

**University of Alberta**

Effect of Sonication on the Particle Size of Kaolinite Clays

by

Maedeh Marefatallah

A thesis submitted to the Faculty of Graduate Studies and Research  
in partial fulfillment of the requirements for the degree of

Master of Science

in

Chemical Engineering

Department of Chemical and Materials Engineering

©Maedeh Marefatallah

Spring 2013

Edmonton, Alberta

Permission is hereby granted to the University of Alberta Libraries to reproduce single copies of this thesis and to lend or sell such copies for private, scholarly or scientific research purposes only. Where the thesis is converted to, or otherwise made available in digital form, the University of Alberta will advise potential users of the thesis of these terms.

The author reserves all other publication and other rights in association with the copyright in the thesis and, except as herein before provided, neither the thesis nor any substantial portion thereof may be printed or otherwise reproduced in any material form whatsoever without the author's prior written permission.

تقدیم به پدرم، مادرم و مهدی...

به پاس بودن های همیشه شان...

## **Abstract**

In oil sands mining operations, water-based mixtures containing coarse sand grains and fine mineral solids (including clays) are ubiquitous. The clay fraction can have a detrimental effect on the separation of bitumen from the oil sand matrix, on the hydrotransport pipelines, and on water recycle. As such, the particle size and concentration of the colloidal clay particles and the rheology of aqueous suspension of these particles must be monitored.

The Particle Size Distribution (PSD), along with pH and ion concentration in the continuous phase, govern particle-particle and particle-continuous phase interactions. These interactions in turn dictate the overall behavior of mixtures containing clays. Therefore, any factor that can bias or alter the clay PSD of the mineral solids must be investigated. For example these mixtures are typically exposed to sonication before particle size analyses are conducted. In this study, the effect of sonication on the kaolinite clay PSD - as an analog of the clays found in the oil sands - was examined. The size measurements were carried out using a Flow Particle Image Analyzer (Sysmex FPIA-3000). This study demonstrates that sonication results in a reduction of the number of large particles and also an increase in the proportion of the smallest particles. Results of experiments conducted on slurries having different pH, electrolyte concentrations and solids concentrations showed that these factors, along with sonication time and power, have a significant effect on the extent of the particle size reduction.

## **Acknowledgements**

First of all, I would like to express my gratitude and appreciation to my supervisor, Dr. Sean Sanders, for his insights, encouragements, guidance, and support throughout my M.Sc. project.

Next, I would like to thank my colleagues in the Pipeline Transport Process Research Group for the useful conversations we had in our meetings and their valuable feedbacks on my research work. Specially, I would like to thank Terry Runyon for her continuous help throughout my research.

Thanks to the NSERC industrial research chair in pipeline transport processes for funding this project.

Special thanks to Andrea Sedgwick, from Total E&P Canada, for providing the tailings samples used in this study and Jessie Smith for her help in preparation of these industrial tailings samples for my experiments. I would also like to acknowledge Dr. Zhenghe Xu for providing access to his laboratory equipment.

I wish to express my sincere appreciation to Lily Laser and Marion Pritchard from Chemical and Materials Engineering Department. There were so many times that their greetings and beautiful smiles changed my long busy days to happy nice ones.

Finally, I would like to express my deepest appreciation to my family who always believed in me and supported me.

## Table of Contents

<b>1. Problem Statement</b> .....	1
<b>2. Literature review</b> .....	8
2.1. Overview/Chapter highlights.....	8
2.2. Role of clays in oil sands mining and extraction.....	9
2.2.1. Clay content of the ore .....	9
2.2.2. Clay-bitumen interaction .....	10
2.2.3. Sludging in the separation vessel.....	11
2.2.4. Design and operation of hydrotransport pipelines .....	11
2.2.5. Settling behaviour of tailings.....	12
2.2.6. Chemistry of recycled water .....	13
2.3. Solids particle size distributions in the oil sands industry .....	13
2.4. Effect of particle size on the rheology of clays .....	15
2.5. Explanation of the behaviour of aqueous clay suspensions .....	17
2.5.1. van der Waals and electrostatic forces .....	17
2.5.2. DLVO theory .....	19
2.6. Kaolinite as a model clay .....	21
2.7. Sonication.....	24
2.7.1. Effect of sonication on the particle size of solids .....	29
2.7.2. Effect of sonication on the particle size of clays .....	30
<b>3. Experimental method</b> .....	37
3.1. Materials.....	37
3.1.1. Kaolinite clay.....	37
3.1.5. FPIA Consumables.....	38

3.1.6. Industrial oil sand tailings.....	38
3.2. Equipment .....	40
3.2.1. Sonication test system.....	40
3.2.2. Sysmex Flow Particle Image Analyzer-3000 (FPIA) .....	44
3.2.3. Application of the FPIA in literature.....	49
3.3. Procedures .....	51
3.3.1. Sample preparation.....	51
3.3.2. FPIA tests .....	51
3.3.3. Sonication tests .....	53
3.3.4. Mastersizer tests.....	54
3.3.5. Cryo-SEM tests.....	55
3.3.6. Tailings tests .....	57
3.4 Experimental programme .....	58
3.4.1 Test parameter selection and development.....	58
3.4.2 Benchmarking data – Effect of solids concentration, pH, and flocculant addition on kaolinite PSD (no sonication) .....	59
3.4.3 Sonication tests (time and amplitude) .....	60
<b>4. Evaluation of experimental setup.....</b>	<b>61</b>
4.1. Introduction and test objectives .....	61
4.2. Sysmex-FPIA 3000 operations .....	62
4.2.1. Repeatability of FPIA results.....	62
4.3. Effect of mixing and pre-test cooling .....	69
4.3.1. Effect of mixing .....	71
4.3.2. Effect of cooling and heating during the mixing .....	75
4.4. Summary .....	76

<b>5. Preliminary evaluation of factors affecting kaolinite PSD</b> .....	78
5.1 Introduction and objectives .....	78
5.2. Effect of sample concentration on measured PSD.....	79
5.3. Sample pH .....	82
5.4. Flocculant addition.....	86
5.5. Summary .....	90
<b>6. The effect of sonication on kaolinite PSD</b> .....	91
6.1 Introduction and objectives .....	91
6.2. Effect of sonication time .....	93
6.2.1. Comparison of particle size distributions .....	94
6.2.2. Comparison of populations of primary particles, flocs, and aggregates .....	98
6.2.3. Evaluation of the Floc Reduction Ratio (FRR) .....	103
6.2.4. The influence of solids concentration .....	105
6.3. Validation of results.....	107
6.3.1. Laser diffraction method .....	107
6.3.2. Cryogenic SEM studies .....	110
6.3.3. Settling behavior .....	114
6.4. Effect of sonication amplitude on kaolinite PSD measurements .....	118
6.5. Case study I: effect of sample pH.....	122
6.6. Case study II: effect of flocculant addition .....	131
6.7. Sonication of Oil Sands Tailings samples.....	136
6.8. Summary .....	145
<b>7. Conclusions and recommendations</b> .....	148

7.1. Conclusions .....	148
7.2. Recommendations.....	150
<b>8. References</b> .....	<b>152</b>
Appendix A: Repeatability of FPIA results .....	172
Appendix B: calculations of chi-square tests.....	174
Appendix C: Effect of FPIA mixer speed on kaolinite PSD .....	200
Appendix D: Effect of sonication time- Comparison of particle size distributions.. .....	205
Appendix E: Effect of sonication time- Comparison of populations of primary particles, flocs, and aggregates.....	208
Appendix F: Effect of sonication time- Evaluation of the Floc Reduction Ratio (FRR) .....	211
Appendix G: Laser diffraction method.....	212
Appendix H: Cryogenic SEM studies .....	216
Appendix I: Effect of sonication amplitude on the kaolinite PSD .....	219
Appendix J: Case study I: effect of sample pH.....	227
Appendix K: Case study II: effect of flocculant addition.....	229

## List of Tables

Table 2.1 Summary of literature on the sonication of clay materials.....	31
Table 3.1 Particle size range for each FPIA-3000 measuring mode.....	45
Table 3.2 Particle size frequency table produced by FPIA software .....	47
Table 3.3 The characteristics of samples used for cryo-SEM studies and settling tests .....	56
Table 4.1 The chi-square test statistics for results shown in Figures 4.1 and 4.2.	65
Table 6.1 Experimental matrix for the investigation of the effects of sonication time, sonication amplitude and sample concentration on kaolinite PSD.....	93
Table 6.2 The amount of sonication energy delivered to each sample as a function of sonication time and amplitude .....	97
Table 6.3 Particle size range classifications used in the present study.....	99
Table 6.4 Calculations of total sonication energy for three kaolinite samples ...	120
Table 6.5 Dean Stark Results for tailings sieved, bead treated sample, mass basis .....	137
Table 6.6 Dean Stark Results for tailings sieved, bead treated sample, percentages .....	137

## List of Figures

Figure 1.1 Generalized scheme of the hot water extraction process. Reprinted with permission of John Wiley & Sons, Inc (©2004), Masliyah, J., Zhou, Z. J., Xu, Z., Czarnecki, J. & Hamza, H. Understanding Water-Based Bitumen Extraction from Athabasca Oil Sands. <i>The Canadian Journal of Chemical Engineering</i> 82, 628–654 (2004).....	2
Figure 2.1 Particle size distributions of three solids fractions separated from a sample of mature fine railings. Reprinted with permission of John Wiley & Sons, Inc (©2009), Adeyinka, O. B., Samiei, S., Xu, Z. & Masliyah, J. H. Effect of particle size on the rheology of Athabasca clay suspensions. <i>The Canadian Journal of Chemical Engineering</i> 87, 422–434 (2009).....	16
Figure 2.2 Relative viscosity of suspensions comprised of different ratios of fraction 1 and 2. Reprinted with permission of John Wiley & Sons, Inc (©2009), Adeyinka, O. B., Samiei, S., Xu, Z. & Masliyah, J. H. Effect of particle size on the rheology of Athabasca clay suspensions. <i>The Canadian Journal of Chemical Engineering</i> 87, 422–434 (2009).....	17
Figure 2.3 Attraction, repulsion, and net interaction energy between two charged particles. Reprinted with permission of John Wiley & Sons, Inc (©2006), Masliyah, J. H. & Bhattacharjee, S. <i>Electrokinetic and Colloid Transport Phenomena</i> .....	21
Figure 2.4 Kaolinite particle charge distribution .....	22
Figure 2.5 Different particle-particle association modes.....	23
Figure 2.6 Sonication probe immersed in a sample .....	28
Figure 3.1 Particle size distribution of sieved, bead treated tailings sample measured by FPIA: $c=10$ g/L .....	39
Figure 3.2 Misonix Sonicator-4000 and its components .....	41
Figure 3.3 View of the Sonicator-4000's screen.....	42
Figure 3.4 Cooling system components.....	43
Figure 3.5 Large-tip opening transfer pipette (13-711-5B Fisher Scientific).....	53
Figure 3.6 Cryo-SEM copper stage.....	57

Figure 4.1 Repeatability tests: Cumulative Particle size distributions for 10 samples from a single mixture (c= 10 g/L).....	63
Figure 4.2 Repeatability tests: Cumulative particle size distributions for 6 different mixtures having the same concentration (c=10 g/L).....	63
Figure 4.3a Effect of FPIA mixer speed on the measured PSD (c=10 g/L, RPM=50, 300).....	67
Figure 4.3b Effect of FPIA mixer speed on the measured PSD (c=10 g/L, RPM=300, 550).....	67
Figure 4.3c Effect of FPIA mixer speed on the measured PSD (c=10 g/L RPM=50, 300, 550, 700) .....	67
Figure 4.4 Effect of RPM target on the cumulative partice size distribution (c=10 g/L) .....	68
Figure 4.5a Effect of pre-test cooling (23 °C-18°C) on the kaolinite PSD (c=40 g/L) .....	70
Figure 4.5b Effect of pre-test cooling (18 °C-11°C) on the kaolinite PSD (c=40 g/L) .....	70
Figure 4.5c Effect of pre-test cooling (23 °C-5 °C) on the kaolinite PSD (c=40 g/L) .....	70
Figure 4.6 Effect of mixing on the Sauter mean diameter of kaolinite samples: c=40 g/L.....	72
Figure 4.7a Effect of mixing on the kaolinite PSD (c=40 g/L).....	74
Figure 4.7b Effect of mixing on the kaolinite PSD (c=40 g/L) .....	74
Figure 4.8 Effect of sample temperature variation on the Sauter mean diameter during sample preparation .....	76
Figure 5.1 Kaolinite PSD at two concentrations: c=2 g/L and 40 g/L, (pH~ 4.6).. .....	80
Figure 5.2 Kaolinite PSD at concentration of c=8 g/L, (pH~ 4.6).....	80
Figure 5.3 Kaolinite PSD at concentration of: c=24 g/L, (pH~ 4.6).....	81
Figure 5.4 Effect of solids concentration on the kaolinite PSD (c=2, 8, 24, and 40 g/L),(pH~ 4.6) .....	81
Figure 5.5 Kaolinite PSD at natural and high pH (pH~4.6 and 11), c=40 g/L .....	84

Figure 5.6 Kaolinite PSD at natural and high pH (pH~4.6 and 11), c=40 g/L.....	84
Figure 5.7 Kaolinite PSD at natural and high pH (pH~4.6 and 11), c=8 g/L.....	85
Figure 5.8 Kaolinite PSD at natural and high pH (pH~4.6 and 11), c=2 g/L.....	85
Figure 5.9. Effect of flocculant addition on the kaolinite PSD (c=40 g/L) pH = 4.6 (no flocculant), pH~11 (flocculant added) CaCl <sub>2</sub> .2H <sub>2</sub> O: Kaolinite (mass ratio)=0.1.....	87
Figure 5.10 Effect of flocculant addition on the kaolinite PSD (c=24 g/L) pH ~4.6 (no flocculant), pH~11 (flocculant added) CaCl <sub>2</sub> .2H <sub>2</sub> O: Kaolinite (mass ratio)=0.1.....	87
Figure 5.11 Effect of flocculant addition on the kaolinite PSD (c=8g/L) pH ~4.6 (no flocculant), pH~11 (flocculant added) CaCl <sub>2</sub> .2H <sub>2</sub> O: Kaolinite (mass ratio)=0.1.....	88
Figure 5.12 Effect of flocculant addition on the kaolinite PSD (c=2g/L) pH ~4.6 (no flocculant), pH~11 (flocculant added) CaCl <sub>2</sub> .2H <sub>2</sub> O: Kaolinite (mass ratio)=0.1.....	88
Figure 5.13 Sauter mean diameter of kaolinite suspensions (c=2, 8, 24, 40 g/L) at three conditions: a) pH~4.6, no NaOH addition, no flocculant addition; b) pH ~11 (NaOH added); c) pH ~11 and flocculant addition, CaCl <sub>2</sub> .2H <sub>2</sub> O: Kaolinite (mass ratio) = 0.1.....	89
Figure 6.1 Kaolinite PSD for non-sonicated samples: c=10, 20, and 40 g/L; pH~4.6 .....	92
Figure 6.2 Effect of sonication time on the kaolinite PSD: c=40 g/L; pH~4.6; Sonication amplitude: 100% .....	94
Figure 6.3 Effect of sonication time on the kaolinite PSD: c=20 g/L; pH~4.6; Sonication amplitude: 100% .....	95
Figure 6.4 Effect of sonication time on the kaolinite PSD: c=10 g/L; pH~4.6; Sonication amplitude: 100% .....	95
Figure 6.5 Proportion of the dispersed phase population of primary particles, expressed in %, as a function of sonication time, for sample concentrations of 10, 20, and 40 g/L. Sonication amplitude: 100%.....	101

Figure 6.6 Proportion of the dispersed phase population of flocs, expressed in %, as a function of sonication time, for sample concentrations of 10, 20, and 40 g/L. Sonication amplitude: 100% .....	102
Figure 6.7 Proportion of the dispersed phase population of aggregates, expressed in %, as a function of sonication time, for sample concentrations of 10, 20, and 40 g/L. Sonication amplitude: 100%.....	104
Figure 6.8 Floc reduction ratio (FRR) at each sonication time: c=10, 20, and 40 g/L; Sonication amplitude: 100%.....	105
Figure 6.9 Kaolinite PSD after different sonication times measured by Malvern Mastersizer c=40 g/L, Sonication times: 0, 3, 10, 20, 30, 40, 50 and 60 minutes, Sonication amplitude: 100% .....	108
Figure 6.10 Sauter mean diameter (d <sub>32</sub> ) of kaolinite sample at different sonication times.....	110
Figure 6.11 Cryo-SEM image of non-sonicated kaolinite sample; sample (1-1); c=20 g/L, 1000X.....	112
Figure 6.12 Settling behaviour of 4 kaolinite samples at t=30 minutes; amplitude: 100%.....	112
Figure 6.13 Cryo-SEM image of non-sonicated kaolinite sample; sample (1-1); c=20 g/L, 2000X.....	113
Figure 6.14 Cryo-SEM image of sonicated kaolinite sample; sample (1-2); c=20 g/L; 2000X; sonication time: 30 minutes; amplitude: 100% .....	113
Figure 6.15 Sample PSD measured by FPIA; Sample (1-1) and (1-2); c=20 g/L; Sonication time: 30 minutes; amplitude: 100% .....	114
Figure 6.16 Settling behaviour of 4 kaolinite samples at t=0; Sample (1-1): non-sonicated, c=20 g/L; Sample (1-2): c=20 g/L, sonicated for 30 minutes, amplitude: 100%; Sample (2-1): non-sonicated, c=10 g/L; Sample (2-2): c=10 g/L, sonicated for 30 minutes, Sonication amplitude: 100% .....	115
Figure 6.17 Settling behaviour of 4 kaolinite samples at t=30 minutes; Sample (1-1): non-sonicated, c=20 g/L; Sample (1-2): c=20 g/L, sonicated for 30 minutes, Sonication amplitude: 100%; Sample (2-1): non-sonicated, c=10 g/L; Sample (2-2): c=10 g/L, sonicated for 30 minutes, Sonication amplitude: 100% .....	116

Figure 6.18 Settling behaviour of 4 kaolinite samples at t=90 minutes; Sample (1-1): non-sonicated, c=20g/L; Sample (1-2): c=20g/L, sonicated for 30 minutes, Sonication amplitude: 100%; Sample (2-1): non-sonicated, c=10g/L; Sample (2-2): c=10g/L, sonicated for 30 minutes, Sonication amplitude: 100% .....	117
Figure 6.19 Settling behaviour of 4 kaolinite samples at t=24 hours; Sample (1-1): non-sonicated, c=20g/L; Sample (1-2): c=20g/L, sonicated for 30 minutes, amplitude: 100%; Sample (2-1): non-sonicated, c=10g/L; Sample (2-2): c=10g/L, sonicated for 30 minutes, amplitude: 100%.....	118
Figure 6.20 Effect of sonication amplitude on the kaolinite PSD: c=40 g/L; Sonication amplitude: 50%, 75%, and 100%.....	119
Figure 6.21 Effect of sonication amplitude on the floc reduction ratio (FRR): c=40 g/L.....	122
Figure 6.22 Influence of pH on the sonication effect: c= 40 g/L; pH=4.6; Sonication amplitude: 100% .....	124
Figure 6.23 Influence of pH on the sonication effect: c= 40 g/L; pH=8.2; Sonication amplitude: 100% .....	124
Figure 6.24 Influence of pH on the sonication effect: c= 40 g/L; pH=11.4; Sonication amplitude: 100% .....	125
Figure 6.25 Flocc percentage at different sonication times for three different pH values; c=40 g/L, Sonication amplitude: 100% .....	126
Figure 6.26 Floc reduction ratio (FRR) at different sonication times for three different pH values; c=40 g/L, Sonication amplitude: 100% .....	126
Figure 6.27(a) FPIA images of largest aggregates ( $71.328 \mu\text{m} < d < 63.241 \mu\text{m}$ ) in the sonicated kaolinite sample: c=40g/L; pH=8.2; Sonication time of 30 minutes; Sonication amplitude of 100% .....	128
Figure 6.27(b) FPIA images of largest aggregates ( $63.172 \mu\text{m} < d < 61.123 \mu\text{m}$ ) in the sonicated kaolinite sample: c=40g/L; pH=8.2; Sonication time of 30 minutes; Sonication amplitude of 100%.....	129
Figure 6.27(c) FPIA images of largest aggregates ( $61.072 \mu\text{m} < d < 58.206 \mu\text{m}$ ) in the sonicated kaolinite sample: c=40g/L; pH=8.2; Sonication time of 30 minutes; Sonication amplitude of 100%.....	130

Figure 6.28 Effect of sonication on the non-flocculated kaolinite sample: c=20 g/L; sonication amplitude: 100% .....	133
Figure 6.29 Effect of sonication on the flocculated kaolinite sample: c=20 g/L; CaCl <sub>2</sub> to kaolinite mass ratio = 0.1; sonication amplitude: 100%.....	133
Figure 6.30 Percentage of individual particles in the flocculated and non-flocculated samples at different sonication times; c=20 g/L; CaCl <sub>2</sub> to kaolinite mass ratio = 0.1;sonication amplitude: 100%.....	134
Figure 6.31 Flocc percentage in the flocculated and non-flocculated samples at different sonication times; c=20 g/L; CaCl <sub>2</sub> to kaolinite mass ratio = 0.1; sonication amplitude: 100%.....	134
Figure 6.32 Percentage of aggregates in the flocculated and non-flocculated samples at different sonication times; c=20 g/L; CaCl <sub>2</sub> to kaolinite mass ratio = 0.1; amplitude: 100%.....	135
Figure 6.33 Floc reduction ration (FRR) in the flocculated and non-flocculated samples at different sonication times; c=20 g/L; CaCl <sub>2</sub> to kaolinite mass ratio=0.1; amplitude: 100%.....	135
Figure 6.34(a)-(f) Effect of sonication on the PSD of tailings sample: c=10 g/L; amplitude 100%.....	139
Figure 6.35(a)-(d) Effect of sonication on the kaolinite clay PSD and tailings sample PSD: c=10 g/L; sonication amplitude 100%.....	142
Figure 6.36 Flocc percentage of kaolinite and industrial tailings sample at different sonication times; c=10 g/L; amplitude 100% .....	143
Figure 6.37 Floc reduction ratio (FRR) of kaolinite and industrial tailings sample at different sonication times; c=10 g/L; amplitude 100% .....	144

## List of Symbols

$P_{\max}$	Maximum pressure amplitude
$n_{\infty}$	ionic number concentration in the bulk solution
$\epsilon_0$	permittivity of vacuum
$\kappa^{-1}$	Debye length
A	spherical particle radius
C	Concentration
$c_s$	speed of sound in the sample fluid
df	Degree of freedom
E	elementary charge
FRR	Floc Reduction Ratio
G	gram
H	separation distance
$k_B$	Boltzmann constant
L	Litre
PSD	Particle Size Distribution
t	Time
T	absolute temperature
v	Frequency
z	absolute value of valency of the electrolyte
$\alpha$	absorption coefficient
$\rho$	Density of the fluid
$\epsilon$	dielectric permittivity of medium
$\epsilon$	dielectric permittivity of medium
$\varphi$	surface potential (zeta potential)

## 1. Problem Statement

Alberta's oil sands deposits are ranked as the third largest crude oil reserves in the world, after Saudi Arabia and Venezuela<sup>1</sup>. The initial established reserves are estimated to have over 170 billion barrels (National Energy Board, 2004)<sup>2</sup>. According to the Alberta Energy Resources Conservation Board (ERCB), in 2011 the production of crude bitumen from the oil sands was 1.7 million barrels per day. This amount is anticipated to increase to 3.7 million barrels per day by 2021<sup>3</sup>.

Alberta's oil sands are comprised of 55-80% inorganic materials (mainly quartz), 4-18% bitumen, 5-34% fines (solid particles smaller than 44  $\mu\text{m}$ ), and 2-15% water<sup>4,5</sup>. Bitumen high viscosity and the presence of sands particles make the bitumen recovery from oil sands reserves more challenging than for conventional crude oil reserves.

Two methods are currently used for commercial bitumen production from oil sands: in-situ and open pit mining. Open pit mining is used for deposits buried less than 75 meters below the surface<sup>6</sup>. In 2007, the total crude bitumen production was 1.327 million barrels per day: 0.793 million bbl/d from mining operations and 0.534 million bbl/d from in-situ operations<sup>6</sup>.

Currently, the Clark Hot Water Extraction (CHWE) process is used in most commercial bitumen extraction plants in Alberta to recover bitumen from surface mined oil sands<sup>7,8</sup>. Figure 1.1 illustrates the process of the hot water bitumen

extraction used in open pit mining<sup>8</sup>. CHWE is a water based process in which heated water is added to the oil sands ore and the resulting slurry is transported to the extraction unit with hydrotransport pipelines<sup>9</sup>. Within the hydrotransport pipelines bitumen liberation from the sand grains occurs where the size of the oil sands lumps is reduced because of the shear forces<sup>8</sup>. The liberated bitumen droplets attach to the existing air bubbles in the slurry<sup>9</sup>. When the slurry reaches the extraction plant, the first stage of separation is then carried out in the gravity separation vessel<sup>9</sup>.

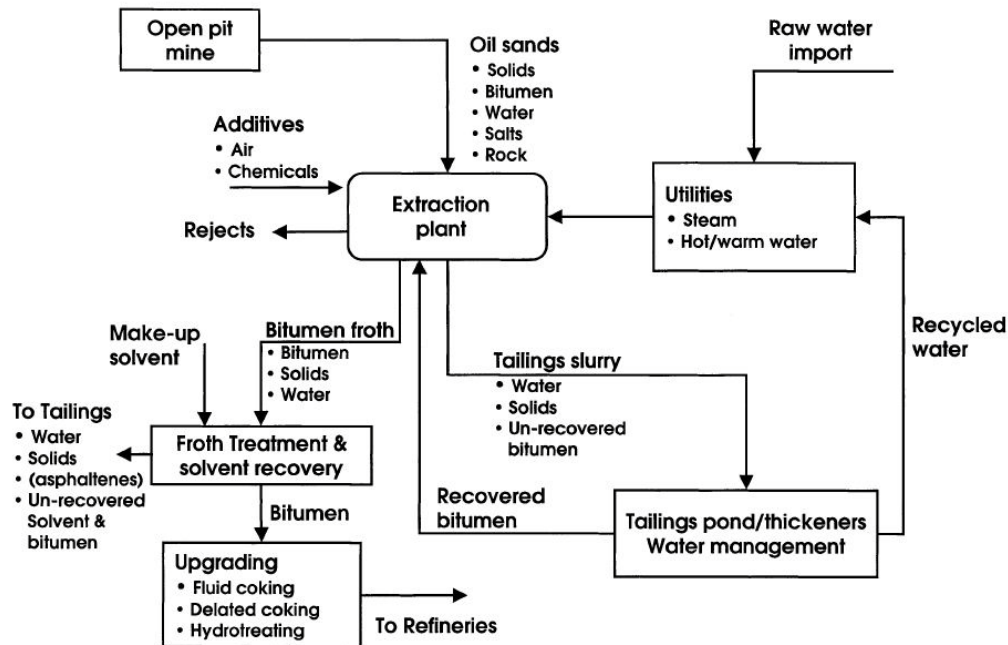


Figure 1.1 Generalized scheme of the hot water extraction process<sup>8</sup>. Reprinted with permission of John Wiley & Sons, Inc (©2004), Masliyah, J., Zhou, Z. J., Xu, Z., Czarnecki, J. & Hamza, H. Understanding Water-Based Bitumen Extraction from Athabasca Oil Sands. *The Canadian Journal of Chemical Engineering* 82, 628–654 (2004).

In the separation vessel the aerated bitumen and solids are separated based on their density<sup>9</sup>. The aerated bitumen, having low density, floats to the top of separation vessel and forms oil sands froth stream while the coarse solids, having

higher density, settle at the bottom of the vessel and form the tailings stream<sup>9</sup>. The froth stream is sent to the froth treatment unit for bitumen recovery and the tailings will transport and further discharge to the tailings pond<sup>8,9</sup>. The middle layer, called the middlings, of the separation vessel is also withdrawn for further bitumen separation<sup>9</sup>. The middlings are dilute slurries having a low solids content (10-21 wt %)<sup>10,11</sup>.

The froth stream normally contains 60% bitumen, 30% water, and 10% solids. The bitumen in the froth stream is recovered by the addition of solvents in a froth treatment unit. The recovered bitumen from the froth treatment unit will be sent to upgrading units. The remaining mixture of solids, water, and un-recovered bitumen is added to the tailings stream<sup>8</sup>.

The tailings stream from the extraction plant is typically discharged to the tailings ponds for solid-liquid separation<sup>8,9</sup>. In the tailings ponds, the coarse solids rapidly separate from the fine solids and settle at the bottom of the tailings ponds. The recovered water from tailings ponds is recycled back to the extraction unit<sup>8</sup>.

As of 2006, the production of oil sands has increased to about 1.2 million barrels per day<sup>12</sup>. To produce 1 barrel of bitumen from oil sands ores by the bitumen extraction process, 2-4 barrels of fresh water are required. In Alberta, this fresh water is withdrawn from Athabasca River. The total amount of water used for oil sands production in 2005 was 359 million cubic meters<sup>13</sup>. The huge water consumption and the production of large volumes of tailings at the end of the

bitumen extraction process are two important environmental issues currently facing the oil sands industry.

The great amounts of produced tailings are discharged into the tailings ponds and are believed to cause a negative environmental impact on the surrounding soil, water, and air<sup>12</sup>. Currently, tailings ponds cover a land area greater than 50 km<sup>2</sup><sup>14</sup>. The large volumes and resulting environmental impact of tailing ponds make recycling water from tailings treatments a crucial aspect of the current extraction processes<sup>12</sup>.

The difficulties in tailings treatment are primarily because of the slow settling of fine particles, which are mostly clays, in the tailings suspension. It takes many years of settling to reach a solid concentration of about 30 wt %<sup>9,15</sup>. At this point the fine tailings are called mature fine tailings (MFT)<sup>9</sup>.

The average mineral content of MFT is about 30 wt%. More than 97 wt% of these minerals are fines (particles smaller than 44 µm)<sup>16</sup>. While 22-67% of the clay fraction of tailings (particles smaller than 2 µm) is kaolinite, illite and montmorillonite are the next most abundant clay minerals, comprising 7-10 wt% and 1-8 wt% of clay fraction<sup>17</sup>.

Understanding the clay minerals is vital for any oil sands process. The clay fraction can have a detrimental effect on the separation of bitumen from the oil sand matrix, pipeline transport of oil sands mixtures, tailings management, and water recycle<sup>9,10,18-21</sup>. Due to these effects, the particle size, concentration and rheology of colloidal clay slurries must be monitored.

As clay slurries are colloidal systems, Particle Size Distribution (PSD), pH and continuous phase ion concentration govern particle-particle and particle-continuous phase interactions<sup>22</sup>. Further, these interactions dictate the overall behavior of clay-containing mixtures<sup>22</sup>.

In the oil sands mining and extraction process, samples (such as ore samples, primary froth and secondary froth, middlings, extraction tailings, fine tailings, and mature fine tailings) are collected from various process streams for PSD analysis<sup>11</sup>. Light scattering is one of the most common particle size measurement methods used in the oil sands industry<sup>11</sup>. Light scattering methods are sensitive to the presence of aggregates<sup>23,24</sup>; therefore, samples must be pretreated prior to the size measurement tests. These methods are mostly dispersion methods which de-aggregate the suspensions. Sonication, dispersant addition, and pH adjustment are examples of these dispersion methods<sup>23,24</sup>.

Because of the importance of accurately determining the PSD of the “fines” (<44  $\mu\text{m}$ ), factors that can bias the PSD measurement should be investigated. The parameters that enhance particle agglomeration or de-agglomeration primarily affect PSD measurements for fine particles. Delgado and Matijevic<sup>23</sup> and Jeeravipoolvam et al<sup>25</sup> showed in separate studies that sample preparation and size measurement techniques can affect the measured PSD of colloidal dispersions<sup>23</sup>, specifically oil sands fine particles<sup>25</sup>. Since mixtures are typically exposed to sonication before particle size analysis is conducted<sup>11</sup>, it is important to investigate the effect of sonication on the PSD.

Most studies done on the clay mineralogy of the Athabasca oil sands agree that kaolinite is one of the most dominant clay minerals in the oil sands industry<sup>19,26-33</sup>. Thus, numerous studies have been done using kaolinite mixtures as surrogate materials for oil sands fine solids slurries<sup>34-38</sup>. Mihiretu et al<sup>34</sup> compared the rheological behaviour of a kaolinite slurry with that of an actual MFT sample of the same solids content. The results of their work showed that kaolinite slurries represent the fine tailings material very well<sup>34</sup>. They explained this similarity by the fact that about 76% of the fine tailings in the oil sands process are kaolinite<sup>34</sup>. Additionally, kaolinite clay slurries have been used extensively in this research group<sup>39,40</sup> and their behaviour is well characterized. Consequently kaolinite has been used as a “model” clay for the present study. The particle size is used as a surrogate for rheology and processability of the slurry in the present study. The effect of particle size on the rheology of clay slurries is discussed in Section 2.4 of the present study.

In this work, the effect of the time and intensity of sonication on the kaolinite suspension PSD was examined. Experiments were conducted using slurries with various pH, electrolyte concentrations and solids concentrations. The kaolinite size distribution was analyzed using a Sysmex FPIA-3000 flow particle image analyzer (FPIA). The FPIA enables characterization of PSD using automated imaging techniques.

The objectives of the present study are therefore:

- Study the particle size distribution of non-sonicated kaolinite samples at different solids concentrations, at low and high sample pH, in the absence or presence of the flocculant
- Compare the particle size distribution of non-sonicated and sonicated kaolinite mixtures
- Study the extent of size reduction due to sonication at different sonication time and amplitudes
- Study the extent of size reduction due to sonication for samples with different kaolinite concentrations, having different pH values, and flocculated samples comparing to non-flocculated ones
- Validate the conclusions of this study by reproducing the results (variation of kaolinite PSD) using other methods: laser diffraction method, cryogenic-SEM studies, and settling behavior observations

## **2. Literature review**

### **2.1. Overview/Chapter highlights**

Kaolinite is studied in the present work as an analog of the clays found in the oil sands. Clays play an important role in different steps of bitumen extraction and tailings treatment. The role of clays in the oil sands mining and extraction is discussed in this chapter under 6 topics: clay content of the ore, clay-bitumen interaction, sludging in the separation vessel, design and operation of hydrotransport pipelines, settling behaviour of tailings, and chemistry of recycled water. The importance of the knowledge of clay minerals in each section is described.

Among various suspension characteristics, particle size distribution has been chosen to study in the present work. The importance of solids particle size distribution and its effect on the suspension rheology are discussed in Sections 2.3 and 2.4.

In the present work, the kaolinite particle size distribution is studied under different suspension conditions such as high pH values, and the flocculant addition. Analysis of different behaviours of kaolinite suspensions, as a colloidal system, at each condition is done using the principles of the behaviour of aqueous clay suspension. The dominant forces that dictate the particle-particle interactions in a colloidal suspension are discussed in Section 2.5.

Furthermore, the characteristics of kaolinite as a model clay is discussed in Section 2.6.

Finally, the principles of sonication as the dispersion method often used in sample preparation for PSD measurements in the oil sands industry are discussed in Section 2.7.

## **2.2. Role of clays in oil sands mining and extraction**

Clay-bitumen interactions, sludging in the separation vessel, design and operation of hydrotransport pipelines, settling behaviour of tailings and the chemistry of recycled water are some of the topics in which knowledge of clay minerals is necessary<sup>9,10,18-21</sup>.

Various studies have been conducted on the mineralogy of clays in the oil sands extraction process. The type, particle size, and the amount of the clay minerals present in different process streams have been studied by numerous researchers<sup>19,28-31,41-44</sup>. The results of these studies can be used to track specific clay minerals in different process streams and units and thus their impact on the operation of each process unit in the oil sands extraction process<sup>19</sup>.

### **2.2.1. Clay content of the ore**

Traditionally, in addition to the bitumen content, the fine clay content (fines, which are solid particles < 44 µm in diameter) has been used to classify different oil sands ores and also to predict bitumen separation behaviour<sup>45,46</sup>. The quantity of fines is important as it at least partially determines the processability of the

ore<sup>5</sup>. As the percentage of fines present in an ore increases, the bitumen recovery from that ore typically decreases<sup>47</sup>. It has been suggested that the clay fraction (particles smaller than 2  $\mu\text{m}$ ) and the ultrafine clay fraction (particles smaller than 0.2  $\mu\text{m}$ ) of the fines govern the processability of an ore<sup>14,48</sup>.

### **2.2.2. Clay-bitumen interaction**

The clay-bitumen interaction impacts the bitumen flotation in separation vessels, and the quality of oil sands froth and consequently the efficiency of the bitumen extraction process<sup>19,20</sup>. The study of Sparks et al<sup>18</sup> also confirmed that the clay fraction of the fines hinders the bitumen recovery by interfering with the bitumen-water interactions. The interactions between bitumen and clay are affected by the presence of different cations on the surface of the clay. Clay-bitumen interactions change both the clay's surface and the bitumen composition<sup>29,43,49,50</sup>. Different clays play different roles in the process of bitumen extraction, depending on their type, and the presence of specific cations<sup>51</sup>. For example, in the presence of calcium ions, montmorillonite negatively impacts the conditioning process, while kaolinite does not<sup>51</sup>. In addition to clay type, clay concentration is also important. Schramm<sup>10</sup> carried out in-situ measurements of middlings viscosity in a commercial size gravity separation vessel. His results demonstrated that low concentrations of fine solids in the oil sands slurry resulted in a high aerated bitumen rise velocity, which increased the bitumen recovery rate<sup>10</sup>.

Besides type and concentration of clays, the particle size distribution is another determining characteristic of the clay that can affect bitumen flotation. Decreased

particle size (increased surface area) typically results in an increase in the yield strength<sup>52</sup> of the oil sands slurry which hinders the bitumen flotation<sup>33</sup>.

### **2.2.3. Sludging in the separation vessel**

Sludging is an operational condition in which a highly viscous suspension is formed in the primary separation vessel<sup>9</sup>. This layer of viscous suspension hinders the flotation of aerated bitumen and thus results in low bitumen separation efficiency<sup>9</sup>. A recent study showed that in addition to the fines content, the ultra-fine fraction ( $< 0.3 \mu\text{m}$ ) can also contribute to the sludging in a separation vessel<sup>48</sup>. Slurries containing significant amounts of ultra-fines are colloidal systems; therefore, the particle-particle interactions can change the rheological behaviour of these slurries, including middlings, in the separation vessel<sup>9</sup>. Several studies investigated possible causes of, and methods to avoid sludge formation in the separation vessel<sup>9,10,48</sup>. The results from these studies suggested that the factors causing the sludging are high solids concentration, high concentration of ultra-fines, high electrolyte content, and the presence of specific clay types<sup>9,10,48</sup>. Adeyinka et al<sup>9</sup> studied the effect of particle size distribution on the rheology of clay suspensions. Since an increase in viscosity can cause sludging, their results are useful for predicting the properties of slurries which are at risk of causing sludging in the separation vessel.

### **2.2.4. Design and operation of hydrotransport pipelines**

Two of the important parameters for design and operation of hydrotransport pipelines are the minimum operating velocity, also known as the deposition

velocity, and the pipeline pressure gradient. To minimize pipe wear rates, hydrotransport pipelines are operated at velocities just greater than the deposition velocity<sup>6</sup>. In the oil sands industry, the SRC Two-Layer model is used to predict deposition velocity and pipelines pressure drop<sup>53,54</sup>. Beside particle size and concentration of fine, the carrier fluid (fine + water) viscosity is one of the important parameters used in the prediction of pressure drop and deposition velocity by SRC Two-Layer model<sup>54</sup>. The carrier fluid viscosity is a function of the volume fraction and the particle size distribution of fines<sup>40</sup>. Therefore, the mineral solids particle size distribution (PSD) is required for the design and operation of hydrotransport pipelines<sup>6</sup>, particularly if fine particle (clay) size is used as an indicator of the expected viscosity of the (fines + water) fraction.

#### **2.2.5. Settling behaviour of tailings**

The flocculation behaviour of clays controls the settling behaviour of tailings<sup>20,21</sup>. This is due to the fact that sedimentation behaviour of slurries containing sands and fine clays is affected by sand size distribution, solids content (both fines and sands), and rheological properties of the (fine + water) mixture<sup>34,55,56</sup>. The rheological properties of fine-water mixtures are, in turn, influenced by the fines content (concentration), fines size distribution, and water chemistry<sup>25</sup>. The particle-particle and particle-fluid interactions are affected by the water chemistry. These interactions dictate the overall behavior including the settling process of clay-containing slurries<sup>34</sup>.

### **2.2.6. Chemistry of recycled water**

The water recycled from the tailings treatment is used in the bitumen extraction process<sup>57</sup>. Water chemistry has an important effect on the charge associated with the clay particles, which influences their flocculation, settling, and consolidation behavior<sup>21</sup>. In turn, the charge exchange capacity of the clay particles can affect the water chemistry, causing further changes in the extraction unit<sup>21</sup>.

Mikula et al<sup>21</sup> found that in addition to the effect of water chemistry on the oil sands tailings behaviour, the role of clays in the chemistry of the process water is also important. They also show that, in addition to tailings treatment options, the fines content in the ore also determines the volume of water used to produce a barrel of bitumen<sup>21</sup>. Therefore, the amount of fresh water required depends on the fine content in the ore<sup>21</sup>.

### **2.3. Solids particle size distributions in the oil sands industry**

As described in the previous section, the particle size distribution of the clay fraction can have a significant effect on the separation of bitumen from oil sand, on the pipeline transport of oil sands mixtures, on tailings management, and on water recycle. Furthermore, knowledge of clay mineral behaviour, and specifically clay particle size distribution, can be used to improve models used in the design and operation of thickeners, tailings ponds, and the extraction process<sup>58</sup>. As such, the particle size distribution of the clay component of different streams in the oil sands mining and bitumen extraction process must be monitored. For all these reasons, the measurement of the mineral solids PSD of an

oil sands ore is one of the first and most important steps in characterization the oil sands ore<sup>6</sup>.

Adegoroye<sup>59</sup> studied the characteristics of 5 different oil sands ores. Their results showed that each oil sands ore has a different particle size distribution. In particular, the fraction of ultra-fine, clay, and fine solids changes with ore type<sup>59</sup>, and the percentage of kaolinite clay are also different for each ore. The Dean Stark analysis presented in their work showed that the amount of kaolinite is in the range of 19% to 54% in the clay fraction of each of the 5 ores whereas this amount is in the range of 8-45% in the silt fraction of these ores<sup>59</sup>.

Kaminsky<sup>33</sup> indicates in her study that the solids particle size distribution of an ore changes significantly over different steps of the oil sands extraction process. Therefore, in addition to the measurement of the solids PSD of an oil sands ore, the analysis of particle size distribution for samples taken from different oil sands process streams (e.g. primary and secondary froth, middlings, and tailings) is necessary<sup>33</sup>.

Jeeravipoolvam et al<sup>25</sup> indicated in their study that the particle size distribution of tailings material is significantly affected by the extraction process. Their results demonstrated that the particle size distribution of thickened fine tailings is different from the fine tailings from Clark's Hot Water Extraction (CHWE). They studied the particle size distribution, water chemistry and morphology of two different oil sand fine tailings<sup>25</sup>. They compared these characteristics of the fine tailings from Syncrude's CHWE tailings with those of thickened tailings from

Albian Sands Energy Inc. Albian Sands' plant is a low energy, non-additive extraction process developed as an alternative to the CHWE. Different operations carried out in these two extraction processes affect specifically the clay particles, leading to different tailings behaviour. They showed in their study that the extraction process, specifically the additive used in the process to alter the pH, produces significant differences in the structures of clays in tailings. They suggest that the effectiveness of different extraction processes, and the tailings properties of each, can be understood and predicted through (i) particle size distribution and (ii) water chemistry measurements<sup>25</sup>. They also emphasized that these measurements should be done under the extraction process conditions<sup>25</sup>.

#### **2.4. Effect of particle size on the rheology of clays**

The effect of particle size on the rheology of various suspensions has been studied by many researchers<sup>60-73</sup>. However, only a few studies focus on the impact of particle size on the rheological properties of oil sands slurries<sup>9,74</sup>. Velho and Gomes<sup>75</sup> indicated in their study that there is a close relationship between the rheology of kaolin suspensions and kaolinite particle size. They showed that suspensions containing larger particles exhibit lower viscosities. Brenner<sup>52</sup> showed that particle size reduction leads to an increase in the yield strength of slurries. Separate studies<sup>30,34</sup> showed that the addition of sand particles (with greater diameter than fines) reduces the yield strength and apparent viscosity of tailings suggesting that slurries which contain sand and clay are more workable than suspensions containing only kaolinite.

Adeyinka et al<sup>9</sup> studied the effect of particle size distribution of fine tailings on the rheology of clay suspensions. They separated three fractions of solids from a single MFT sample<sup>9</sup>. The particle size distribution of each fraction is shown in Figure 2.1. Their results indicate that at a given solids concentration, the sample with smaller particles (0.03 $\mu\text{m}$ -2.5  $\mu\text{m}$ ,  $d_{50}$ =0.14  $\mu\text{m}$ ) has higher viscosities comparing to the sample with larger particles (1 $\mu\text{m}$ -25  $\mu\text{m}$ ,  $d_{50}$ =5.96  $\mu\text{m}$ )<sup>9</sup>. Their results also indicate that solids concentration is not sufficient to predict the rheological behaviour of clay suspensions<sup>9</sup>. Figures 2.2 show that at the same solids concentration, the relative viscosity of clay suspensions differ because the size distribution of solids in the suspensions differs<sup>9</sup>.

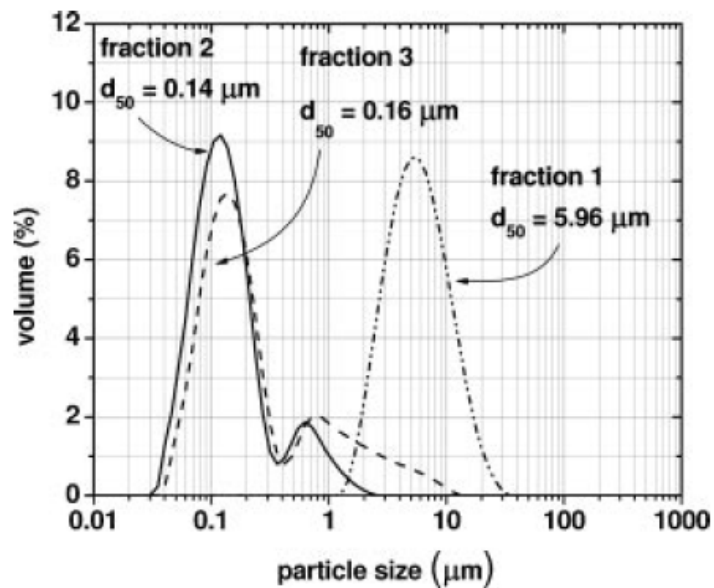


Figure 2.1 Particle size distributions of three solids fractions separated from a sample of mature fine railings<sup>9</sup>. Reprinted with permission of John Wiley & Sons, Inc (©2009), Adeyinka, O. B., Samiei, S., Xu, Z. & Masliyah, J. H. Effect of particle size on the rheology of Athabasca clay suspensions. *The Canadian Journal of Chemical Engineering* 87, 422–434 (2009).

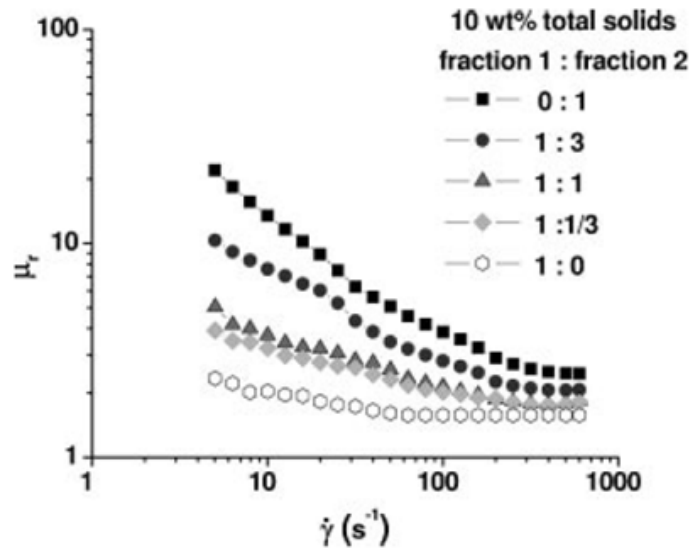


Figure 2.2 Relative viscosity of suspensions comprised of different ratios of fraction 1 and 2<sup>9</sup>. Reprinted with permission of John Wiley & Sons, Inc (©2009), Adeyinka, O. B., Samiei, S., Xu, Z. & Masliyah, J. H. Effect of particle size on the rheology of Athabasca clay suspensions. *The Canadian Journal of Chemical Engineering* 87, 422–434 (2009).

## 2.5. Explanation of the behaviour of aqueous clay suspensions

Overall behaviour of a colloidal system, such as clay suspension, is governed by various factors such as particle size and shape, physical and chemical properties of the surface, chemical and physical properties of the continuous phase, particle-particle, and particle-continuous phase interactions<sup>22</sup>. The particle-particle interactions can be primarily attributed to Van der Waals attractive forces and electrostatic repulsive forces<sup>22</sup>.

### 2.5.1. van der Waals and electrostatic forces

van der Waals attractive forces are dominant in the particle-particle interactions of clay suspensions. These attractive forces are based on the fact that similar particles are attracted to each other due to the molecular interactions<sup>6</sup>.

The other dominant forces in the clays particle-particle interaction are electrostatic forces<sup>6</sup>. Since particles having similar charges repel each other and clay particles carry a net negative charge, the electrostatic forces between clay particles in the clay suspensions are mostly repulsive<sup>6,22</sup>.

The magnitude of electrostatic forces is influenced by the thickness of a charged atmosphere around the particle called an electric double layer<sup>6,22</sup>. The electric double layer is developed due to the change in the ionic environment of a charged particle. The presence of a charged particle in an electrolyte solution influences the distribution of ions in the environment surrounding the particle<sup>6,22</sup>.

The thickness of electric double layer is called the Debye length ( $\kappa^{-1}$ ) and is defined as:

$$\kappa^{-1} = \left( \frac{\epsilon k_B T}{2e^2 z^2 n_\infty} \right)^{1/2} \quad (2.1)$$

where:

$\kappa^{-1}$ : Debye length, m

$\epsilon$ : dielectric permittivity of medium, C/Vm

$k_B$ : Boltzmann constant ( $1.38 \times 10^{-23}$  J/K)

T: absolute temperature, K

e: elementary charge ( $1.602 \times 10^{-19}$  C)

z: absolute value of valency of the electrolyte

$n_{\infty}$ : ionic number concentration in the bulk solution,  $m^{-3}$

As shown in Equation (2.1), the Debye length is a property of the electrolyte solution<sup>22</sup>. The thickness of the electric double layer of a clay particle suspended in water is a function of particle charge and the concentration and valence of ions in the solution<sup>6,36,76</sup>.

### 2.5.2. DLVO theory

The Derjaguin, Landau, Verwey, and Overbeek (DLVO) theory explains the net interaction of particles in a clay suspension. In this theory, the net force between particles is calculated as the summation of van der Waals attractive forces and the electrostatic repulsion<sup>6,22</sup>:

$$F_{net} = F_R + F_A \quad (2.2)$$

where

$$F_R = \frac{2\pi\epsilon\epsilon_0ka_1a_2}{a_1+a_2} \left[ \frac{2\varphi_1\varphi_2e^{-kh}}{1+e^{-kh}} - \frac{(\varphi_1-\varphi_2)^2e^{-2kh}}{1-e^{-2kh}} \right] \quad (2.3)$$

$$F_A = -\frac{Aa_1a_2}{6h^2(a_1+a_2)} \quad (2.4)$$

where

a: spherical particle radius, m

$\epsilon$ : dielectric permittivity of medium, C/Vm

$\epsilon_0$ : permittivity of vacuum,  $8.854 \times 10^{-12}$  C/Vm

$\kappa^{-1}$ : Debye length, m

$\varphi$ : surface potential (zeta potential), V

h: separation distance, m

When two clay particles with the same sign charges approach one another, an electrostatic repulsion occurs between their electric double layers. When their electric double layers overlaps, the required energy to overcome this repulsion increases. On the other hand, the van der Waals attraction applies to the clay particles when the distance between them decreases<sup>6,22</sup>. Figure 2.3 illustrates the attraction, repulsion, and net interaction energy between two charged particles<sup>22</sup>. The solid lines (U(1), U(2), and U(3)) show the net interaction energy between two particles at three different conditions. Each solid line is the summation of van der Waals attraction energy curve ( $U_A$ ) and the electrostatic repulsion energy curve ( $U_R(1)$ ,  $U_R(2)$ ,  $U_R(3)$ ) at each condition. The peak of curve U(1) represents the energy barrier for flocculation of two particles with a repulsion energy curve of  $U_R(1)$ <sup>22,36,76</sup>. Flocculation occurs when two particles have enough kinetic energy to overcome the energy barrier. The energy barrier is lowered when the thickness of the electric double layer is reduced.

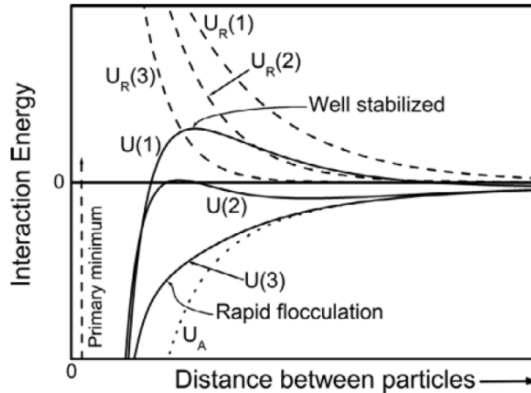


Figure 2.3 Attraction, repulsion, and net interaction energy between two charged particles<sup>22</sup>. Reprinted with permission of John Wiley & Sons, Inc (©2006), Masliyah, J. H. & Bhattacharjee, S. *Electrokinetic and Colloid Transport Phenomena*.

## 2.6. Kaolinite as a model clay

Kaolinite is reported to be one of the most dominant clay minerals in oil sands industry<sup>19,26-33</sup>. Besides being a dominant clay mineral present in oil sands ores, water-based mixtures, and tailings, kaolinite is an important industrial mineral having many applications. Kaolinite is used in different industries such as ceramics production, paper industry, inks and paints manufacturing, and cementation of radioactive waste<sup>75,77,78</sup>. The size reduction of kaolinite particles is important for some applications because the particle size reduction can improve the surface reactivity of kaolinite which is a matter of great interest for these industries<sup>77-79</sup>.

Kaolinite  $[Al_2O_3 \cdot 2SiO_2 \cdot 2H_2O]$  is an aluminium phyllosilicate with a 1:1 crystalline structure<sup>78</sup>. Kaolinite primary particles are thin roughly hexagonal platelets<sup>80</sup>. While the largest dimension of a kaolinite primary particle is between 0.1 to 2  $\mu m$ , its thickness ratio is between 10:1 and 30:1<sup>81</sup>. The basal (face) surfaces of a kaolinite particle carry a permanent negative charge, while the

charge of the edges is dependent upon on pH, as shown in Figure 2.4<sup>81</sup>. Van Olphen<sup>82</sup> suggested that kaolinite particles have positively charge edges, based on the photograph provided by Thiessen<sup>83</sup>. This photograph was an electron-microscopic image of dilute slurry of kaolin particles mixed with negatively charged gold particles. Van Olphen<sup>82</sup> explained that the attachment of negatively-charged gold particles to the edges of kaolin particles confirmed the positive charge on the edges.

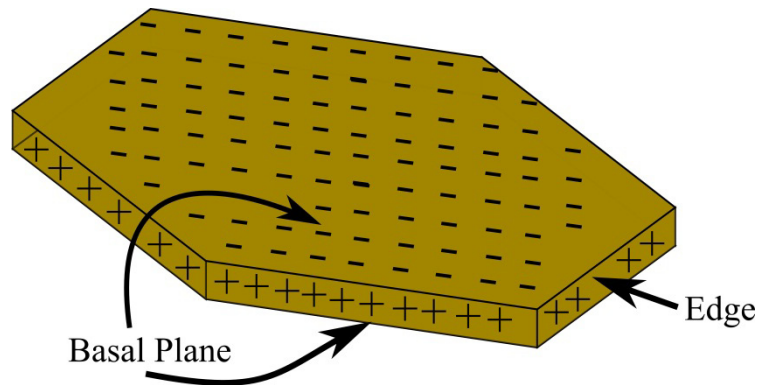


**Figure 2.4 Kaolinite particle charge distribution<sup>81</sup>**

The charged kaolin particles flocculate due to the particle-particle interaction forces. Three main modes of kaolinite particle association are face-to-face, edge-to-edge and edge-to-face, as shown in Figure 2.5<sup>82</sup>. The preferred mode of formation depends on the net particle-particle interaction force, i.e. a balance between van der Waals attraction forces and electrostatic repulsion forces. Therefore, different modes of particle association occur at different continuous phase pH and ion concentration values<sup>81</sup>.

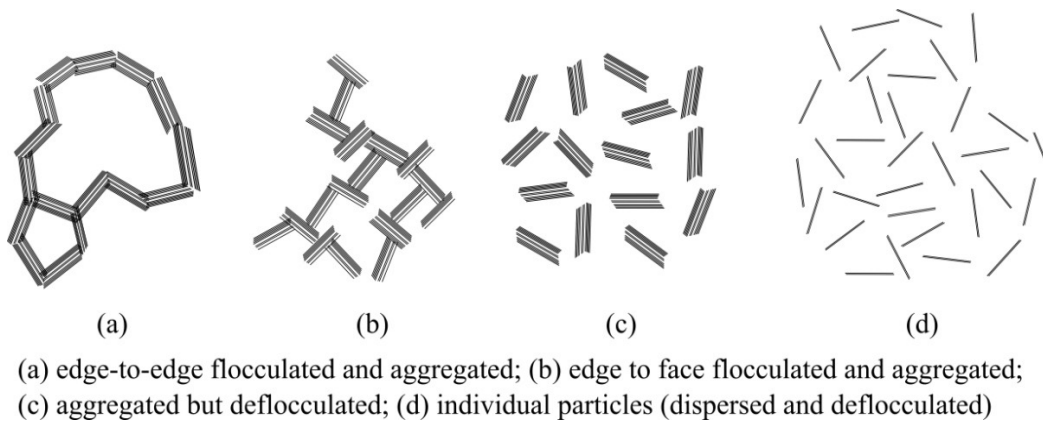


**Figure 2.5 Different particle-particle association modes** <sup>82</sup>

Under acidic conditions ( $\text{pH} < 6.5$ ), the edges of the kaolinite particle become positively charged due to the binding of aluminium (at the edges) and hydrogen ions in the water<sup>80</sup>. This causes an electrostatic attraction between the edges and faces of the kaolinite particles. This leads to an increase in the number face-to-edge association modes. This floc structure is often called the “card-house” structure<sup>80</sup>.

Under alkaline conditions, the edges become neutral or negatively charged by adsorbing  $\text{OH}^-$  ions. Consequently, the net attractive force between edges and faces is not sufficient to maintain the flocs<sup>80,81,84</sup>. Under these conditions, particles deflocculate<sup>80,81,84</sup>. Nasser and James<sup>81</sup> reported that at pH 9 flocs were broken down completely. Michaels and Bolger<sup>80</sup> also mentioned that at high pH ( $\text{pH} > 7$ ), the probability of particle de-flocculation increases rapidly.

At high electrolyte concentrations, the thickness of the electric double layer decreases. Therefore, the van der Waals attractive forces between faces can

overcome the electrostatic repulsion. Under these conditions, the face-to-face association mode is favoured. The floc structure formed in the face-to-face configuration is often referred to as the “card-pack” structure<sup>80,81</sup>.

$\text{Ca}^{2+}$  and  $\text{Mg}^{2+}$  are two dominant ions present in the formation water in the oil sands matrix. Some studies have shown that the presence of cations such as  $\text{Ca}^{2+}$  and  $\text{Mg}^{2+}$  in the water increases the settling rate of clays<sup>21,85</sup>, specifically for kaolinite clays<sup>34</sup>. The adsorption of cations such as  $\text{Ca}^{2+}$ , by neutralizing the electric charges on the particles, decreases the thickness of the electric double layer. Under these conditions, the electrostatic repulsion between particles decreases. The reduction in the repulsive forces leads to strong particle interactions and thus a high degree of flocculation in the slurry<sup>86</sup>. In the present study,  $\text{CaCl}_2 \cdot 2\text{H}_2\text{O}$  is used as a flocculant for this reason.

## **2.7. Sonication**

In the oil sands industry, clay-containing samples are often pretreated prior to the size measurement tests<sup>11</sup>. Sonication, as a dispersion method, is often part of the sample preparation steps for PSD measurements<sup>11,23,24</sup>. In this section, the principles of the ultrasound treatment and the determining parameters of sonication energy are discussed. Then the results of various studies investigating the effect of sonication on clays and non-clays are summarized in Sections 2.6.1 and 2.6.2).

Sonication is the act of applying sound (usually ultrasound) energy to agitate particles in a sample. The frequency ranges from 20 kHz to 10 MHz of the sonic spectrum are called ultrasound<sup>87</sup>.

When sound passes through an elastic medium as a longitudinal wave, it creates an acoustic pressure in the medium,  $P_A$ , which varies with time,  $t$  :

$$P_A = P_{\max} \sin (2\pi vt) \quad (2.5)$$

where,

$v$  : Frequency (Hz)

$P_{\max}$ : Maximum pressure amplitude (Pa)

Therefore, we can define an acoustic intensity,  $I$ , as the energy transmitted through 1  $m^2$  of fluid per unit time:

$$I = \frac{(P_{\max})^2}{2\rho c} \quad (2.6)$$

where,

$\rho$ : Density of the fluid in which the speed of sound is  $c$

$c$ : speed of sound in the sample fluid

The intensity of ultrasound varies with distance,  $d$ , from its source due to the attenuation caused by viscous forces resulting in heat generation in the fluid.

Ultrasound intensity can be defined as:

$$I = I_0 \exp(-2\alpha d) \quad (2.7)$$

where  $\alpha$  is the absorption coefficient which depends on factors such as the viscosity and thermal conductivity of the medium<sup>88</sup>. As the attenuation and dissipation of acoustic energy can be influenced by suspension viscosity it is important to keep the suspension viscosity constant during sonication<sup>88, 89</sup>.

The acoustic energy passing through the medium as sound waves vibrates the molecules of the medium. This vibrational motion changes the distances between molecules. When the ultrasound intensity increases, there is a point at which the molecular structure breaks down in some locations and cavitation bubbles are created in the medium<sup>87,88</sup>. The origin of ultrasound effects is the acoustic cavitation<sup>87</sup>. Cavitation is the process of the formation, growth, and implosive collapse of bubbles in the liquid medium<sup>90-93</sup>.

Sonication of slurries consisting of solid particles in a liquid medium leads to shock-waves and microjets which are caused by cavitation bubble collapse. The impacts of the shock-waves and the production of microjets, along with increased inter-particle collisions, can result in solids particle size reduction<sup>87</sup>. Because of this effect, sonication has been used for many years as a dispersion method.

Ultrasonic treatment can be conducted either by immersing an ultrasonic probe into the suspension (direct sonication) or by dipping the sample container into a liquid bath where ultrasound waves travel through liquid to reach the sample<sup>94</sup>. Delgado and Matijevic<sup>23</sup> showed that the sonication effect is more significant when an ultrasonic probe is used. Sonication with an ultrasonic probe (direct

method) is more effective because it does not have to overcome the barriers bath sonication has to reach the sample. Figure 2.6 shows a sonication probe immersed in a sample. Ultrasound is produced by the piezoelectric ceramic located in the ultrasound horn. The piezoelectric transducer converts electrical energy to mechanical energy<sup>91</sup>. The sonication probe transfers the sound energy from the transducer to the suspension<sup>94</sup>. The probe vibrates at a fixed frequency (usually 20 kHz) but the intensity can be variable<sup>91</sup>.

Bubble breakage results in extreme local heating which leads to an overall bulk heating of the sonicated suspension<sup>87</sup>. Increased temperature of the suspension will cause evaporation, which changes the sample volume as well as sample physical properties (such as viscosity)<sup>89</sup>. On the other hand, it is important to keep suspension viscosity constant during sonication, because the attenuation and dissipation of acoustic energy can be influenced by suspension viscosity<sup>88,95</sup>. A higher suspension viscosity results in the greater attenuation of sonication energy<sup>89</sup>. A cooling bath can be used to avoid temperature increase in the sonicated sample. In the present study, the kaolinite suspension is placed in a jacketed beaker connected to a cooling bath. The circulation of cold liquid between the walls of beaker maintains the suspension temperature constant at/about 20°C.

The total amount of energy delivered to the sample is a function of sonication power and sonication time.

$$E = P * t \tag{2.8}$$

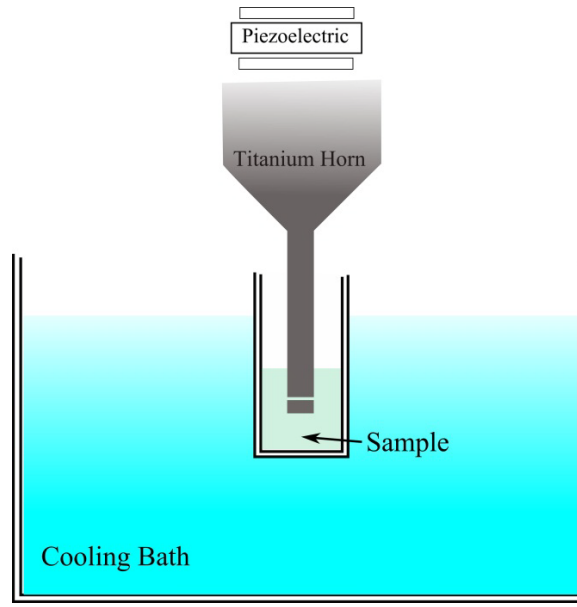


**Figure 2.6 Sonication probe immersed in a sample <sup>91</sup>**

Therefore, the effect of sonication on two samples that are sonicated with the same sonication power for different time periods will not be the same<sup>89</sup>. Sonication time and power, as instrument parameters, determine the amount of energy delivered to the sample. On the other hand, sample volume and solids concentration, as system parameters, determine the response of the sample to the delivered acoustic energy<sup>89</sup>.

Assuming constant sample volumes, a sample with a higher solids concentration will be more affected by the higher frequency of particle collisions than the more dilute sample will. Increased collision frequency can lead to agglomeration of particles or breakage of aggregates<sup>89</sup>. In this study samples with three different solids concentration ( $c=10, 20, 40$  g/L) have been investigated to study the influence of solids concentration on the sonication effect on the kaolinite PSD.

The impact of sample volume on the disruptive effect of sonication can be measured as energy density. Energy density is defined as the amount of delivered energy per unit of sample volume (J/mL). This means that the disruptive effect of sonication is greater for samples with smaller volumes<sup>89</sup>. The sample volume is kept constant at 140 mL for all samples tested in the present study.

### **2.7.1. Effect of sonication on the particle size of solids**

The effect of ultrasound treatment on the particle size of different materials (clays and non-clays) has been studied for years<sup>24,75,95-100</sup>. Since the focus of the current study is the effect of sonication on the particle size of kaolinite as an analog of the clays found in the oil sands, a few examples of studies on non-clay materials are explained. Studies that analyzed the particle size reduction of clays due to sonication are then described.

Hassanjani-Roshan et al<sup>96</sup> showed that ultrasound treatment dispersed Titania (TiO<sub>2</sub>) nano-particles. They explained that the particle size reduction caused by sonication results from the shock-waves created by acoustic cavitation. Desroches et al<sup>24</sup> used sonication, pH adjustment, and dispersant addition to obtain primary particle size of CeO<sub>2</sub> powder suspensions. They reported that sonication decreases the size of particles by enhancing particle de-agglomeration<sup>24</sup>. Keenan et al<sup>95</sup> studied the effect of sonication on the size and rheology of fruit smoothies. They reported that sonication caused a reduction in the particle size as well as a decrease in viscosity<sup>95</sup>.

### 2.7.2. Effect of sonication on the particle size of clays

Recently, various researches have studied sonication as a technique for particle size reduction of clay materials<sup>77,97,98,100-109</sup>. They observed that sonication produces delamination and particle size reduction of the clay platelet particles<sup>77,97,98,100-109</sup>. Delamination decreases the particle thickness and increases the number of particles and thus the specific surface area. In fact, sonication is part of an accepted delamination method for kaolinite clays<sup>75</sup>.

Table 2.1 summarizes the clay types and the sonication time and intensity used by various studies investigating the effect of sonication on the particle size of different clays. The results of these studies are as follows:

- 1) Lapidés and Yariv<sup>97</sup>, Pacula et al<sup>98</sup>, and Poli et al<sup>104</sup> studied the effect of ultrasound treatment on the size and morphology of montmorillonite clays. Lapidés and Yariv<sup>97</sup> studied the effect of ultrasound treatment on dilute and concentrated suspensions of Wyoming bentonite (Na-montmorillonite). Sonication resulted in production of small (submicron) particles in the dilute suspension. In the concentrated sample, the volume percentage of submicron particles decreased from 90% to 10%, while the population of larger particles (1-7  $\mu\text{m}$ ) increased<sup>97</sup>. For the dilute samples de-aggregation and delamination of clay particles were reported<sup>97</sup>. In the other two studies sonication resulted in a decrease in the size and volume percentage of larger particles. At the same time, the population of the smallest particles increased<sup>98,104</sup>. They suggested that sonication caused

disruption of clay aggregates and delamination of clay particles. Furthermore, Poli et al (2008) reported that by increasing the sonication time the size reduction increases gradually <sup>104</sup>.

**Table 2.1 Summary of literature on the sonication of clay materials**

Refs	Clay type	Sonication Power	Sonication time	Results
Lapides and Yariv <sup>97</sup>	Wyoming bentonite	Total Energy: 13 to 130 kJ	-	(1)
Pacula et al <sup>98</sup>	montmorillonite	100 W	100 minutes	(1)
Poli et al <sup>104</sup>	montmorillonite	70 W and 35 W	5 to 60 minutes	(1)
Perez-Maqueda et al <sup>100</sup>	vermiculite	750W	10 to 100 hours	(2)
Perez-Rodriguez et al <sup>101</sup>	vermiculite	600W	10 to 150 hours	(2)
Wiewiora et al <sup>102</sup>	vermiculite	600W	10 to 150 hours	(2)
Perez-Maqueda et al <sup>105</sup>	talc	600W	10 to 100 hours	(3)
Perez-Maqueda et al <sup>106,110</sup>	Muscovite and biotite	750W	10 to 100 hours	(4)
Perez-Rodriguez et al <sup>107</sup>	mica	750 W	10 to 100 hours	(4)
Franco et al <sup>108</sup>	dickite	750 W	10 and 20 hours	(5)
Franco et al <sup>77</sup>	kaolinite	600 and 750 W	10 and 20 hours	(6)
Perez-Maqueda et al <sup>78</sup>	kaolinite	600 W	5 to 100 hours	(7)

- 2) Perez-Maqueda et al<sup>100</sup> reported that two populations of micron-sized and submicron particles appeared in the vermiculite samples after sonication for 10 to 40 hours. Their results showed that while the size and volume percentage of larger particles decreased with sonication time, the volume percentage of smallest particles increased. They also found that the crystallite size of vermiculite particles reduces significantly in the first stage of sonication (10 hours) while from 10 to 30 hours the vermiculite plates' size remain unchanged (delamination of clays was still happening.) Their study demonstrated that longer sonication times promoted flocculation and aggregation of vermiculite particles. They added that even after 100 hours of ultrasound treatment vermiculite clay particles retained their crystal structure<sup>100</sup>. Perez-Rodriguez et al<sup>101</sup> and Wiewiora et al<sup>102</sup> completed previous studies with examining the effect of 10 to 150 hours of sonication on the vermiculite clays PSD. Their results confirmed delamination and degradation of clay particles as well as the primary particles size reduction, while the crystalline structure of vermiculite did not damage<sup>101,102</sup>.
- 3) Perez-Maqueda et al<sup>105</sup> indicated in their study of talc particles that sonication caused both delamination and plate diameter reduction. The crystalline structure of the parent mineral did not change. The volume percentage of the smallest particles increased while the volume percentage of the largest ones decreased. For prolonged sonication times re-aggregation of particles was detected<sup>105</sup>.

- 4) Perez-Maqueda et al<sup>106,110</sup>, Perez-Rodriguez et al<sup>107</sup> examined the effect of sonication on different clay materials in the mica group. They investigated the ultrasound treatment effect on muscovite, biotite, and phlogopite<sup>106,107,110</sup>. Their results showed that sonicated samples had two kinds of particles: micron-sized and submicron particles. The volume percentage of micron-sized particles decreases while the volume percentage of submicron particles increases after sonication. A gradual particle size reduction occurred when the sonication time was increased. A significant delamination and a reduction in the plate diameter in the lateral dimension were detected. Even after 100 hours of sonication the crystalline structure was not damaged and the sonicated particles retained the plate-like shape characteristic of micas. Sonicated samples (even after 100 hours) did not contain any aggregates<sup>106,107</sup>.
- 5) Franco et al<sup>108</sup> indicated in their study that sonication completely exfoliates the book-like piles of dickite particles. They reported that in addition to the exfoliation of flocs lateral breakage of particles happened after sonication<sup>108</sup>. Ultrasound treatment did not cause any changes in the crystalline structure of dickite<sup>108</sup>. Sonication caused a decrease in the volume percentage and the size of the largest particles from 12  $\mu\text{m}$  to 3.4  $\mu\text{m}$  and 3  $\mu\text{m}$  after 10 and 20 hours treatments, respectively. The population of smallest particles increased significantly, while their modal size increased slightly from 0.4  $\mu\text{m}$  to 0.5  $\mu\text{m}$ <sup>108</sup>. The particle size distribution of untreated sample showed that dickite particles were in the

size range of 0.2 to 70  $\mu\text{m}$ . The sonicated samples PSD showed no particles larger than 30  $\mu\text{m}$ <sup>108</sup>.

- 6) Franco et al<sup>77</sup> suggested that sonication is an effective method for particle size reduction of kaolinite clays. They expressed that sonication reduces the particle size of kaolinite to the submicron range without any major changes in the crystalline structure and lamellar morphology of these clay particles<sup>77</sup>. They also showed that different variables can control the effect of sonication on the size reduction of kaolinite clays. Sample volume, sonication time and power were reported as controlling parameters in their study<sup>77</sup>. They reported that sonication significantly reduces the particle size of kaolinite clay by delamination and lateral breaking of clay aggregates which result in a reduction in other particle size dimension. They suggest that the size reduction by sonication can be controlled by three variables: sonication time, power, and the sample volume. They studied the effect of sample volume, sonication time, and sonication power on two kaolinite samples<sup>77</sup>. Two samples had same proportion of mass of kaolinite to the volume of de-ionized water in their study<sup>77</sup>. The particle size analyses were conducted using a low-angle laser light scattering (Malvern Mastersizer) which estimates the percentage of particle volume vs particle size<sup>77</sup>. Samples were continuously sonicated from 10 to 75 hours with two different sonicators of output 700 and 600 W<sup>77</sup>. The particle size distributions of both samples were the same before sonication, and each had particles in the size range of 0.1 to 30  $\mu\text{m}$ . In

each sample there were three populations of particles with maxima at 0.5, ~1.8, and 9.9  $\mu\text{m}$ <sup>77</sup>. Sonication decreased the population of ~1.8 and 9.9  $\mu\text{m}$  while the proportion of the smallest particles (0.5  $\mu\text{m}$ ) increases significantly. Higher sonication power (700 W) and lower sample volume can lead to a reduction in the size of smallest particles and produce kaolinite particles with sizes smaller than 0.5  $\mu\text{m}$ . Results from a scanning electron micrograph (SEM) and a transmission electron micrograph (TEM) of the non-sonicated and sonicated samples confirmed the results obtain by Malvern Mastersizer<sup>77</sup>. In the conditions of lower sonication power (600 W) and higher sample volume the effect of sonication is less comparing to the other conditions<sup>77</sup>. Their results also showed that long sonication time results in appearance of large size particles (10.4  $\mu\text{m}$  and 17.5  $\mu\text{m}$ ). They suggested that prolonged sonication of kaolinite can lead to agglomeration of some particles that were activated by acoustic energy<sup>77</sup>. Delgado and Matiyevic<sup>23</sup> also confirmed that prolonged sonication may promote aggregation of colloidal particles<sup>23</sup>. Franco et al (2004) showed that when sample is sonicated with the sonicator with output power of 600 W, the effect of sonication on the particle size of kaolinite is less comparing to sonicator with 700W output power. Size reduction occurs in both conditions but the lower power sonicator cannot decrease the size of smallest particles while the higher power sonicator can produce particles smaller than 0.5  $\mu\text{m}$ <sup>77</sup>.

7) Perez-Maqueda et al<sup>78</sup> confirmed Franco et al<sup>77</sup> results by comparing the effect of sonication on the particle size of kaolinite and pyrophyllite<sup>78</sup>. Non-sonicated sample of both kaolinite and pyrophyllite contains wide particle size ranges from submicron to the flocs and aggregates of particles of several tens of microns. After 40 hour sonication with a sonicator of 600 W output significant size reduction in all directions occurred for both samples. Sonication caused delamination and breakage of the plates which led to narrower particle size distributions for both samples<sup>78</sup>. They reported that sonication yielded to production of plate-like particles having the same shape and crystalline structure of the original clays<sup>78</sup>.

As the results of the above mentioned studies indicate sonication resulted in a reduction of particle size of different clays. Most of these studies investigated the influence of long periods of sonication (up to 150 hours). In this study the effect of 10 seconds to 60 minutes of sonication on the kaolinite PSD has been investigated, (Chapter 6). Kaolinite clay has been chosen as an analog of the clays found in the oil sands. Furthermore, the effect of sonication amplitude has been studied (Section 6.4). In all the studies mentioned above, clay suspensions are prepared by adding the clays powder to de-ionized water i.e. natural pH values and no flocculant added. In the present study, the influence of sonication on the kaolinite suspensions with different pH values and with the presence of  $\text{Ca}^{2+}$  ions, as flocculant, has been studied (Sections 6.5 and 6.6). Finally, the sonication effect on a sample of industrial clay-containing tailings is discussed in Section 6.7.

### **3. Experimental method**

#### **3.1. Materials**

##### **3.1.1. Kaolinite clay**

The kaolinite clay used in this study was obtained from Dry Branch Kaolin Clay Company, Georgia, USA. All the kaolinite powder used in this study to make suspensions for experimental tests was collected from a single bag in attempt to minimize possible inconsistencies in the experimental results because of differences in the source clay.

##### **3.1.2. De-ionized water**

All samples were prepared using de-ionized water since tap water contains different mineral ions which would affect flocc/aggregate size. Freshly de-ionized water collected from “Elix Advantage Water Purification System” (Millipore SAS, France) was used.

##### **3.1.3. Calcium chloride**

Calcium chloride,  $\text{CaCl}_2$ , (0.3 M solution) was added as a flocculant to selected kaolinite suspensions.  $\text{Ca}^{2+}$  is one of the dominant ions present in oil sands matrix. The addition of divalent cations such as  $\text{Ca}^{2+}$  to the clay suspensions result in aggregation of clay particles<sup>111</sup>. As previously discussed in Section 2.5, the presence of calcium ions in the clay suspensions enhances the attractive forces between the clay particles due to the associated decrease of the surface charge and collapse of the electric double layer<sup>111</sup>.

#### **3.1.4. Sodium hydroxide**

Sodium hydroxide, NaOH (0.25 M solution) has been used for pH adjustment of selected kaolinite suspensions.

#### **3.1.5. FPIA Consumables**

##### ***Sheath liquid***

The FPIA uses sheath liquid in the Sheath-Flow cell to press the sample flow in the way that the largest surface of each particle in the sample faces the camera <sup>112</sup>.

The sheath liquid is an electrolytic sheath solution composed of sodium chloride (7.1 g/L), surfactant (0.6 g/l), Tris buffer (2.0 g/l), and EDTA-2K (0.2 g/l).

##### ***Polymer microspheres***

Uniform size polystyrene latex microspheres (Model 5200A) from Duke Scientific Corporation with 2.0  $\mu\text{m}$  in diameter have been used for calibration purposes (focus adjustment step; see Section 3.3.2). The polystyrene latexes have been previously used by others for calibration of size measurement instruments <sup>23</sup>.

The polystyrene latex particles are dispersed in the sheath fluid with the 10 wt% concentration. These latex microspheres have a density of 1.05  $\text{g}/\text{cm}^3$  and refractive index of 1.59<sup>112</sup>.

#### **3.1.6. Industrial oil sand tailings**

Samples of industrial oil sand tailings used to study the effect of sonication on “real” clay-containing suspension. The results of the experiments conducted are described in Section 6.7 of the present study. These industrial tailings samples

were kindly provided by Andrea Sedgwick, Sr. Engineer Tailings Processing at Total E&P Canada. Tailings materials were produced with the Batch Extraction Unit (BEU) methodology<sup>113</sup>. Sample preparation procedure of the tailings raw slurry is explained in Section 3.3.7. Considering the FPIA-3000 limitations on particle size and concentration, particles larger than 75 microns were removed by sieving the tailings prior to measurements. In addition, by using RHS beads (Reusable Hydrocarbon Sorbent), much of the bitumen in the tailings was also removed. The sieved, bead treated samples used in this study are prepared by my colleague in pipeline transport process group, Jessie Smith. The results of Dean Stark analysis for sieved, bead treated samples are provided in Table 6.5 and 6.6 in Section 6.7. The Dean Stark analysis is done by Jessie Smith as a part of her MSc thesis<sup>114</sup>. The particle size distribution for the sieved, bead treated tailings sample diluted with the filtrate water ( $c=10$  g/L) is shown in Figure 3.1.

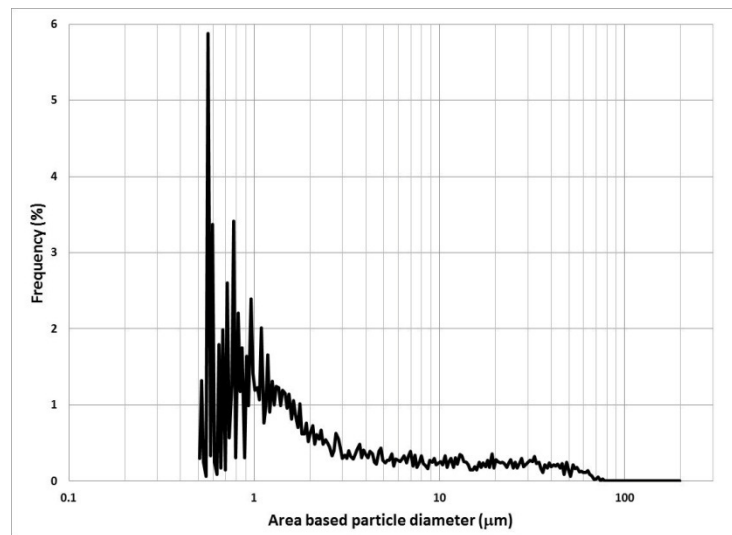


**Figure 3.1 Particle size distribution of sieved, bead treated tailings sample measured by FPIA:  $c=10$  g/L**

## 3.2. Equipment

### 3.2.1. Sonication test system

Direct sonication was performed by using a Misonix Sonicator-4000 which is shown in Figure 3.2<sup>115</sup>. Sonicator-4000 has a 20 KHz converter, a high intensity tapered probe and a maximum power output of 600 W. The standard tapered titanium probe is ½ inch in diameter and produces maximum amplitude of 120  $\mu\text{m}$ <sup>115</sup>. During all the experiments, the probe tip is directly immersed about 1.5 ~ 2 cm below the sample surface in the jacketed beaker.

Figure 3.3 shows different parameters which appear on the Sonicator-4000's screen during each test. The output amplitude can be adjusted between 1%-100% before each test and the sonication time can be controlled by the start and pause buttons. The values for sonication power (Watts) and energy (Joules) are displayed during each test.

The principles of operation of probe sonicator were explained in Section 2.6 of this work. In Section 2.6, sonication time and sonication power were introduced as the two controlling parameters which dictate the total amount of acoustic energy. It is important to note that operation of the Sonicator-4000 in “manual” mode allows the user to set the amplitude of sonication at any value between 1-100%. As such, the sonication power cannot be adjusted and thus the relationship and difference between sonication power and amplitude needs further explanation.

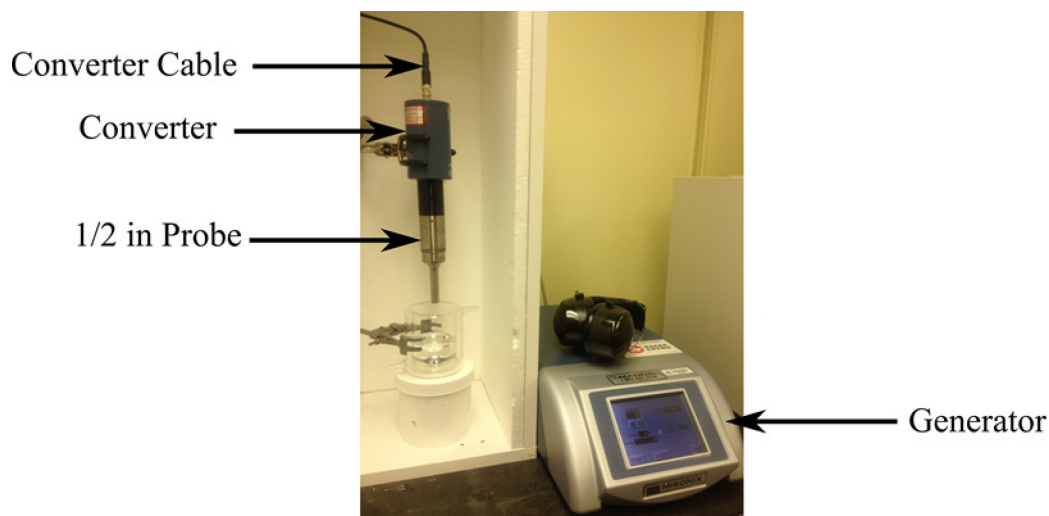


**Figure 3.2. Misonix Sonicator-4000 and its components<sup>115</sup>**

Sonication power (Watts) is the amount of electrical energy that is being delivered to the convertor. The value of sonication power can be read on the Sonicator-4000 LCD (Figure 3.3) during each test. The Convertor transforms the electrical energy to mechanical energy by means of a piezoelectric. This mechanical energy causes the probe to move up and down. The amplitude represents the distance of one movement up and down. The amplitude is manually controlled by the user changing the settings on the Sonicator's touchscreen (see Figure 3.3)<sup>116</sup>. When the output amplitude is set at 100%, the distance of probe movement will be 120  $\mu\text{m}$ .

While the amplitude and intensity have a direct relationship, their relationship with sonication power varies with sample characteristics. For example, when the output amplitude is set at 100% for two samples having different viscosities, the intensity for both samples will be the same, but the sonication power will be different. For the sample with the higher viscosity, the sonicator needs more power to move the probe over the same distance (keeping the amplitude at 100%).

Therefore, the sonication power will be greater for the sample with the higher viscosity<sup>116</sup>.



**Figure 3.3. View of the Sonicator-4000's screen**

As explained in Section 2.6, high power sonication causes an increase in the sample temperature. Sample temperature is one of the parameter that can affect the total amount of delivered energy. Therefore, in this work the sample temperature was kept constant at 20 °C during sonication. The cooling system required for this purpose is composed of a cylindrical jacketed beaker connected to a refrigerated circulator. This system has been used in other studies as well<sup>105,108</sup>. Sample temperature was checked with a thermometer to ensure that it remained at/near 20 °C during sonication.

The cooling system of this work was comprised of the following components:

1. The digital (Model 3016 D) Fisher Scientific Isotemp Refrigerated Circulator with a temperature range of -20 to +200°C. The circulator

reservoir was filled with a 50/50 mixture, by volume, of laboratory grade ethylene glycol and filtered tap water.

2. Kontes Reaction-Jacketed beaker: Two hose connections, 250 mL capacity, 47mm I.D. x 73mm inner height; 80mm O.D. x 85mm outer height, Figure 3.3.
3. Fisherbrand Pure Natural Rubber Tubing: Amber, Thick Wall, I.D. x O.D. 9.5 x 15.9 mm, Wall thickness 3.2 mm.
4. Fisher Scientific Traceable Kangaroo Thermometer which is shown in the photograph of Figure 3.4.



**Figure 3.4. Cooling system components**

### **3.2.2. Sysmex Flow Particle Image Analyzer-3000 (FPIA)**

Particle size analyses were conducted using a Sysmex FPIA-3000. The FPIA (Malvern Instruments Ltd., UK) provides visualization and characterization of the particle size and shape, using an automated imaging technique<sup>112</sup>. The FPIA can measure particles in the size range of 0.8–300  $\mu\text{m}$ <sup>112</sup>.

The sample is fed into the sample chamber of the FPIA, which is equipped with an ultrasonic probe and a mixing rotor, both of which can be used for sample dispersion. The sample is passed through the measurement cell (Sheath-Flow cell) by means of a jet nozzle<sup>112</sup>. In the Sheath-Flow cell, sheath liquid flows parallel to the sample flow, pressing it in a manner so that the sample flow becomes sandwiched and flat. This ensures all particles in the sample lay in the same focusing plane and are oriented with their largest surface facing the camera<sup>112</sup>.

Next, a strobe light illuminates the particles as they pass through the transparent measurement cell, and their images are captured by a charge coupled device (CCD) camera<sup>112</sup>. The CCD camera captures 60 images per second. The generated images of the individual particles are next automatically analyzed by the instrument's image analysis software<sup>112</sup>.

The image analysis software uses a mathematical grey-scale calculation method. In this method, a threshold value is applied to separate the image of each particle from the background. In this way, the edges of each particle are defined and with these data the particle image analyzer is able to calculate the desired parameters, e.g. actual area and perimeter of the particles, their length, width, and maximum

distance, as well as other morphological parameters like size and shape distributions. The particle size and shape information is generated from analysis of up to 360,000 particles in the sample. The results, such as size distribution and particle shape distribution, are displayed in histograms. In addition, images of all particles are stored as part of the data file to provide further visual understanding of the measurement data.

The FPIA has different modes of detection which differ primarily by magnification. The particle size ranges of each measuring mode are described in Table 3.1. When the standard primary lens (10x) is used, the low-power field mode (LPF) allows for analysis of coarse particles in the size range of 6 to 160  $\mu\text{m}$ . The high-power field (HPF) mode allows analysis of fine particles in the size range of 1.5 to 40  $\mu\text{m}$ .

**Table 3.1. Particle size range for each FPIA-3000 measuring mode** <sup>112</sup>

<b>Measuring mode</b>	<b>High power field- HPF (2x secondary lens)</b>	<b>Low power field-LPF (0.5x secondary lens)</b>
High-mag unit: Primary lens = 20x	Particle size range: 0.8–20 $\mu\text{m}$	Particle size range: 4–80 $\mu\text{m}$
Standard unit: Primary lens = 10x	Particle size range: 1.5–40 $\mu\text{m}$	Particle size range: 8–160 $\mu\text{m}$
Low-mag unit: Primary lens = 5x	Particle size range: 3–80 $\mu\text{m}$	Particle size range: 16–300 $\mu\text{m}$

The FPIA mixer speed can be adjusted from 50 to 750 RPM. Both low and high speeds of mixing motor may cause problems in the FPIA performance or the accuracy of measurements. Low speed mixing can result in blockage inside the sample chamber, nozzle or sheath-flow cell which will cause malfunction of the FPIA instrument. High speed mixing may change the size and/or structure of the kaolinite aggregates.

All the FPIA measurements of this study have been done with 10x objective lens and High Power Field (HPF) magnification mode. The internal sonication of the FPIA has been turned off and the mixer speed has been set at 300 rpm for all the samples.

The FPIA software provides particle size frequency tables for each sample. In the provided particle size frequency table the measurement range is divided to 226 segments. As an example, Table 3.2 shows the first and last rows of the particle size frequency table for a sample of 10 g/L kaolinite in water. The first column of this table presents the size range of each segment and the second column presents the number of particles detected by the FPIA camera in the size range of each segment. The third column shows the *frequency percentage* of each segment, which is calculated as:

$$\text{Freq.(\%)} = 100 \times \frac{\text{Number of particles in each segment}}{\text{Total number of detected particles in the sample}} \quad (4.1)$$

The fourth column of the particle size frequency table indicates *cumulative percentage* of particles detected in each segment. The cumulative percentage of

particles is defined as the percentage of particles finer than the size range of each segment.

CE Diameter(II)			
Range	Num.	Freq.(%)	Cuml.(%)
0.500->0.513	75	0.17	0.17
0.513->0.527	312	0.70	0.87
0.527->0.541	35	0.08	0.95
0.541->0.556	25	0.06	1.00
0.556->0.571	851	1.91	2.91
0.571->0.586	93	0.21	3.12
0.586->0.602	625	1.40	4.52
0.602->0.618	67	0.15	4.67
0.618->0.635	29	0.07	4.74
0.635->0.652	410	0.92	5.66
0.652->0.669	55	0.12	5.78
0.669->0.687	402	0.90	6.68
0.687->0.706	69	0.15	6.83
0.706->0.725	533	1.20	8.03
0.725->0.744	153	0.34	8.37
0.744->0.764	279	0.63	9.00
0.764->0.785	572	1.28	10.28
0.785->0.806	76	0.17	10.45
0.806->0.827	459	1.03	11.48
0.827->0.850	341	0.76	12.24
0.850->0.872	399	0.89	13.14
0.872->0.896	87	0.19	13.33
0.896->0.920	382	0.86	14.19
0.920->0.945	284	0.64	14.82
0.945->0.970	461	1.03	15.86
0.970->0.996	404	0.91	16.76
0.996->1.023	294	0.66	17.42
1.023->1.050	348	0.78	18.20
1.050->1.079	367	0.82	19.03
1.079->1.108	597	1.34	20.37
1.108->1.137	334	0.75	21.11
1.137->1.168	320	0.72	21.83
1.168->1.199	506	1.13	22.97
1.199->1.231	305	0.68	23.65

CE Diameter(II)			
Range	Num.	Freq.(%)	Cuml.(%)
81.20->83.38	0	0.00	100.00
83.38->85.62	0	0.00	100.00
85.62->87.92	0	0.00	100.00
87.92->90.29	0	0.00	100.00
90.29->92.71	0	0.00	100.00
92.71->95.20	0	0.00	100.00
95.20->97.76	0	0.00	100.00
97.76->100.4	0	0.00	100.00
100.4->103.1	0	0.00	100.00
103.1->105.9	0	0.00	100.00
105.9->108.7	0	0.00	100.00
108.7->111.6	0	0.00	100.00
111.6->114.6	0	0.00	100.00
114.6->117.7	0	0.00	100.00
117.7->120.9	0	0.00	100.00
120.9->124.1	0	0.00	100.00
124.1->127.4	0	0.00	100.00
127.4->130.9	0	0.00	100.00
130.9->134.4	0	0.00	100.00
134.4->138.0	0	0.00	100.00
138.0->141.7	0	0.00	100.00
141.7->145.5	0	0.00	100.00
145.5->149.4	0	0.00	100.00
149.4->153.4	0	0.00	100.00
153.4->157.5	0	0.00	100.00
157.5->161.8	0	0.00	100.00
161.8->166.1	0	0.00	100.00
166.1->170.6	0	0.00	100.00
170.6->175.2	0	0.00	100.00
175.2->179.9	0	0.00	100.00
179.9->184.7	0	0.00	100.00
184.7->189.7	0	0.00	100.00
189.7->194.8	0	0.00	100.00
194.8->200.0	0	0.00	100.00

Table 3.2 Particle size frequency table produced by FPIA software

The particle size calculated by the FPIA is an *Area based particle diameter*. The FPIA detects each particle, captures a 2D image of that particle and calculates the actual area of the particle. The FPIA then provides the diameter of a circle with

the same area as the particle (i.e. the area based particle diameter is called CE Diameter in the FPIA software).

The area based particle diameter is calculated as:

$$d = 2 \times \left( \frac{A_p}{\pi} \right)^{1/2}$$

(4.2)

Where:

d: Area based particle diameter

$A_p$ : actual area of the detected particle

In this study, we used the number-weighted diameter (CE Diameter (N)). All particles are weighted equally in the particle size distribution.

To draw each PSD graph in the present study, first the mid-point of each size region in frequency tables (provided by the FPIA software) is calculated as:

$$\frac{1}{2} \times (x_1 + x_2) \text{ for the size range } x_1 \rightarrow x_2$$

These mid-points are used as the X-axis values of the PSD graphs. For each point on the X-axis the corresponding Y-axis value is the frequency percentage of particles as calculated using Equation 4.1, which can be derived from the third column of the size frequency table (from the FPIA measurements).

### 3.2.3. Application of the FPIA in literature

The FPIA has been recently used for measurements of size and morphological parameters of different materials. Several researchers in food process science, microbiology and health science utilized the FPIA to measure size and shape of different biomaterials and carbohydrates. Red cells <sup>117</sup>, DNA nanoparticles <sup>118</sup>, protein aggregates <sup>119–121</sup>, bacteria <sup>122</sup>, pollen species <sup>123</sup>, viral suspensions <sup>124</sup>, *Lipomyces lipofer* <sup>125</sup>, Maltodextrins and cyclic dextrin <sup>126</sup> are examples of these materials examined by the FPIA.

The FPIA has been used to study size and shape parameters of inorganic materials as well. Komabayashi et al (2008a&b, 2009) used Sysmex-FPIA3000 in their studies of particle size and shape analysis of calcium hydroxide, mineral trioxide aggregates (MTA) and Portland cement. The particle sizes reported in these articles range from 0.5 to 40  $\mu\text{m}$  <sup>127–129</sup>. Krause et al (2009) assessed the shape of carbon nanotubes agglomerates in aqueous surfactant dispersions using the Sysmex-FPIA. The results of the particle size distribution showed that particle sizes range from 1.6  $\mu\text{m}$  to 20  $\mu\text{m}$  <sup>130</sup>. Tanaka et al (2008) utilized Sysmex-FPIA-2100 to determine the shape of toner powder particles. Toner powder is a polymer composite consisting of polyester resin, carbon black and wax. The mean particle diameter of the toner varied within the range 5.5–6.5  $\mu\text{m}$  <sup>131</sup>. In a study by Arnold et al (2003) the particle size distribution of crystallized lithium iron phosphate before and after a heat treatment in nitrogen was determined with a Sysmex-FPIA2100 <sup>132</sup>. The shape of LTCC powder, which is mixture of glass and alumina

powders, have been measured by the FPIA in two studies by Besendorfer and Roosen (2008) and Rauscher and Roosen (2009) <sup>133,134</sup>. Brugger et al (2007) measured the droplet size of emulsifier microgels using the FPIA <sup>135</sup>.

Although the FPIA has been used by in numerous studies on the size and shape of organic and inorganic materials, the only work available in the literature which shows the use of the FPIA for size and shape study of clay minerals is done by Lape et al (2004). They used the Sysmex-FPIA 2100 to measure the size distribution of exfoliated muscovite mica <sup>136</sup>.

While dilute clay slurries, being an aqueous suspension of particles with specific gravity of less than 3, meet some important the FPIA-3000 constraints, there is some concern about the instrument particle size limit. The FPIA manual indicates that the size range of particles measured by the FPIA should be 0.8 to 300  $\mu\text{m}$ .

Clay slurries contain particle size ranges of the colloidal domain. In complete dispersed conditions the particle sizes are of the order of  $10^{-1} \mu\text{m}$  <sup>22</sup>. Clay particles flocculate under most circumstances and can grow in size to as much as “several hundred microns or larger” <sup>137</sup> and become too large to be tested by the FPIA-3000. Therefore, the instrument should be used cautiously for flocculated clay slurries. This is more important for polymer-induced flocculated clay slurries.

### **3.3. Procedures**

#### **3.3.1. Sample preparation**

The sample preparation procedure steps for the kaolinite in water mixtures are listed below:

1. Turn on the cooling bath and set the bath liquid temperature at 10 °C.
2. Weigh the proper amount of kaolinite clay powder and pour it into the jacketed beaker.
3. Add 140 mL of distilled water to the kaolinite powder
4. Place the beaker under the mixer and adjust the height of the shaft so that the distance between the bottom of the beaker to the bottom of the impeller is equal to the diameter of impeller
5. Set the mixer speed at 500 RPM and mix the sample for 30 minutes.
6. Make the FPIA ready for measurements; see Section 3.3.2.

#### **3.3.2. FPIA tests**

The FPIA needs to be prepared for measurements before each series of tests. The background check and the auto focus (calibration) must be completed before the FPIA is ready to make measurements.

In the background check, the FPIA software checks the initial background of images and shows the number of particles detected before any sample is injected into the instrument. The FPIA manual mentions that the maximum number of particles detected is 10. If the number of particles detected is larger than 10, the

background check should be repeated. After running the background check, the FPIA software will define the initial background as the original background for the upcoming tests. It is recommended that users run the background check before each series of measurements.

The calibration step (the focus adjustment) should be done using the polystyrene latex microspheres ( $d=2.0\ \mu\text{m}$ ). The FPIA software runs the auto focus adjustment automatically. If there is a problem with auto focus adjustments, the focus adjustment should be done manually.

The preparation steps for the FPIA measurements are listed below:

1. Check all the connections of the tubes to the FPIA apparatus, the sheath liquid container, and the liquid waste container.
2. Turn on the FPIA and open the FPIA software on the connected computer.
3. Run the “Background Check”.
4. Run the “Auto focus”.
5. Add 5 mL of fresh diluted polystyrene latex microspheres suspension.
6. Adjust the testing parameters such as sample name, magnification mode (set at HPF), RPM (set at 300), and sonication power (set at “not applied”).
7. Use the large-tip opening transfer pipette and cut off the tip of the pipette, as shown in Figure 3.5.
8. Take first sample for size measurement after it has been mixed for 30 minutes. Use the open tip pipette.

9. While the FPIA is running the measurement for the first sample, quickly place the jacketed beaker under the sonicator probe while it is still connected to the bath with two tubes.



**Figure 3.5. Large-tip opening transfer pipette (13-711-5B Fisher Scientific)**

### **3.3.3. Sonication tests**

After samples are mixed for 30 minutes and the FPIA is ready for tests, start the sonication step of the tests as follows:

1. Put the sonication probe into the sample. The depth of the probe tip should be the same for all experiments (1.5~2 cm). The probe should be exactly at the center of the beaker.
2. Put the thermometer into the sample. Turn on the thermometer and record the sample temperature at the beginning and during the sonication period.

Use tape to attach the thermometer to the sonication probe. In this way the thermometer location is always the same for all samples (see Figure 3.3).

3. Turn on the sonicator and set the amplitude (100%, 75%, or 50%) but do not start sonication.
4. Make the FPIA ready for measurement (Section 3.3.2).
5. Push the start button of the sonicator and be ready to take samples 10 seconds after starting the sonicator.
6. Use the open tip pipette to obtain a sample. Pour the sample into the FPIA chamber.
7. Take samples at 5, 10, 20, 30, 40, 50 and 60 minutes of sonication.
8. During the 60 minutes of sonication, monitor the sample temperature and ensure it is about 20°C. If necessary, alter the bath liquid temperature to keep the sample temperature at/near 20°C.

#### **3.3.4. Mastersizer tests**

The particle size distributions of two samples before and after sonication were analyzed using a Malvern Mastersizer 2000. Malvern Mastersizer-2000 uses the laser diffraction technique. During measurements, particles pass through the laser beam and scatter light at different angles and intensities depending on their size. Lower intensity light will be scattered by smaller particles at wide angle while larger particles scatter the light of higher intensity at a narrow angle. Transmission of light occurs as well, which can be computed by considering the refractive index in the measurements. In this study, Kaolinite was chosen as the

reference for refractive index of samples. The map of scattering intensity versus light angle is the source used to calculate the particle size distributions<sup>138,139</sup>.

The samples tested using Malvern Mastersizer had kaolinite concentrations of 10 and 40 g/L and were prepared as explained in Section 3.3.1. Both samples were sonicated at 100% amplitude for as long as 60 minutes, as explained in Section 3.3.3.

### **3.3.5. Cryo-SEM tests**

Cryogenic Scanning Electron Microscope (SEM) studies were carried out on two samples of kaolinite clays. Samples with concentrations of 10 g/L and 20 g/L were prepared as explained in Section 3.3.1 and sonicated for 30 minutes at 100% amplitude as explained in Section 3.3.3. Table 3.3 lists the characteristics of the four samples that were studied using the Cryo-SEM.

Numerous examples of SEM images of clay suspensions can be found in the literature<sup>77,78,98,104,106</sup>. All were taken using a drying technique, which can alter the structure of flocs and aggregates during the ice formation step. Du et al<sup>140</sup> suggest that cryo-vitrification can overcome the limits of freeze-drying techniques. For this reason, the cryogenic SEM is used in this study to obtain the images of kaolinite particles before and after sonication.

The SEM used for the present study was a JEOL model, JSM.6301F located in the Scanning Electron Microscope Laboratory of Earth and Atmospheric Sciences Department at University of Alberta.

**Table 3.3. The characteristics of samples used for cryo-SEM studies and settling tests**

Sample name and number	Kaolinite concentration (g/L)	Sonicated for (minutes)
Not-sonicated 20 g/L (1-1)	20	0
Sonicated 20 g/L (1-2)	20	30
Not-sonicated 10 g/L (2-1)	10	0
Sonicated 10 g/L (2-2)	10	30

Four kaolin samples (Table 3.2) were prepared for cryogenic SEM studies in our lab and 10 mL of each sample was put in a glass jar. The jars were then transported to the SEM laboratory. A rectangular copper specimen mount (31×9.5×7 mm, L×W×H) with four similar cavities of 2 mm in diameter and 1 mm in depth was used (see Figure 3.6). Each glass jar was turned end over end by hand four times before sampling. Then, using an open tip pipette, a drop of each sample was taken from the middle of the jar and mounted on the top of the copper stage. The copper stage was then submerged immediately in a cup of liquid nitrogen slush. The liquid nitrogen had been cooled to its freezing point using the Emitech K1250 cryogenic system. The frozen samples were then fractured (below the surface of the liquid nitrogen) using hand-held pliers to expose a fresh surface. This preparation technique is known as freeze-fracturing. Next, the stage was removed from the liquid nitrogen cup and placed within the SEM vacuum chamber for the sublimation step. The temperature of the chamber was kept below -40°C, which prevents recrystallization of the ice on the surface. After the sample kept in the SEM chamber for complete sublimation (about 1 hour), it is

bombarded with gold in a process known as sputtering. Samples were then ready for observation at a vacuum pressure of  $8 \times 10^{-6}$  torr and a temperature of  $-130^{\circ}\text{C}$ . The images were collected at magnifications ranging from 1000 to 20,000 times and are shown in Section 6.7.2.

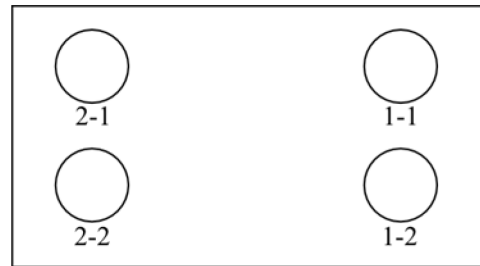


**Figure 3.6 Cryo-SEM copper stage**

### **3.3.6. Tailings tests**

Effect of sonication on the industrial tailings sample PSD is discussed in Section 6.8 of this work. Sample preparation steps for the industrial tailings, provided by Jessie Smith as a part of her MSc thesis<sup>114</sup>, are as follows:

1. Pour the raw slurry mixture onto a 75 micron (200 mesh) sieve. Place a pail beneath to collect fluid and fine particles.
2. Add around 200 mL of sieved sample to the glass jar.
3. Add RHS beads (approximate ratio of 6:1 by weight beads to bitumen) to each jar of tailings.
4. Place the jar containing the RHS beads and tailings sample in a hot water bath (about  $45^{\circ}\text{C}$ ) for 5 minutes.

5. Place the jar in rotating mixer and mix for 10 minutes. Remove from mixer and allow jar to stand until RHS beads rise to the top of the container. Remove beads using metal strainer.
6. Repeat Steps 2 through 5 an additional 5 times for the same sample to ensure maximum bitumen removal.
7. Vacuum filter the bead-treated sample using a Buchner funnel and 2.5  $\mu\text{m}$  filter paper (Whatman 5 Qualitative Paper). Repeat three times to ensure total solids removal.
8. Use the filtrate water (prepared in Step 7) to dilute samples prior to testing in the FPIA.

### **3.4 Experimental programme**

#### **3.4.1 Test parameter selection and development**

The sonication process need to be investigated from two points of view: the energy source and the energy target. The energy source is the Sonicator-4000. The energy target is the kaolinite clay suspension. The effect of sonication on the kaolinite PSD is a direct function of total effective acoustic energy received by the kaolinite suspension. The amount of energy received by kaolinite suspension is affected by instrument parameters as well as system-specific parameters<sup>89</sup>. Sonication time and amplitude dictate the total amount of acoustic energy delivered to the sample.

The system-specific parameters, on the other hand, are the sample volume, the sample temperature, and the controlling parameters which dictate the nature of

initial kaolinite PSD. The particle size distribution of kaolinite clay (before sonication) is controlled by three dominant factors: *kaolinite concentration*, *sample pH*, and *flocculant addition*.

In this work, the sample volume and temperature are kept constant. Sonication time and amplitude, kaolinite concentration, suspension pH and the addition of flocculant are selected as the test parameters.

A preliminary investigation was carried out to verify that the experimental setup or measuring device is not influencing the measured PSD's. The results of this preliminary investigation are discussed in Chapter 4. This chapter also includes the results of an investigation on the Sysmex-FPIA 3000 operations, the effect of mixing and the effect of pre-test cooling on measured PSD's.

### **3.4.2 Benchmarking data – Effect of solids concentration, pH, and flocculant addition on kaolinite PSD (no sonication)**

For a comprehensive study of sonication effect on the kaolinite PSD, samples with different initial particle size distributions needed to be studied. Solids concentration, sample pH, and the addition of flocculant as three system-specific parameters are investigated in this work. As explained in section 2.4 and 2.5, these are the main parameters which can influence the initial kaolinite PSD.

The aim of this set of experiments is to discover at which conditions kaolinite clay samples have the largest and smallest particle sizes. These conditions will define the boundaries of the size of initial samples (not-sonicated samples). Samples will

be selected within these boundaries for further investigation of sonication impacts.

The preliminary evaluation of factors affecting kaolinite PSD is explained in Chapter 5 of the present study.

### **3.4.3 Sonication tests (time and amplitude)**

Selected samples from investigation in Chapter 5 will be treated by ultrasound and their PSDs after sonication will be compared to the initial ones. The test parameters explained in section 3.4.1 will be studied in Chapter 6. In this chapter, the main objective of the present study will be addressed.

Three samples with the kaolinite concentration of 40 g/L, 20 g/L, and 10 g/L will be sonicated. The pH of these samples is about 4.6 and there is no flocculant addition.

The effect of sonication time and amplitude will be studied for three sonication amplitudes of 50%, 75%, and 100% (discussed in section 6.3) and for sonication times from 10 seconds to 60 minutes (discussed in section 6.2).

The effect of solids concentration will be explained in section 6.4. The effect of sonication on the samples with different pH will be discussed later in section 6.5. In addition, the changes in the flocculated samples PSD due to sonication will be studied in section 6.6.

## **4. Evaluation of experimental setup**

### **4.1. Introduction and test objectives**

In this chapter, the performance of the experimental setup is evaluated to verify that neither the current experimental setup nor the measuring device is influencing the measured PSD. In the evaluation of the experimental setup performance the following factors are investigated:

- Reproducibility of the FPIA measurements
- Sample preparation techniques
- The FPIA internal mixing

The repeatability of the experimental results and the possible effects of FPIA operation on the kaolinite PSD are discussed in Section 4.2. The effects of two important parts of the sample preparation procedure, sample mixing and pre-cooling, on kaolinite PSD are discussed in Section 4.3.

Systematic effects of flow through the FPIA chamber are not considered in this study because any effect would be similar for both sonicated and non-sonicated samples. However, the results produced with the FPIA were validated using other techniques such as laser diffraction and scanning electron microscopy. These results are described in Section 6.3.

## **4.2. Sysmex-FPIA 3000 operations**

In this section the repeatability of the experimental results is investigated. The repeatability of sample preparation procedures and reproducibility of the FPIA measurements are discussed in section 4.2.1. The repeatability of sample preparation procedure is investigated by comparing the PSD's of multiple different samples made under the same conditions (same solid concentrations and sample pH). Additionally, the reproducibility of the FPIA measurements is studied by comparing the measured PSD's for samples taken from a single kaolinite mixture. The effect of the FPIA internal mixer on the kaolinite PSD is explained in section 4.2.2.

### **4.2.1. Repeatability of FPIA results**

In this section, two series of experiments were carried out to assess the repeatability of the FPIA results. In the first series of experiments, ten consecutive measurements were carried out on samples from a single kaolinite suspension to test the reproducibility of the FPIA measurements. Figure 4.1 illustrates the results of these tests for a single mixture, with  $c=10$  g/L. Similar results for higher concentrations (20 g/L and 40 g/L) are shown in Appendix A.

In the second series of experiments, six separate mixtures were prepared to test the repeatability of the sample preparation procedures. Each mixture PSD was measured separately and compared to that of the other mixtures. Figure 4.2 shows the results of these measurements for 6 mixtures with  $c=10$  g/L. Similar results for higher concentrations (20 g/L and 40 g/L) are shown in Appendix A.

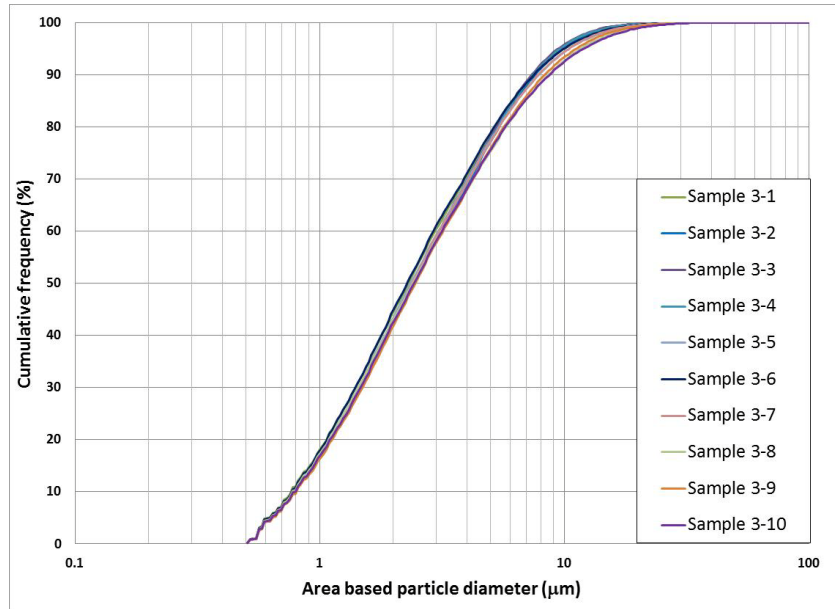


**Figure 4.1 Repeatability tests: Cumulative Particle size distributions for 10 samples from a single mixture (c= 10 g/L)**

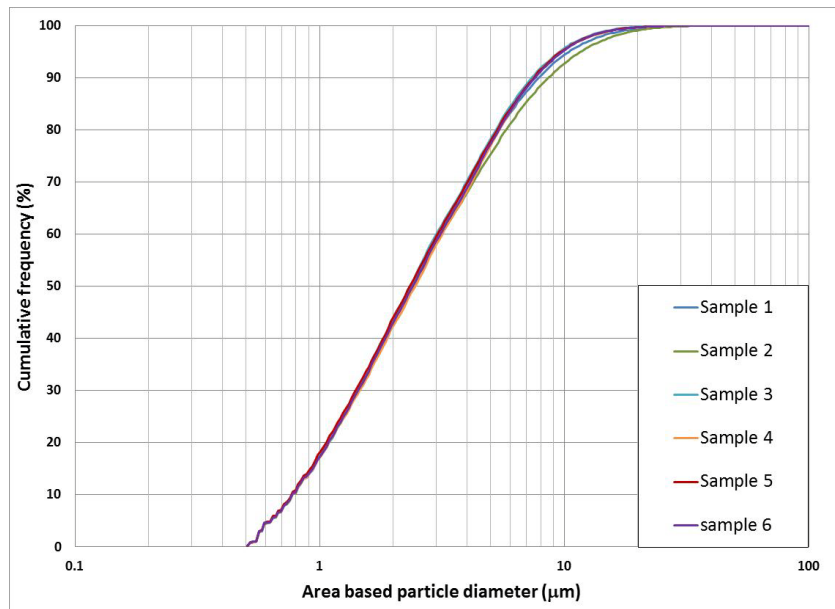


**Figure 4.2. Repeatability tests: Cumulative particle size distributions for 6 different mixtures having the same concentration (c=10 g/L)**

Figures 4.1 and 4.2 indicate that the FPIA results are very repeatable and show only small variations, which may be related to the colloidal nature of the kaolinite mixtures. In colloidal suspensions, the continuous random motion of particles results in the collision between particles leading to the formation of flocs and aggregates<sup>22</sup>. The success of these collisions (i.e. coagulation) is strongly affected by the slurry conditions (solids concentration, pH, and electrolyte concentration)<sup>22</sup>. The collision frequency, on the other hand, depends on the solids concentration and the random motion of the particles<sup>22</sup>. The random nature of particles motion and collision supports the idea that slurries with the same conditions (solids concentration, pH, and ionic strength) may have slightly different PSDs.

To test whether the differences between particle size distributions shown in Figures 4.1 and 4.2 are statistically significant, the chi-square goodness of fit test has been carried out separately for the each set of results. The chi-square statistic is a measure of how far the measured values are from the expected values (expectation for random variations)<sup>141</sup>. The null hypothesis in this study is that there is no significant difference between the particle size distributions of samples prepared at the same conditions. If the null hypothesis is true, the differences between the size distributions are just due to the random variations<sup>141</sup>. To test the null hypothesis the observed value and expected values are compared<sup>141</sup>.

The expected and chi-square values are calculated as<sup>141</sup>:

$$\text{expected value} = \frac{\text{row total} \times \text{column total}}{\text{table total}} \quad (4.1)$$

$$\chi^2 = \sum \frac{(\text{measured value} - \text{expected value})^2}{\text{expected value}} \quad (4.2)$$

The probability of occurrence of the calculated chi-square value for specific *degree of freedom* (df) of the data set is defined as P-value. df is calculated as<sup>141</sup>:

$$\text{df} = (\text{number of rows} - 1) \times (\text{number of columns} - 1) \quad (4.3)$$

The P-value verifies if the null hypothesis is true or it should be rejected<sup>141</sup>. If the P-value is equal or less than 0.05 the null hypothesis will be rejected which means the difference between the populations is not due to random variations<sup>141</sup>. On the other hand, if the P-value is larger than 0.05 (up to 1), the null hypothesis is true which means the difference between the compared populations are not statistically significant<sup>141</sup>. In this study the chi-square and the P-value are calculated with Microsoft Excel.

The test statistics for two sets of experiments are shown in Table 4.1.

**Table 4.1**The chi-square test statistics for results shown in Figures 4.1 and 4.2

	Results shown in Figure 4.1	Results shown in Figure 4.2
Chi-Square	13.8174	4.2759
df (degree of freedom)	1953	1085
P-Value	1.000	1.000

As shown in Table 4.1 the calculated P-value for both of the results shown in Figures 4.1 and 4.2 is equal to 1.000 which verifies the null hypothesis that the differences among the populations shown in each figure are not statistically

significant and the differences between them are due to random variations. The detailed calculations of chi-square tests are provided in Appendix B.

#### **4.2.2. Effect of FPIA mixer speed on kaolinite PSD**

As described in Chapter 3, the FPIA sample chamber is equipped with an ultrasonic probe and a mixer to help disperse the sample. The FPIA allows the operator to adjust the speed of the mixing motor and the sonication power of the ultrasound probe. Both the probe and mixer may influence the measured kaolinite PSD.

Since the objective of the present study is to investigate the effect of sonication on the kaolinite PSD, it is important to control all sources of sonication of the sample. To accurately characterize the applied sonication only the Misonix Sonicator-4000 was used and for all the measurements carried out by the FPIA the internal ultrasound treatment is set to “Not Apply” (off).

With the internal sonicator of FPIA turned off, the effect of the FPIA internal mixer on the sample PSD is studied. The PSD of a single kaolinite suspension sample was measured with four different mixer motor RPM settings to investigate the influence of mixer speed on the measurements carried out by FPIA. Figures 4.3a through 4.3c show the PSD of a 10 g/L kaolinite in water sample, for four different RPM targets (internal mixer speeds) of 50, 300, 550, and 700 RPM. Figure 4.5 illustrates the cumulative particle size distributions for the same series of measurements. Similar results for higher concentrations (20 g/L and 40 g/L) are shown in Appendix C.

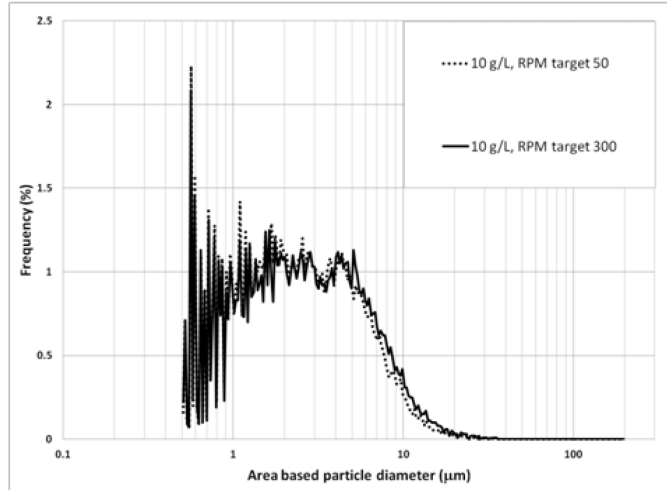


Figure 4.3a Effect of FPIA mixer speed on the measured PSD ( $c=10$  g/L, RPM=50, 300)

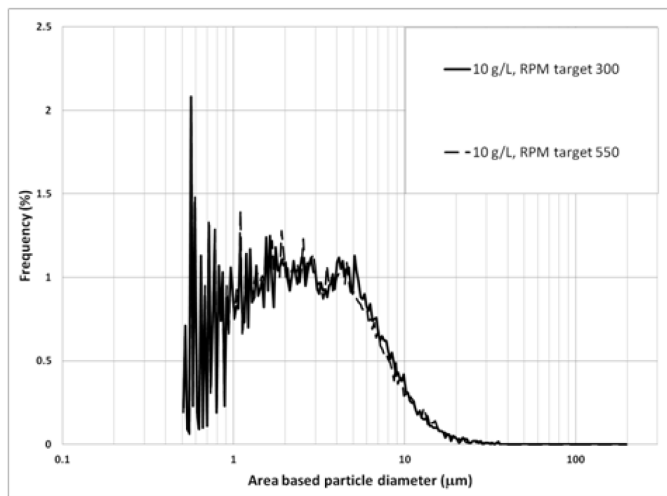


Figure 4.3b Effect of FPIA mixer speed on the measured PSD ( $c=10$  g/L, RPM=300, 550)

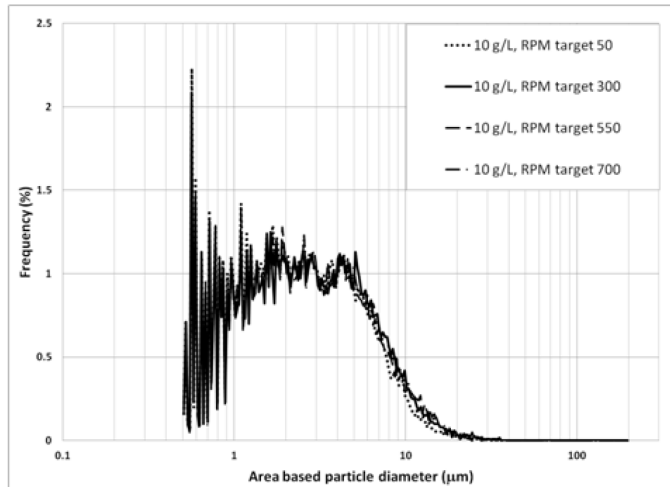
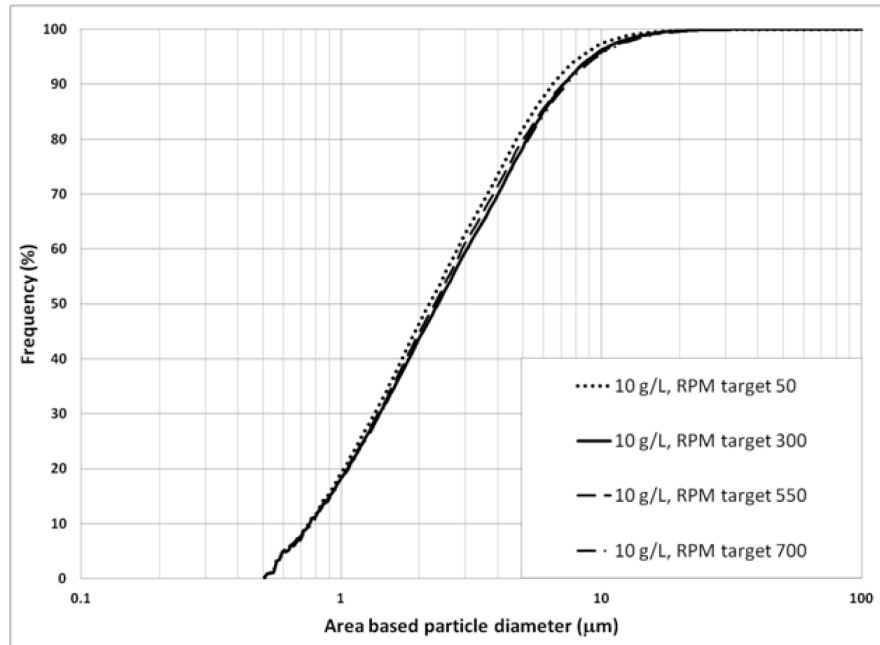


Figure 4.3c Effect of FPIA mixer speed on the measured PSD ( $c=10$  g/L RPM=50, 300, 550, 700)

The results presented in these figures demonstrate that the RPM setting of the internal mixing motor of the FPIA does not have a significant effect on the kaolinite PSD.



**Figure 4.4 Effect of RPM target on the cumulative particle size distribution (c=10 g/L)**

Based on these results, the FPIA mixer speed was set at N=300 RPM for all experiments. This value was chosen because it was high enough to prevent blockages from forming in the FPIA chamber.

### **4.3. Effect of mixing and pre-test cooling**

High intensity ultrasound treatment introduces a large amount of energy to the suspensions, which increases the sample temperature dramatically in a short time. An increase in the temperature alters important physical properties of the sample (i.e. viscosity). Additionally, surface evaporation caused by sudden increases in temperature can lead to changes in sample volume and solids concentration during the experiments. In this study, the temperature was kept constant to avoid these issues.

Recall that the sample preparation procedure requires that a sample be mixed for 30 minutes. The sample is also cooled during the mixing step. Either or both of these steps (i.e. mixing and cooling) could impact the kaolinite PSD. Therefore, tests were conducted to evaluate the potential effect(s) that these steps had on the kaolinite PSD.

In order to maintain the sample temperature at 20°C during sonication, the samples need to be cooled during the mixing stage. A set of experiments was conducted to make sure that the pre-test cooling of the kaolinite samples does not change their PSDs. In this set of experiments, the mixing and the cooling of the samples began simultaneously. The PSD of a 40 g/L kaolinite suspension was then measured during the cooling process from room temperature (23°C) to 5°C. Figures 4.5a through 4.5c show the kaolinite PSD's at different temperatures.

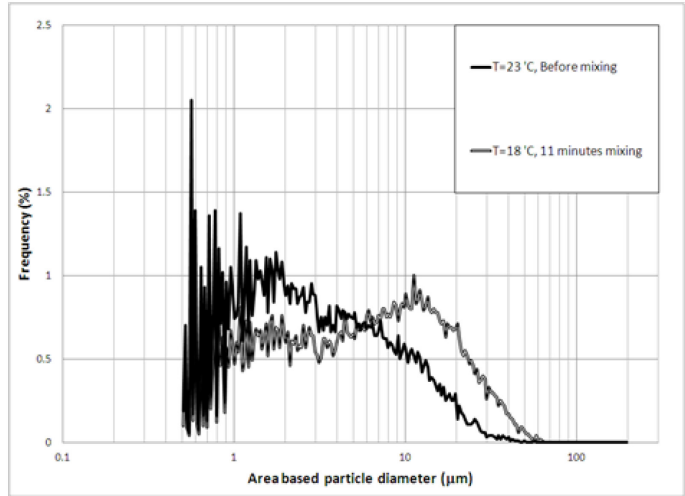


Figure 4.5a Effect of pre-test cooling (23 °C-18°C) on the kaolinite PSD (c=40 g/L)

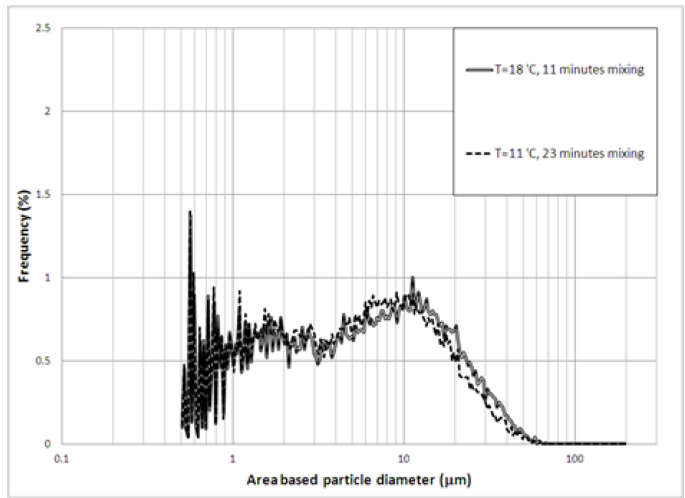


Figure 4.5b Effect of pre-test cooling (18 °C-11°C) on the kaolinite PSD (c=40 g/L)

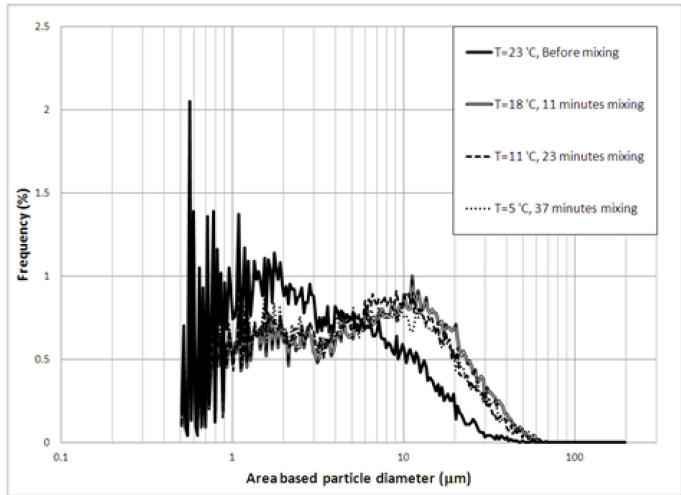


Figure 4.5c Effect of pre-test cooling (23 °C-5 °C) on the kaolinite PSD (c=40 g/L)

Figures 4.5a through 4.5c show that by cooling the sample from 23 °C to 18 °C (5 °C decrease) the PSD changes significantly. It should be noted that it took 11 minutes for the sample to reach 18°C from room temperature. Unlike the first 11 minutes, Although further mixing and cooling of the sample for 26 minutes (from the eleventh minute) decreases the sample temperature by 13 °C (from 18 °C to 5 °C) the sample PSD does not change significantly. The fact that the PSD changes during the mixing and cooling process only occur during the first 11 minutes (when the sample temperature is decreased by 5°C from room temperature) suggests the possibility of having another cause for the PSD changes. Besides pre-test cooling and mixing another possible cause of this change could be the fact that the sample is not at its stable state in the beginning of the mixing (the first 11 minutes).

Two sets of experiments were designed to distinguish which of these factors caused the change in PSD. In the first series of experiments, the variations of the kaolinite PSD were tracked during mixing at constant temperature. In the second series of experiments, the sample was cooled to 5°C and then heated to room temperature. The variations in the PSD during both the cooling and the heating steps were investigated.

#### **4.3.1. Effect of mixing**

The Sauter mean diameter ( $d_{32}$ ) of kaolinite mixtures have been studied in this section to investigate the overall changes of kaolinite particle size during mixing time. However, the entire particle size distributions of these samples are also

studied later in this section. Figure 4.6 shows the changes in the Sauter mean diameter of two kaolinite samples ( $c=40$  g/L) during mixing. The Sauter mean diameter is the average diameter based on unit surface per unit volume of the particles in the solution:

$$d_{32} = \frac{\sum_{i=1}^{226} n_i d_i^3}{\sum_{i=1}^{226} n_i d_i^2} \quad (4.1)$$

where  $n_i$  is the number of detected particles in the  $i^{\text{th}}$  segment in the frequency table provided by the FPIA software and  $d_i$  is the mean diameter of the  $i^{\text{th}}$  segment.

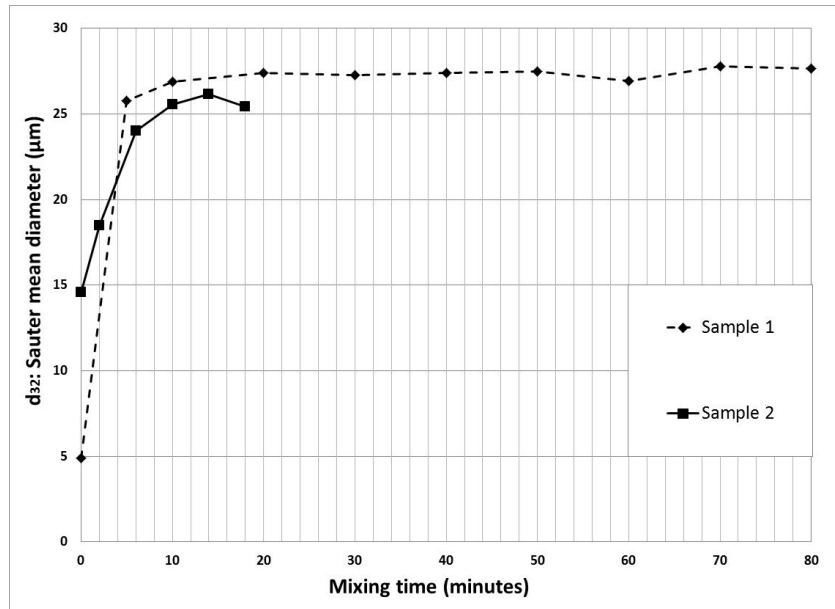


**Figure 4.6 Effect of mixing on the Sauter mean diameter of kaolinite samples:  $c=40$  g/L**

Sample 1 was mixed for 80 minutes and the values of  $d_{32}$  after different mixing times were obtained. It can be seen from the results of Figure 4.6 that there is a dramatic increase in  $d_{32}$  during the first 10 minutes of mixing and then the Sauter

mean diameter does not vary significantly with continued mixing ( $t > 10$  minutes).

The very low mean diameter of the sample at time  $t=0$  is due to the initial settling of the kaolinite particles at the bottom of the beaker, making a two-phase suspension. The samples were collected from the same depth of the beaker for all data points. At time  $t=0$ , sampling from the same depth resulted in a significantly lower mean diameter due to the low concentration of small particles suspended in the supernatant phase. Additionally, changes in the sample PSD of another kaolinite in water sample with the same solids concentration ( $c=40$  g/L) were studied over first 18 minutes of mixing. The squares in Figure 4.6 show the Sauter mean diameter of this sample at different mixing times. These results indicate that the Sauter mean diameter dramatically increases during the first 6 minutes of mixing and does not change significantly with continued mixing (from 6 to 18 minutes).

Since the Sauter mean diameter ( $d_{32}$ ) of a suspension is single value meant to represent an entire particle size distribution, a fuller picture of the effect of the mixing process is probably obtained by studying the changes in the sample PSD with mixing. The PSD's for the 40 g/L kaolinite suspension are shown in Figures 4.7a and 4.7b.

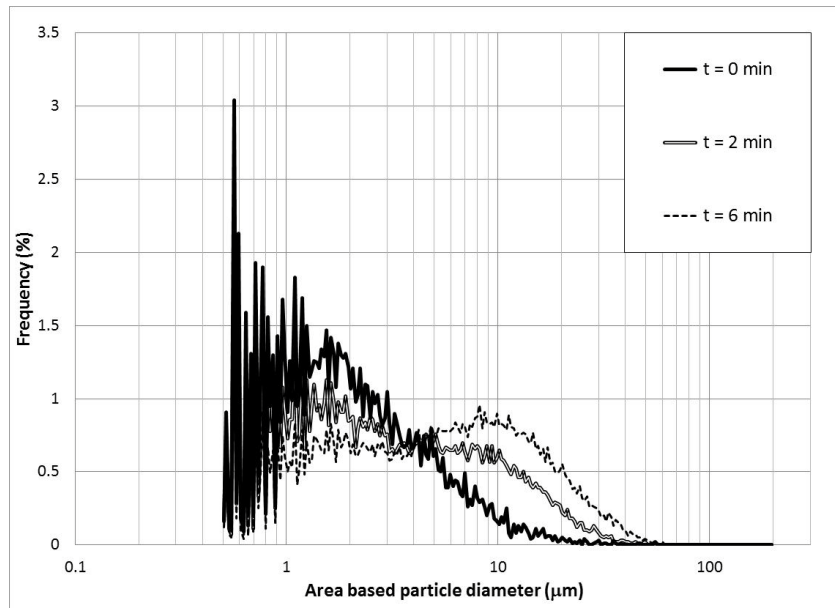


**Figure 4.7a Effect of mixing on the kaolinite PSD (c=40 g/L)**

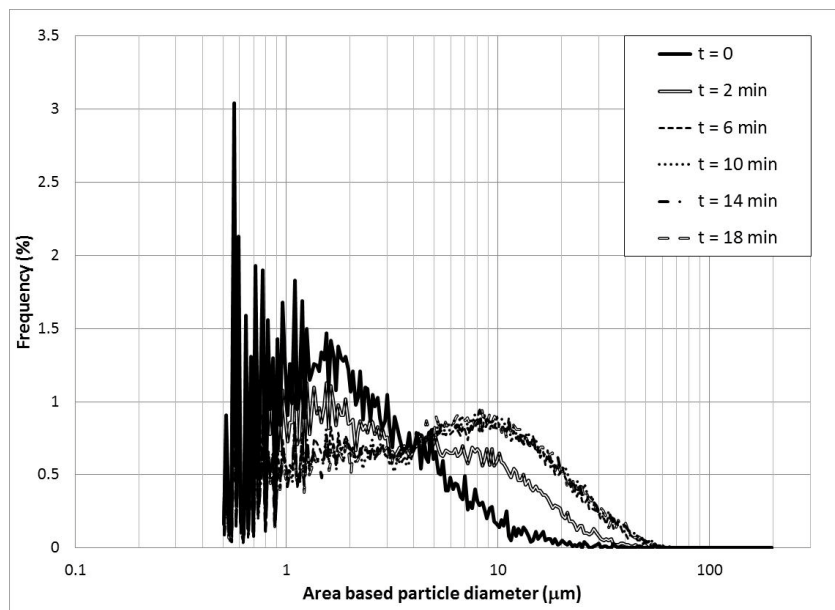


**Figure 4.7b Effect of mixing on the kaolinite PSD (c=40 g/L)**

Figures 4.7 a and 4.7b show that it takes approximately 6 to 10 minutes for each sample to reach the stable state and after this state is reached, mixing does not affect the PSD. Therefore, it can be concluded that the mixing that is applied for 30 minutes during the pre-test cooling step does not have any impact on the kaolinite PSD. Although based on these findings 10 minutes of mixing is sufficient for sample preparation, in this study, samples are mixed for 30 minutes to be consistent with the experimental procedures used for preparation of similar mixtures by other researchers (in oil sands industry and literature).

These findings suggest that the significant change in the PSD between 23°C and 18°C samples, shown in Figures 4.5a through 4.5c, is a result of the sample not being in a stable state. In other words, changes in the PSD were not caused by pre-test cooling or the mixing. Furthermore, the similarity of sample PSD's at 18°C, 11°C and 5°C, shown in Figure 4.5c, reinforces the above-mentioned reasoning.

#### **4.3.2. Effect of cooling and heating during the mixing**

A second series of experiments was designed to provide a better understanding of possible effects caused by changing the temperature of the samples prior to sonication. In this set of runs, cooling and mixing were started simultaneously. While continuously mixing the sample, the sample was first cooled from room temperature (23°C) to 5°C. In the second phase the sample was heated until the original temperature (23°C) was reached.

In Figure 4.8 changes in the Sauter mean diameter can be seen only in the first 10 minutes of the cooling and mixing. This finding reinforces the idea that sample PSDs are unstable in the first 10 minutes of sample preparation. Therefore, the changes in the measured  $d_{32}$  are not related to cooling or mixing. Additionally, Figure 4.8 illustrates that heating the sample from 5°C to 23°C does not affect the Sauter mean diameter.

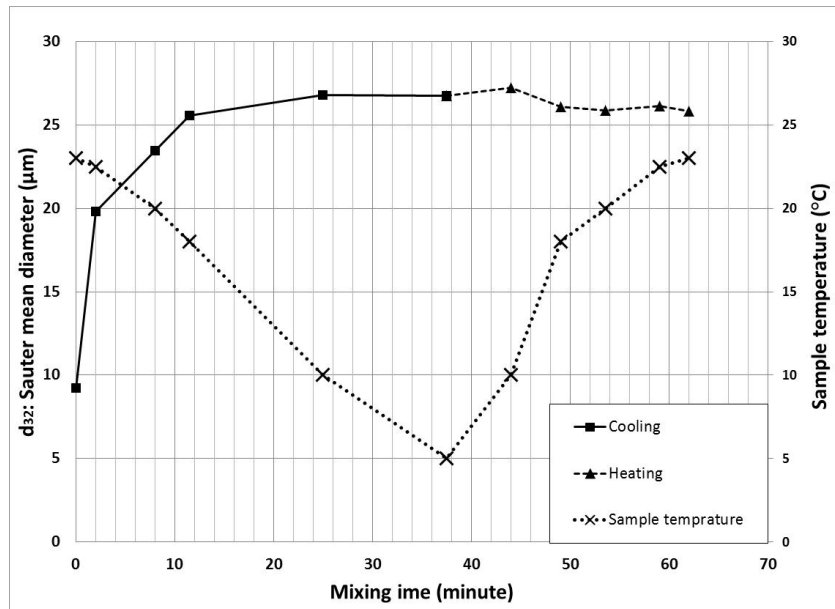


**Figure 4.8 Effect of sample temperature variation on the Sauter mean diameter during sample preparation**

#### 4.4. Summary

The performance of the experimental setup has been evaluated in this chapter.

The results presented in this chapter demonstrate that:

- The FPIA results are highly repeatable and show only small variations

- The sample preparation procedure used in this study allows us to produce repeatable results for the same sample conditions (same solids concentration and sample pH)
- The FPIA internal mixer does not have a significant effect in the measured kaolinite PSD
- The sample mixing and pre-test cooling do not influence the kaolinite suspension PSD

Therefore, it has been shown that neither the experimental setup nor the measuring device (FPIA) has a significant effect on the measured PSD.

## **5. Preliminary evaluation of factors affecting kaolinite PSD**

### **5.1 Introduction and objectives**

Factors that affect kaolinite PSD are known to include the sample concentration, the sample pH, and the addition of  $\text{CaCl}_2$  as a flocculant<sup>9,80,81,86,142</sup>. Increasing the solids concentration increases the particle size of the kaolinite suspensions by increasing the number of large particles<sup>9,22,142</sup>. As previously discussed in Chapter 2, increasing the sample pH results in de-flocculation of kaolinite flocs and thus leads to a reduction in particle size of kaolinite suspensions<sup>80,81</sup>. The addition of  $\text{CaCl}_2$ , as a flocculant, results in strong particle interactions and high flocculation degrees<sup>86</sup>. Therefore, the addition of  $\text{CaCl}_2$  significantly increases the particle size of kaolinite suspensions.

In the present study, a set of experiments was performed to study the effect of each parameter on the sample PSD. The results of these tests are compared to those available in the literature. The consistency of these results with previous studies provides confidence in the ability of the FPIA to make reliable size measurements for kaolinite mixtures.

Furthermore, the results of this set of experiments determine the conditions at which kaolinite clay samples have the largest and smallest particle sizes. These conditions define the boundaries of the particle size found in un-sonicated samples in this work. For a comprehensive study of the effect of sonication, samples with different initial PSDs (within the particle size boundaries defined below) were treated by ultrasound. The PSDs after sonication are compared to the

initial PSDs to show the effect that sonication has on different initial kaolinite PSDs, and on different modes of particle aggregation (see Section 2.3, 2.4, and 2.5).

## **5.2. Effect of sample concentration on measured PSD**

The particle size distributions of four samples, with kaolinite concentrations of 2, 8, 24, and 40 g/L, were measured to determine the effect of solids concentration on the particle size distribution. The results are shown in Figures 5.1 through 5.3. It should be mentioned that the pH of all these samples is about 4.6 and is roughly the same for all samples. For the sample with  $c=2$  g/L (Figure 5.1), nearly all of the particles are finer than 10  $\mu\text{m}$ . Compared to the 2 g/L sample, the sample with  $c=8$  g/L (Figure 5.2) has more particles that are larger than 6  $\mu\text{m}$  and fewer particles in the size range of 1 to 6  $\mu\text{m}$ . Figure 5.3 shows that compared to the 8 g/L sample, the sample with  $c=24$  g/L has more particles that are larger than 5  $\mu\text{m}$  and fewer particles that are smaller than 5  $\mu\text{m}$ .

The population of particles larger than 25  $\mu\text{m}$  is similar for the samples with  $c=24$  g/L and  $c=40$  g/L, but the sample with the higher solids concentration has a larger number of particles in the size range of 2  $\mu\text{m}$  to 20  $\mu\text{m}$  and fewer particles finer than 2  $\mu\text{m}$ .

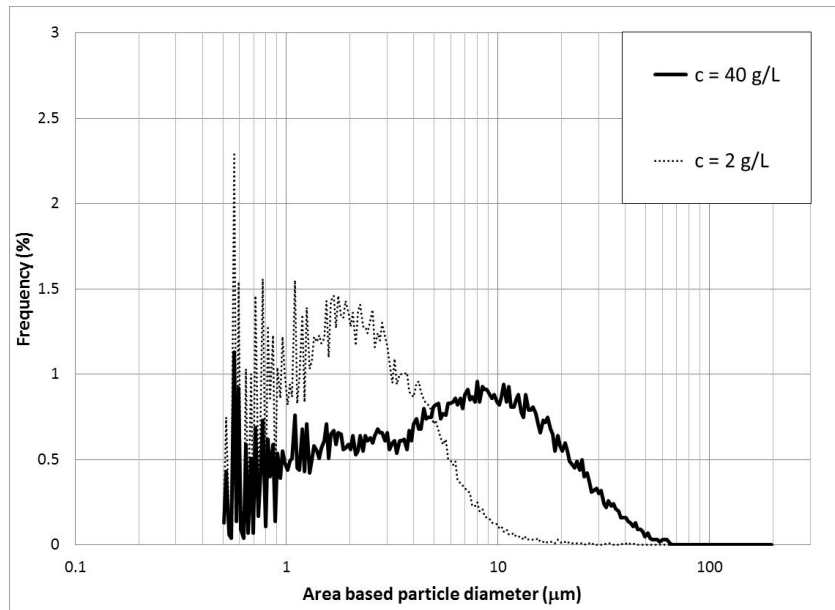


Figure 5.1 Kaolinite PSD at two concentrations:  $c=2$  g/L and  $40$  g/L, (pH~ 4.6)

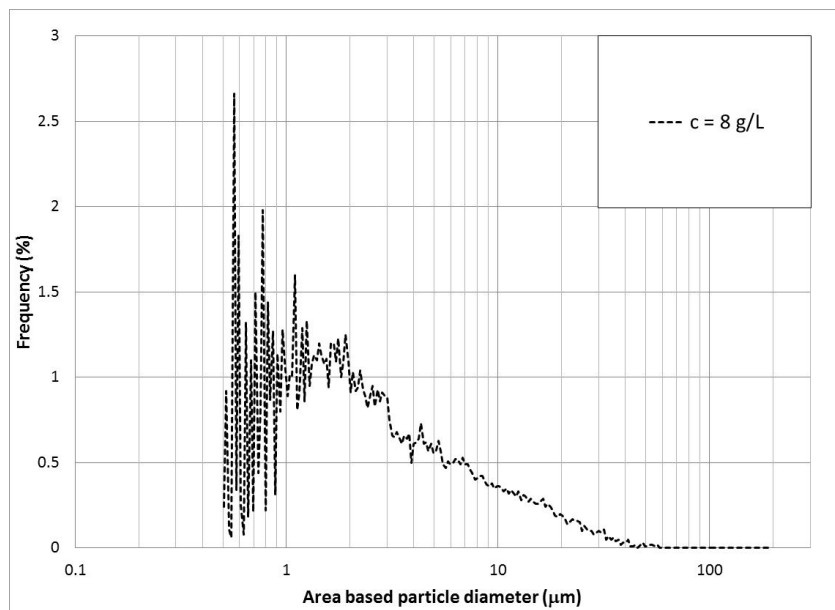


Figure 5.2 Kaolinite PSD at concentration of  $c=8$  g/L, (pH~ 4.6)

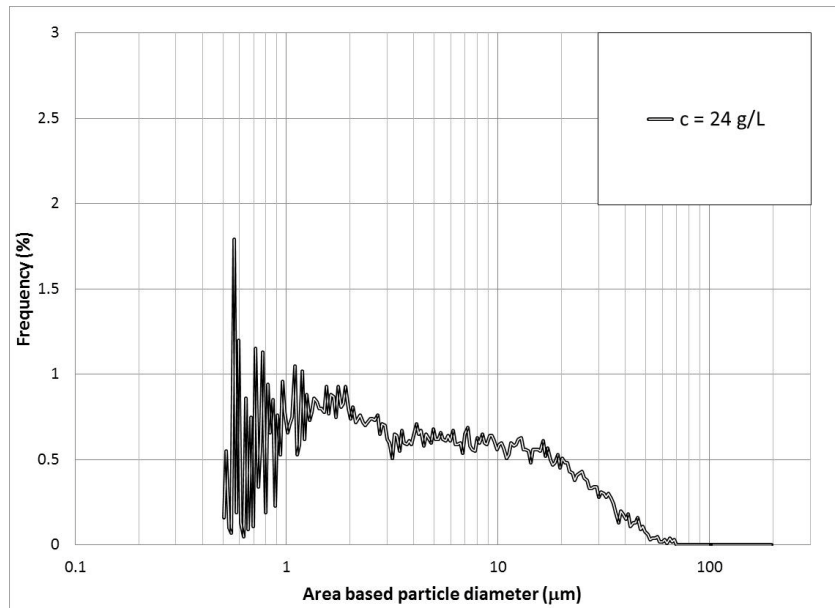


Figure 5.3 Kaolinite PSD at concentration of:  $c=24$  g/L, (pH~ 4.6)

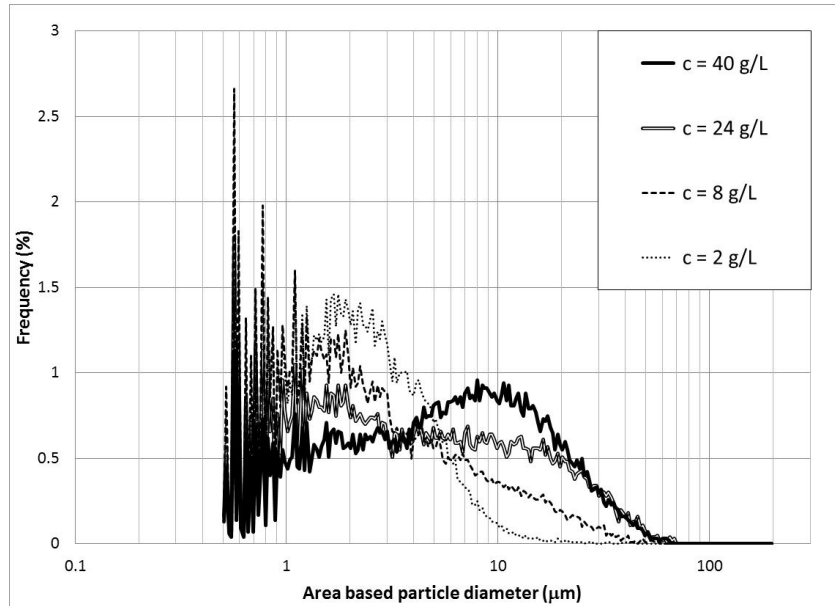


Figure 5.4 Effect of solids concentration on the kaolinite PSD ( $c=2, 8, 24,$  and  $40$  g/L) (pH~ 4.6)

Figure 5.4 compares the PSD's of all four samples. It can be deduced from this figure that for samples with higher concentrations, the population of large particles ( $5 \mu\text{m} < d$ ) is greater and the number of fine particles ( $d < 2 \mu\text{m}$ ) is lower. It can be concluded that by increasing the kaolinite concentration, the population of larger particles increases.

This conclusion is consistent with the findings of previous studies. When a kaolinite slurry solids concentration increases, the interparticle distances decrease which leads to more collisions between particles<sup>9,142</sup>. The higher number of collisions between particles increases the chance of successful collisions<sup>22</sup>. Such collisions result in the formation of larger flocs and aggregates<sup>22</sup>. The greater number of large particles observed for samples with high concentrations is the result of more frequent and more successful collisions between particles.

### **5.3. Sample pH**

Another factor that can change the kaolinite PSD is the sample pH. The addition of sodium hydroxide (NaOH) to the samples increases the pH by increasing the concentration of  $\text{OH}^-$  in the suspension. By adsorbing  $\text{OH}^-$  ions, the edges of a particle become neutral or negatively charged<sup>80,81</sup>. Under these conditions the electrostatic forces between edges and faces are no longer attractive, resulting in de-flocculation of flocs and aggregates<sup>80,81,84</sup>. Nasser and James<sup>81</sup> reported that at pH=9, flocs were broken down completely. Michaels and Bolger<sup>143</sup> also mentioned that at a high pH, above 7, the probability of de-flocculation increases rapidly.

Here, the sodium hydroxide (NaOH, 0.25 M) was added to the four samples described in Section 5.2 to investigate the effect of pH on kaolinite PSD. The pH of these samples was adjusted to pH=11 (approximately) and then size distributions were measured with the FPIA. The results are shown in Figures 5.5 through 5.8. As the PSD's shown in Figures 5.5 through 5.8 demonstrate, increasing the sample pH decreases the particle size of the kaolinite suspension. This reduction in size appears in the figures as a significant decrease in the number of particles larger than 2  $\mu\text{m}$  and an associated increase in the population of particles finer than 2  $\mu\text{m}$ . These findings verify the results found in the literature, which indicate that kaolinite particles de-flocculate at high pH and the E-F (edge-to-face) associations will no longer exist in the suspension<sup>81</sup>. At high pH values, kaolinite suspensions contain a large number of individual primary particles along with a small number of flocs, mostly produced through of F-F (face-to-face) associations<sup>81</sup>.

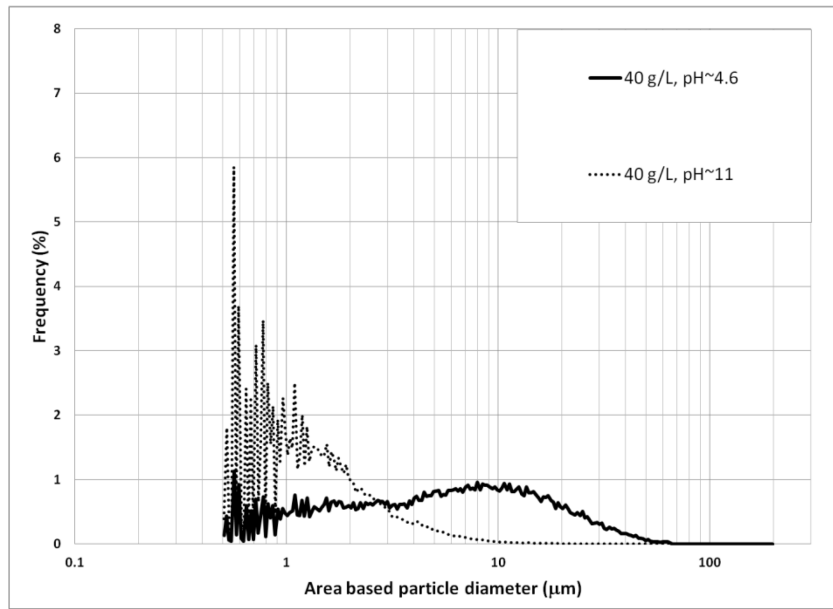


Figure 5.5 Kaolinite PSD at natural and high pH (pH~4.6 and 11), c=40 g/L

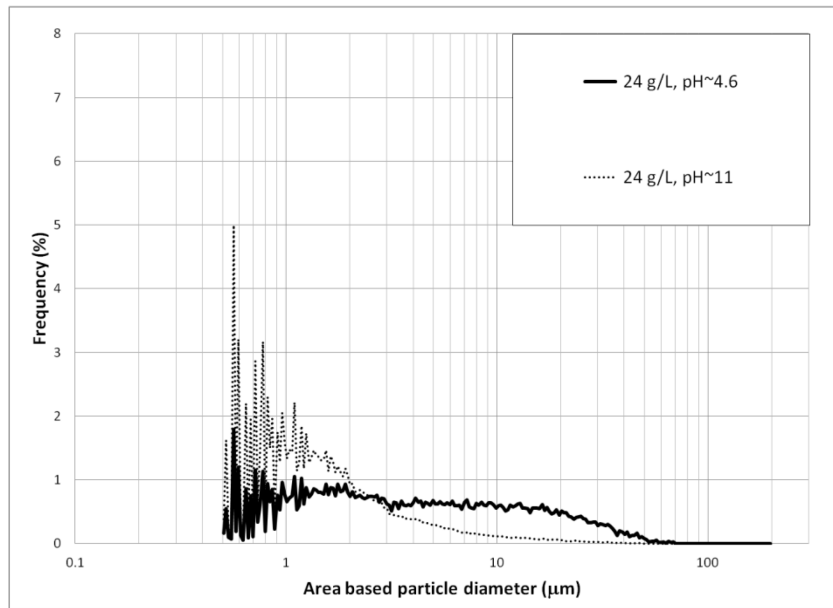


Figure 5.6 Kaolinite PSD at natural and high pH (pH~4.6 and 11), c=24 g/L

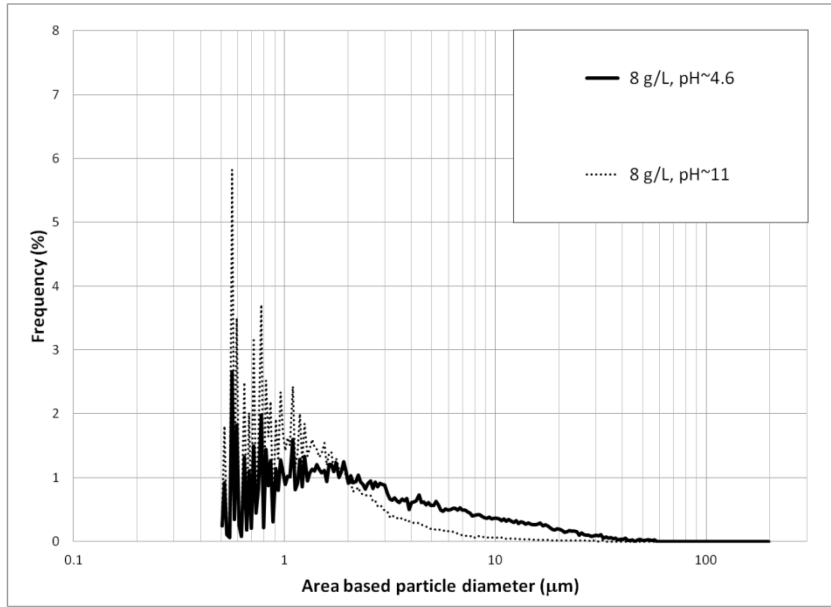


Figure 5.7 Kaolinite PSD at natural and high pH (pH~4.6 and 11), c=8 g/L

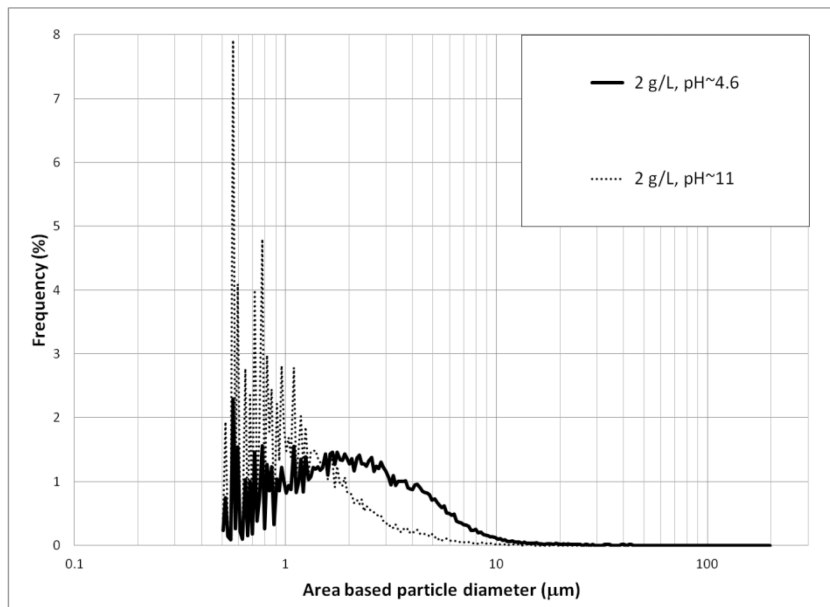
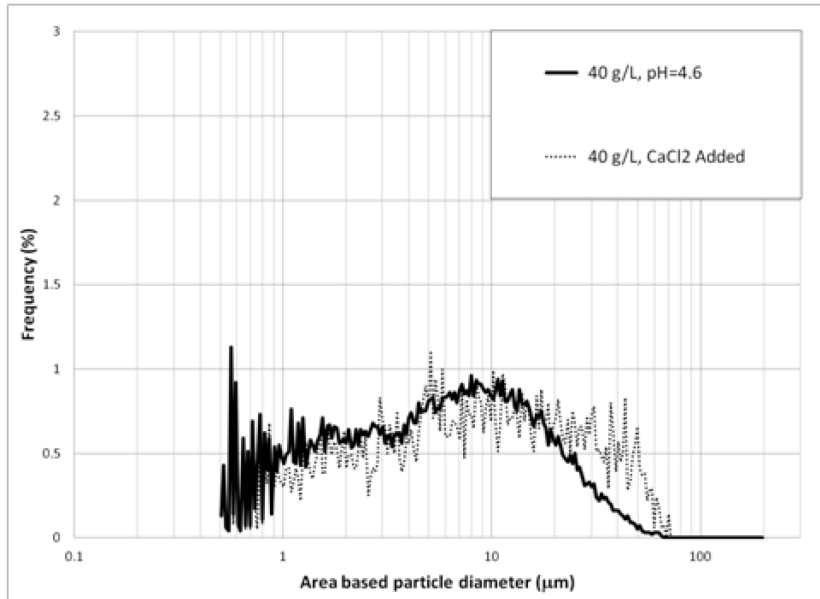


Figure 5.8 Kaolinite PSD at natural and high pH (pH~4.6 and 11), c=2 g/L

#### 5.4. Flocculant addition

Flocculant addition can drastically alter the kaolinite suspension PSD's<sup>34,85,86,144</sup>. Here,  $\text{CaCl}_2$  is added as a flocculant to the same samples described in Sections 5.2 and 5.3. The mass ratio of  $\text{CaCl}_2 \cdot 2\text{H}_2\text{O}$  to kaolinite was constant at 0.1 for all of the samples. The addition of  $\text{CaCl}_2$  was done after increasing the sample pH to about 11. At that high sample pH most of the aggregates and flocs are broken to individual particles<sup>81</sup>, as described in Section 5.3. The addition of  $\text{CaCl}_2$  decreases the thickness of the electric double layer surrounding the particles and results in a reduction in the electrostatic repulsion between faces<sup>86</sup>. Under these conditions, high density aggregates produces through F-F (face-to-face) associations are expected. These associations are sometimes referred as “card-pack” flocs. Figures 5.9 through 5.12 compare the samples PSD's at a natural pH (no NaOH addition) with that of samples with the addition of  $\text{CaCl}_2$  at a high pH. It can be seen from these graphs that the population of large particles significantly increases after flocculant addition. It is also noticeable that samples with low concentrations are more affected by the addition of  $\text{CaCl}_2$  compared to the sample with  $c=40$  g/L. These results are consistent with previous studies in the literature<sup>86</sup>.



**Figure 5.9. Effect of flocculant addition on the kaolinite PSD ( $c=40$  g/L)  
 pH = 4.6 (no flocculant), pH~11 (flocculant added)  
 CaCl<sub>2</sub>.2H<sub>2</sub>O: Kaolinite (mass ratio) = 0.1**

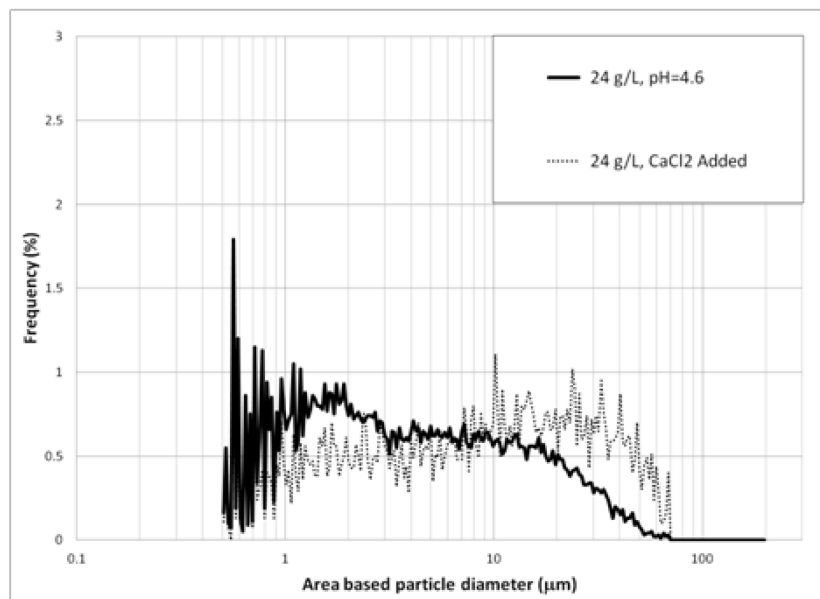


**Figure 5.10. Effect of flocculant addition on the kaolinite PSD ( $c=24$  g/L)  
 pH ~4.6 (no flocculant), pH~11 (flocculant added)  
 CaCl<sub>2</sub>.2H<sub>2</sub>O: Kaolinite (mass ratio) = 0.1**

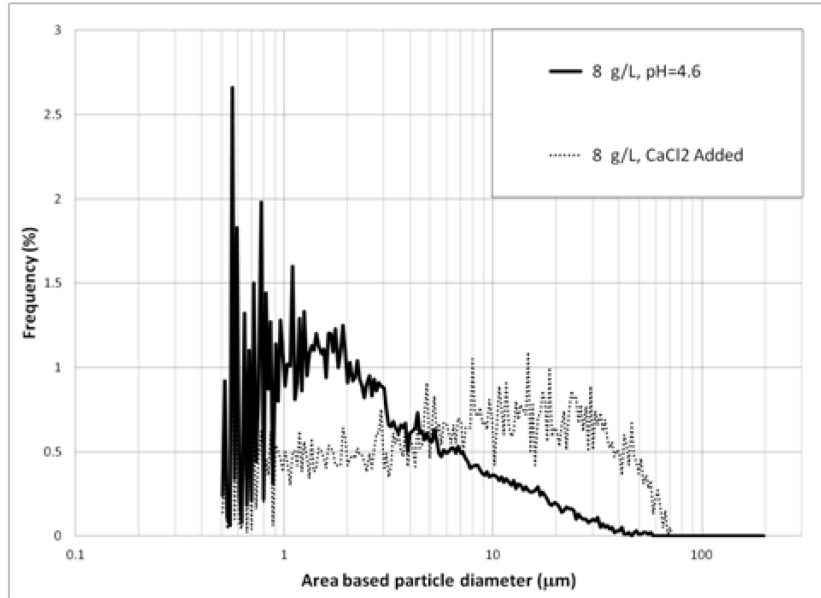


**Figure 5.11. Effect of flocculant addition on the kaolinite PSD (c=8g/L)  
 pH ~4.6 (no flocculant), pH~11 (flocculant added)  
 CaCl<sub>2</sub>.2H<sub>2</sub>O: Kaolinite (mass ratio) = 0.1**

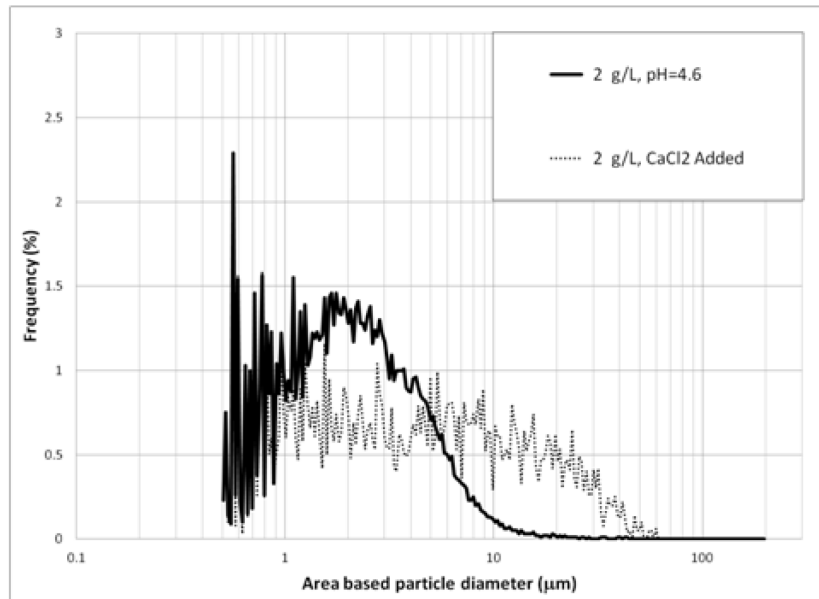


**Figure 5.12. Effect of flocculant addition on the kaolinite PSD (c=2g/L)  
 pH ~4.6 (no flocculant), pH~11 (flocculant added)  
 CaCl<sub>2</sub>.2H<sub>2</sub>O: Kaolinite (mass ratio) = 0.1**

Figure 5.13 illustrates the Sauter mean diameter ( $d_{32}$ ) for the samples used in this section. The solid circles show the  $d_{32}$  of samples with different kaolinite concentrations (no NaOH addition, no flocculant addition,). The solid triangles show the  $d_{32}$  of the same samples at high suspension pH and the solid squares show the  $d_{32}$  of these samples after flocculant addition (at high pH). The results of Figure 5.13 indicate that at each concentration, samples with high pH (no flocculant addition) have the smallest particle sizes while the flocculated samples contain the largest particles. Figure 5.13 shows the conditions at which the kaolinite suspensions studied here have the largest and smallest particle sizes. These conditions were used to select the samples for the study of the effect of sonication on the kaolinite suspension PSD.

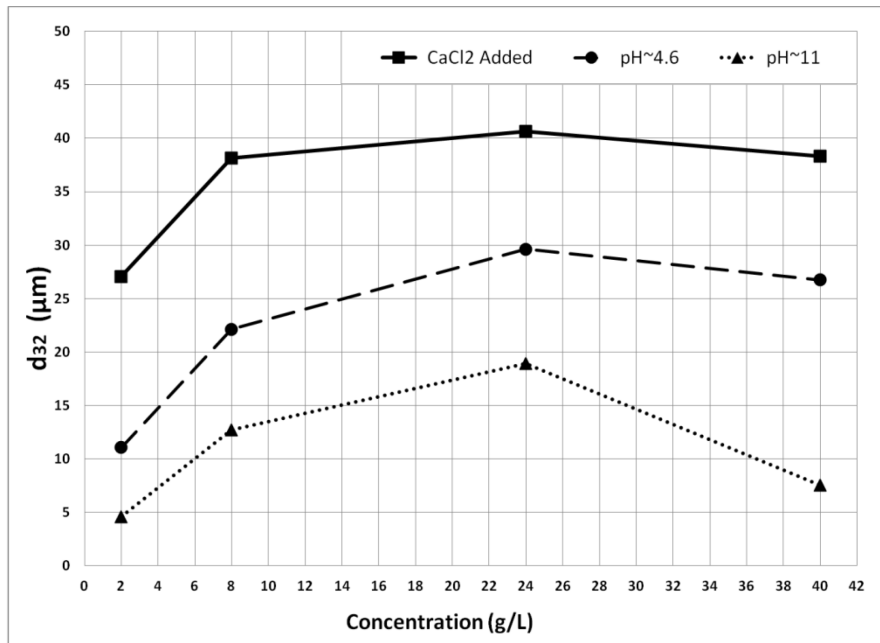


**Figure 5.13. Sauter mean diameter of kaolinite suspensions ( $c=2, 8, 24, 40$  g/L) at three conditions: a) pH~4.6, no NaOH addition, no flocculant addition; b) pH ~11 (NaOH added); c) pH ~11 and flocculant addition,  $\text{CaCl}_2 \cdot 2\text{H}_2\text{O}$ : Kaolinite (mass ratio) = 0.1**

The selection of solids concentrations for the sonication tests has two limitations. The fact is that water-based mixtures containing clays in the oil sands extraction process usually have high solids concentrations. However, the FPIA is not able to produce reliable measurements at concentrations above 40 g/L. Therefore, the upper limit of solids concentration is chosen as 40 g/L in this work. The lower limit of the kaolinite concentration is chosen as 10 g/L. An intermediate solids concentration of 20 g/L was also selected for testing. By selecting a range of kaolinite suspension concentrations, it is possible to investigate the combined effects of concentration and sonication on kaolinite PSD's (Section 6.5).

## **5.5. Summary**

The main factors that affect the kaolinite PSD are studied in this chapter. The results presented in this chapter are used to determine appropriate conditions at which the main samples need to be tested for the study of sonication effect on the kaolinite PSD. Furthermore, presented results indicate that the kaolinite PSD can be significantly affected by sample pH and the flocculant addition. Therefore, in addition to the study of the samples with different solids concentration, effect of sonication on the particle size of samples with different pH values and different flocculant additions should be investigated.

On the other hand, the consistency of the results presented in this chapter to the previous studies in the literature indicates that the FPIA produces reliable results in the solids concentration range and the sample conditions applied in this work.

## 6. The effect of sonication on kaolinite PSD

### 6.1 Introduction and objectives

In the previous chapters of this study, three important results were described:

- It was proven that the sample preparation procedure and subsequent analysis with the FPIA yields reproducible results;
- Critical pre-sonication procedures, including mixing and sample cooling, do not impact the sample PSD; and
- The sample PSD responds in an expected way to changes in pH and/or flocculant addition

The main objective of the present study will be addressed in this chapter. With the effects of the experimental parameters characterized, it is now possible to study the effect of sonication on the kaolinite PSD. Three samples with concentrations of 10 g/L, 20 g/L, and 40 g/L are selected to study the effect of sonication. Figure 6.1 shows the sample PSD at each concentration before sonication. It should be noted that the pH of these samples is about 4.6 (no electrolyte addition) and there is no flocculant addition.

The sonication process should be investigated from two points of view: energy source and energy target. The energy source is a Sonicator-4000 which delivers sonication energy. Recall that the two controlling parameters are *sonication time* and *sonication amplitude*. The energy target is the kaolinite clay suspension. As

discussed in Chapter 5, the nature of the initial particle size distribution of the kaolinite clay is controlled by three dominant parameters: *kaolinite concentration*, *mixture pH*, and *flocculant addition*. Therefore, the influence of each of these parameters need to be investigated along with the effect that sonication has on the kaolinite PSD.

Section 6.2 describes the effect of sonication time on the kaolinite clay PSD. After validating these results with other techniques (Section 6.3), the effect of sonication amplitude on the kaolinite PSD is discussed in Section 6.4. All of the experiments described in Section 6.2 and 6.4 are carried out on samples with three different concentrations. In Sections 6.5 and 6.6 two case studies have been used to investigate the sonication effect on samples having different pH values and on flocculated samples, respectively. Finally, the effect of sonication on the PSD of an industrial tailings sample is evaluated.

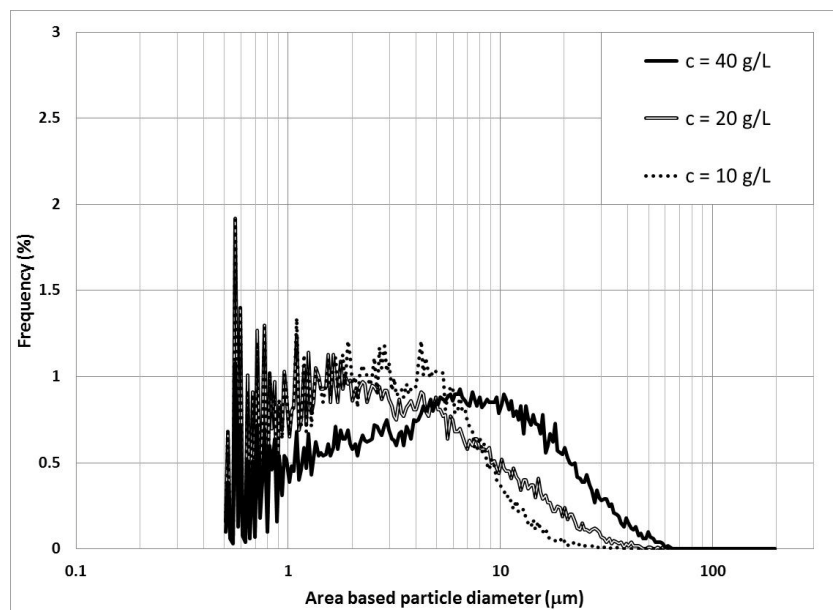


Figure 6.1 Kaolinite PSD for non-sonicated samples:  $c=10, 20,$  and  $40$  g/L;  $pH\sim 4.6$

## 6.2. Effect of sonication time

Different concentrations of kaolinite clay in de-ionized water were continuously sonicated for periods ranging from 10 seconds to 60 minutes to measure the impact of sonication. For this set of experiments, the experimental matrix shown in Table 6.1 was designed. As Table 6.1 indicates, three different concentrations of kaolinite clay (10, 20, and 40 g/L) with a total sample volume of 140 mL were prepared. These three samples were subjected to continuous sonication with three amplitudes of 50%, 75%, and 100%. For each of these amplitudes, the PSD was measured at 9 sonication times: 0 seconds, 10 seconds, and 5, 10, 20, 30, 40, 50, and 60 minutes.

**Table 6.1 Experimental matrix for the investigation of the effects of sonication time, sonication amplitude and sample concentration on kaolinite PSD**

Concentration (g/L)	Sonication amplitude (%)	Sonication time (minutes)								
		0	0.17	5	10	20	30	40	50	60
40	100%	0	0.17	5	10	20	30	40	50	60
	75%	0	0.17	5	10	20	30	40	50	60
	50%	0	0.17	5	10	20	30	40	50	60
20	100%	0	0.17	5	10	20	30	40	50	60
	75%	0	0.17	5	10	20	30	40	50	60
	50%	0	0.17	5	10	20	30	40	50	60
10	100%	0	0.17	5	10	20	30	40	50	60
	75%	0	0.17	5	10	20	30	40	50	60
	50%	0	0.17	5	10	20	30	40	50	60

### 6.2.1. Comparison of particle size distributions

Figures 6.2 through 6.4 illustrate the differences in the PSD's for samples with concentrations of 10, 20, and 40 g/L, with PSD's measured after specific sonication times. The sonication amplitude is set at 100% for these tests. Results for lower amplitudes (50% and 75%) are shown in Appendix D.

These graphs show a decrease in the percentage of particles in the size range of 2.5 to 25  $\mu\text{m}$  (40 g/L), 1.5 to 15  $\mu\text{m}$  (20 g/L), and greater than 1.5  $\mu\text{m}$  (10 g/L). It can be seen from Figures 6.2 through 6.4 that the number of particles smaller than stated concentration-specific size ranges increases after sonication. Additionally, a slight increase in the number of particles larger than 25  $\mu\text{m}$  in the 40 g/L sample, and 15  $\mu\text{m}$  in the 20 g/L sample occurs.

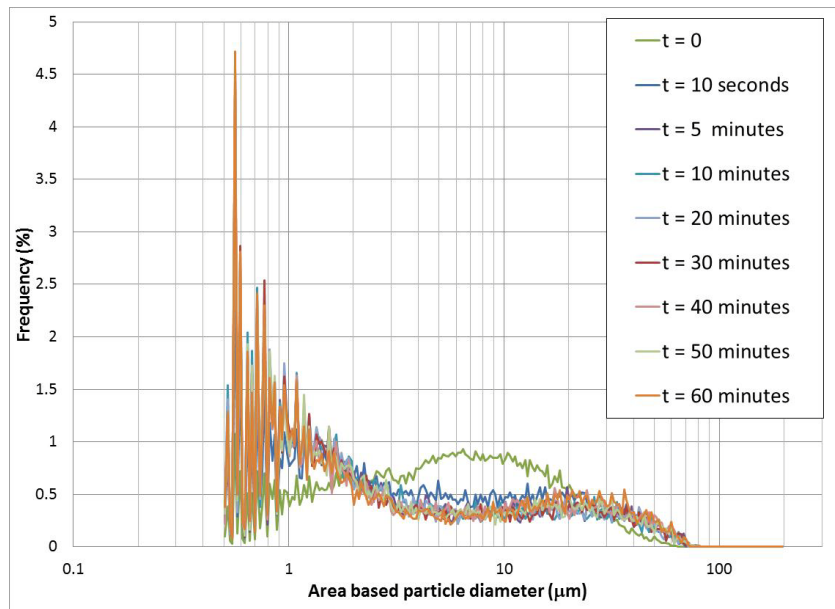


**Figure 6.2 Effect of sonication time on the kaolinite PSD: c=40 g/L; pH~4.6; Sonication amplitude: 100%**

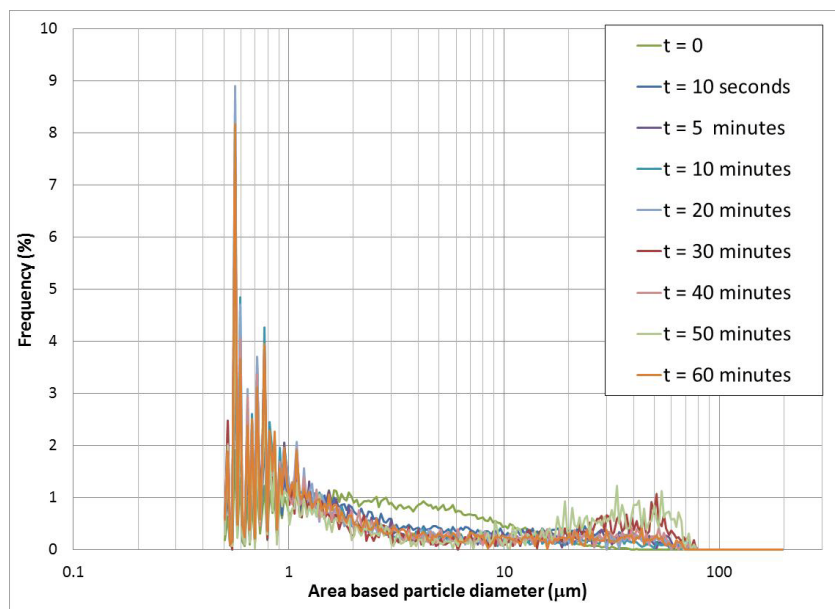


**Figure 6.3 Effect of sonication time on the kaolinite PSD: c=20 g/L; pH~4.6; Sonication amplitude: 100%**

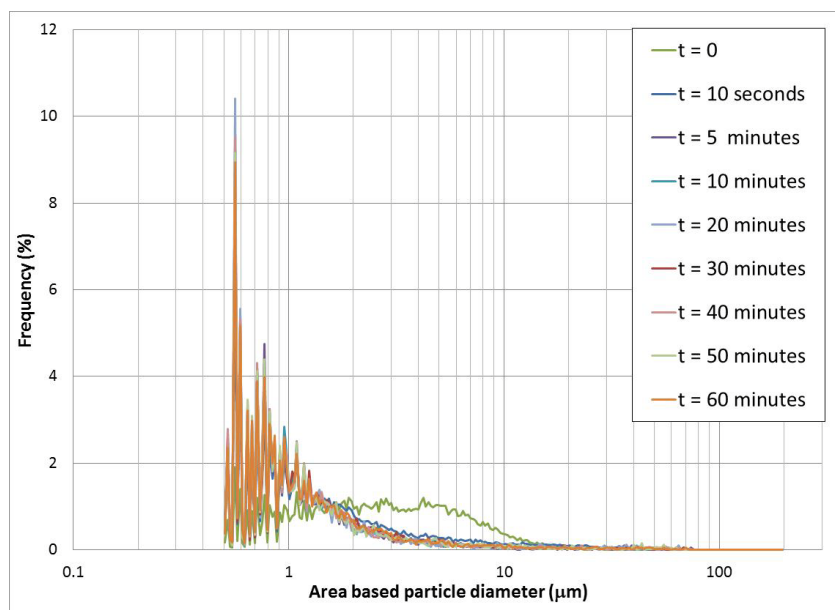


**Figure 6.4 Effect of sonication time on the kaolinite PSD: c=10 g/L; pH~4.6; Sonication amplitude: 100%**

These results illustrate that sonication alters the kaolinite clay PSD such that the proportion of large particles decreases while the proportion of the fine particles

increases. This overall reduction of particle size occurred for all the sonication times and amplitudes tested here.

Size reduction due to sonication was most noticeable within the first 10 minutes of sonication. The sample PSD did not change for sonication times greater than 10 minutes. As discussed in Section 2.6, sonication of slurries consisting of solid particles in a liquid leads to agitation of particles and formation of shock-waves and microjets in the liquid medium<sup>87</sup>. The agitation of particles results in an increased frequency of inter-particle collisions<sup>87</sup>, which can lead to agglomeration of particles or breakage of aggregates<sup>89</sup>. On the other hand, the shock-waves and microjets can cause particle size reduction<sup>87</sup>. Therefore, both particle-size reduction and agglomeration of particles should be expected. This can explain the formation of a small number of “large” particles (greater than 25  $\mu\text{m}$ ), as seen in Figures 6.2 and 6.3. In some cases, the ultrasound-activated particles form large aggregates<sup>23,77</sup>, which has been observed in previous studies<sup>77</sup>. Delgado and Matiyevic<sup>23</sup> suggested that prolonged sonication, especially with a probe sonicator, can promote the aggregation of colloidal particles. Similar results were obtained in subsequent study by Peters<sup>87</sup>.

Sonication time and power determine the amount of energy delivered to the sample<sup>89</sup>. Table 6.2 shows the amount of energy delivered to each sample during the experiments. Sonication power is displayed on the Sonicator-4000 screen during each treatment. The total amount of energy delivered to the sample is calculated based on Eq 2.8. The results of Table 6.2 show that by increasing the

sonication time, the amount of sonication energy delivered to the sample increases significantly. However, this does not result in continued size reduction. Figures 6.2 through 6.4 show that a certain number of particles (in the size range of 2 to 20  $\mu\text{m}$ ) remain intact after sonication. Although the delivered sonication energy during 60 minutes is about six times greater than that delivered during the first 10 minutes, the population of this fraction of particles does not change after 10 minutes of sonication. The effect of sonication on the kaolinite clay PSD is a function of the number of particle-particle attachments in the flocs and aggregates structures and the energy required to break down any such attachments.

**Table 6.2 The amount of sonication energy delivered to each sample as a function of sonication time and amplitude**

Concentration (g/L)	Amplitude (%)	Power (W)	Sonication time			
			10 sec	5 min	10 min	60 min
			Sonication energy (J)			
40	100	73	730	21 900	43 800	248 000
	75	57	570	17 100	34 200	196 000
	50	42	420	12 600	25 200	142 000
20	100	75	750	22 500	45 000	253 000
	75	56	560	16 800	33 600	192 000
	50	41	410	12 300	24 600	139 000
10	100	77	770	23 100	46 200	252 000
	75	56	560	16 800	33 600	192 000
	50	41	410	12 300	24 600	141 000

The platelet-shaped kaolinite particles can associate in edge-to-edge (EE), edge-to-face (EF), and face-to-face (FF) modes<sup>82</sup>. The energy required to separate two kaolinite particles attached in the F-F association is greater than that for E-F, which in turn is greater than the separation energy required for the E-E configuration<sup>145,146</sup>. The reason why sonication cannot separate some of the particle-particle linkages may be related to the fact that the delivered sonication energy is not sufficient to separate F-F associations.

### **6.2.2. Comparison of populations of primary particles, flocs, and aggregates**

Up to this point, it was qualitatively observed that sonication altered the kaolinite PSD such that large particles were broken down into smaller particles. Comparing the PSD graphs (Figures 6.2 through 6.4), it can be observed that the influence of sonication on the PSD is not the same for all of the conditions tested. The full size range of particles was divided into three regions, which are shown in Table 6.3, to better quantify the effect of sonication on the kaolinite samples. The first size region ( $< 2 \mu\text{m}$ ) is defined based on the kaolinite primary particle size, reported as 0.1 to  $2 \mu\text{m}$ <sup>80,81</sup>. Particles smaller than  $2 \mu\text{m}$  are defined as individual or primary particles in this study.

The results of Section 6.2.2 showed that particles larger than  $2 \mu\text{m}$  can be divided to two size range based on their response to the sonication. Specifically, the proportion of particles in the size ranges of 2 to  $20 \mu\text{m}$  decreases significantly after sonication, while the proportion of particles larger than  $20 \mu\text{m}$  increases slightly during the first 10 minutes of sonication and remains approximately

constant afterwards. The different responses of these particles to sonication is the reason that two additional size ranges are defined in Table 6.3. The particles in these size regions are larger than individual particles. This means they are flocs or aggregates of primary particles. There is not a clear particle size range defined (or calculated) for flocs and/or aggregates in the literature. Both flocs and aggregates are groups of individual particles joined together to form a larger cluster. Michaels and Bolger<sup>80</sup> defined flocs as small clusters of particles and aggregates as clusters of flocs grouped together. Considering this definition, the particles in the size range of 2 to 20  $\mu\text{m}$  are defined as flocs in this study. Particles larger than 20  $\mu\text{m}$  are defined as aggregates. An exact boundary does not exist so a reasonable value was selected for this study.

**Table 6.3 Particle size range classifications used in the present study**

<b>Classification</b>	<b>Definition</b>
<i>Individual particles</i>	$d < 2 \mu\text{m}$
<i>Flocs</i>	$2 \mu\text{m} \leq d \leq 20 \mu\text{m}$
<i>Aggregates</i>	$20 \mu\text{m} < d$

Figures 6.5 through 6.7 illustrate the proportions of these regions for the 10 g/L, 20 g/L and 40 g/L samples as a function of sonication time. The sonication amplitude is 100% (120  $\mu\text{m}$ ) in these tests. Similar results for lower amplitudes (75% and 50%) are shown in Appendix E.

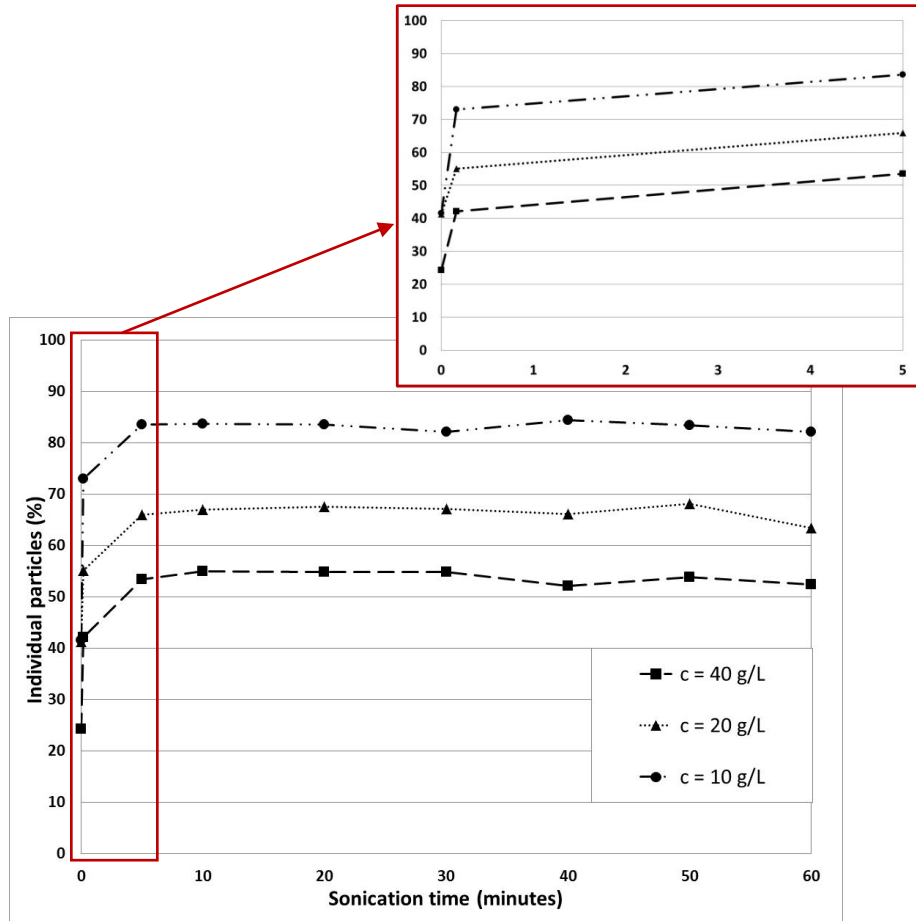
Figure 6.5 demonstrates that the percentage of individual particles always increases after sonication. While the extent of this increase depends on the kaolinite concentration and the sonication time, it occurs in every sample. Furthermore, Figure 6.5 illustrates that although there is a sharp increase in the percentage of individual particles during the first 10 minutes of sonication, this percentage does not change significantly with continued sonication ( $t > 10$  minutes).

Figure 6.6 also indicates that the percentage of flocs always decreases after sonication. The extent of this reduction also depends on the solids concentration and sonication time. As was the case for the individual particles, a significant reduction in the number of flocs occurs during the first 10 minutes of sonication. Between 10 minutes and 60 minutes of sonication, the percentage of flocs changes very little compared to the initial decrease in their population.

It is notable that even 10 seconds of sonication has a significant impact on the percentage of flocs in all three samples.

The results of Figure 6.7 indicate that the percentage of aggregates also increases through sonication. It is worth noting that the aggregates constitute a small portion of the entire particle size distribution for each of the three samples tested in this study. Before sonication, approximately 0.5% to 10% of the population is aggregates, while 56-66% is flocs and 24-42% is individual particles. After 60 minutes of sonication, the percentage of aggregates increases so that they now

represent 1.7% to 16% of the population, while this range is 16-32% of the particles are in the ‘floc’ size range, while 53-82% are individual particles.



**Figure 6.5 Proportion of the dispersed phase population of primary particles, expressed in %, as a function of sonication time, for sample concentrations of 10, 20, and 40 g/L. Sonication amplitude: 100%**

In summary, Figures 6.5 through 6.7 illustrate that through sonication the percentage of flocs is reduced. They are mostly broken down to individual particles, except for a few which form aggregates. Equation 6.1 shows the relationship among the three size classifications used in this study. The total percentage of the three regions adds to 100%. Based on Equation 6.1, the variation in the percentage of flocs at any time is equal to the summation of

variations in the percentage of individual particles and the percentage of aggregates (see Equation 6.2).

$$\% \text{ Individual particles} + \% \text{ Flocs} + \% \text{ Aggregates} = 100 \quad (6.1)$$

$$\Delta(\% \text{ Flocs}) = \Delta(\% \text{ Individual particles}) + \Delta(\% \text{ Aggregates}) \quad (6.2)$$

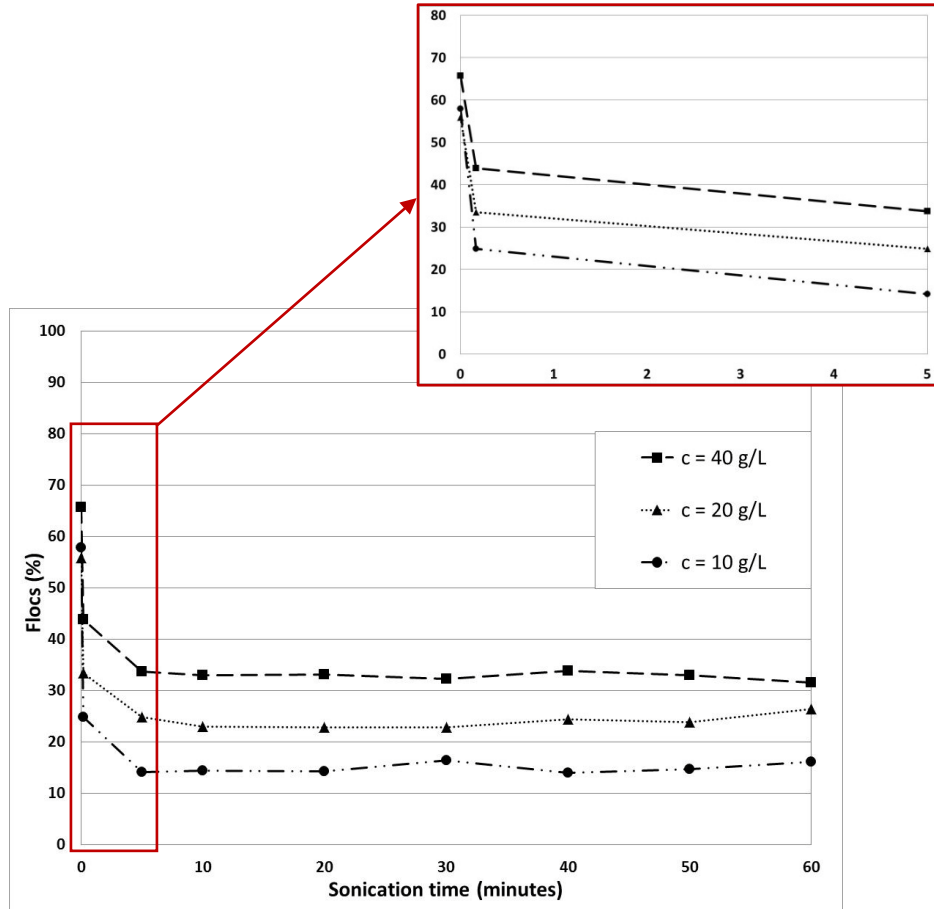


**Figure 6.6** Proportion of the dispersed phase population of flocs, expressed in %, as a function of sonication time, for sample concentrations of 10, 20, and 40 g/L. Sonication amplitude: 100%

Considering the results shown up to this point along with Equations 6.1 and 6.2, the floc population is selected as the parameter which best represents the size

reduction due to sonication. The percentage of flocs universally decreases regardless of sonication time, sonication amplitude, and solids concentration.

### **6.2.3. Evaluation of the Floc Reduction Ratio (FRR)**

To quantify the effect of sonication on particle size reduction, the floc reduction ratio (FRR) is defined as the ratio of the percentage of flocs at each time to the percentage of the flocs in the sample before sonication. The FRR parameter allows for the analysis of changes in the floc population independent of the initial values:

$$\text{FRR} = \frac{\% \text{Flocs (t)}}{\% \text{Flocs (t=0)}} \quad (6.3)$$

Figure 6.8 illustrates the calculated FRR at each sonication time, for the three different concentrations. The amplitude in these tests is set at 100% (120  $\mu\text{m}$ ). Similar results for lower amplitudes (75% and 50%) are shown in Appendix F. It should be noted that in contrast to graphs showing the number of flocs (as a % of the population), the FRR graphs start with an initial value of one. All values fall between zero and one for all sonication times.

The results shown in Figure 6.8 indicate that for the 10 g/L sample, sonication breaks down 75% of the flocs that were initially in the suspension. Additionally, 58% of the flocs are broken during the first 10 seconds of sonication. The remaining 17% are broken down between 10 seconds and 5 minutes of sonication. Sonication time longer than 10 minutes did not change the FRR significantly.

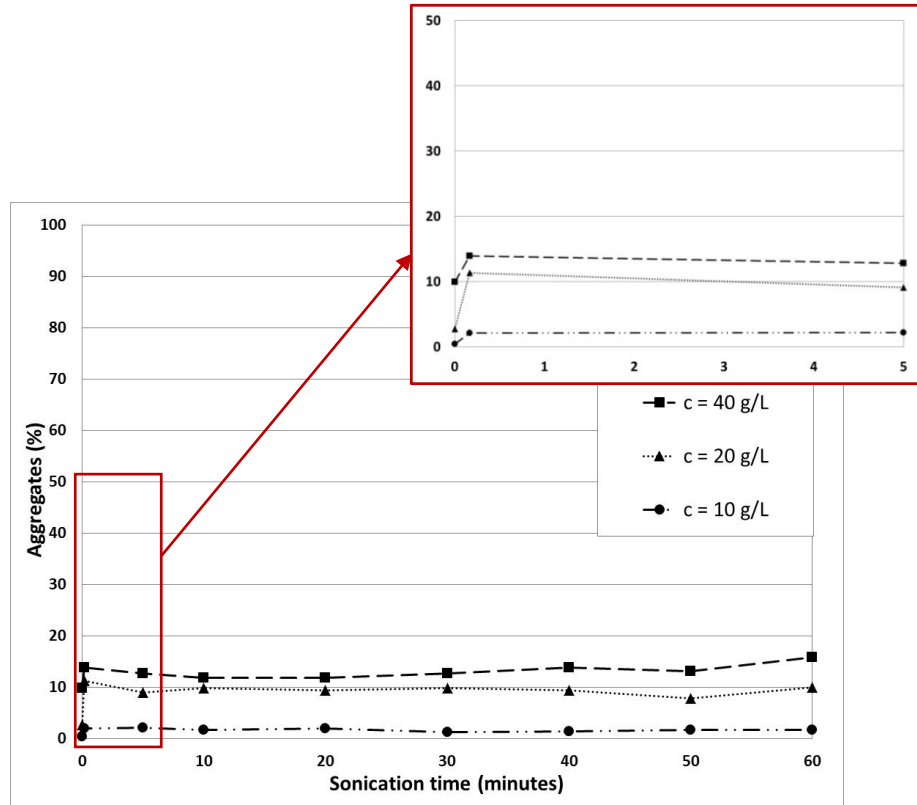


**Figure 6.7 Proportion of the dispersed phase population of aggregates, expressed in %, as a function of sonication time, for sample concentrations of 10, 20, and 40 g/L. Sonication amplitude: 100%**

For the 20 g/L sample, 40% of the flocs are broken during the first 10 seconds of sonication. This number increases to 56% at 5 minutes and 59% at 10 minutes of sonication. After 10 minutes, continued sonication results in a slight increase in the FRR, with the final value approaching 48%. As discussed earlier, the ultrasound-activated particles experience more inter-particle collisions; in other words, flocs and aggregates can also form during sonication.

For the 40 g/L sample, the percentage of flocs in the sample after sonication is 50%. During first 10 seconds of sonication, 32% of the flocs are broken. Between

10 seconds and 5 minutes the remaining 18% also disappear from the floc size range, through size reduction (primarily) and aggregation.

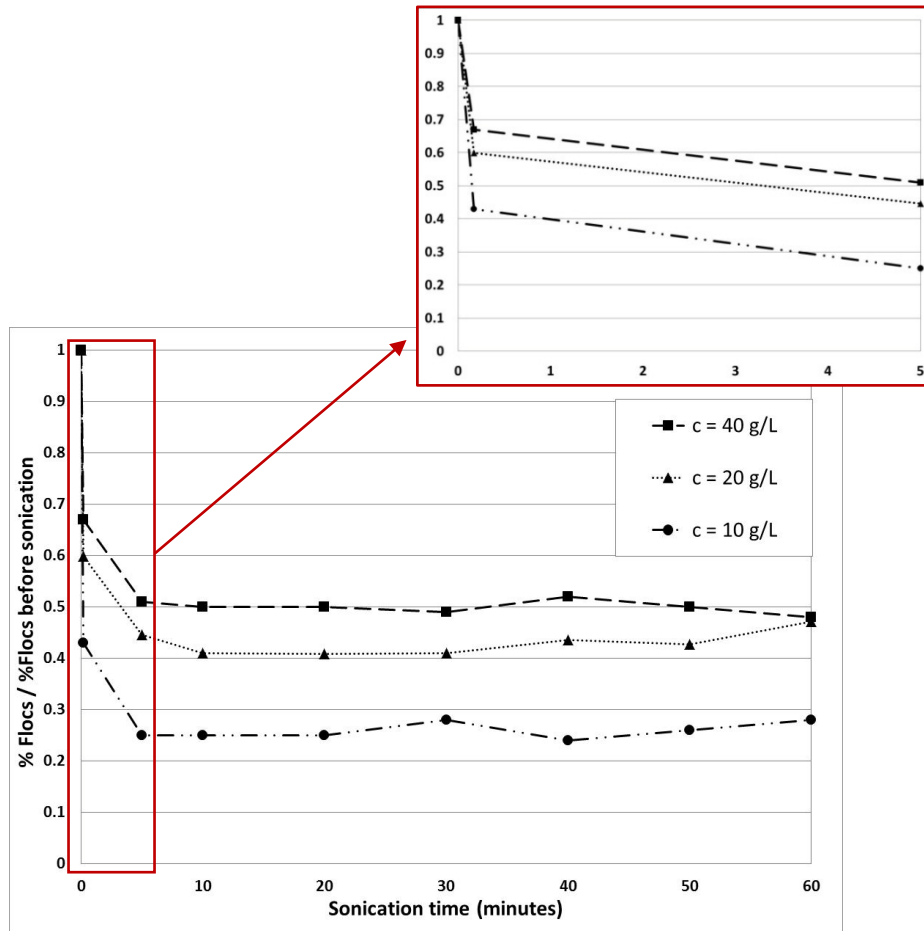


Figure 6.8 Floc reduction ratio (FRR) at each sonication time:  $c=10, 20,$  and  $40 \text{ g/L}$ ; Sonication amplitude: 100%

#### 6.2.4. The influence of solids concentration

The experimental results presented thus far demonstrate that the sonication effect on the kaolinite PSD is dependent upon sample concentration. It can be seen in Figures 6.5 and 6.6 that the  $40 \text{ g/L}$  sample has the lowest change in the percentage of individual particles and flocs while the  $10 \text{ g/L}$  sample has the greatest. These observations suggest that dilute samples are more affected by sonication than

more concentrated ones. Additionally, the variation of floc reduction ratio (FRR) with sonication time is shown in Figure 6.8. The results shown in this figure indicate that at all sonication times, the size reduction has its highest value in the sample with  $c=10$  g/L and its lowest value in the sample with  $c=40$  g/L.

Recall that Figure 6.1 compares the initial sample PSD (non-sonicated samples) for three kaolinite mixtures that are the primary focus of this study. This figure shows that the 40 g/L sample contains more flocs and aggregates (particles larger than 5  $\mu\text{m}$ ) than the 20 g/L sample. It also illustrates that there are no aggregates (larger than 20  $\mu\text{m}$ ) in the 10 g/L sample prior to sonication. Furthermore, the number of flocs in the size range of 8-20  $\mu\text{m}$  is the lowest in the dilute (10 g/L) sample. The results shown in Figure 6.1 verify that by increasing the concentration of samples the chance of particle-particle collision increases and this leads to production of more randomly formed flocs and aggregates.

Since the total amount of sonication energy is similar for three samples, the same amount of energy is introduced to samples with different populations of flocs and aggregates. Under these conditions, the sample with fewer flocs and aggregates will be more greatly affected by sonication because the energy received by each floc or aggregate is higher. This finding supports the aforementioned theory that samples with lower concentrations are more strongly affected by sonication.

## 6.3. Validation of results

### 6.3.1. Laser diffraction method

Particle size distribution of a kaolinite mixture was analyzed with a Malvern Mastersizer-2000 before and after sonication. A set of experiments which were previously done using the FPIA (Section 6.2) were repeated. The sample PSD's for mixtures with  $c=40$  g/L and  $c=10$  g/L were measured with the Mastersizer. This sample was then sonicated with the Sonicator-4000 with 100% amplitude for periods of time up to 60 minutes. Only the results obtained for the 40 g/L are presented here. The results for the 10 g/L sample are provided in Appendix G. They follow similar trends as shown here for the 40 g/L sample.

Figures 6.9 show the particle size distributions in terms of *percentage of total particle volume* versus *particle diameter* for the 40 g/L kaolinite suspension subjected to sonication for different amounts of time.

Before sonication, the kaolinite particle size distribution is broad but monomodal, with modal size centered at 8  $\mu\text{m}$ . After 3 min of sonication the curve still shows monomodal particle size distribution but it is narrower compared to the initial PSD (sample with no sonication) and the modal size is shifted to 4.08  $\mu\text{m}$ . After 10 minutes of sonication the size distribution becomes a bimodal with the modal sizes centered at 4.7  $\mu\text{m}$  and 0.15  $\mu\text{m}$ . A small volume that represents very large particles (with the particle size around 780  $\mu\text{m}$ ) is detected in the sample after 10 minutes of sonication.

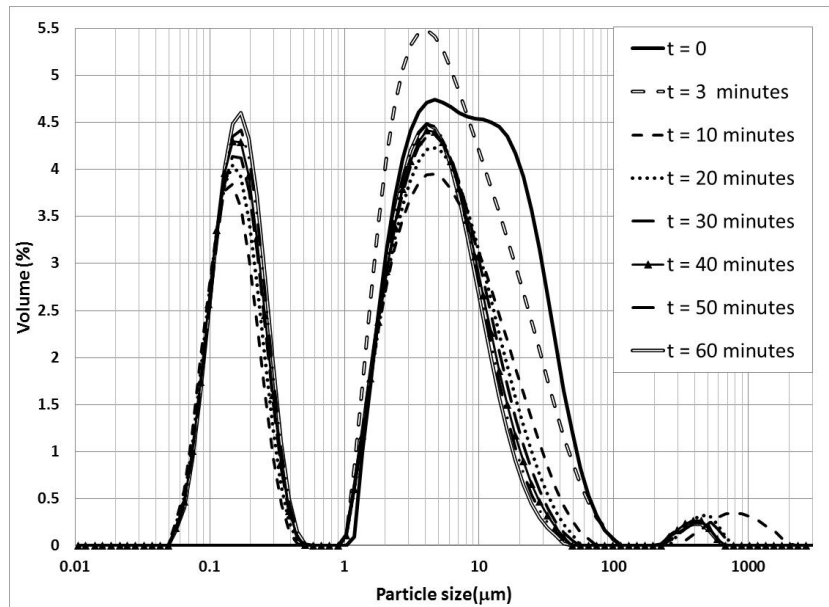


**Figure 6.9 Kaolinite PSD after different sonication times measured by Malvern Mastersizer  $c=40$  g/L, Sonication times: 0, 3, 10, 20, 30, 40, 50 and 60 minutes, Sonication amplitude: 100%**

After 20 minutes of sonication, the curve is bimodal with the same modal sizes as at 10 minutes. Comparing the two last curves (10 minutes and 20 minutes sonication), very large particles sizes shifted from  $780 \mu\text{m}$  to  $450 \mu\text{m}$  with a slight decrease in their volume percentages (from 0.35% to 0.32%). Furthermore, between 10 and 20 minutes of sonication, a decrease in the volume percentage of particles in the size range of  $10 \mu\text{m}$  to  $75 \mu\text{m}$  occurs. At the same time, there is an increase in the volume percentage of particles in the size ranges of  $2 \mu\text{m}$  to  $10 \mu\text{m}$  and  $0.13 \mu\text{m}$  to  $0.5 \mu\text{m}$ . Between 20 and 60 minutes of sonication, there is not a significant change in the particle size distribution of the sample; however, there is a slight decrease in the volume percentage of particles in the size range of  $5 \mu\text{m}$  to  $60 \mu\text{m}$  and an increase in the volume percentage of particles in the  $2 \mu\text{m}$  to  $7 \mu\text{m}$  range. In this same time interval, the population of smaller particles (with modal

size centered at 0.15  $\mu\text{m}$ ) continuously increases from 4.05% to 4.60%. In addition the portion of very large particles shifts from modal size of 450  $\mu\text{m}$  to 390  $\mu\text{m}$  with a slight decrease in the particles' volume percentages from 0.32% to 0.23%.

Figure 6.10 shows the Sauter mean diameter ( $d_{32}$ ) of the kaolinite clay sample as a function of sonication time. The Sauter mean diameter ( $d_{32}$ ) in this graph is calculated by the Malvern Mastersizer 2000 software. It can be seen that there is a significant decrease in the mean diameter of the sample after 10 minutes of sonication. Although there is a slight decrease in the mean size of the samples between 10 and 60 minutes of sonication, changes in the mean diameter are negligible.

The results presented here are in agreement with the FPIA results discussed in Section 6.2: specifically, that sonication breaks flocs into the individual particles. The modal size of 0.15  $\mu\text{m}$  shown in Figure 6.9 is approximately the primary particle size of kaolinite used in this study (as reported by the producer). This verifies that the production of individual particles is the dominant effect of sonication. In addition, the formation of large aggregates is also confirmed by the results obtained using a laser diffraction method. Finally, the Mastersizer measurements are in good agreement with the FPIA results, as both show that a significant size reduction occurs in the first 10 minutes of sonication (see Figure 6.10).

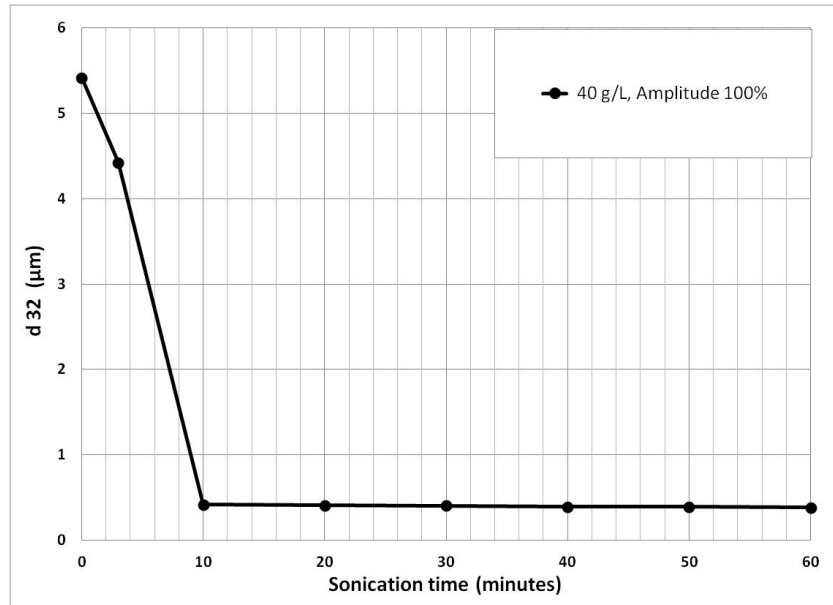


**Figure 6.10 Sauter mean diameter (d<sub>32</sub>) of kaolinite sample at different sonication times measured by Malvern Mastersizer software; c=40 g/L; Amplitude: 100%**

### 6.3.2. Cryogenic SEM studies

Cryogenic Scanning Electron Microscope (Cryo-SEM) studies were conducted using kaolinite suspensions with c=10 and 20 g/L. These samples were sonicated for 30 minutes with 100% amplitude. Table 3.3 in Chapter 3 shows characteristics of four samples visually studied by Cryo-SEM. Because the results obtained at the two concentrations are similar, only the results obtained at 20 g/L are discussed here. The results for the more dilute samples (10 g/L) are presented in Appendix H.

Figures 6.11 through 6.14 show images of the kaolinite clay particles, before and after sonication, at magnifications of 1000 and 2000X. Comparing each pair of images (Figure 6.11 with 6.12 and Figure 6.13 with 6.14), it can be seen that there

is a significant change in the size of the kaolinite particles. Figures 6.12 and 6.14 show that after 30 minutes of sonication the networks of particles break down to smaller flocs and aggregates.

It is noticeable in both Figure 6.12 and Figure 6.14 that the number of particles detected is increases after sonication. This suggests that aggregates and flocs are broken down to a number of smaller flocs and individual particles. In Figure 6.11 and Figure 6.13 (before sonication), the particles appear to be mostly in the 10 to 20  $\mu\text{m}$  size range, whereas in Figure 6.12 and Figure 6.14 (after sonication) particle sizes are reduced to  $\leq 5 \mu\text{m}$ . It should be noted that although some large aggregates can still be seen in Figures 6.12 and 6.14, the number of detected particles smaller than 2  $\mu\text{m}$  has increased significantly. Comparing the overall sizes of particles in Figures 6.11 through 6.14 with the sample PSD measured with the FPIA, shown in Figure 6.15, it can be seen that there is good agreement between the FPIA 3000 measurements and the Cryo-SEM images.

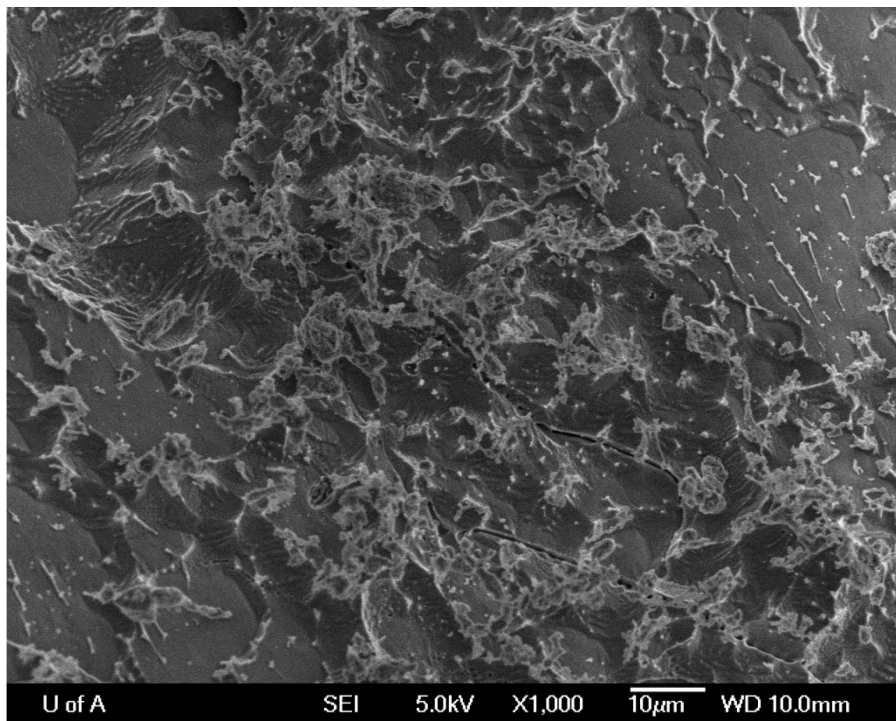


Figure 6.11 Cryo-SEM image of non-sonicated kaolinite sample; sample (1-1); c=20 g/L, 1000X

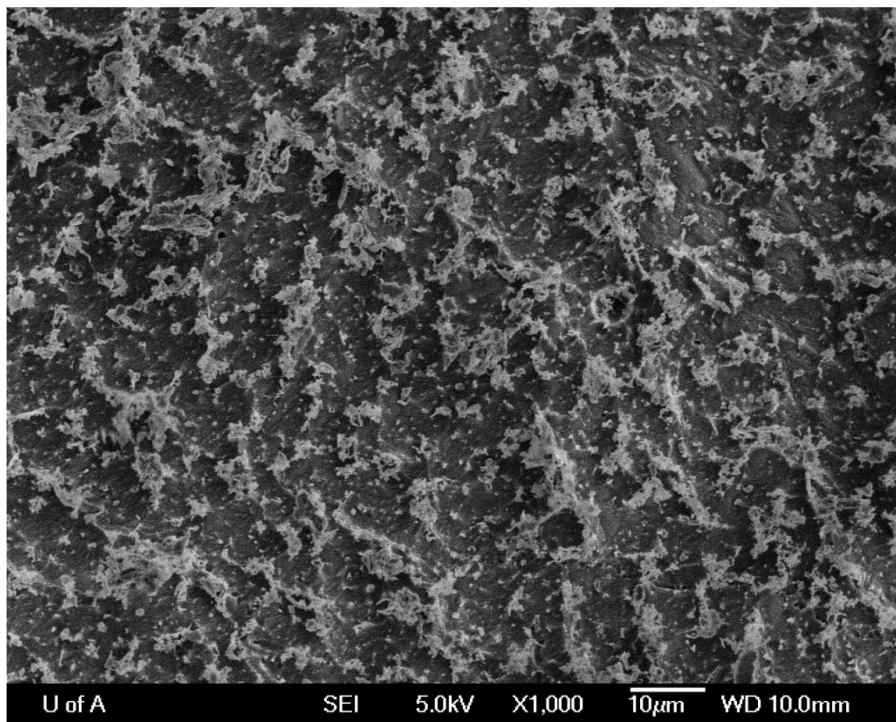


Figure 6.12 Cryo-SEM image of sonicated kaolinite sample; sample (1-2); c=20 g/L; 1000X; sonication time: 30 minutes; amplitude: 100%

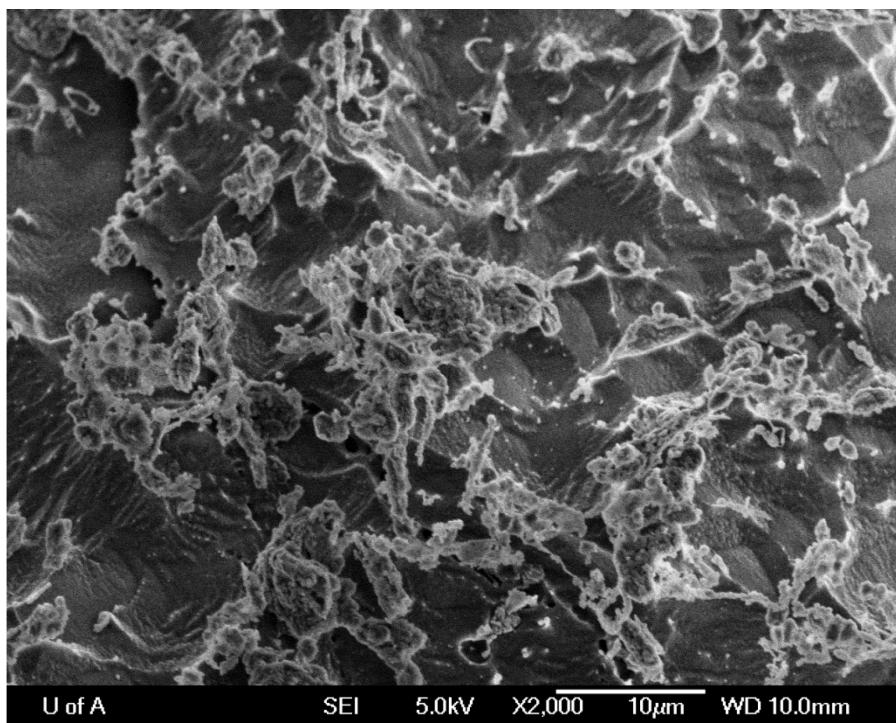


Figure 6.13 Cryo-SEM image of non-sonicated kaolinite sample; sample (1-1);  $c=20$  g/L, 2000X

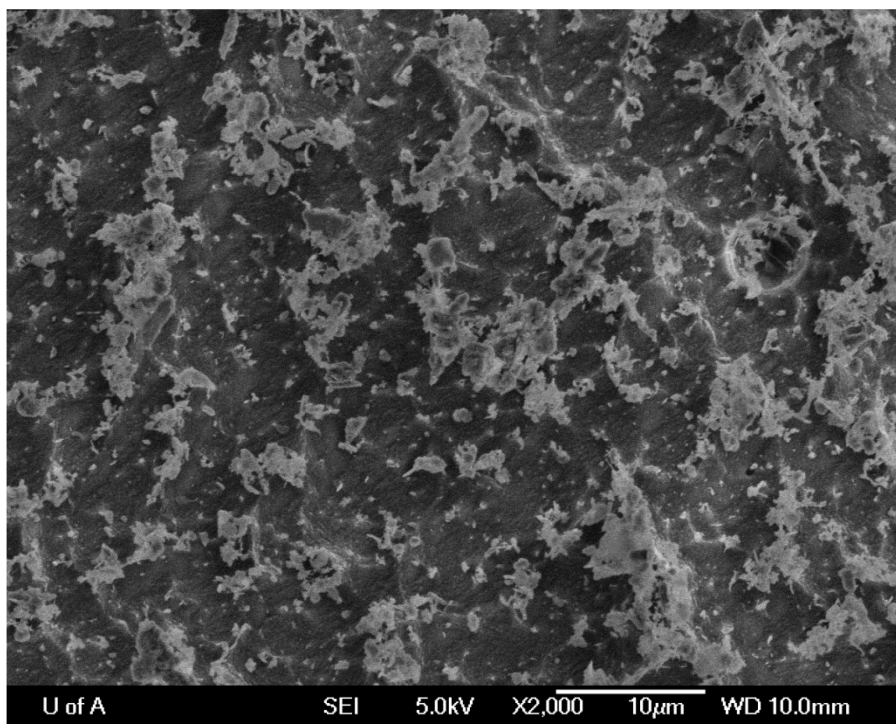
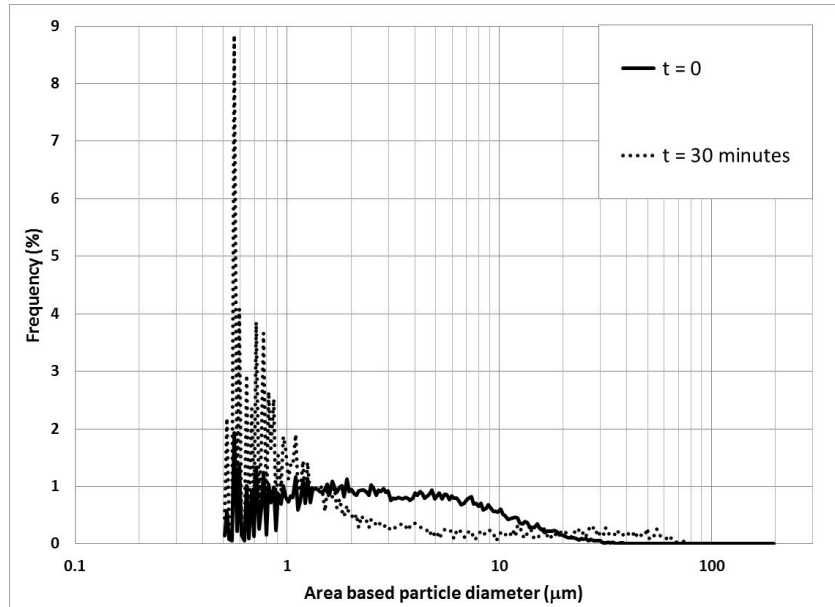


Figure 6.14 Cryo-SEM image of sonicated kaolinite sample; sample (1-2);  $c=20$  g/L; 2000X; sonication time: 30 minutes; amplitude: 100%



**Figure 6.15 Sample PSD measured by FPIA; Sample (1-1) and (1-2);  $c=20$  g/L; Sonication time: 30 minutes; amplitude: 100%**

### 6.3.3. Settling behavior

The settling behavior of non-sonicated and sonicated kaolinite clay samples is shown and described in this section. Samples with concentrations of 20 g/L and 10 g/L were sonicated for 30 minutes with 100% amplitude. Table 3.2 summarizes the characteristics of four samples shown in the following images.

Figures 6.16 through 6.19 show all four samples at start of the settling test ( $t=0$ , Figure 6.16), after 30 minutes of settling (Figure 6.17), after 90 minutes of settling (Figure 6.18), and after 24 hours of settling (Figure 6.19).

After 30 minutes of settling, it can be observed that the particles in the non-sonicated samples started to settle whereas the sonicated samples appear in the photo to be one phase. After 90 minutes of settling, the non-sonicated 20 g/L

sample shows a sedimented bed and almost clear supernatant whereas both sonicated samples appear in the photo to remain in one phase.

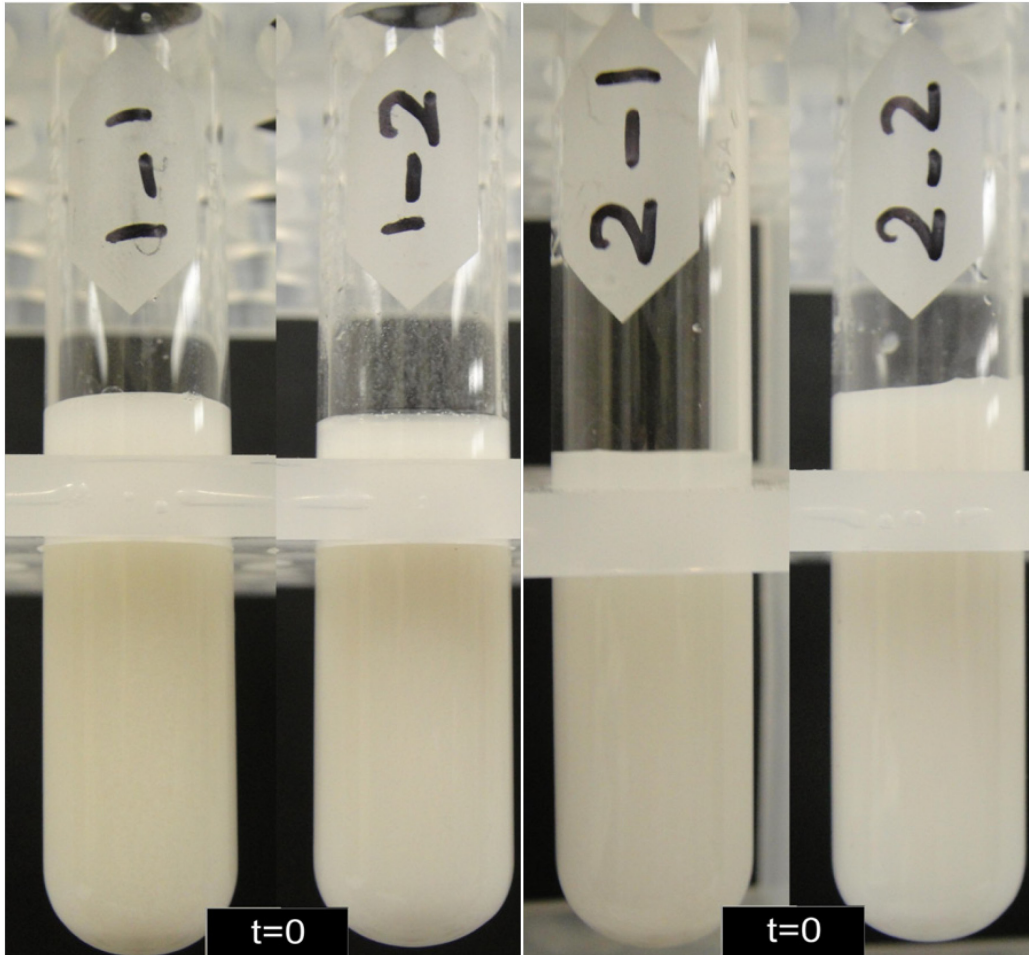


**Figure 6.16 Settling behaviour of 4 kaolinite samples at  $t=0$ ; Sample (1-1): non-sonicated,  $c=20$  g/L; Sample (1-2):  $c=20$  g/L, sonicated for 30 minutes, amplitude: 100%; Sample (2-1): non-sonicated,  $c=10$  g/L; Sample (2-2):  $c=10$  g/L, sonicated for 30 minutes, Sonication amplitude: 100%**

After 24 hours of settling, sedimentation is clearly observed for the non-sonicated samples and there is a distinct interface between the sediment beds and the clear supernatant. Sonicated samples also started to settle after 24 hours. Their interfaces are still near the top of the suspension and the supernatant is not clear.

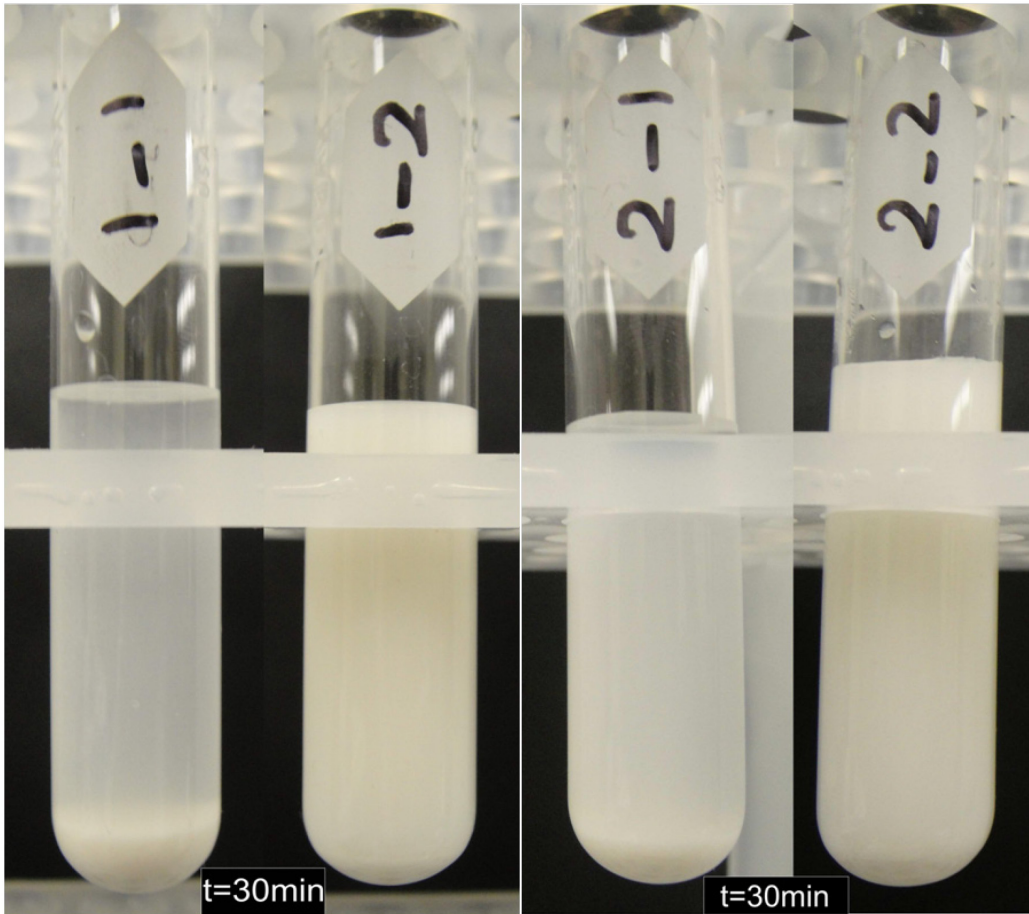


**Figure 6.17 Settling behaviour of 4 kaolinite samples at t=30 minutes;**  
**Sample (1-1): non-sonicated, c=20 g/L;**  
**Sample (1-2): c=20 g/L, sonicated for 30 minutes, Sonication amplitude: 100%;**  
**Sample (2-1): non-sonicated, c=10 g/L;**  
**Sample (2-2): c=10 g/L, sonicated for 30 minutes, Sonication amplitude: 100%**

Nasser and James<sup>81</sup> suggest that kaolinite particles settle as individual particles in the dispersed form and the interface is not clear under this condition. The flocculated particles, however, settle together, producing a sharp interface between the sediment bed and the supernatant<sup>81</sup>. Therefore, it can be said that the settling results shown in Figures 6.16 to 6.19 are in a qualitative agreement with the results obtained in Section 6.2. Comparison of the settling behavior of non-sonicated with sonicated samples shows that kaolinite particles are in the dispersed form after sonication. Due to their small sizes, the applied gravity force

cannot overcome the buoyancy and drag forces, which keep them suspended in the supernatant phase for long periods of time.

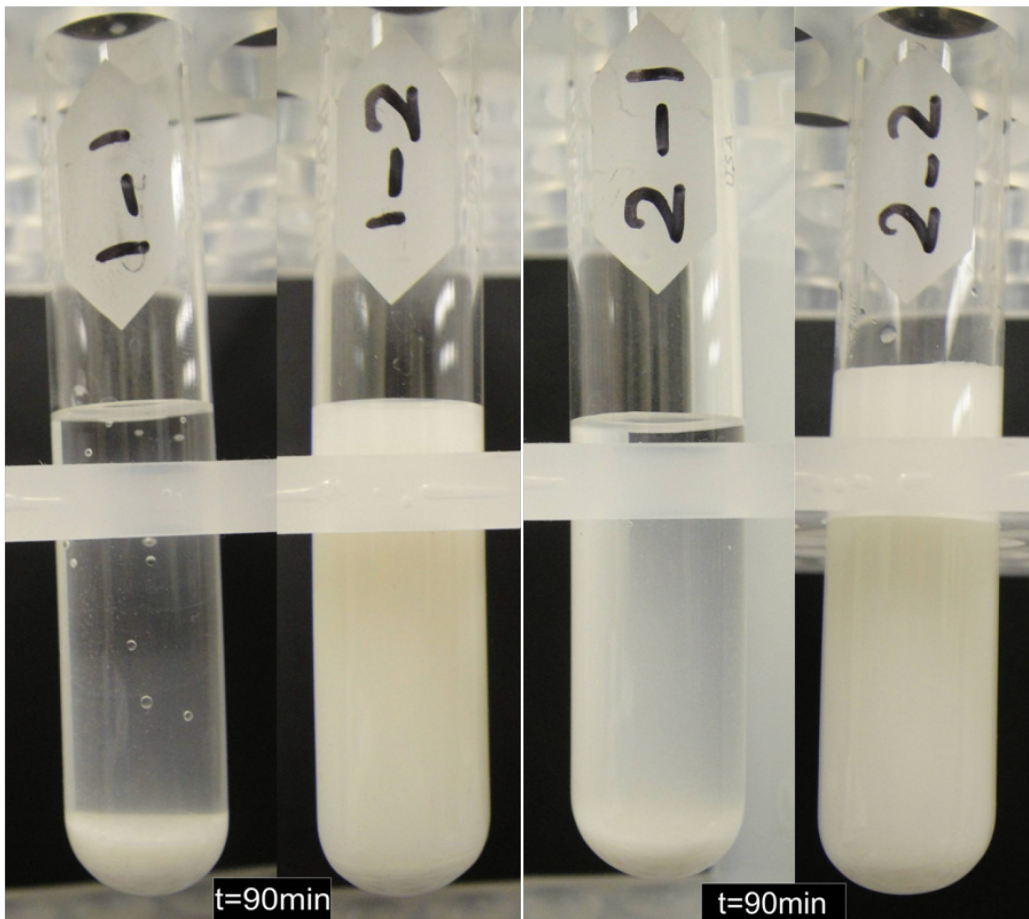


**Figure 6.18 Settling behaviour of 4 kaolinite samples at t=90 minutes;**  
**Sample (1-1): non-sonicated, c=20g/L;**  
**Sample (1-2): c=20g/L, sonicated for 30 minutes, Sonication amplitude: 100%;**  
**Sample (2-1): non-sonicated, c=10g/L;**  
**Sample (2-2): c=10g/L, sonicated for 30 minutes, Sonication amplitude: 100%**

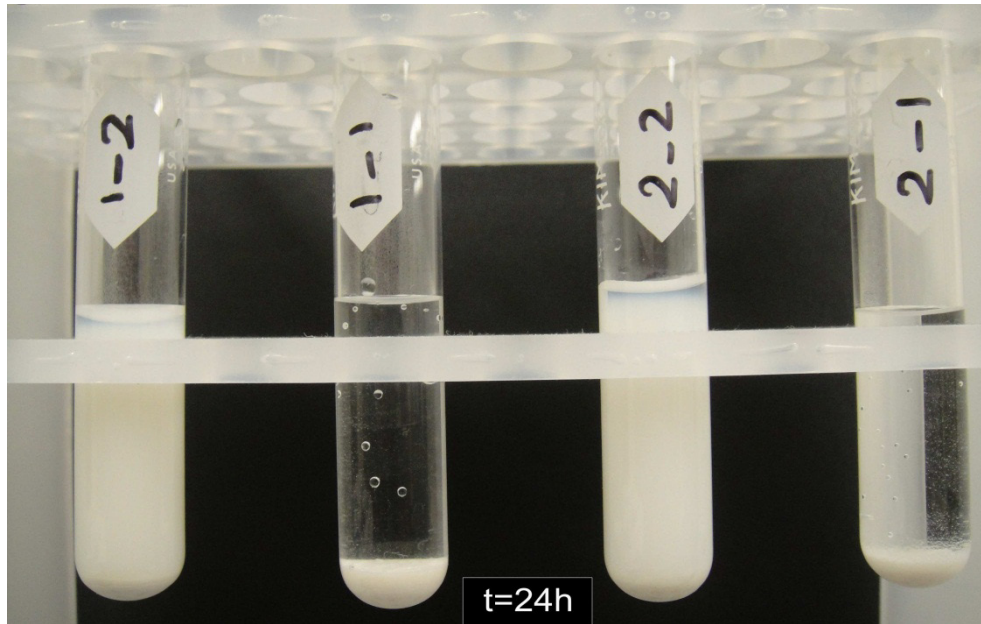


**Figure 6.19 Settling behaviour of 4 kaolinite samples at  $t=24$  hours;**  
**Sample (1-1): non-sonicated,  $c=20\text{g/L}$ ;**  
**Sample (1-2):  $c=20\text{g/L}$ , sonicated for 30 minutes, amplitude: 100%;**  
**Sample (2-1): non-sonicated,  $c=10\text{g/L}$ ;**  
**Sample (2-2):  $c=10\text{g/L}$ , sonicated for 30 minutes, amplitude: 100%**

#### **6.4. Effect of sonication amplitude on kaolinite PSD measurements**

Sonication amplitude is another parameter of ultrasound treatment that determines the amount of sonication energy. As previously explained (in Section 3.2.1), the amplitude of the Misonix Sonicator-4000 can be adjusted from 1 to 100% (where 100% represents 120  $\mu\text{m}$  tip displacement). Values of 50%, 75%, and 100% of the maximum sonication amplitude were examined in this study to investigate the influence of sonication amplitude on the measured kaolinite PSD. For this purpose the three main samples, described in Section 6.2, with the solids concentrations of 10, 20, and 40  $\text{g/L}$ , were subjected to ultrasound treatment using different sonication amplitudes. Figure 6.20 illustrates the changes in kaolinite

PSD after 60 minutes of treatment for the sample with  $c=40$  g/L. Similar results for samples with  $c=10$  g/L and  $c=20$  g/L are shown in Appendix I.

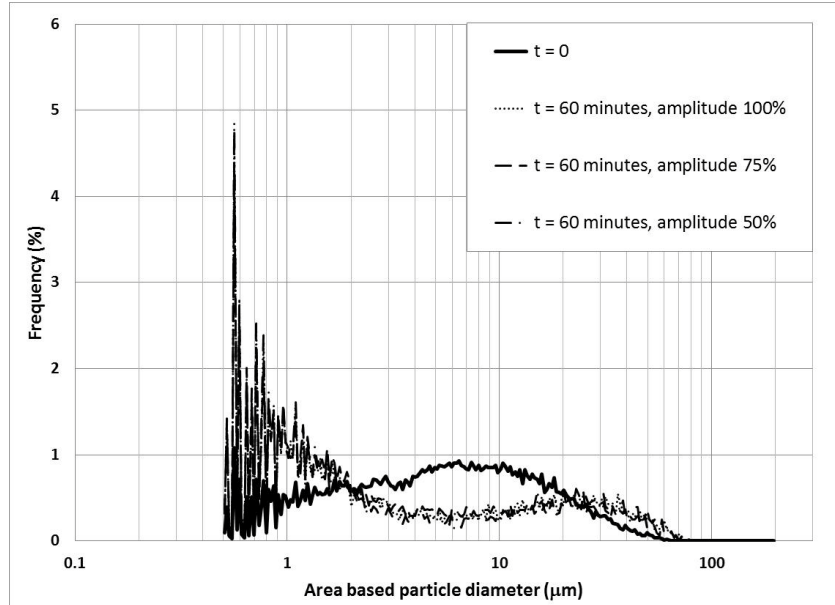


**Figure 6.20 Effect of sonication amplitude on the kaolinite PSD:  $c=40$  g/L; Sonication amplitude: 50%, 75%, and 100%**

The results presented in this figure indicate that decreasing the amplitude to 50% or 75% does not alter the sonicated sample PSD. To study the reason behind this finding, it is necessary to calculate the total amount of sonication energy introduced to the sample during 60 minutes of treatment.

The screen of the Sonicator-4000 continuously displays the sonication power (in Watts) and the delivered sonication energy (in Joules) during the ultrasound treatment. Table 6.4 shows the values of these parameters for each test. It should be noted that sonication power is not constant during sonication period (as explained in Section 3.2.1) and it decreases slightly during the 60 minute

treatment period. The values shown in the third column of Table 6.4 represent the range of sonication power during each 60 minute test.

**Table 6.4 Calculations of total sonication energy for three kaolinite samples**

<b>Concentration (g/L)</b>	<b>Sonication Amplitude (%)</b>	<b>Sonication Power (W)</b>	<b>Total Sonication Energy (J)</b>	<b>Total Sonication Energy (%)</b>
40	100	73-65	248 000	100
	75	57-53	196 000	80
	50	42-37	142 000	57
20	100	75-67	253 000	100
	75	56-52	192 000	76
	50	41-37	139 000	55
10	100	77-65	252 000	100
	75	56-52	192 000	76
	50	41-38	141 000	56

The fourth column in this table shows the total amount of energy introduced to sample during 60 minutes (calculated by Sonicator-4000). As can be seen, the amount of sonication energy does not change linearly with amplitude. Hence, the percentage of total sonication energy is calculated as:

$$\text{Total Sonication Energy (\%)} = \frac{\text{Total Sonication Energy (at each amplitude)}}{\text{Total Sonication Energy (at amplitude 100\%)}} \times 100 \quad (6.4)$$

The percentage of total sonication energy is shown in the last column of Table 6.4. The values of the last column indicate that by decreasing the sonication amplitude from 100% to 75% or 50%, the sonication energy decreases to 80% or 57% of the total amount of energy, respectively. For 40 g/L sample, the total sonication energy at an amplitude of 75% can be 80% of the total sonication energy introduced to the sample at amplitude 100%. Similarly, the total sonication energy at amplitude of 50% can be 57% of the total sonication energy introduced to the sample at amplitude 100%. These percentages are different for 20 g/L and 10 g/L samples (see Table 6.4).

Although a 25% or 50% reduction in sonication amplitude means decreasing the sonication energy to ~78% or ~56% of its initial value, it seems that this reduction in the sonication energy does not have a significant effect on the size of the kaolinite particles. By comparing the values shown in Table 6.2 with those of Table 6.4, it can be seen that the amount of energy provided at 50% amplitude is still greater than the energy required to break a certain fraction of flocs in the samples. Therefore, decreasing the sonication amplitude to 50% or 75% does not significantly change the sonication effect on the kaolinite clay PSD.

The FRR values for the samples with  $c = 40$  g/L after sonication with 50%, 75%, and 100% amplitude are calculated and shown in Figures 6.21. Similar results for lower concentrations ( $c = 10$  and 20 g/L) are provided in Appendix I. The results shown in Figure 6.21 indicate that the reduction in the floc population does not change when decreasing the sonication amplitude (from 100% to 75% or 50%).

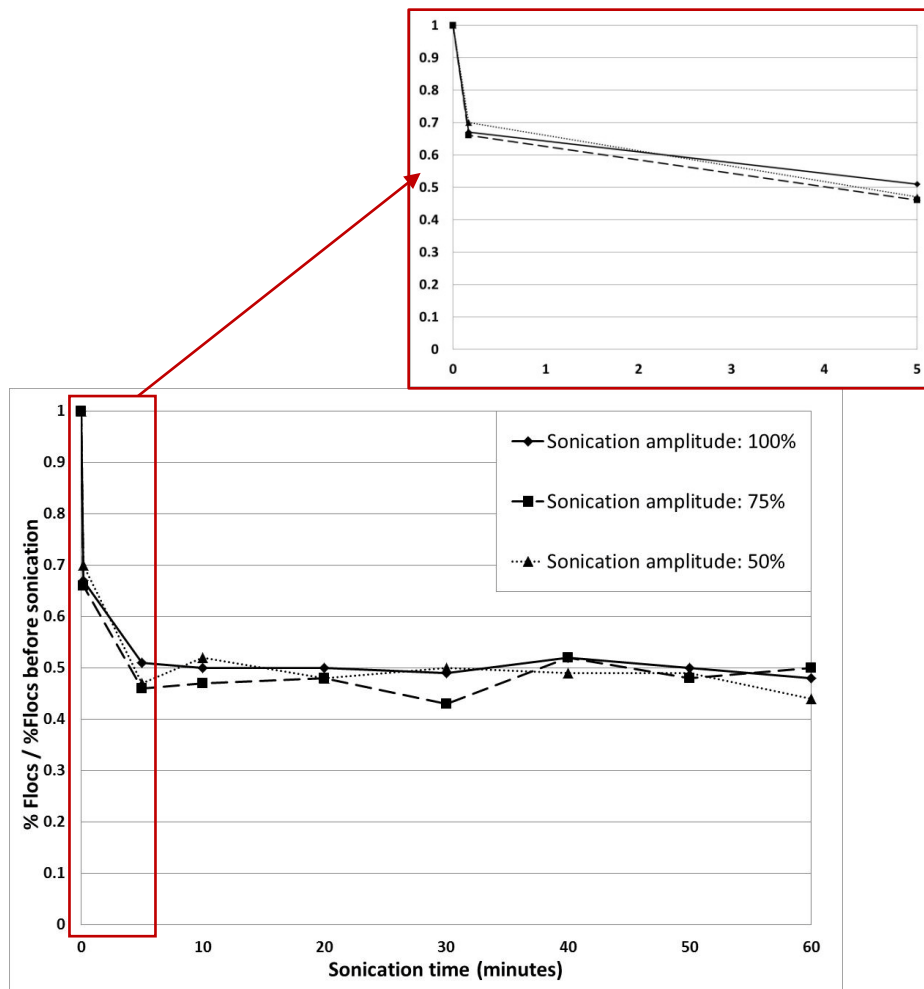


Figure 6.21 Effect of sonication amplitude on the floc reduction ratio (FRR):  $c=40$  g/L

### 6.5. Case study I: effect of sample pH

A sample with 40 g/L kaolinite concentration is used to investigate the sonication effect on the kaolinite PSD at different pH values. Figures 6.22 through 6.24 show the variations in sample PSD due to 10 minutes of sonication at pH values of 4.6,

8.2 and 11.4. Similar results for longer sonication times are provided in Appendix J.

The results shown in these figures indicate that the sonication effect changes when the sample pH is increased. At sonication periods of 10, 20, and 30 minutes, the sample at pH 8.2 is less affected by sonication than the sample at pH of 4.6. The percentage of individual particles increases and percentage of flocs decreases with sonication. The magnitude of the changes is greater for the sample at pH 4.6 than the sample at pH 8.2. It can be observed that the trend of changes in the sample PSD at pH 8.2 is similar to the natural kaolinite in water sample (pH=4.6); however, the magnitudes of the reduction in the percentage of flocs and the increase in the percentage of individual particles are lowered. The third sample, having a high pH of 11.4 is not affected by sonication because it mostly consists of individual particles and small flocs prior to the sonication.

As explained in Section 5.3, increasing the sample pH leads to breakage of E-F linkages and de-flocculation of the kaolinite particles. The remaining flocs in the sample, at high pH, are mostly produced through F-F associations<sup>81</sup>. The initial sample PSD (for non-sonicated samples) shown in Figures 6.22 through 6.24 confirm this finding. The reason why sonication does not significantly change the kaolinite PSD at pH 8 can be due to the fact that there is only a small number of E-F and E-E linkages that sonication can break. The rest of the flocs have F-F associations, which sonication cannot break. At pH 11.4, it can be seen in Figure 6.24 that there are no flocs or aggregates larger than 10  $\mu\text{m}$ . It seems that, at this

high pH, the suspension no longer contains flocs with E-F or E-E associations. The existing flocs are formed from the strong attachments of the F-F mode and thus are not affected by sonication.

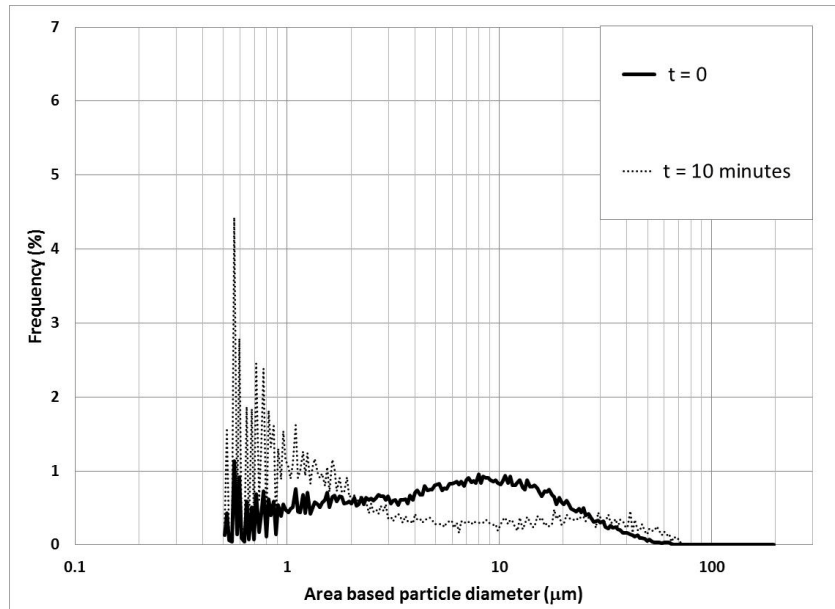


**Figure 6.22 Influence of pH on the sonication effect:  $c = 40 \text{ g/L}$ ;  $\text{pH}=4.6$ ; Sonication amplitude: 100%**

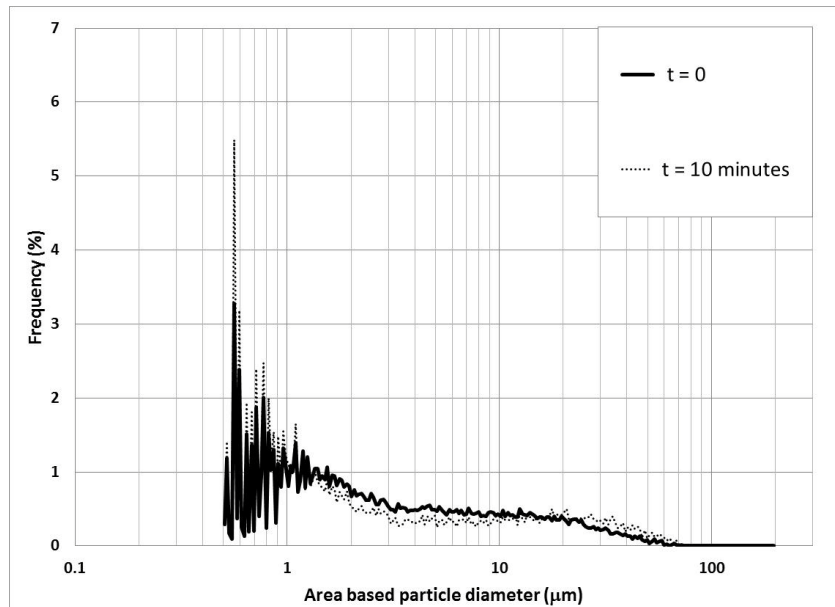


**Figure 6.23 Influence of pH on the sonication effect:  $c = 40 \text{ g/L}$ ;  $\text{pH}=8.2$ ; Sonication amplitude: 100%**

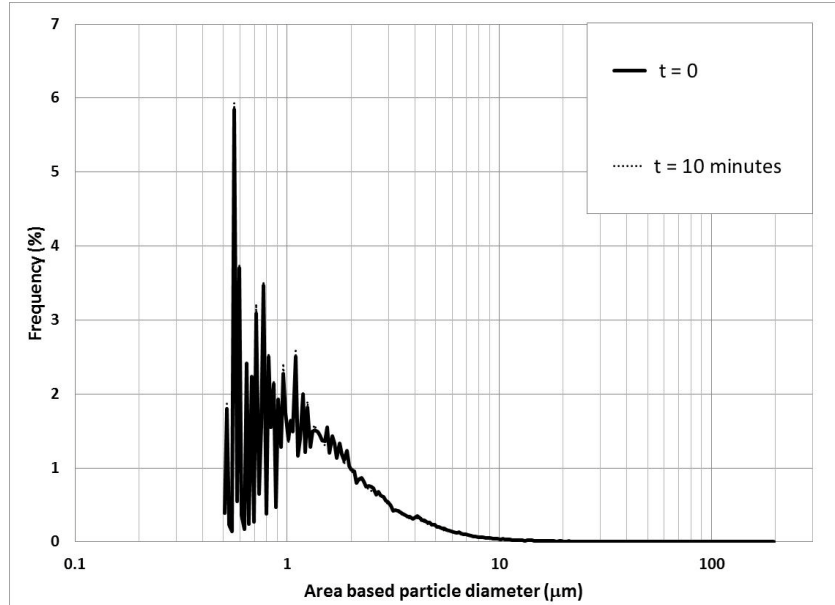


**Figure 6.24 Influence of pH on the sonication effect:  $c=40$  g/L;  $\text{pH}=11.4$ ; Sonication amplitude: 100%**

Figures 6.25 and 6.26 illustrate the reduction of the flocs percentage and floc reduction ratio (FRR) for three samples with pH of 4.6, 8.2, and 11.4. Figures 6.25 and 6.26 show that the sample with pH 4.6 is more affected by sonication than the sample with pH=8. In comparison with these samples, the sample with pH=11, which mostly consisted individual particles and small flocs, was not affected by sonication. Even after 30 minutes of sonication, less than 3% of the flocs were either broken down to individual particles (or formed aggregates).

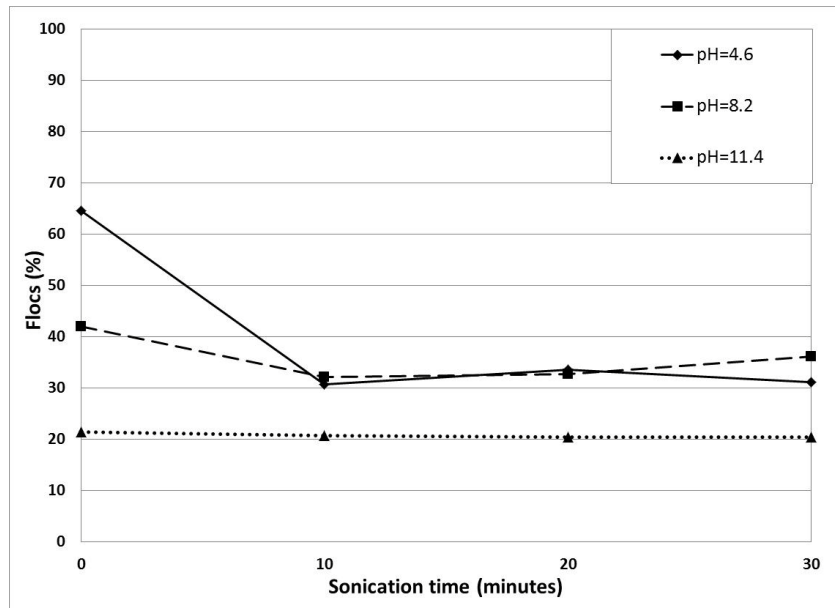


Figure 6.25 Flocs percentage at different sonication times for three different pH values;  
 c=40 g/L, Sonication amplitude: 100%

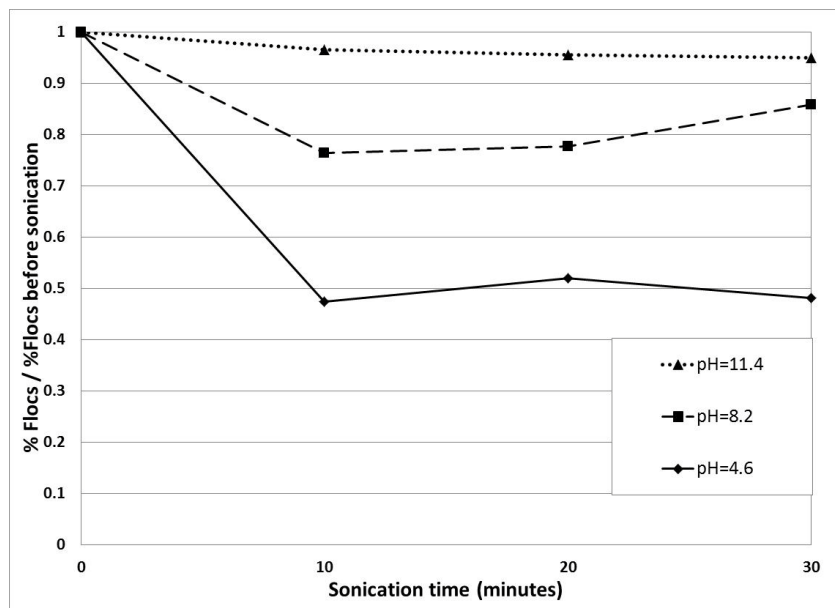
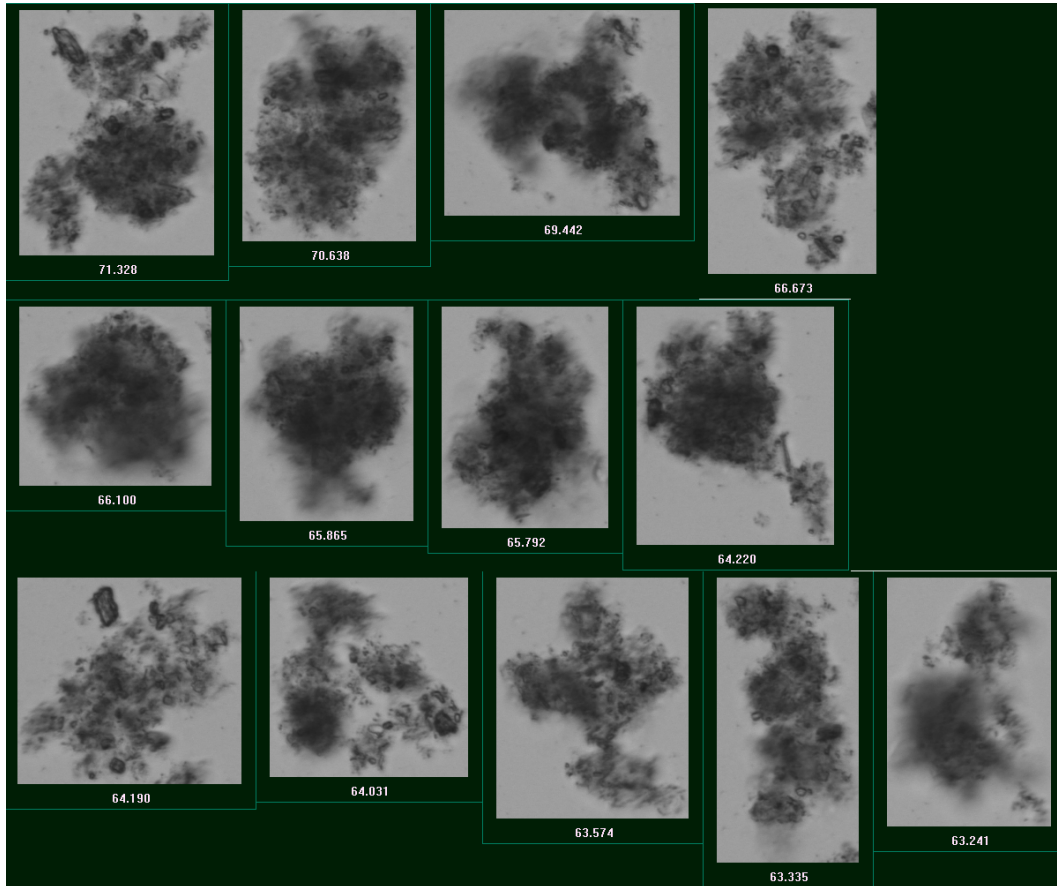


Figure 6.26 Floc reduction ratio (FRR) at different sonication times for three different pH values; c=40 g/L, Sonication amplitude: 100%

An increase in the population of “large” aggregates after sonication has been shown in different graphs in this chapter. The reason suggested in this work for the increase in the number of large aggregates is that due to sonication, some ultrasound-activated kaolinite particles encounter one another and form large aggregates. There might be another possibility for the existence of large aggregates in the sample after sonication: specifically, that these large aggregates are formed of inert (non-flocculating) particles such as silica that have larger primary particle sizes compared to kaolinite particles. If that is the case, it should be expected that sonication would not change the size of these large, inert particles. It is important to determine if these larger particles are aggregates formed through sonication or if they are inert particles that are always present.

To distinguish between these two possibilities, we investigated the images of particles captured by the FPIA in a 40 g/L sample after sonication. The sample studied here has a high pH value of 8.2. As previously discussed, at high pH values most kaolinite particles deflocculate and the overall particle size decreases. This means that there is a very small number of large aggregates of kaolinite particles before sonication. Figures 6.27(a) through 6.27(c) illustrate the images of the largest aggregates in the sonicated kaolinite sample ( $c=40$  g/L,  $\text{pH}=8.2$ ). It can be seen in these figures that although some of the largest aggregates contain inert particles (most likely silica particles), most of the large aggregates in the sonicated sample are formed of kaolinite particles. This verifies the reason suggested in this study that large aggregates are a result of collision of ultrasound-activated kaolinite particles.

In addition, Malvern Mastersizer measurements also confirm this finding by showing no large aggregates in the sample before sonication and the production of very large aggregates after sonication (see Figure 6.9).



**Figure 6.27(a) FPIA images of largest aggregates ( $71.328 \mu\text{m} < d < 63.241 \mu\text{m}$ ) in the sonicated kaolinite sample:  $c=40\text{g/L}$ ;  $\text{pH}=8.2$ ; Sonication time of 30 minutes; Sonication amplitude of 100%.**

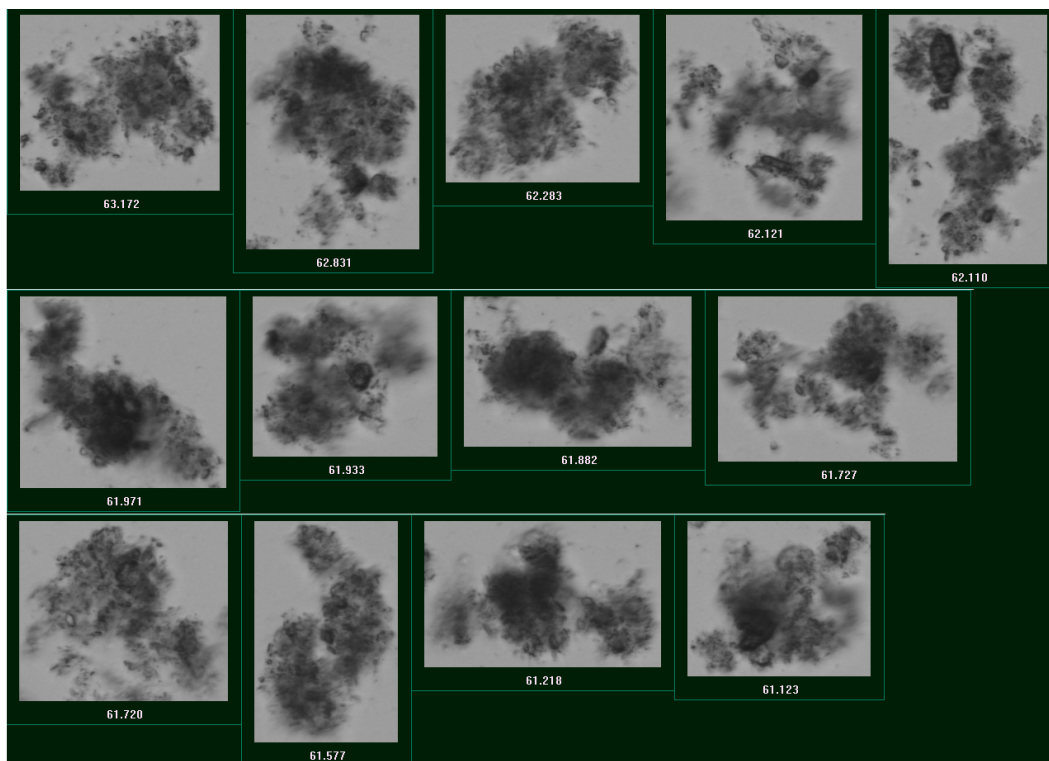


**Figure 6.27(b) FPIA images of largest aggregates ( $63.172 \mu\text{m} < d < 61.123 \mu\text{m}$ ) in the sonicated kaolinite sample:  $c=40\text{g/L}$ ;  $\text{pH}=8.2$ ; Sonication time of 30 minutes; Sonication amplitude of 100%.**

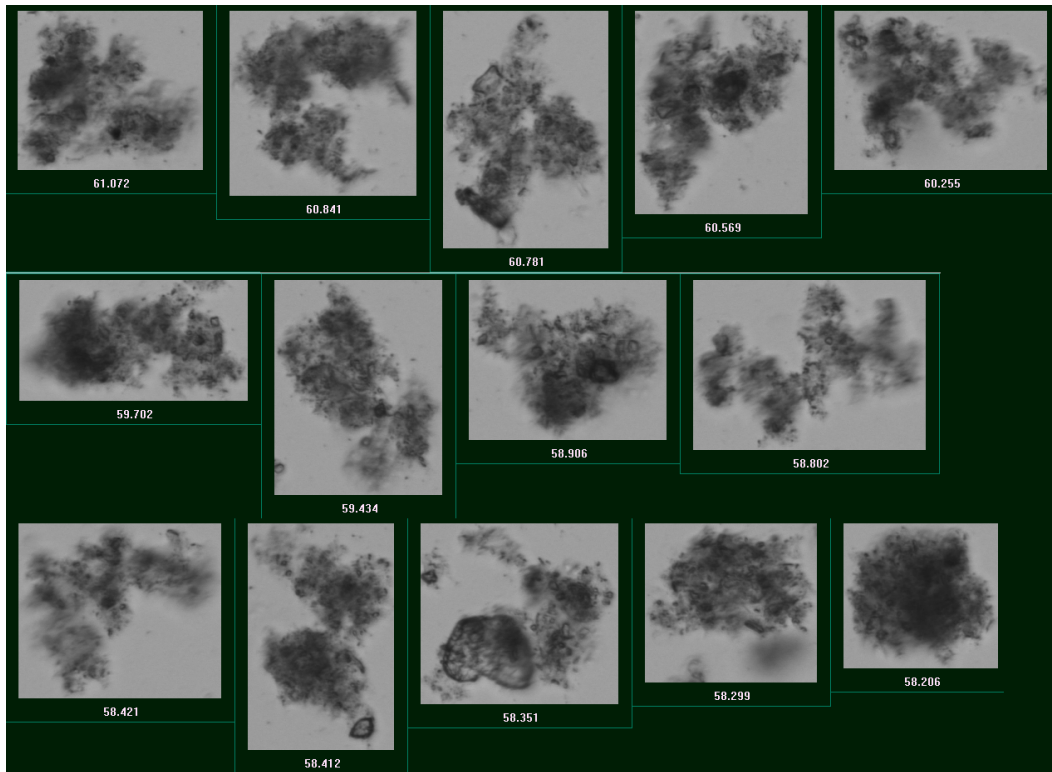


**Figure 6.27(c) FPIA images of largest aggregates ( $61.072 \mu\text{m} < d < 58.206 \mu\text{m}$ ) in the sonicated kaolinite sample:  $c=40\text{g/L}$ ;  $\text{pH}=8.2$ ; Sonication time of 30 minutes; Sonication amplitude of 100%.**

## 6.6. Case study II: effect of flocculant addition

A sample with 20 g/L kaolinite concentration is used to study the effect of sonication on a flocculated sample of kaolinite.  $\text{CaCl}_2$  is added to the sample at pH of approximately 11. The mass ratio of  $\text{CaCl}_2$  to kaolinite is kept at 0.1.

At high pH, the addition of  $\text{Ca}^{2+}$ , as a divalent cation (with the opposite charge to the basal surface and edge surface of kaolinite clay) results in reduction of the thickness of both electric double layers (on the face and edge surface). In addition, high  $\text{Ca}^{2+}$  concentration (0.3 M calcium chloride used in this study) makes the kaolinite zeta potential less negative by increasing the ionic strength of the suspension. These two phenomena will reduce the electrostatic repulsion between particles and make the van der Waals forces dominant. The van der Waals forces at the surfaces of kaolinite platelets cause attraction between basal surfaces and formation of “card-pack” flocs<sup>81,84</sup>.

The results of Figures 6.27 and 6.28 show the changes in the (non-flocculated) kaolinite PSD and flocculated sample PSD after 10 seconds of sonication. Similar results for longer sonication times are provided in Appendix K. These figures show that changes in the flocculated sample PSD are similar to the non-flocculated sample PSD. In both conditions the percentage of particles in the size range of 2  $\mu\text{m}$  to 20  $\mu\text{m}$  decreases whereas there is an increase in the populations of particles smaller than 2  $\mu\text{m}$  and of particles larger than 20  $\mu\text{m}$ . However, the sonication effect on the flocculated sample PSD is negligible compared to effect on the non-flocculated sample PSD. The reason why sonication does not

significantly change the flocculated sample PSD is related to the structure of the flocs and aggregates found in the sample. The addition of  $\text{CaCl}_2$  at high pH results in the formation of denser flocs and aggregates, with a greater fraction produced through F-F associations. As discussed in previous sections, sonication cannot break F-F linkages. Figures 6.29 through 6.31 show the percentage of individual particles, flocs, and aggregates in the flocculated and non-flocculated samples at each sonication time. These figures confirm that flocculated samples have more flocs and aggregates and less individual particles. The flocculated sample is less affected by sonication.

Figure 6.32 shows the changes in the floc reduction ratio (FRR) of both the flocculated and non-flocculated samples. It can be seen that in the flocculated sample only 15-30% of the flocs are broken due to sonication while this number is about 60% for the non-flocculated samples.

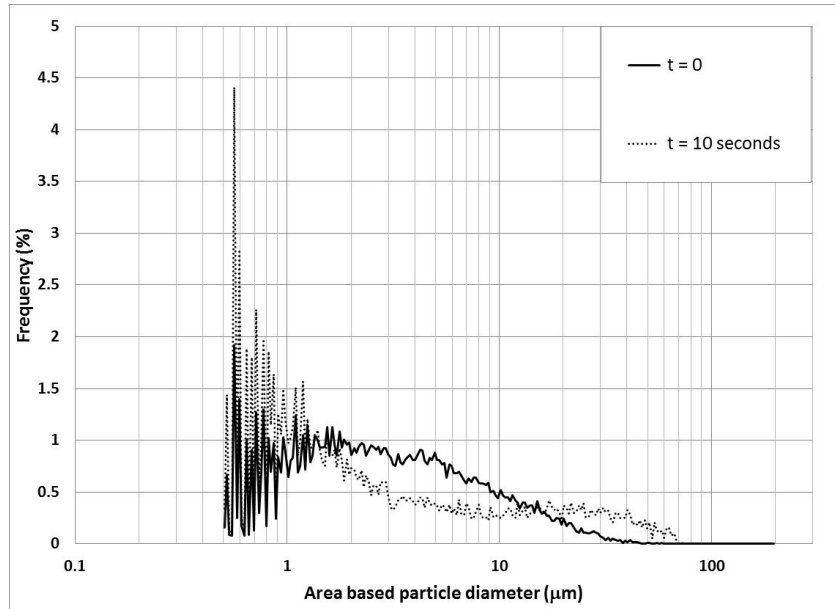


**Figure 6.28 Effect of sonication on the non-flocculated kaolinite sample:  $c=20$  g/L; sonication amplitude: 100%**

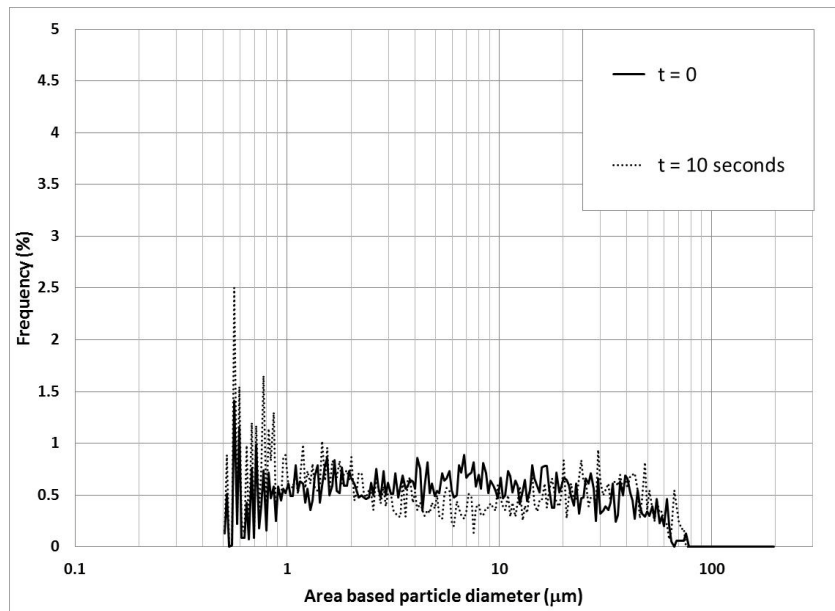


**Figure 6.29 Effect of sonication on the flocculated kaolinite sample:  $c=20$  g/L;  $\text{CaCl}_2$  to kaolinite mass ratio = 0.1; sonication amplitude: 100%**

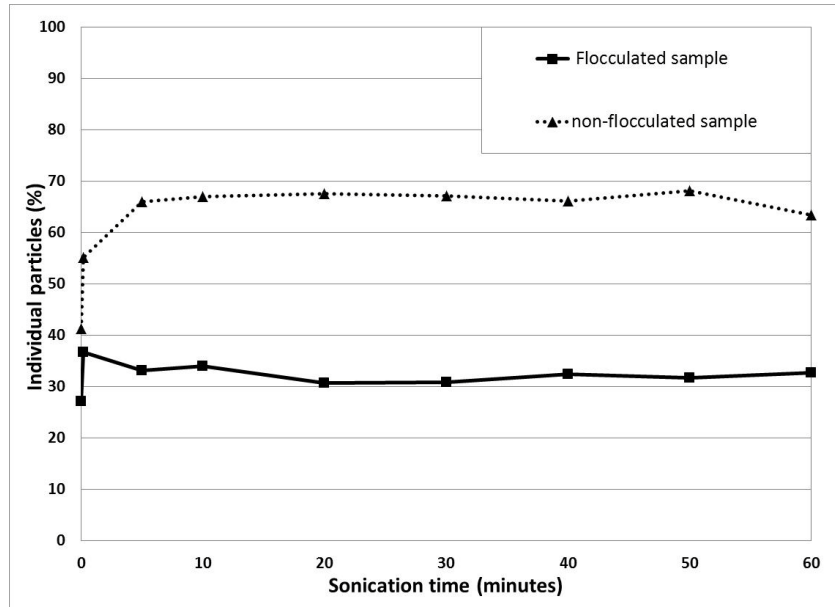


**Figure 6.30 Percentage of individual particles in the flocculated and non-flocculated samples at different sonication times;  $c=20$  g/L;  $\text{CaCl}_2$  to kaolinite mass ratio = 0.1; sonication amplitude: 100%**

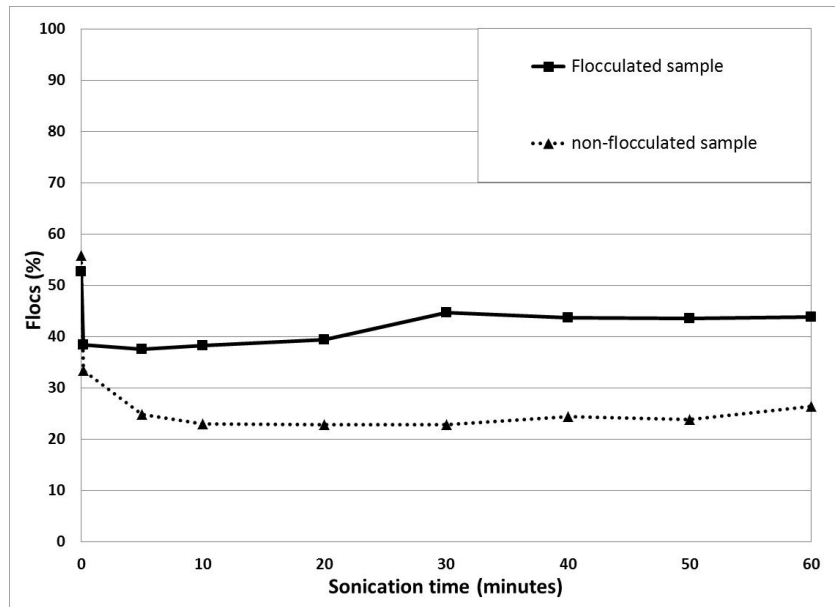


**Figure 6.31 Flocs percentage in the flocculated and non-flocculated samples at different sonication times;  $c=20$  g/L;  $\text{CaCl}_2$  to kaolinite mass ratio = 0.1; sonication amplitude: 100%**

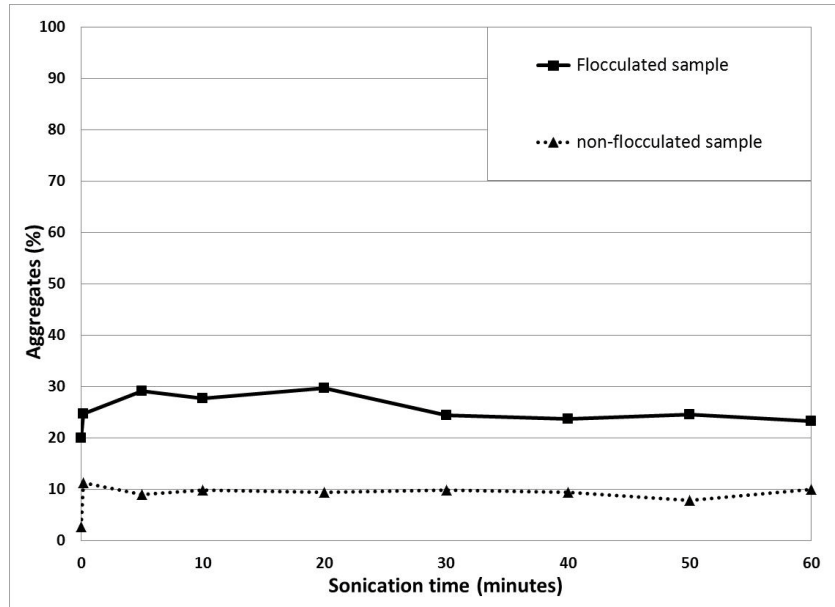


Figure 6.32 Percentage of aggregates in the flocculated and non-flocculated samples at different sonication times;  $c=20$  g/L;  $\text{CaCl}_2$  to kaolinite mass ratio = 0.1; amplitude: 100%

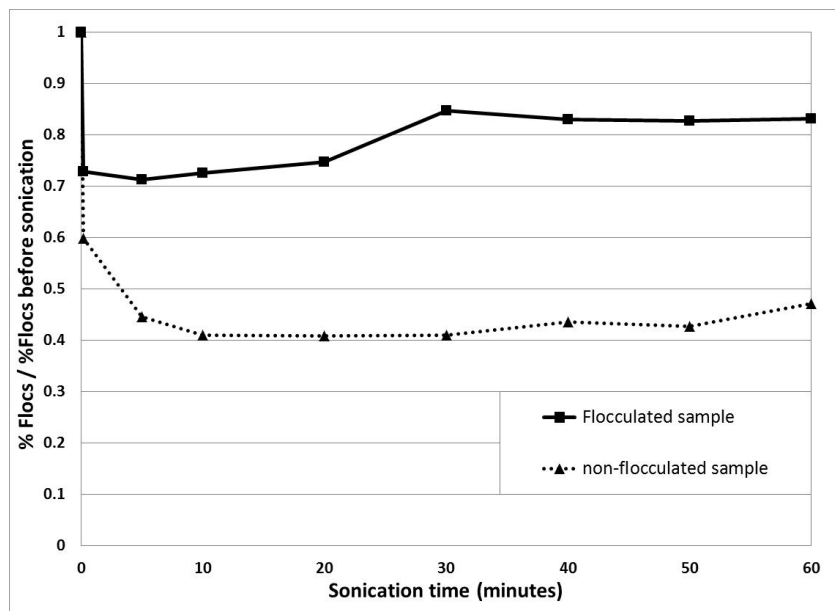


Figure 6.33 Floc reduction ratio (FRR) in the flocculated and non-flocculated samples at different sonication times;  $c=20$  g/L;  $\text{CaCl}_2$  to kaolinite mass ratio = 0.1; amplitude: 100%

## 6.7. Sonication of Oil Sands Tailings samples

In this section, the effect of sonication on an industrial tailings sample is discussed. This sample was kindly provided by Andrea Sedgwick, Sr. Engineer Tailings Processing at Total E&P Canada. Tailings were produced with the Batch Extraction Unit (BEU) methodology<sup>113</sup>. For the PSD measurements, the FPIA-3000 was used again to investigate the sonication effect. Samples were prepared following the procedure described in Section 3.3.7. Considering the FPIA-3000 limitations on particle size and sample concentration, particles larger than 75 microns were removed by sieving the tailings prior to making FPIA measurements. In addition, some of the bitumen in the tailings was removed using the RHS beads.

Table 6.5 and 6.6 show the results of Dean Stark analyses for sieved, bead treated samples. These results indicate that 87.92 g of tailings sample contains 84.76 g of water, 2.90 g of solids (including clays), and 0.26 g of bitumen. A sample of 10 g/L solid concentrations is prepared using the filtered process water to study the sonication effect on the tailings sample. Filtered process water (98 g) is added to 42 g of sieved and bead treated tailings sample (containing 40.5 g water, 1.4 g solids, and 0.12 g Bitumen).

A 10 g/L tailings sample was mixed and sonicated for 60 minutes with 100% amplitude. The mixing, sonication, and PSD measurement procedures are similar to those used for the kaolinite samples.

**Table 6.5 Dean Stark Results for tailings sieved, bead treated sample, mass basis**

<b>Sample name</b>	<b>Bitumen wt (g)</b>	<b>Water wt (g)</b>	<b>Mineral dry wt (g)</b>	<b>Cumulative wt (g)</b>
Tailings	0.26	84.76	2.90	87.92

**Table 6.6 Dean Stark Results for tailings sieved, bead treated sample, percentages**

<b>Sample name</b>	<b>% Bitumen</b>	<b>% Water</b>	<b>% Minerals</b>
Tailings	0.296	96.406	3.298

Figures 6.33(a) through 6.33(f) show the effect of sonication on the tailings sample PSD. Figure 6.33(a) demonstrates that after 10 seconds of sonication, the number of particles larger than 1.5  $\mu\text{m}$  decreases which results in an increase in the number of particles smaller than 1.5  $\mu\text{m}$ . Although the change in the percentage of large particles is small, most of the large particles, especially particles larger than 10  $\mu\text{m}$ , were broken to smaller particles. The percentage of aggregates (particles larger than 20  $\mu\text{m}$ ) decreases from 9.17% to 3.45% after 10 seconds of sonication. On the other hand, the percentage of individual particles (particles smaller than 2  $\mu\text{m}$ ) increases from 63% to 84% after 10 seconds of sonication.

Figure 6.33(b) illustrates that after 5 minutes of sonication, the number of particles larger than 2  $\mu\text{m}$  decreases which results in an increase in the number of particles smaller than 2  $\mu\text{m}$ . The percentages of aggregates (particles larger than

20  $\mu\text{m}$ ) decreases from 9.2% to 0.4%. The population of individual particles (particles smaller than 2  $\mu\text{m}$ ) increases from 63% to 87%.

Figures 6.33(c) through 6.33(f) show that from 5 minutes to 60 minutes of sonication, the tailings sample PSD does not change significantly. This suggests that most of the changes in the tailings sample PSD, caused by sonication, happen in the first 5 to 10 minutes of treatment.

Results presented in Figure 6.33 indicate that 60 minutes of sonication decreases the particle size of solids. The percentage of large particles (larger than 20  $\mu\text{m}$ ) decreases from 9.2% to 0.4%. On the other hand, after 60 minutes of sonication, the percentage of small particles (smaller than 2  $\mu\text{m}$ ) increases from 63% to 89%.

The changes in the industrial tailings sample PSD and the kaolinite in water sample PSD (as an idealized fine tailings sample) are compared in Figures 6.34(a) through 6.34(d). Both samples have the same concentration and are sonicated for the same amount of time, using the same sonication amplitude.

Figures 6.34(a) through 6.34(d) illustrate the effect of 30 minutes of sonication on the two types of suspensions.

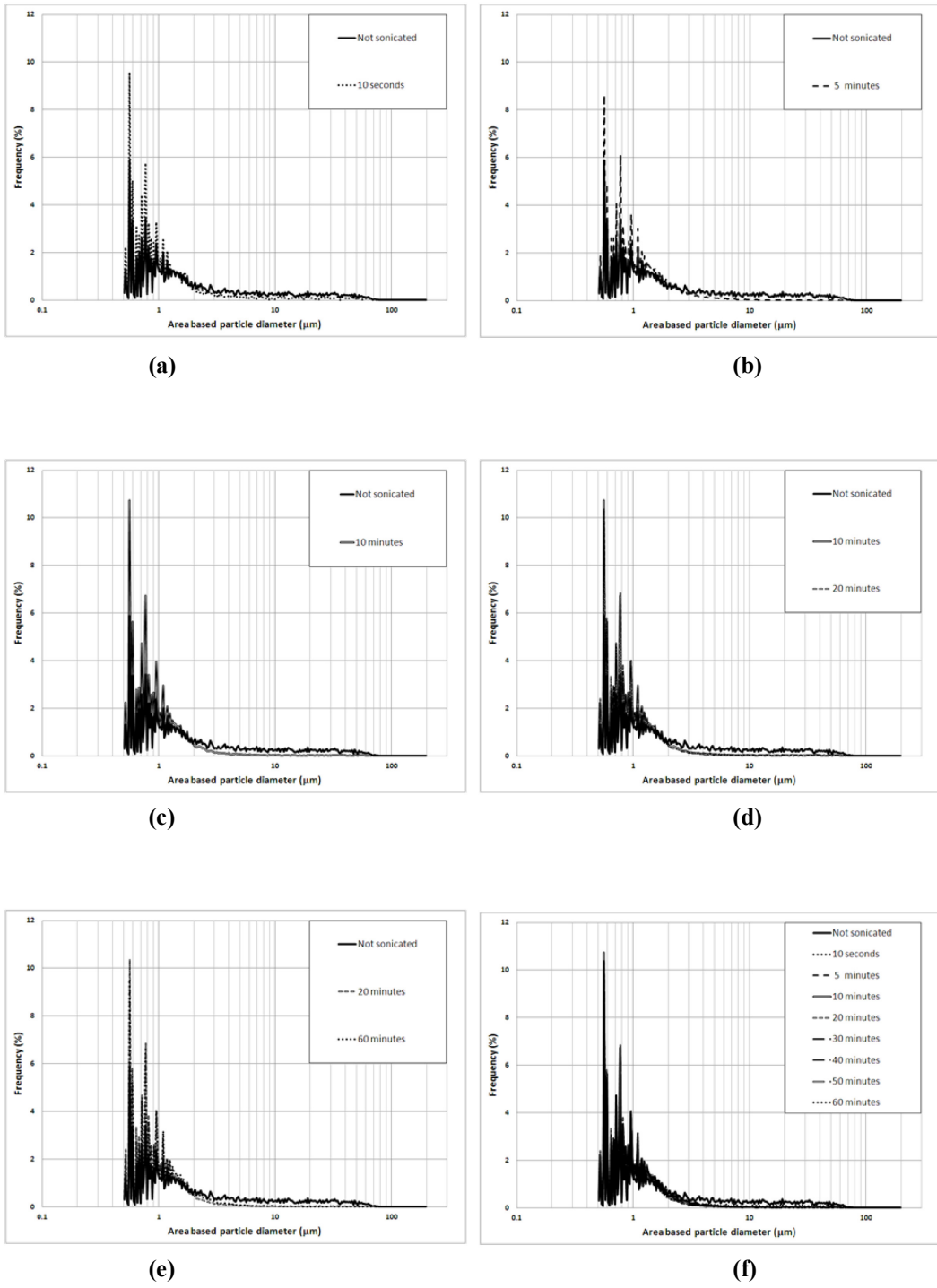


**Figure 6.34 (a)-(f) Effect of sonication on the PSD of tailings sample:  $c=10$  g/L; amplitude 100%**

Figure 6.34(a) shows how the PSD of the industrial tailing sample changes after 30 minutes of sonication. As previously explained, the large particles are broken to small particles. While the population of particles larger than 20  $\mu\text{m}$  becomes negligible after sonication, the percentage of individual particles (particles smaller than 2  $\mu\text{m}$ ) increases from 63% to 91%. The portion of flocs (particles in the size range of 2  $\mu\text{m}$  to 20  $\mu\text{m}$ ) also decreases from 28% to 8.5%.

Figure 6.34(b) shows how the kaolinite sample PSD changes after 30 minutes of sonication. Particles in the size range of 1.5  $\mu\text{m}$  to 20  $\mu\text{m}$  (flocs) are broken down to particles smaller than 1.5  $\mu\text{m}$  with sonication. The population of aggregates (particles larger than 20  $\mu\text{m}$ ) is negligible before and after sonication in this sample. Therefore, 30 minutes sonication appears to break most of the flocs down to the individual particles.

The results shown in Figure 6.34(c) compare the kaolinite in water PSD and industrial tailings sample PSD after 30 minutes of sonication. There is not a significant difference between the idealized and actual tailing samples PSDs, after ultrasound treatment.

The results shown in Figure 6.34(d) verify that although the initial (non-sonicated) kaolinite PSD and tailings PSD are different, sonication decreases the size of particles in both samples in the way that the particle size distributions of both kaolinite and tailings become quite similar after 30 minutes of ultrasound treatment.

Figure 6.35 illustrates the changes in percentage of flocs of both kaolinite and industrial tailings samples after 60 minutes of sonication. The trends of changes are similar: both have a sharp decrease during the first 5 minutes of sonication. In both samples, there is no significant change in the percentage of flocs after 10 minutes of ultrasound treatment. Furthermore, similar to Figures 6.34(c) and 6.34(d) the values of flocs percentage in both samples are similar after 5 minutes of sonication. Although the difference in the flocs percentages of samples prior to sonication is 30%, the values converge after 5 minutes of sonication; so that the differences in the flocs percentage of the two samples becomes less than 8% at all points in time after 10 minutes.

Figure 6.36 shows the changes in the floc reduction ratio (FRR) of both kaolinite and tailings samples. This figure confirms the findings that changes in the kaolinite PSD and tailings sample PSD are similar in trends of variations as well as in the extent of size reduction. The percentage of initial flocs that remained in the sample after sonication is about 35% for the industrial tailings sample whereas this number is about 25% for the kaolinite sample.

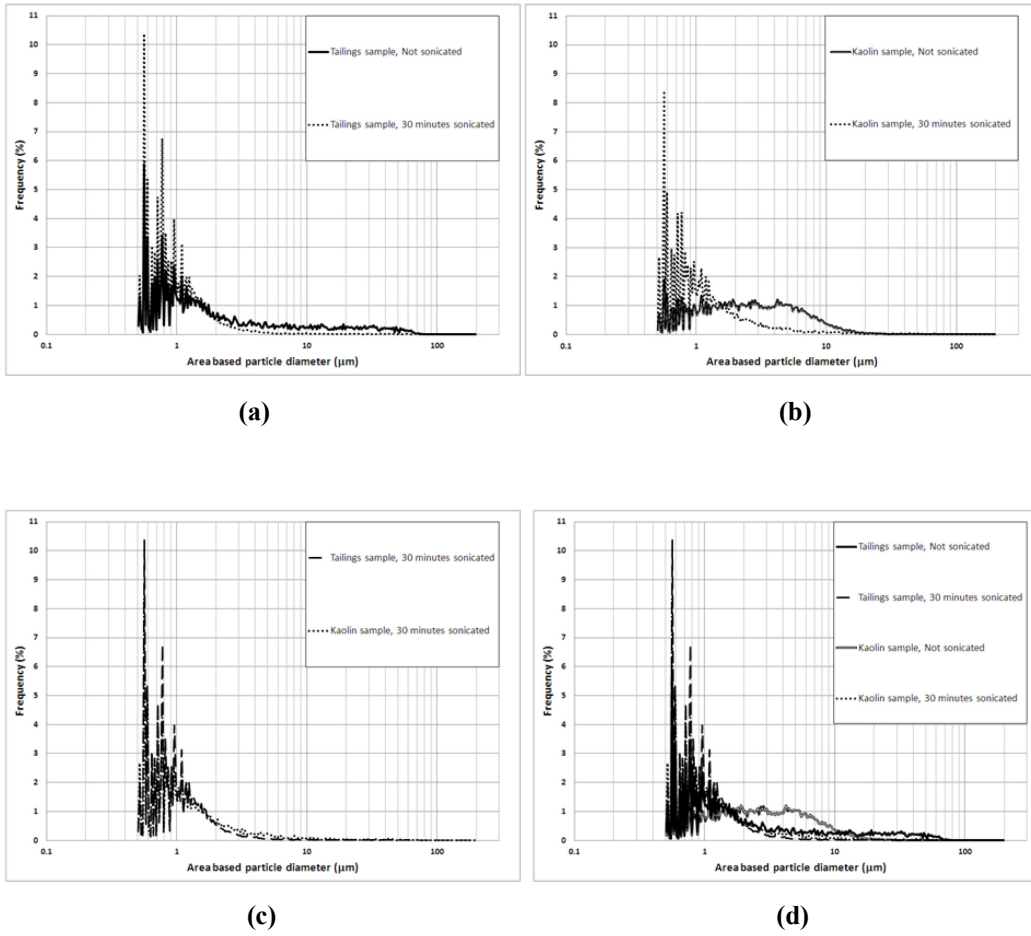


**Figure 6.35(a)-(d) Effect of sonication on the kaolinite clay PSD and tailings sample PSD:  
c=10 g/L; sonication amplitude 100%**

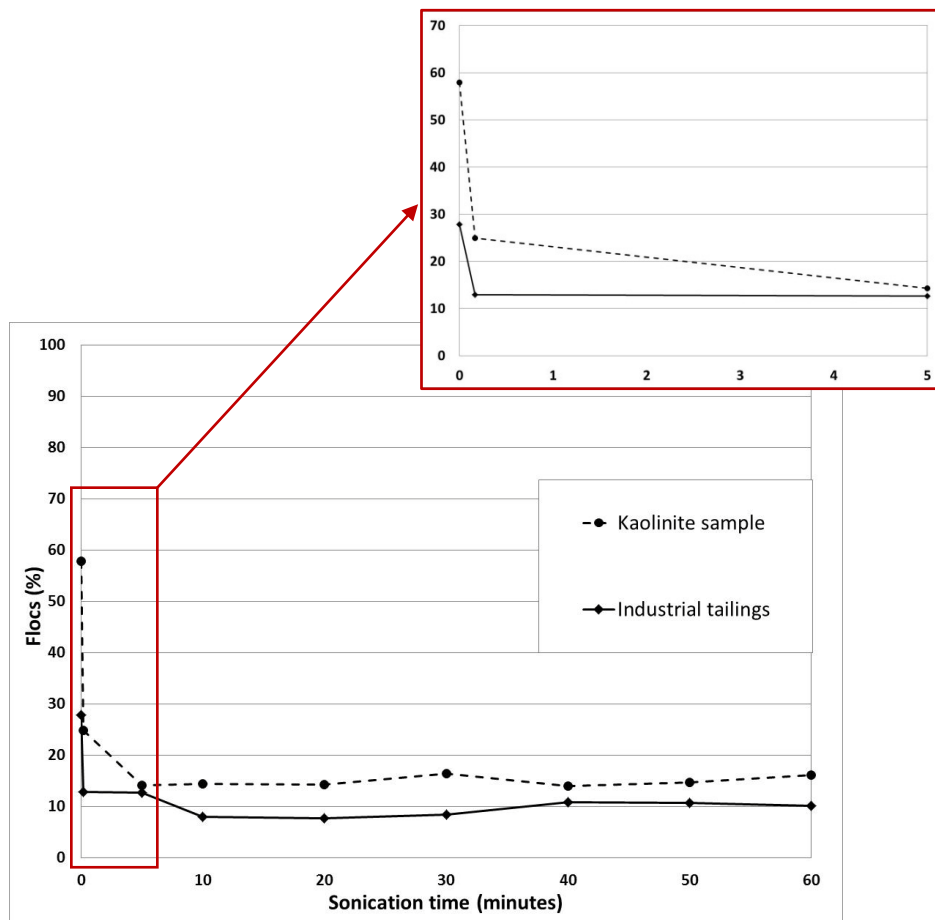
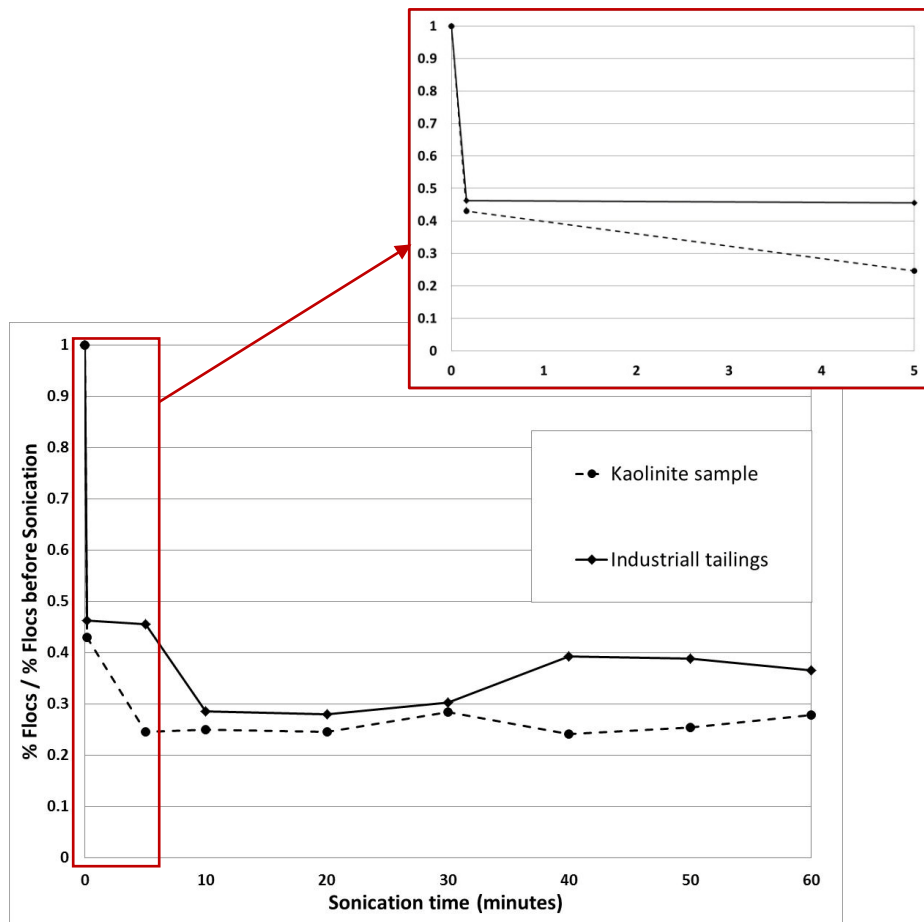


Figure 6.36 Flocs percentage of kaolinite and industrial tailings sample at different sonication times;  $c=10$  g/L; amplitude 100%



**Figure 6.37 Floc reduction ratio (FRR) of kaolinite and industrial tailings sample at different sonication times;  $c=10$  g/L; amplitude 100%**

## 6.8. Summary

The results of this chapter show that sonication results in a significant particle size reduction in kaolinite suspensions. This reduction occurs primarily through the breaking of flocs into individual particles. In addition, a small fraction of the ultrasound-activated particles group together to form big aggregates.

The influence of different parameters on the effect of sonication on the kaolinite PSD was studied. The results can be summarized as follows:

- *Effect of sonication time*

The most significant size reduction effect occurs during the first 10 minutes of sonication. Continued treatment (after ten minutes) does not have a significant additional effect on the particle size distribution of kaolinite samples.

- *Effect of sonication amplitude*

Decreasing the sonication amplitude to 75% or 50% does not significantly change the extent of sonication effect on the kaolinite clay PSD. The reason behind this is that the amount of sonication energy provided at 50% amplitude (sonication time > 10 seconds) is greater than the energy required to break a certain fraction of flocs in the samples.

- *Effect of solids concentration*

The size reduction is most significant in the dilute sample (c=10 g/L). The effect, while still important, is not as strong in the most concentrated sample (c=40 g/L).

In the dilute sample, with lower number of flocs and aggregates, the energy received by each floc or aggregate is higher than the more concentrated samples.

- *Effect of sample pH*

The sample at pH 4.6 is more affected by sonication than the sample at pH 8.2. In comparison with these samples, the sample at pH~11 was not affected by sonication. Since increasing the sample pH results in breakage of E-F associations and de-flocculation of kaolinite particle, samples at pH 8.2 contain only a small number of E-F and E-E linkages that sonication can break. At pH 11.4, the kaolinite suspension no longer contains flocs with E-F or E-E associations. Therefore, sonication has no effect on this sample.

- *Effect of flocculant addition*

Non-flocculated kaolinite suspensions are more affected by sonication than flocculated suspensions. Flocculated samples contain denser flocs and aggregates, with a greater fraction produced through F-F associations and sonication cannot break these strong linkages.

Furthermore, the FPIA results have been validated using other independent measuring techniques. The results from laser diffraction method, cryo-SEM studies, and study of settling behavior were in good qualitative agreement with the FPIA results. All showed that sonication produces a significant reduction in kaolinite particle size.

Finally, the effect of sonication on the particle size of an industrial tailings sample has also been studied. The results showed that although the non-sonicated kaolinite PSD and tailings PSD are different, the particle size distributions for both kaolinite and tailings become quite similar after the ultrasound treatment.

## 7. Conclusions and recommendations

### 7.1. Conclusions

- The particle size distribution of non-sonicated kaolinite suspensions at three different solids concentrations ( $c=10, 20, \text{ and } 40 \text{ g/L}$ ), at pH values of 4.6 and 11.4, and in the presence of  $\text{CaCl}_2$ , as a flocculant, was studied. The consistency of these results produced here to previous studies found in the literature indicates that the size measurement instrument used for this study provides meaningful results in the solids concentration range and the sample conditions applied in this work.
- The particle size distributions of non-sonicated and sonicated kaolinite suspensions were compared. The results showed that sonication resulted in a significant reduction in kaolinite particle size. This reduction occurred primarily by breaking down flocs to individual (primary) particles. In addition, some of the ultrasound-activated particles formed large aggregates.
- The extent of size reduction due to sonication was studied at different sonication times ( $t=0, 10 \text{ seconds, } 5, 10, 20, 30, 40, 50, \text{ and } 60 \text{ minutes}$ ) and amplitudes (amplitude: 50%, 75%, and 100%). The results of this study showed that most of the size reduction occurred within the first ten minutes of sonication. Continued ultrasound treatment ( $t > 10 \text{ minutes}$ ) did not have a significant effect on the kaolinite suspension PSD. On the other hand, decreasing the sonication amplitude to 75% or 50% did not

significantly change the extent of sonication effect on the kaolinite suspension PSD's. Sonication at 50% amplitude still provides the energy required to break down the flocs.

- The extent of size reduction due to sonication for samples with different kaolinite concentrations ( $c=10, 20, \text{ and } 40 \text{ g/L}$ ), having different pH values (pH 4.6, 8.2, and 11.4), and flocculated samples comparing to non-flocculated ones was also studied. The results of this study showed that:
  - Samples with lower concentrations were more affected by sonication. At all sonication times, the maximum size reduction was observed for the most dilute sample ( $c=10 \text{ g/L}$ ) and the size reduction effect was less pronounced in the most concentrated sample ( $c=40 \text{ g/L}$ ).
  - Samples with pH 4.6 were more affected by sonication than the samples with pH 8. The sample with pH 11.4 was not affected by sonication. Sample with high pH values contain only a small number of weak particle linkages (E-F and E-E associations) that sonication can break.
  - The non-flocculated kaolinite suspension PSD was more affected by sonication than the flocculated suspension was. Flocculated samples contain denser flocs and aggregates, with a greater fraction produced through F-F associations and sonication cannot break these strong linkages.

- The conclusions of this study were validated qualitatively using other measuring methods: laser diffraction method, cryogenic-SEM studies, and settling behavior observations. The results from these methods were in good agreement with the FPIA results, with all methods indicating that sonication produces a significant reduction in kaolinite particle size. The results from laser diffraction size analysis tests confirmed the finding of this study; namely, that the size reduction due to sonication occurred primarily over the first 10 minutes of treatment and continued sonication beyond that time did not significantly alter the kaolinite suspension PSD.
- The primary objective of this study was to investigate the sonication effect on the kaolinite clay PSD. In addition to this investigation on the kaolinite suspension, as a model clay, the effect of sonication on the particle size distribution of a real industrial tailings sample was also studied. The results showed that although the non-sonicated kaolinite PSD and tailings PSD were different, sonication decreased the size of particles in both samples such that the particle size distributions for both kaolinite and tailings became quite similar after the ultrasound treatment.

## **7.2. Recommendations**

- Additional studies should be conducted to study the changes caused by sonication on other characteristics of kaolinite clay particles such as floc structure/morphology, specific surface area, and the thermal behaviour.

- Additional experiments should be carried out to study the sonication effect on particle size of real industrial clay-containing suspensions. For this purpose, samples taken from different process streams and different tailings ponds should be analyzed.

## 8. References

1. Government of Alberta, *Alberta Energy-Oil Sands* (2007). at  
<<http://www.energy.gov.ab.ca/OurBusiness/oilsands.asp>>
2. National Energy Board Canada's Oil Sands: opportunities and challenges to 2015. (2004). at  
<<http://www.neb.gc.ca/clfnsi/rnrgynfimt/nrgyrprt/lsnd/pprntnsndchllngs20152006/qapprntnsndchllngs20152006-eng.html>>
3. Alberta Energy Resources Conservation Board. at  
<<http://www.ercb.ca/learn-about-energy/energy-in-alberta/production-reserves>>
4. Bichard, J. A., *Oil sands composition and behaviour research. The research papers of John A. Bichard 1957-1965.*, AOSTRA technical publication series, (Alberta Oil Sands Technology and Research Authority: Edmonton, AB, 1987).
5. Kasperski, K. L., *Review of research on aqueous extraction of bitumen from mined oil sands.*, [Division No. CWRC 01-17 (CF)]. (Natural Resources Canada, CANMET-WRC: 2001).
6. Masliyah, J., *Course Notes - ChE 534 Fundamentals of Oilsands Extraction.*, (Department of Chemical and Materials Engineering, University of Alberta: Edmonton, AB, 2009).
7. Camp, F. W., *The tar sands of Alberta.*, (Cameron Engineers Inc: Colorado, USA, 1976).

8. Masliyah, J., Zhou, Z. J., Xu, Z., Czarnecki, J. and Hamza, H., Understanding Water-Based Bitumen Extraction from Athabasca Oil Sands, *The Canadian Journal of Chemical Engineering* **82**, 628–654 (2004).
9. Adeyinka, O. B., Samiei, S., Xu, Z. and Masliyah, J. H., Effect of particle size on the rheology of Athabasca clay suspensions, *The Canadian Journal of Chemical Engineering* **87**, 422–434 (2009).
10. Schramm, L., The Influence Of Suspension Viscosity On Bitumen Rise Velocity And Potential Recovery In The Hot Water Flotation Process For Oil Sands, *Journal of Canadian Petroleum Technology* **28**, 73-80 (1989).
11. Starr, J. and Bulmer, J. T., *Syncrude Analytical Methods for Oil Sand and Bitumen Processing*, (Alberta Oil Sands Technology and Research Authority: 1979).
12. Li, H., Zhou, J. and Chow, H. A. W., Comparison of polymer applications to treatment of oil sands fine tailings, *Proceeding First International Oil Sands Tailings Conference*, 77–84 (2008).
13. *Sustainable Development Business Case Report: Clean Conventional Fuel - Oil and Gas*. (Sustainable Development Technology Canada: 2006).
14. Hooshier, A., Characterization of Clay Minerals in the Athabasca Oil Sands in Water Extraction and Nonaqueous Solvent Extraction Processes, Edmonton, Alberta. PhD thesis, University of Alberta (2011).
15. MacKinnon, M., Development of the tailings pond at Syncrude’s oil sands plant 1978-1987, *AOSTRA Journal of Research* **5**, 109–133 (1989).

16. Thomas, T., Afacan, A., Masliyah, J., Xu, Z., Wang, Y. and Liu, J., Recovery of Hydrocarbons from Mature Fine Tailings of Oil Sands Extraction, *Proceedings of the 2nd International Oil Sands Tailings Conference* 141–148 (2010).
17. Kasperski, K. L., A review of properties and treatment of oil sands tailings, *AOSTRA Journal of Research* **8**, 11–53 (1992).
18. Sparks, B., Kotlyar, L., O'Carroll, J. and Chung, K., Athabasca oil sands: effect of organic coated solids on bitumen recovery and quality, *Journal of Petroleum Science and Engineering* **39**, 417–430 (2003).
19. Kaminsky, H. A. W., Etsell, T. H., Ivey, D. G. and Omotoso, O., Distribution of clay minerals in the process streams produced by the extraction of bitumen from Athabasca oil sands, *The Canadian Journal of Chemical Engineering* **87**, 85–93 (2009).
20. Uhlik, P., Hooshar, A., Kaminsky, H. A. W., Ivey, D. G. and Liu, Q., Cation Exchange Capacity of Clay Fractions from Oil Sands Process Streams, *Proceeding First International Oil Sands Tailings Conference*, 64–72 (2008).
21. Mikula, R. J., Omotoso, O. and Kasperski, K. L., The chemistry of oil sands tailings: production to treatment, *Proceeding First International Oil Sands Tailings Conference*, 23–33 (2008).
22. Masliyah, J. H. and Bhattacharjee, S., *Electrokinetic and Colloid Transport Phenomena*, (John Wiley and Sons: 2006).

23. Delgado, A. and Matijevic, E., Particle Size Distribution of Inorganic Colloidal Dispersions: A comparison of different techniques, *Particle & Particle Systems Characterization* **8**, 128–135 (1991).
24. Desroches, M. J., Castillo, I. A. and Munz, R. J., Determination of Particle Size Distribution by Laser Diffraction of Doped-CeO<sub>2</sub> Powder Suspensions: Effect of Suspension Stability and Sonication, *Particle & Particle Systems Characterization* **22**, 310–319 (2005).
25. Jeeravipoolvam, S., Scott, J. D., Donahue, R. & Ozum, B., Characterization of oil sands thickened tailings, *Proceeding First International Oil Sands Tailings Conference*, 132–142 (2008).
26. Raymond, B. W., Clay Mineral Concentration in Tailings of Great Canadian Oil Sands, Montana, United States, MSc Thesis, Montana College of Mineral Science and Technology, (1969).
27. Kessick, M. A., Ion exchange and dewaterability of clay sludges, *International Journal of Mineral Processing* **6**, 277–283 (1980).
28. Roberts, J. O. L., Yong, R. N. and Erskine, H. L., Surveys of Some Tar Sand Sludge Ponds: Results and Interpretations, presented at the *Applied Oil Sands Geoscience Conference*, June 11-13, Edmonton, AB (1980).
29. Ignasiak, T. M., Kotlyar, L., Longstaffe, F. J., Strausz, O. P. and Montgomery, D. S., Separation and characterization of clay from Athabasca asphaltene, *Fuel* **62**, 353–362 (1983).

30. Don Scott, J., Dusseault, M. B. and David Carrier, W., Behaviour of the clay/bitumen/water sludge system from oil sands extraction plants, *Applied Clay Science* **1**, 207–218 (1985).
31. Kotlyar, L. S., Characterization of Colloidal Solids from Athabasca Fine Tails, *Clays and Clay Minerals* **41**, 341–345 (1993).
32. Brady, N. C. and Weil, R. R., *Elements of the Nature and Properties of Soils*, (Prentice Hall: New Jersey, USA, 2003).
33. Kaminsky, H. A. W., Characterization of an Athabasca oil sands ore and process streams, Edmonton, Alberta., PhD Thesis, University of Alberta (2008).
34. Mihiretu, Y., Chalaturnyk, R. and Scott, D., Tailings segregation fundamentals from flow behaviour perspectives, *1st International Oil Sands Tailings Conference*. 112–120 (2008).
35. Litzenberger, C. G. and Sumner, R. J., Flow Behaviour of Kaolin Clay Slurries, *BHR Group Hydrotransport* **16**, 77–91 (2004).
36. Litzenberger, C. G., Rheological Study of Kaolin Clay Slurries, Saskatoon, Canada, M.Sc. Thesis, University of Saskatchewan (2003).
37. Sumner, R. J., Munkler, J. J., Carriere, S. M. and Shook, C. A., Rheology of kaolin slurries containing large silica particles, *Journal of Hydrology and Hydromechanics* **48**, 110–124 (2000).
38. Mohamedelhassan, E., Electrokinetic sedimentation and dewatering of clay slurries, *First International Oil Sands Tailings Conference*. 153–160 (2008).

39. Vaezi G, F., Sanders, R. S. and Masliyah, J. H., Flocculation kinetics and aggregate structure of kaolinite mixtures in laminar tube flow, *J Colloid Interface Sci* **355**, 96–105 (2011).
40. Asadi Shahmirzadi, A., The Effect of Fine Flocculating Particles and Fine Inerts on Carrier Fluid Viscosity, Edmonton, Alberta., MSc Thesis, University of Alberta (2012).
41. Dusseault, M. B. and Scafe, D., Mineralogical and engineering index properties of the basal McMurray Formation clay shales, *Canadian Geotechnical Journal* **16**, 285–294 (1979).
42. Omotoso, O., Mikula, R. J., Urquhart, S., Sulimma, H. and Stephens, P., Characterization of clays from poorly processing oil sands using synchrotron techniques, *Clay Science* **12**, 88–93 (2006).
43. Wallace, D., Tipman, R., Komishke, B., Wallwork, V. and Perkins, E., Fines/Water Interactions and Consequences of the Presence of Degraded Illite on Oil Sands Extractability, *The Canadian Journal of Chemical Engineering* **82**, 667–677 (2004).
44. Mercier, P. H. J., Page, Y. L., Tu, Y. and Kotlyar, L., Powder X-ray Diffraction Determination of Phyllosilicate Mass and Area versus Particle Thickness Distributions for Clays from the Athabasca Oil Sands, *Petroleum Science & Technology* **26**, 307–321 (2008).
45. Chong, J., Ng, S., Chung, K. H., Sparks, B. D. and Kotlyar, L. S., Impact of fines content on a warm slurry extraction process using model oilsands, *Fuel* **82**, 425–438 (2003).

46. Sanford, E. C., Processibility of athabasca oil sand: Interrelationship between oil sand fine solids, process aids, mechanical energy and oil sand age after mining, *The Canadian Journal of Chemical Engineering* **61**, 554–567 (1983).
47. Liu, J., Xu, Z. and Masliyah, J., Role of fine clays in bitumen extraction from oil sands, *AIChE Journal* **50**, 1917–1927 (2004).
48. Tu, Y., O’Carroll, J. B., Kotlyar, L. S., Sparks, B. D., Ng, S., Chung, K. H., and Cuddy, G., Recovery of bitumen from oilsands: gelation of ultra-fine clay in the primary separation vessel, *Fuel* **84**, 653–660 (2005).
49. Clementz, D. M., Interaction of petroleum heavy ends with montmorillonite, *Clays and Clay Minerals* **24**, 312–319 (1976).
50. Czarnecka, E. and Gillott, J. E., Formation and characterization of clay complexes with bitumen from Athabasca oil sand, *Clays and Clay Minerals* **28**, 197–203 (1980).
51. Kasongo, T., Zhou, Z., Xu, Z. and Masliyah, J., Effect of clays and calcium ions on bitumen extraction from athabasca oil sands using flotation, *The Canadian Journal of Chemical Engineering* **78**, 674–681 (2000).
52. Brenner, H., Rheology of a dilute suspension of axisymmetric Brownian particles, *International Journal of Multiphase Flow* **1**, 195–341 (1974).
53. Sanders, R. S., Schaan, J., Hughes, R. and Shook, C., Performance of Sand Slurry Pipelines in the Oil Sands Industry, *The Canadian Journal of Chemical Engineering* **82**, 850–857 (2004).

54. Gillies, R. G., Shook, C. A. and Xu, J., Modelling Heterogeneous Slurry Flows at High Velocities, *The Canadian Journal of Chemical Engineering* **82**, 1060–1065 (2004).
55. Caughill, D. L., Morgenstern, N. R. and Scott, J. D., Geotechnics of nonsegregating oil sand tailings, *Canadian Geotechnical Journal* **30**, 801–811 (1993).
56. Boratyneć, D., Fundamentals of rapid dewatering of composite tailings, Edmonton, Canada, MSc. Thesis, University of Alberta (2003).
57. Donahue, R., Segó, D. C., Burke, B., Krahn, A., Kung, J., and Islam, N., Impact of ion exchange properties on the sedimentation properties of oil sands mature fine tailings and synthetic clay slurries, *Proceedings of the First International Oil Sands Tailings Conference* 55–63 (2008).
58. Kaminsky, H. W., Uhlik, P., Hooshiar, A., Shinbine, A., Etsell, T. H., Ivey, D. G., Liu, Q., and Omotoso, O., Comparison of morphological and chemical characteristics of clay minerals in the primary froth and middlings from oil sands processing by high resolution transmission electron microscopy, *Proceedings of the First International Oil Sands Tailings Conference* 102–111 (2008).
59. Adegoroye, A. Y., Characterization of Solids Isolated from Different Oil Sand Ores, Edmonton, Canada, PhD thesis, University of Alberta (2010).
60. Lionberger, R. A., Viscosity of bimodal and polydisperse colloidal suspensions, *Physical Review E* **65**, 061408(1-11), (2002).

61. Cheng, D. C. H., Kruszewski, A. P., Senior, J. R. and Roberts, T. A., The effect of particle size distribution on the rheology of an industrial suspension, *Journal of Materials Science* **25**, 353–373 (1990).
62. Dabak, T. and Yucel, O., Modeling of the concentration particle size distribution effects on the rheology of highly concentrated suspensions, *Powder Technology* **52**, 193–206 (1987).
63. Parkinson, C., Matsumoto, S. and Sherman, P., The influence of particle-size distribution on the apparent viscosity of non-newtonian dispersed systems, *Journal of Colloid and Interface Science* **33**, 150–160 (1970).
64. Olhero, S. and Ferreira, J. M., Influence of particle size distribution on rheology and particle packing of silica-based suspensions, *Powder Technology* **139**, 69–75 (2004).
65. Leong, Y. K., Scales, P. J., Healy, T. W. and Boger, D. V., Effect of Particle Size on Colloidal Zirconia Rheology at the Isoelectric Point, *Journal of the American Ceramic Society* **78**, 2209–2212 (1995).
66. Do Amaral, M., Van Es, S. and Asua, J. M., Effect of the particle size distribution on the low shear viscosity of high-solid-content latexes, *Journal of Polymer Science Part A: Polymer Chemistry* **42**, 3936–3946 (2004).
67. Chun, J., Oh, T., Luna, M. and Schweiger, M., Effect of particle size distribution on slurry rheology: Nuclear waste simulant slurries, *Colloids and Surfaces A: Physicochemical and Engineering Aspects* **384**, 304–310 (2011).

68. Vlasak, P. and Chara, Z., Effect of Particle Size Distribution and Concentration on Flow Behavior of Dense Slurries, *Particulate Science and Technology* **29**, 53–65 (2011).
69. Bhattacharya, I., Panda, D. and Bandopadhyay, P., Rheological behaviour of nickel laterite suspensions, *International Journal of Mineral Processing* **53**, 251–263 (1998).
70. Subbanna, M., Pradip and Malghan, S., Shear yield stress of flocculated alumina–zirconia mixed suspensions: effect of solid loading, composition and particle size distribution, *Chemical Engineering Science* **53**, 3073–3079 (1998).
71. Dondi, M., Iglesias, C., Dominguez, E., Guarini, G. and Raimondo, M., The effect of kaolin properties on their behaviour in ceramic processing as illustrated by a range of kaolins from the Santa Cruz and Chubut Provinces, Patagonia (Argentina), *Applied Clay Science* **40**, 143–158 (2008).
72. Rasteiro, M. G. and Salgueiros, I., Rheology of Particulate Suspensions in Ceramic Industry, *Particulate Science and Technology* **23**, 145–157 (2005).
73. Matijasic, G. and Glasnovic, A., Influence of Dispersed Phase Characteristics on Rheological Behavior of Suspensions, *Chem. Biochem. Eng. Q.* **16**, 165–172 (2002).
74. Samiei, S., Role of ultra-fine solid fractions on rheology of oil sands suspensions, Edmonton, Alberta. PhD Thesis, University of Alberta (2007).

75. Velho, J. A. G. L. and Gomes, C. D. S. F., Characterization of Portuguese kaolins for the paper industry: beneficiation through new delamination techniques, *Applied Clay Science* **6**, 155–170 (1991).
76. Masliyah, J. H., *Electrokinetic transport phenomena*, (Alberta, Oil Sands Technology and Research Authority: 1994).
77. Franco, F., Pérez-Maqueda, L. A. and Pérez-Rodríguez, J. L., The effect of ultrasound on the particle size and structural disorder of a well-ordered kaolinite, *Journal of Colloid and Interface Science* **274**, 107–117 (2004).
78. Pérez-Maqueda, L. A., Franco, F. and Pérez-Rodríguez, J. L., Comparative study of the sonication effect on the thermal behaviour of 1:1 and 2:1 aluminium phyllosilicate clays, *Journal of the European Ceramic Society* **25**, 1463–1470 (2005).
79. Franco, F., Pérez-Maqueda, L. A. & Pérez-Rodríguez, J. L., The influence of ultrasound on the thermal behaviour of a well ordered kaolinite, *Thermochimica Acta* **404**, 71–79 (2003).
80. Michaels, A. S. and Bolger, J. C., Settling Rates and Sediment Volumes of Flocculated Kaolin Suspensions, *Ind. Eng. Chem. Fund.* **1**, 24–33 (1962).
81. Nasser, M. S. and James, A. E., Settling and sediment bed behaviour of kaolinite in aqueous media, *Separation and Purification Technology* **51**, 10–17 (2006).
82. Olphen, H. V., *An Introduction to Clay Colloid Chemistry*, (John Wiley and Sons: 1977).

83. Thiessen, P. A., Wechselseitige Adsorption von Kolloiden, *Zeitschrift für Elektrochemie und angewandte physikalische Chemie* **48**, 675–681 (1942).
84. Yukselen-Aksoy, Y. and Kaya, A., A study of factors affecting on the zeta potential of kaolinite and quartz powder, *Environmental Earth Sciences* **62**, 697–705 (2011).
85. Islam, N., The role of cation exchange on the sedimentation behavior of oil sands tailings, Edmonton, Alberta. MEng Thesis, University of Alberta (2008).
86. Zbik, M. S., Smart, R. S. C. and Morris, G. E., Kaolinite flocculation structure, *Journal of Colloid and Interface Science* **328**, 73–80 (2008).
87. Peters, D., Ultrasound in materials chemistry, *J. Mater. Chem.* **6**, 1605–1618 (1996).
88. G. J. Price, *Current Trends in Sonochemistry*, 1st ed. (Royal Society of Chemistry: 1992).
89. Taurozzi, J., Hackley, V. & Wiesner, M., Protocol for preparation of nanoparticle dispersion from powdered material using ultrasonic disruption, (CEINT/NIST US: 2010).
90. Doktycz, S. J. & Suslick, K. S., Interparticle Collisions Driven by Ultrasound, *Science* **247**, 1067–1069 (1990).
91. Suslick, K. S., The Chemical Effects of Ultrasound, *Scientific American* **260**, 80–86 (1989).
92. Suslick, K. S., The Sonochemical Hot Spot, *American Chemical Society* **108**, 5641–5642 (1986).

93. Prozorov, T., Prozorov, R. & Suslick, K. S., High Velocity Interparticle Collisions Driven by Ultrasound, *J. Am. Chem. Soc.* **126**, 13890–13891 (2004).
94. Berlan, J. & Mason, T. J., Sonochemistry: from research laboratories to industrial plants, *Ultrasonics* **30**, 203–212 (1992).
95. Keenan, D. F., Tiwari, B. K., Patras, A., Gormley, R., Butler, F., and Brunton, N. P., Effect of sonication on the bioactive, quality and rheological characteristics of fruit smoothies, *International Journal of Food Science & Technology* **47**, 827–836 (2012).
96. Hassanjani-Roshan, A., Kazemzadeh, S. M., Vaezi, M. R. & Shokuhfar, A., The effect of sonication power on the sonochemical synthesis of titania nanoparticles, *Journal of Ceramic Processing Research* **12**, 299–303 (2011).
97. Lapidés, I. & Yariv, S., The effect of ultrasound treatment on the particle-size of Wyoming bentonite in aqueous suspensions, *Journal of Materials Science* **39**, 5209–5212 (2004).
98. Pacuła, A., Bielańska, E., Gawęł, A., Bahranowski, K. & Serwicka, E. M., Textural effects in powdered montmorillonite induced by freeze-drying and ultrasound pretreatment, *Applied Clay Science* **32**, 64–72 (2006).
99. Hinds, I. C., Electric Birefringence for Monitoring Size Changes in Clay Suspensions, *Clay Minerals* **31**, 549–556 (1996).
100. Pérez-Maqueda, L. A., Caneo, O. B., Poyato, J. & Pérez-Rodríguez, J. L., Preparation and characterization of micron and submicron-sized vermiculite, *Physics and Chemistry of Minerals* **28**, 61–66 (2001).

101. Pérez-Rodríguez, J. L., Carrera, F., Poyato, J. & Pérez-Maqueda, L. A.,  
Sonication as a tool for preparing nanometric vermiculite particles,  
*Nanotechnology* **13**, 382–387 (2002).
102. Wiewióra, A., Pérez-Rodríguez, J. L., Perez-Maqueda, L. A. & Drapala, J.,  
Particle size distribution in sonicated high- and low-charge vermiculites,  
*Applied Clay Science* **24**, 51–58 (2003).
103. Pérez-Maqueda, L. A., de Haro, M. C. J., Poyato, J. & Pérez-Rodríguez, J.  
L., Comparative study of ground and sonicated vermiculite, *Journal of  
Materials Science* **39**, 5347–5351 (2004).
104. Poli, A. L., Batista, T., Schmitt, C. C., Gessner, F. & Neumann, M. G.,  
Effect of sonication on the particle size of montmorillonite clays, *J Colloid  
Interface Sci* **325**, 386–390 (2008).
105. Pérez-Maqueda, L. A., Duran, A. & Pérez-Rodríguez, J. L., Preparation of  
submicron talc particles by sonication, *Applied Clay Science* **28**, 245–255  
(2005).
106. Pérez-Maqueda, L. A., Franco, F., Avilés, M. A., Poyato, J. & Pérez-  
Rodríguez, J. L., Effect of Sonication on Particle-Size Distribution in  
Natural Muscovite and Biotite, *Clays and Clay Minerals* **51**, 701–708  
(2003).
107. Pérez-Rodríguez, J. L., Wiewióra, A., Drapala, J. & Pérez-Maqueda, L. A.,  
The effect of sonication on dioctahedral and trioctahedral micas, *Ultrason  
Sonochem* **13**, 61–67 (2006).

108. Franco, F., Cecila, J. A., Pérez-Maqueda, L. A., Pérez-Rodríguez, J. L. & Gomes, C. S. F., Particle-size reduction of dickite by ultrasound treatments: Effect on the structure, shape and particle-size distribution, *Applied Clay Science* **35**, 119–127 (2007).
109. Pérez-Rodríguez, J. L., Pascual, J., Franco, F., Jiménez de Haro, M. C., Duran, A., Ramírez del Valle, V. and Pérez-Maqueda, L. A., The influence of ultrasound on the thermal behaviour of clay minerals, *Journal of the European Ceramic Society* **26**, 747–753 (2006).
110. Pérez-Maqueda, L. A., Blanes, J. M., Pascual, J. & Pérez-Rodríguez, J. L., The influence of sonication on the thermal behavior of muscovite and biotite, *Journal of the European Ceramic Society* **24**, 2793–2801 (2004).
111. Long, J., Li, H., Xu, Z. & Masliyah, J. H., Role of colloidal interactions in oil sand tailings treatment, *AIChE Journal* **52**, 371–383 (2006).
112. Sysmex FPIA-3000/FPIA-3000S operator's manual, Kobe, Japan. (Sysmex Corporation: 2006).
113. Sandford, E. & Seyer, F., Batch Extraction Unit for Tar Sands Processing Studies, Syncrude Canada Ltd, Edmonton, Canada (1978).at  
<[http://web.anl.gov/PCS/acsfuel/preprint%20archive/Files/23\\_4\\_MIAMI%20BEACH\\_09-78\\_0054.pdf](http://web.anl.gov/PCS/acsfuel/preprint%20archive/Files/23_4_MIAMI%20BEACH_09-78_0054.pdf)>
114. Smith, J., Correlations of carrier fluid rheology with clay aggregate size and concentration for oil sands slurries, presented at the 83rd Annual Meeting of the Society of Rheology, Cleveland, US, (2011).

115. Misonix Sonicators - Sonicator 4000. at  
<<http://www.sonicator.com/sonicator4000.aspx>>
116. Qsonica, manufacturers of Misonix Sonicators *Power vs Intensity*. at  
< <http://www.sonicator.com/pdf/PowervsIntensity.pdf>>
117. Saigo, K., Hashimoto, M., Kumagai, S., Tanaka, C. & Imoto, S., Usefulness of particle image analyzer for evaluation of fragmented red cells, *Transfusion and Apheresis Science* **33**, 71–73 (2005).
118. Collins, L., Kaszuba, M. & Fabre, J. W., Imaging in solution of (Lys)<sup>16</sup>-containing bifunctional synthetic peptide/DNA nanoparticles for gene delivery, *Biochimica et Biophysica Acta (BBA) - General Subjects* **1672**, 12–20 (2004).
119. Nicorescu, I. , Riaublanc, A., Loisel, C., Vial, C., Djelveh, G., Cuvelier, G. and Legrand, J., Impact of protein self-assemblages on foam properties, *Food Research International* **42**, 1434–1445 (2009).
120. Promeyrat, A., Bax, M. L. , Traoré, S. , Aubry, L., Santé-Lhoutellier, V., and Gatellier, P., Changed dynamics in myofibrillar protein aggregation as a consequence of heating time and temperature, *Meat Science* **85**, 625–631 (2010).
121. Promeyrat, A., Gatellier, P., Lebret, B., Kajak-Siemaszko, K., Aubry, L., and Santé-Lhoutellier, V., Evaluation of protein aggregation in cooked meat, *Food Chemistry* **121**, 412–417 (2010).

122. Mathys, A., Inactivation mechanisms of *Geobacillus* and *Bacillus* spores during high pressure thermal sterilization, Berlin, Germany. Doctor of Engineering Thesis, Berlin University of Technology. (2008).
123. Mitsumoto, K., Yabusaki, K. & Aoyagi, H., Classification of pollen species using autofluorescence image analysis, *Journal of Bioscience and Bioengineering* **107**, 90–94 (2009).
124. Langlet, J., Gaboriaud, F. & Gantzer, C., Effects of pH on plaque forming unit counts and aggregation of MS2 bacteriophage, *J. Appl. Microbiol.* **103**, 1632–1638 (2007).
125. Raschke, D. & Knorr, D., Rapid monitoring of cell size, vitality and lipid droplet development in the oleaginous yeast *Waltomyces lipofer*, *J. Microbiol. Methods* **79**, 178–183 (2009).
126. Kagami, Y., Sugimura, S., Fujishima, N., Matsuda, K., Kometani, T. and Matsumura, Y., Oxidative Stability, Structure, and Physical Characteristics of Microcapsules Formed by Spray Drying of Fish Oil with Protein and Dextrin Wall Materials, *Journal of Food Science* **68**, 2248–2255 (2003).
127. Komabayashi, T., D'souza, R. N., Dechow, P. C., Safavi, K. E. and Spångberg, L. S. W., Particle Size and Shape of Calcium Hydroxide, *Journal of Endodontics* **35**, 284–287 (2009).
128. Komabayashi, T. & Spångberg, L. S. W., Particle Size and Shape Analysis of MTA Finer Fractions Using Portland Cement, *Journal of Endodontics* **34**, 709–711 (2008).

129. Komabayashi, T. & Spångberg, L. S. W., Comparative analysis of the particle size and shape of commercially available mineral trioxide aggregates and Portland cement: a study with a flow particle image analyzer, *Journal of Endodontics* **34**, 94–98 (2008).
130. Krause, B., Petzold, G., Pegel, S. & Pötschke, P., Correlation of carbon nanotube dispersability in aqueous surfactant solutions and polymers, *Carbon* **47**, 602–612 (2009).
131. Tanaka, M., Komagata, M., Tsukada, M. & Kamiya, H., Fractal analysis of the influence of surface roughness of toner particles on their flow properties and adhesion behavior, *Powder Technology* **186**, 1–8 (2008).
132. Arnold, G., Garche, J., Hemmer, R., Ströbele, S., Vogler, C., and Wohlfahrt-Mehrens, M., Fine-particle lithium iron phosphate LiFePO<sub>4</sub> synthesized by a new low-cost aqueous precipitation technique, *Journal of Power Sources* **119–121**, 247–251 (2003).
133. Besendörfer, G. & Roosen, A., Particle Shape and Size Effects on Anisotropic Shrinkage in Tape-Cast Ceramic Layers, *Journal of the American Ceramic Society* **91**, 2514–2520 (2008).
134. Rauscher, M. & Roosen, A., Effect of Particle Shape on Anisotropic Packing and Shrinkage Behavior of Tape-Cast Glass–Ceramic Composites, *International Journal of Applied Ceramic Technology* **6**, 24–34 (2009).
135. Brugger, B. & Richtering, W., Magnetic, Thermosensitive Microgels as Stimuli-Responsive Emulsifiers Allowing for Remote Control of

- Separability and Stability of Oil in Water-Emulsions, *Advanced Materials* **19**, 2973–2978 (2007).
136. Lape, N. K., Nuxoll, E. E. & Cussler, E. L., Polydisperse flakes in barrier films, *Journal of Membrane Science* **236**, 29–37 (2004).
137. Nasser, M. S. & James, A. E., Effect of polyacrylamide polymers on floc size and rheological behaviour of kaolinite suspensions, *Colloids and Surfaces A: Physicochemical and Engineering Aspects* **301**, 311–322 (2007).
138. Eshel, G., Levy, G. J., Mingelgrin, U. & Singer, M. J., Critical Evaluation of the Use of Laser Diffraction for Particle-Size Distribution Analysis, *Soil Science Society of America Journal* **68**, 736–743 (2004).
139. Malvern Mastersizer 2000. at  
<<http://www.malvern.com/common/downloads/MRK501.pdf>>
140. Du, J., Pushkarova, R. A. & Smart, R. S. C., A cryo-SEM study of aggregate and floc structure changes during clay settling and raking processes, *International Journal of Mineral Processing* **93**, 66–72 (2009).
141. Moore, D., Notz, W. I. & Fligner, M. A., *The Basic Practice of Statistics*, (W. H. Freeman: 2011).
142. Klein, B., Partridge, S. J. & Laskowski, J. S., Rheology of Unstable Mineral Suspensions, *Coal Preparation* **8**, 123–134 (1990).
143. Michaels, A. S. & Bolger, J. C., Particle Interactions in Aqueous Kaolinite Dispersions, *Ind. Eng. Chem. Fund.* **3**, 14–20 (1964).

144. Mikula, R. J., Omotoso, O. & Kasperski, K. L., The chemistry of oil sands tailings: production to treatment, *Proceeding First International Oil Sands Tailings Conference*, 23–33 (2008).
145. Rand, B. & Melton, I. E., Particle interactions in aqueous kaolinite suspensions: I. Effect of pH and electrolyte upon the mode of particle interaction in homoionic sodium kaolinite suspensions, *Journal of Colloid and Interface Science* **60**, 308–320 (1977).
146. Hsu, J. P. & Tseng, M. T., Electrical Interaction between Two Thin Disks of Finite Thickness, *Langmuir* **14**, 714–718 (1998).

# Appendix A: Repeatability of FPIA results

Concentration: 20 g/L

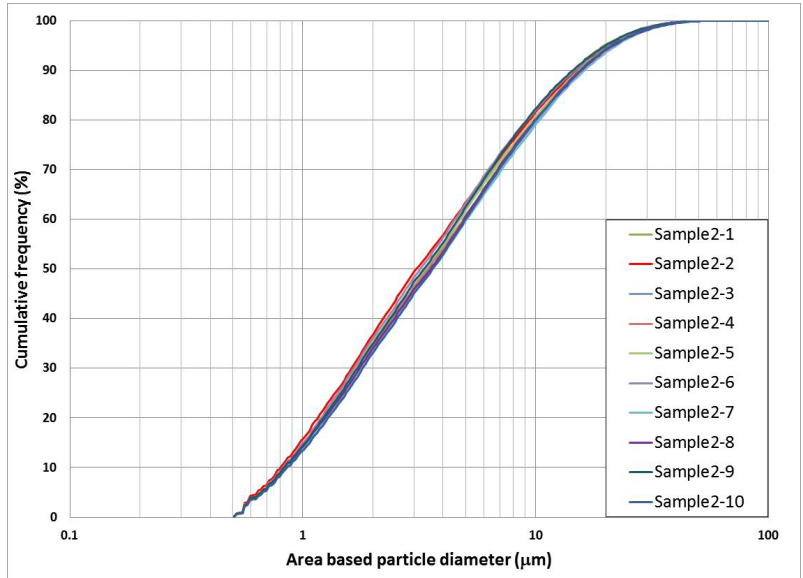


Figure A.1 Repeatability tests: Cumulative Particle size distributions for 10 samples from a single mixture (c= 20 g/L)

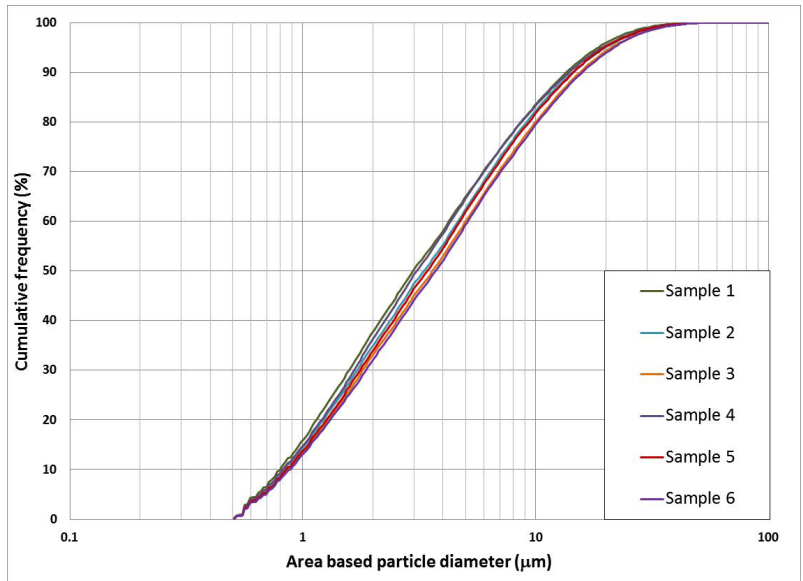
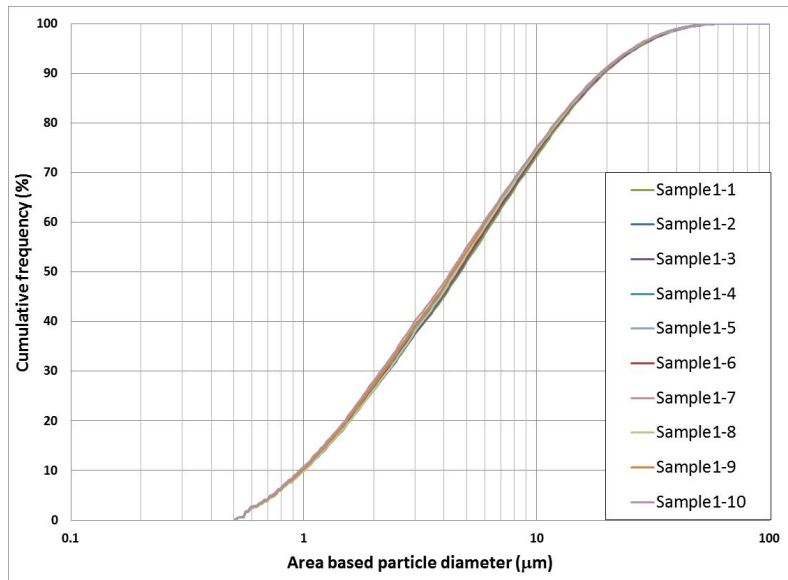
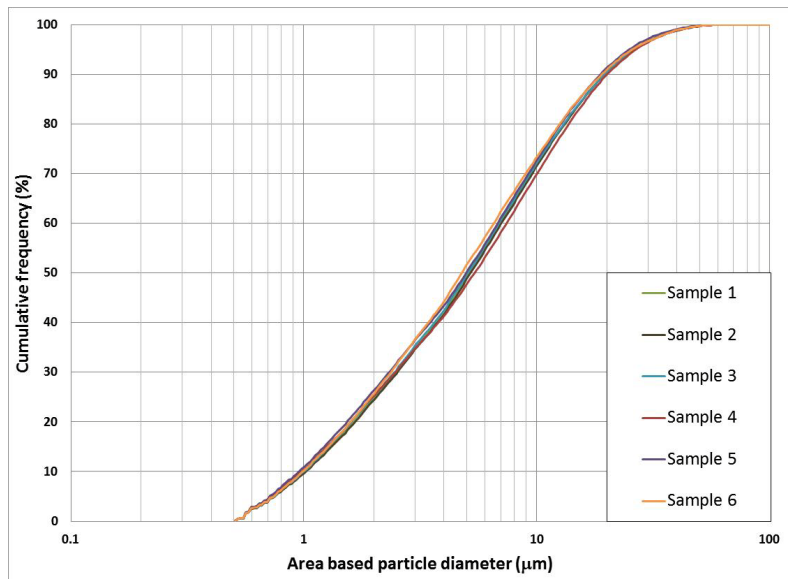


Figure A.2. Repeatability tests: Cumulative particle size distributions for 6 different mixtures having the same concentration (c=20 g/L)

**Concentration: 40 g/L**



**Figure A.3 Repeatability tests: Cumulative Particle size distributions for 10 samples from a single mixture (c= 40 g/L)**



**Figure A.4. Repeatability tests: Cumulative particle size distributions for 6 different mixtures having the same concentration (c=40 g/L)**

## Appendix B: calculations of chi-square tests

Calculations for results presented in Figure 4.1, c=10 g/L

**Table B.1 Observed values of cumulative particle size distributions presented in Figure 4.1 for 10 samples from a single mixture (c= 10 g/L)**

Observed values: cumulative %											
Size (µm)	sample 3-1	sample 3-2	sample 3-3	sample 3-4	sample 3-5	sample 3-6	sample 3-7	sample 3-8	sample 3-9	sample 3-10	total
<=0.6	24.75	21.55	21.47	21.34	22.41	23.93	22.65	22.73	20.72	21.99	223.54
27											
0.644	6.01	5.34	5.38	5.43	5.6	5.85	5.56	5.54	5.16	5.4	55.27
0.661	6.15	5.46	5.49	5.56	5.73	5.97	5.68	5.65	5.27	5.55	56.51
0.678	7.01	6.27	6.35	6.3	6.61	6.83	6.57	6.51	6.15	6.4	65
0.697	7.13	6.41	6.47	6.42	6.74	7	6.69	6.64	6.29	6.5	66.29
0.716	8.43	7.57	7.69	7.58	7.99	8.2	7.88	7.89	7.44	7.65	78.32
0.735	8.77	7.9	7.98	7.87	8.28	8.52	8.22	8.17	7.75	7.92	81.38
0.754	9.48	8.5	8.69	8.51	8.95	9.2	8.86	8.87	8.36	8.57	87.99
0.775	10.82	9.71	9.86	9.74	10.16	10.5	10.05	10.14	9.53	9.84	100.35
0.796	11.01	9.88	10.06	9.93	10.35	10.69	10.24	10.33	9.68	10.03	102.2
0.817	12.12	10.91	11.07	10.98	11.38	11.82	11.24	11.33	10.69	11.05	112.59
0.839	12.91	11.6	11.79	11.7	12.1	12.61	11.9	12.1	11.4	11.75	119.86
0.861	13.88	12.6	12.71	12.61	13.07	13.58	12.86	13.12	12.33	12.77	129.53
0.884	14.09	12.83	12.96	12.85	13.3	13.85	13.11	13.36	12.57	12.99	131.91
0.908	14.96	13.64	13.81	13.65	14.11	14.73	14.01	14.19	13.4	13.8	140.3
0.933	15.61	14.3	14.49	14.32	14.73	15.38	14.68	14.85	14.02	14.48	146.86
0.958	16.67	15.32	15.46	15.34	15.78	16.47	15.65	15.88	14.96	15.55	157.08
0.983	17.56	16.19	16.33	16.18	16.59	17.37	16.53	16.78	15.81	16.34	165.68
1.01	18.3	16.9	17.03	16.84	17.32	18.08	17.26	17.51	16.46	17.06	172.76
1.037	19.09	17.74	17.9	17.69	18.17	18.96	18.03	18.29	17.22	17.87	180.96
1.065	19.94	18.53	18.64	18.49	19.02	19.8	18.86	19.07	18.08	18.67	189.1
1.094	21.25	19.78	19.88	19.75	20.22	21.11	20.09	20.31	19.32	19.93	201.64
1.123	21.96	20.39	20.57	20.44	20.92	21.82	20.75	21.07	19.98	20.55	208.45
1.153	22.69	21.15	21.29	21.24	21.73	22.65	21.51	21.84	20.72	21.24	216.06
1.184	23.9	22.23	22.45	22.36	22.88	23.86	22.72	22.97	21.9	22.3	227.57
1.215	24.61	22.98	23.19	23.1	23.65	24.61	23.41	23.66	22.58	22.98	234.77
1.248	25.77	24.04	24.3	24.22	24.72	25.79	24.55	24.83	23.6	24.11	245.93
1.282	26.58	24.91	25.11	25	25.6	26.67	25.4	25.64	24.42	24.87	254.2
1.316	27.53	25.8	25.98	25.95	26.52	27.57	26.34	26.56	25.24	25.82	263.31
1.351	28.59	26.9	26.97	27	27.59	28.59	27.37	27.52	26.25	26.8	273.58
1.388	29.56	27.89	27.9	27.95	28.68	29.63	28.31	28.57	27.21	27.84	283.54
1.425	30.58	28.86	28.88	28.94	29.6	30.67	29.22	29.54	28.19	28.9	293.38
1.464	31.52	29.89	29.79	29.94	30.59	31.64	30.22	30.55	29.18	29.89	303.21
1.503	32.54	30.88	30.75	30.88	31.6	32.71	31.21	31.58	30.14	30.83	313.12
1.543	33.77	32.15	31.95	32.08	32.86	33.96	32.38	32.77	31.33	31.99	325.24
1.584	34.75	33.05	32.87	32.96	33.77	34.91	33.34	33.7	32.22	32.9	334.47
1.627	35.95	34.18	34.14	34.02	35	36.16	34.51	34.81	33.32	34.07	346.16
1.671	37.13	35.32	35.33	35.19	36.15	37.25	35.61	35.95	34.37	35.23	357.53
1.716	38.13	36.33	36.29	36.18	37.14	38.27	36.55	36.9	35.32	36.21	367.32
1.762	39.27	37.44	37.43	37.3	38.21	39.46	37.69	38.02	36.53	37.31	378.66
1.809	40.37	38.46	38.58	38.36	39.24	40.55	38.79	39.07	37.69	38.39	389.5
1.858	41.35	39.49	39.7	39.38	40.27	41.62	39.83	40.17	38.71	39.52	400.04
1.908	42.61	40.71	40.87	40.58	41.46	42.83	41.12	41.32	39.93	40.74	412.17
1.959	43.64	41.81	42.01	41.71	42.6	44.02	42.21	42.39	41.02	41.78	423.19
2.012	44.72	42.76	43.01	42.77	43.58	45.03	43.25	43.31	42.03	42.7	433.16
2.066	45.81	43.8	44.12	43.84	44.73	46.17	44.26	44.27	43.15	43.73	443.88
2.121	46.68	44.65	45.07	44.77	45.73	47.17	45.2	45.2	44.16	44.71	453.34
2.178	47.73	45.64	46.15	45.84	46.81	48.15	46.22	46.15	45.17	45.76	463.62
2.237	48.75	46.72	47.28	46.92	47.82	49.28	47.36	47.21	46.24	46.79	474.37
2.297	49.78	47.75	48.34	47.97	48.93	50.33	48.42	48.27	47.3	47.81	484.9
2.358	50.91	48.78	49.39	48.95	49.93	51.34	49.49	49.22	48.29	48.81	495.11
2.421	51.99	49.81	50.47	49.98	50.94	52.35	50.51	50.26	49.34	49.79	505.44
2.486	53.06	50.89	51.5	51.01	51.97	53.39	51.55	51.3	50.43	50.85	515.95
2.553	54.17	51.98	52.56	52.12	53.11	54.55	52.67	52.34	51.55	51.92	526.97

2.622	55.19	52.99	53.56	53.18	54.11	55.62	53.73	53.2	52.59	52.89	537.06
2.693	56.28	54	54.73	54.29	55.21	56.73	54.81	54.25	53.7	53.96	547.96
2.765	57.25	55.11	55.8	55.4	56.15	57.87	55.86	55.29	54.74	55.06	558.53
2.839	58.37	56.2	56.95	56.53	57.27	59.07	57.06	56.41	55.83	56.17	569.86
2.915	59.44	57.23	58.07	57.72	58.29	60.04	58.13	57.44	56.84	57.2	580.4
2.994	60.37	58.23	59.12	58.75	59.27	61.1	59.11	58.4	57.78	58.2	590.33
3.074	61.26	59.11	60.09	59.81	60.2	62.05	60.02	59.26	58.7	59.15	599.65
3.157	62.23	60.05	61.03	60.75	61.13	62.89	60.9	60.06	59.62	60.02	608.68
3.241	63.13	61.02	61.95	61.63	62.09	63.79	61.79	60.9	60.49	60.91	617.7
3.328	64.09	62.01	62.96	62.69	63.05	64.69	62.73	61.84	61.44	61.85	627.35
3.418	65.01	62.95	63.99	63.66	63.98	65.55	63.64	62.71	62.33	62.75	636.57
3.51	65.95	63.9	64.99	64.55	64.95	66.47	64.62	63.59	63.25	63.64	645.91
3.604	66.93	64.88	65.98	65.49	65.92	67.43	65.51	64.47	64.18	64.52	655.31
3.701	67.91	65.82	66.95	66.49	66.87	68.29	66.54	65.32	65.11	65.43	664.73
3.8	68.86	66.74	67.86	67.45	67.74	69.18	67.44	66.18	66.03	66.37	673.85
3.902	69.73	67.72	68.84	68.42	68.72	70.15	68.35	67	66.97	67.23	683.13
4.007	70.7	68.72	69.87	69.41	69.74	71.09	69.28	67.9	67.98	68.15	692.84
4.115	71.66	69.79	70.88	70.43	70.7	72.08	70.3	68.91	69	69.14	702.89
4.225	72.67	70.84	71.87	71.46	71.62	73.06	71.31	69.85	69.94	70.08	712.7
4.339	73.63	71.85	72.87	72.49	72.64	74.05	72.27	70.77	70.97	70.98	722.52
4.455	74.59	72.88	73.86	73.42	73.61	74.98	73.25	71.61	71.94	71.86	732
4.575	75.54	73.98	74.78	74.42	74.54	75.93	74.2	72.54	72.88	72.75	741.56
4.698	76.47	75.01	75.78	75.42	75.45	76.87	75.09	73.41	73.74	73.67	750.91
4.824	77.4	76	76.8	76.4	76.38	77.73	76.03	74.25	74.71	74.53	760.23
4.954	78.37	76.92	77.75	77.36	77.22	78.59	76.92	75.08	75.62	75.35	769.18
5.087	79.26	77.85	78.75	78.22	78.08	79.49	77.81	75.91	76.53	76.19	778.09
5.224	80.16	78.76	79.72	79.16	78.9	80.37	78.76	76.73	77.45	77.09	787.1
5.364	80.97	79.68	80.67	80.03	79.76	81.19	79.71	77.61	78.31	77.89	795.82
5.508	81.78	80.63	81.58	81.02	80.59	81.99	80.54	78.49	79.14	78.72	804.48
5.656	82.6	81.57	82.45	81.89	81.45	82.82	81.39	79.34	79.95	79.51	812.97
5.808	83.38	82.41	83.33	82.78	82.25	83.57	82.13	80.12	80.69	80.33	820.99
5.964	84.23	83.29	84.23	83.61	83.04	84.28	82.94	80.95	81.5	81.09	829.16
6.124	85.01	84.16	85.05	84.45	83.78	84.98	83.72	81.66	82.27	81.77	836.85
6.289	85.71	84.92	85.75	85.26	84.51	85.72	84.48	82.38	83.06	82.47	844.26
6.458	86.42	85.7	86.51	86.07	85.25	86.41	85.18	83.14	83.82	83.19	851.69
6.631	87.12	86.47	87.21	86.83	85.93	87.1	85.93	83.89	84.53	83.89	858.9
6.809	87.79	87.16	87.97	87.61	86.61	87.73	86.6	84.65	85.21	84.61	865.94
6.992	88.45	87.88	88.7	88.31	87.25	88.41	87.29	85.31	85.91	85.28	872.79
7.18	89.09	88.62	89.42	88.95	87.87	89.02	87.99	85.97	86.58	85.89	879.4
7.373	89.71	89.26	90.06	89.64	88.53	89.58	88.61	86.58	87.28	86.48	885.73
7.571	90.3	89.93	90.69	90.31	89.2	90.19	89.25	87.16	87.9	87.1	892.03
7.774	90.91	90.54	91.28	90.92	89.72	90.77	89.86	87.79	88.52	87.7	898.01
7.983	91.44	91.14	91.87	91.55	90.3	91.29	90.39	88.4	89.13	88.33	903.84
8.198	91.97	91.7	92.44	92.05	90.82	91.78	90.89	88.96	89.65	88.85	909.11
8.418	92.46	92.22	92.97	92.57	91.38	92.27	91.39	89.49	90.2	89.36	914.31
8.644	92.93	92.71	93.53	93.1	91.91	92.75	91.91	90.04	90.76	89.88	919.52
8.877	93.43	93.25	94.02	93.61	92.42	93.2	92.42	90.57	91.26	90.37	924.55
9.115	93.91	93.75	94.42	94.09	92.94	93.65	92.82	91.06	91.76	90.88	929.28
9.36	94.34	94.13	94.82	94.56	93.37	94.07	93.26	91.57	92.24	91.34	933.7
9.611	94.74	94.59	95.2	94.94	93.79	94.42	93.71	92.01	92.72	91.82	937.94
9.869	95.09	95	95.59	95.32	94.18	94.83	94.13	92.46	93.15	92.27	942.02
10.135	95.47	95.39	95.94	95.72	94.56	95.19	94.55	92.9	93.55	92.75	946.02
10.405	95.79	95.74	96.25	96.07	94.93	95.52	94.92	93.31	93.95	93.14	949.62
10.685	96.14	96.1	96.56	96.4	95.31	95.86	95.31	93.74	94.33	93.52	953.27
10.975	96.46	96.42	96.86	96.74	95.65	96.16	95.64	94.12	94.71	93.84	956.6
11.27	96.75	96.68	97.17	97.01	95.92	96.44	95.95	94.52	95.08	94.2	959.72
11.57	97.01	96.97	97.44	97.27	96.21	96.68	96.24	94.89	95.42	94.55	962.68
11.88	97.23	97.2	97.68	97.49	96.5	96.91	96.52	95.22	95.74	94.87	965.36
12.2	97.48	97.43	97.89	97.7	96.74	97.11	96.81	95.52	96.06	95.17	967.91
12.525	97.67	97.63	98.08	97.91	96.98	97.36	97.06	95.8	96.36	95.44	970.29
12.865	97.85	97.84	98.26	98.07	97.19	97.58	97.29	96.13	96.61	95.73	972.55
13.215	98.03	98.03	98.44	98.24	97.42	97.8	97.51	96.39	96.85	96	974.71
13.57	98.18	98.2	98.6	98.4	97.65	97.99	97.73	96.62	97.11	96.32	976.8
13.93	98.35	98.35	98.79	98.56	97.85	98.17	97.92	96.85	97.36	96.53	978.73
14.3	98.53	98.5	98.93	98.71	98.04	98.35	98.06	97.07	97.55	96.79	980.53
14.685	98.65	98.64	99.06	98.84	98.19	98.5	98.22	97.3	97.78	97.04	982.22
15.08	98.77	98.76	99.14	98.95	98.34	98.63	98.37	97.52	97.95	97.24	983.67
15.485	98.87	98.88	99.22	99.05	98.5	98.75	98.51	97.71	98.09	97.48	985.06
15.905	98.96	99.01	99.3	99.15	98.6	98.85	98.67	97.92	98.24	97.68	986.38

16.335	99.06	99.09	99.38	99.24	98.73	98.95	98.79	98.08	98.38	97.82	987.52
16.77	99.13	99.19	99.45	99.32	98.86	99.05	98.91	98.29	98.52	97.99	988.71
17.22	99.21	99.26	99.51	99.38	98.97	99.14	98.99	98.45	98.67	98.16	989.74
17.685	99.28	99.33	99.58	99.45	99.05	99.22	99.08	98.58	98.8	98.31	990.68
18.16	99.34	99.39	99.65	99.51	99.14	99.3	99.2	98.69	98.9	98.46	991.58
18.645	99.4	99.46	99.68	99.56	99.23	99.37	99.28	98.79	99.01	98.62	992.4
19.145	99.46	99.5	99.72	99.6	99.31	99.42	99.35	98.89	99.11	98.73	993.09
19.66	99.52	99.55	99.75	99.63	99.39	99.51	99.4	99	99.18	98.85	993.78
20.19	99.57	99.6	99.78	99.66	99.44	99.56	99.46	99.1	99.26	98.95	994.38
20.735	99.6	99.64	99.81	99.69	99.5	99.61	99.51	99.19	99.33	99.04	994.92
21.29	99.66	99.68	99.84	99.73	99.55	99.66	99.57	99.27	99.43	99.13	995.52
21.86	99.71	99.71	99.85	99.77	99.6	99.69	99.62	99.33	99.48	99.21	995.97
22.45	99.74	99.75	99.87	99.81	99.64	99.72	99.67	99.39	99.53	99.27	996.39
23.055	99.77	99.79	99.88	99.84	99.7	99.75	99.7	99.46	99.59	99.34	996.82
23.675	99.79	99.81	99.9	99.86	99.72	99.78	99.72	99.52	99.63	99.42	997.15
24.31	99.82	99.83	99.9	99.88	99.75	99.8	99.76	99.55	99.66	99.46	997.41
24.96	99.84	99.85	99.92	99.89	99.77	99.83	99.8	99.62	99.71	99.52	997.75
25.63	99.86	99.86	99.93	99.89	99.8	99.85	99.83	99.66	99.74	99.58	998
26.32	99.88	99.88	99.94	99.9	99.82	99.88	99.86	99.7	99.77	99.63	998.26
27.03	99.89	99.91	99.94	99.92	99.83	99.9	99.88	99.73	99.8	99.67	998.47
27.755	99.91	99.92	99.95	99.93	99.85	99.91	99.9	99.76	99.83	99.69	998.65
28.5	99.93	99.93	99.97	99.93	99.87	99.93	99.91	99.77	99.86	99.75	998.85
29.265	99.93	99.94	99.97	99.94	99.89	99.94	99.92	99.82	99.88	99.77	999
30.05	99.94	99.95	99.97	99.95	99.9	99.94	99.94	99.84	99.89	99.8	999.12
30.86	99.95	99.96	99.98	99.95	99.92	99.95	99.94	99.86	99.91	99.83	999.25
31.69	99.96	99.96	99.98	99.95	99.93	99.95	99.95	99.87	99.92	99.85	999.32
32.54	99.98	99.97	99.98	99.96	99.96	99.96	99.96	99.89	99.94	99.88	999.48
33.415	99.98	99.97	99.98	99.97	99.96	99.97	99.97	99.91	99.95	99.9	999.56
34.31	99.99	99.98	99.98	99.98	99.97	99.98	99.97	99.92	99.97	99.93	999.67
35.23	99.99	99.98	99.99	99.98	99.97	99.98	99.98	99.92	99.97	99.94	999.7
36.18	99.99	99.98	99.99	99.99	99.98	99.98	99.98	99.93	99.98	99.96	999.76
37.15	99.99	99.99	99.99	99.99	99.98	99.98	99.98	99.95	99.99	99.97	999.81
38.145	100	99.99	99.99	99.99	99.98	99.98	99.99	99.95	99.99	99.97	999.83
39.17	100	99.99	99.99	99.99	99.98	99.99	99.99	99.96	100	99.98	999.87
40.225	100	100	100	99.99	99.99	99.99	99.99	99.96	100	99.98	999.9
41.305	100	100	100	99.99	99.99	99.99	99.99	99.97	100	99.99	999.92
42.415	100	100	100	99.99	99.99	99.99	100	99.98	100	99.99	999.94
43.555	100	100	100	99.99	99.99	100	100	99.98	100	100	999.96
44.725	100	100	100	100	99.99	100	100	99.99	100	100	999.98
45.93	100	100	100	100	99.99	100	100	99.99	100	100	999.98
47.165	100	100	100	100	99.99	100	100	99.99	100	100	999.98
48.43	100	100	100	100	99.99	100	100	99.99	100	100	999.98
49.73	100	100	100	100	100	100	100	99.99	100	100	999.99
51.065	100	100	100	100	100	100	100	99.99	100	100	999.99
52.435	100	100	100	100	100	100	100	99.99	100	100	999.99
53.845	100	100	100	100	100	100	100	99.99	100	100	999.99
55.29	100	100	100	100	100	100	100	99.99	100	100	999.99
56.775	100	100	100	100	100	100	100	100	100	100	1000
58.305	100	100	100	100	100	100	100	100	100	100	1000
59.87	100	100	100	100	100	100	100	100	100	100	1000
61.475	100	100	100	100	100	100	100	100	100	100	1000
63.13	100	100	100	100	100	100	100	100	100	100	1000
64.825	100	100	100	100	100	100	100	100	100	100	1000
66.565	100	100	100	100	100	100	100	100	100	100	1000
68.355	100	100	100	100	100	100	100	100	100	100	1000
70.19	100	100	100	100	100	100	100	100	100	100	1000
72.075	100	100	100	100	100	100	100	100	100	100	1000
74.01	100	100	100	100	100	100	100	100	100	100	1000
76	100	100	100	100	100	100	100	100	100	100	1000
78.045	100	100	100	100	100	100	100	100	100	100	1000
80.14	100	100	100	100	100	100	100	100	100	100	1000
82.29	100	100	100	100	100	100	100	100	100	100	1000
84.5	100	100	100	100	100	100	100	100	100	100	1000
86.77	100	100	100	100	100	100	100	100	100	100	1000
89.105	100	100	100	100	100	100	100	100	100	100	1000
91.5	100	100	100	100	100	100	100	100	100	100	1000
93.955	100	100	100	100	100	100	100	100	100	100	1000
96.48	100	100	100	100	100	100	100	100	100	100	1000
99.08	100	100	100	100	100	100	100	100	100	100	1000

101.75	100	100	100	100	100	100	100	100	100	100	1000
104.5	100	100	100	100	100	100	100	100	100	100	1000
107.3	100	100	100	100	100	100	100	100	100	100	1000
110.15	100	100	100	100	100	100	100	100	100	100	1000
113.1	100	100	100	100	100	100	100	100	100	100	1000
116.15	100	100	100	100	100	100	100	100	100	100	1000
119.3	100	100	100	100	100	100	100	100	100	100	1000
122.5	100	100	100	100	100	100	100	100	100	100	1000
125.75	100	100	100	100	100	100	100	100	100	100	1000
129.15	100	100	100	100	100	100	100	100	100	100	1000
132.65	100	100	100	100	100	100	100	100	100	100	1000
136.2	100	100	100	100	100	100	100	100	100	100	1000
139.85	100	100	100	100	100	100	100	100	100	100	1000
143.6	100	100	100	100	100	100	100	100	100	100	1000
147.45	100	100	100	100	100	100	100	100	100	100	1000
151.4	100	100	100	100	100	100	100	100	100	100	1000
155.45	100	100	100	100	100	100	100	100	100	100	1000
159.65	100	100	100	100	100	100	100	100	100	100	1000
163.95	100	100	100	100	100	100	100	100	100	100	1000
168.35	100	100	100	100	100	100	100	100	100	100	1000
172.9	100	100	100	100	100	100	100	100	100	100	1000
177.55	100	100	100	100	100	100	100	100	100	100	1000
182.3	100	100	100	100	100	100	100	100	100	100	1000
187.2	100	100	100	100	100	100	100	100	100	100	1000
192.25	100	100	100	100	100	100	100	100	100	100	1000
197.4	100	100	100	100	100	100	100	100	100	100	1000
Total	16740. 58	16586. 75	16651. 38	16617. 11	16618. 47	16746. 81	16597. 26	16495. 8	16464. 06	16461. 03	165979 .3

**Table B.2 Expected values for data presented in Table B.1**

Expected values										
Size (µm)	Sample 3-1	Sample 3-2	Sample 3-3	Sample 3-4	Sample 3-5	Sample 3-6	Sample 3-7	Sample 3-8	Sample 3-9	Sample 3-10
<=0.6	22.5440	22.3405	22.4277	22.3808	22.3808	22.5529	22.3517	22.2154	22.1751	22.1706
27	09	88	68	25	25	51	65	05	68	972
0.644	5.57397	5.52368	5.54523	5.53363	5.53363	5.57619	5.52644	5.49273	5.48278	5.48167
	95	38	91	24	24	03	73	26	4	86
0.661	5.69903	5.64760	5.66964	5.65778	5.65778	5.70129	5.65043	5.61596	5.60579	5.60466
	35	94	83	12	12	39	49	38	2	18
0.678	6.55525	6.4961	6.52145	6.5078	6.5078	6.55785	6.49935	6.4597	6.448	6.4467
0.697	6.68534	6.62502	6.65087	6.63695	6.63695	6.68799	6.62833	6.58790	6.57596	6.57464
	65	26	57	48	48	81	71	02	8	22
0.716	7.89857	7.82730	7.85784	7.84139	7.84139	7.90170	7.83121	7.78344	7.76934	7.76777
	2	08	56	84	84	48	68	16	4	76
0.735	8.20717	8.13311	8.16485	8.14776	8.14776	8.21042	8.13718	8.08754	8.07289	8.07126
	3	72	54	56	56	82	62	44	6	84
0.754	8.87379	8.79372	8.82803	8.80955	8.80955	8.87731	8.79812	8.74444	8.72860	8.72684
	15	06	67	88	88	11	01	62	8	82
0.775	10.1202	10.0289	10.0681	10.0470	10.0470	10.1243	10.0339	9.97278	9.95472	9.95271
	98	79	16	42	42	12	97	3		3
0.796	10.3068	10.2138	10.2537	10.2322	10.2322	10.3109	10.2189	10.1566	10.1382	10.1361
	7	68	26	64	64	58	78	36	4	96
0.817	11.3547	11.2522	11.2961	11.2725	11.2725	11.3592	11.2578	11.1891	11.1689	11.1666
	02	45	55	11	11	05	74	94	28	762
0.839	12.0878	11.9788	12.0255	12.0003	12.0003	12.0926	11.9848	11.9116	11.8901	11.8877
	81	08	54	83	83	75	01	87	12	148
0.861	13.0631	12.9452	12.9957	12.9685	12.9685	13.0682	12.9517	12.8726	12.8493	12.8467
	01	28	45	44	44	82	05	91	76	854
0.884	13.3031	13.1830	13.2345	13.2068	13.2068	13.3084	13.1896	13.1092	13.0854	13.0828
	24	85	3	29	29		81	16	72	338
0.908	14.1492	14.0215	14.0762	14.0468	14.0468	14.1548	14.0285	13.9430	13.9177	13.9149
	55	82	99	36	36	67	97	14	6	54
0.933	14.8108	14.6771	14.7344	14.7036	14.7036	14.8167	14.6845	14.5949	14.5685	14.5655
	31	88	64	23	23	05	31	47	12	748
0.958	15.8415	15.6985	15.7598	15.7268	15.7268	15.8478	15.7064	15.6106	15.5823	15.5791
	18	75	36	5	5	01	29	1	36	944

0.983	16.7088 28	16.5580 59	16.6226 74	16.5878 82	16.5878 82	16.7154 55	16.5663 43	16.4652 78	16.4354 56	16.4321 424
1.01	17.4228 46	17.2656 34	17.3330 11	17.2967 31	17.2967 31	17.4297 56	17.2742 72	17.1688 89	17.1377 92	17.1343 368
1.037	18.2498 16	18.0851 42	18.1557 17	18.1177 15	18.1177 15	18.2570 54	18.0941 9	17.9838 05	17.9512 32	17.9476 128
1.065	19.0707 35	18.8986 54	18.9724 03	18.9326 92	18.9326 92	19.0782 99	18.9081 09	18.7927 58	18.7587 2	18.7549 38
1.094	20.3353 94	20.1519 02	20.2305 41	20.1881 97	20.1881 97	20.3434 6	20.1619 84	20.0389 83	20.0026 88	19.9986 552
1.123	21.0221 83	20.8324 93	20.9137 89	20.8700 14	20.8700 14	21.0305 21	20.8429 16	20.7157 61	20.6782 4	20.6740 71
1.153	21.7896 51	21.5930 36	21.6773 27	21.6319 27	21.6319 27	21.7982 93	21.6038 39	21.4720 43	21.4331 52	21.4288 308
1.184	22.9504 35	22.7433 46	22.8320 98	22.7843 08	22.7843 08	22.9595 37	22.7547 24	22.6159 07	22.5749 44	22.5703 926
1.215	23.6765 55	23.4629 14	23.5544 74	23.5051 72	23.5051 72	23.6859 45	23.4746 52	23.3314 43	23.2891 84	23.2844 886
1.248	24.8020 41	24.5782 44	24.6741 57	24.6225 12	24.6225 12	24.8118 78	24.5905 41	24.4405 23	24.3962 56	24.3913 374
1.282	25.6360 7	25.4047 48	25.5038 86	25.4505 04	25.4505 04	25.6462 38	25.4174 58	25.2623 96	25.2166 4	25.2115 56
1.316	26.5548 14	26.3152 01	26.4178 92	26.3625 97	26.3625 97	26.5653 46	26.3283 67	26.1677 48	26.1203 52	26.1150 858
1.351	27.5905 43	27.3415 85	27.4482 81	27.3908 3	27.3908 3	27.6014 86	27.3552 64	27.1883 8	27.1391 36	27.1336 644
1.388	28.5950 09	28.3369 88	28.4475 68	28.3880 25	28.3880 25	28.6063 51	28.3511 65	28.1782 05	28.1271 68	28.1214 972
1.425	29.5873 73	29.3203 97	29.4348 15	29.3732 06	29.3732 06	29.5991 08	29.3350 66	29.1561 04	29.1032 96	29.0974 284
1.464	30.5787 29	30.3028 07	30.4210 59	30.3573 85	30.3573 85	30.5908 57	30.3179 68	30.1330 1	30.0784 32	30.0723 678
1.503	31.5781 52	31.2932 13	31.4153 3	31.3495 74	31.3495 74	31.5906 77	31.3088 69	31.1178 66	31.0615 04	31.0552 416
1.543	32.8004 54	32.5044 86	32.6313 29	32.5630 29	32.5630 29	32.8134 64	32.5207 48	32.3223 51	32.2638 08	32.2573 032
1.584	33.7313	33.4269 32	33.5573 75	33.4871 36	33.4871 36	33.7446 78	33.4436 55	33.2396 29	33.1794 24	33.1727 346
1.627	34.9102 36	34.5952 3	34.7302 33	34.6575 39	34.6575 39	34.9240 82	34.6125 38	34.4013 81	34.3390 72	34.3321 488
1.671	36.0569 01	35.7315 48	35.8709 85	35.7959 04	35.7959 04	36.0712 02	35.7494 25	35.5313 31	35.4669 76	35.4598 254
1.716	37.0442 22	36.7099 61	36.8532 16	36.7760 78	36.7760 78	37.0589 15	36.7283 27	36.5042 62	36.4381 44	36.4307 976
1.762	38.1878 61	37.8432 8	37.9909 58	37.9114 39	37.9114 39	38.2030 07	37.8622 13	37.6312 31	37.5630 72	37.5554 988
1.809	39.2810 75	38.9266 3	39.0785 35	38.9967 4	38.9967 4	39.2966 55	38.9461 05	38.7085 1	38.6384 1	38.6306 1
1.858	40.3440 34	39.9799 98	40.1360 13	40.0520 05	40.0520 05	40.3600 36	40 40	39.7559 75	39.6839 68	39.6759 672
1.908	41.5673 45	41.1922 7	41.3530 16	41.2664 6	41.2664 6	41.5838 31	41.2128 78	40.9614 55	40.8872 64	40.8790 206
1.959	42.6787 12	42.2936 09	42.4586 53	42.3697 83	42.3697 83	42.6956 39	42.3147 68	42.0566 22	41.9804 48	41.9719 842
2.012	43.6841 86	43.2900 1	43.4589 43	43.3679 79	43.3679 79	43.7015 12	43.3116 68	43.0474 41	42.9694 72	42.9608 088
2.066	44.7652 98	44.3613 67	44.5344 8	44.4412 66	44.4412 66	44.7830 53	44.3835 61	44.1127 94	44.0328 96	44.0240 184
2.121	45.7193 39	45.3068	45.4836 02	45.3884 01	45.3884 01	45.7374 73	45.3294 67	45.0529 29	44.9713 28	44.9622 612
2.178	46.7560 77	46.3341 83	46.5149 95	46.4176 34	46.4176 34	46.7746 22	46.3573 64	46.0745 56	45.9911 04	45.9818 316
2.237	47.8402 15	47.4085 38	47.5935 42	47.4939 24	47.4939 24	47.8591 89	47.4322 56	47.1428 91	47.0575 04	47.0480 166
2.297	48.9021 65	48.4609 06	48.6500 17	48.5481 88	48.5481 88	48.9215 61	48.4851 51	48.1893 62	48.1020 8	48.0923 82
2.358	49.9318 44	49.4812 93	49.6743 86	49.5704 13	49.5704 13	49.9516 48	49.5060 49	49.2040 32	49.1149 12	49.1050 098
2.421	50.9736 24	50.5136 74	50.7107 95	50.6046 53	50.6046 53	50.9938 42	50.5389 46	50.2306 27	50.1396 48	50.1295 392
2.486	52.0335	51.5640	51.7652	51.6569	51.6569	52.0541	51.5898	51.2751	51.1822	51.1719

	58	43	64	14	14	96	41	11	4	21
2.553	53.1449 25	52.6653 82	52.8709	52.7602 36	52.7602 36	53.1660 03	52.6917 3	52.3702 79	52.2754 24	52.2648 846
2.622	54.1625 01	53.6737 76	53.8832 3	53.7704 47	53.7704 47	54.1839 83	53.7006 29	53.3730 23	53.2763 52	53.2656 108
2.693	55.2617 66	54.7631 22	54.9768 27	54.8617 55	54.8617 55	55.2836 84	54.7905 2	54.4562 65	54.3576 32	54.3466 728
2.765	56.3277 51	55.8194 88	56.0373 15	55.9200 24	55.9200 24	56.3500 92	55.8474 15	55.5067 11	55.4061 76	55.3950 054
2.839	57.4703 81	56.9518 08	57.1740 54	57.0543 83	57.0543 83	57.4931 75	56.9803 01	56.6326 87	56.5301 12	56.5187 148
2.915	58.5333 4	58.0051 76	58.2315 32	58.1096 48	58.1096 48	58.5565 56	58.0341 96	57.6801 52	57.5756 8	57.5640 72
2.994	59.5347 81	58.9975 8	59.2278 09	59.1038 4	59.1038 4	59.5583 94	59.0270 97	58.6669 95	58.5607 36	58.5489 294
3.074	60.4747 03	59.9290 21	60.1628 85	60.0369 58	60.0369 58	60.4986 89	59.9590 04	59.5932 17	59.4852 8	59.4732 87
3.157	61.3853 78	60.8314 79	61.0688 64	60.9410 42	60.9410 42	61.4097 25	60.8619 13	60.4906 18	60.3810 56	60.3688 824
3.241	62.2950 45	61.7329 38	61.9738 41	61.8441 24	61.8441 24	62.3197 53	61.7638 23	61.3870 26	61.2758 4	61.2634 86
3.328	63.2682 48	62.6973 59	62.9420 26	62.8102 82	62.8102 82	63.2933 42	62.7287 27	62.3460 43	62.2331 2	62.2205 73
3.418	64.1980 85	63.6188 06	63.8670 68	63.7333 88	63.7333 88	64.2235 47	63.6506 34	63.2623 27	63.1477 44	63.1350 126
3.51	65.1400 24	64.5522 45	64.8041 5	64.6685 09	64.6685 09	65.1658 6	64.5845 41	64.1905 36	64.0742 72	64.0613 538
3.604	66.0880 14	65.4916 81	65.7472 52	65.6096 37	65.6096 37	66.1142 26	65.5244 47	65.1247 08	65.0067 52	64.9936 458
3.701	67.0380 21	66.4331 16	66.6923 61	66.5527 68	66.5527 68	67.0646 1	66.4663 53	66.0608 67	65.9412 16	65.9279 214
3.8	67.9577 73	67.3445 69	67.6073 71	67.4658 62	67.4658 62	67.9847 27	67.3782 62	66.9672 13	66.8459 2	66.8324 43
3.902	68.8936 61	68.2720 12	68.5384 33	68.3949 76	68.3949 76	68.9209 86	68.3061 69	67.8894 59	67.7664 96	67.7528 334
4.007	69.8729 14	69.2424 3	69.5126 37	69.3671 41	69.3671 41	69.9006 28	69.2770 72	68.8544 39	68.7297 28	68.7158 712
4.115	70.8864 57	70.2468 27	70.5209 54	70.3733 47	70.3733 47	70.9145 72	70.2819 71	69.8532 08	69.7266 88	69.7126 302
4.225	71.8757 95	71.2272 38	71.5051 91	71.3555 24	71.3555 24	71.9043 03	71.2628 73	70.8281 26	70.6998 4	70.6855 86
4.339	72.8661 42	72.2086 49	72.4904 32	72.3387 02	72.3387 02	72.8950 43	72.2447 75	71.8040 38	71.6739 84	71.6595 336
4.455	73.8222	73.1560	73.4415	73.2878	73.2878	73.8514	73.1926	72.7461	72.6144	72.5997
4.575	74.7863 26	74.1115 06	74.4007 15	74.2449 87	74.2449 87	74.8159 88	74.1485 84	73.6962 33	73.5627 52	73.5479 208
4.698	75.7292 74	75.0459 45	75.3388	75.1811	75.1811	75.7593	75.0834	74.6254	74.4902	74.4752
4.824	76.6691 96	75.9773 86	76.2738 76	76.1142 28	76.1142 28	76.6996 05	76.0153 98	75.5516 57	75.4148 16	75.3996 114
4.954	77.5718 03	76.8718 49	77.1718 29	77.0103 02	77.0103 02	77.6025 7	76.9103 08	76.4411 08	76.3026 56	76.2872 724
5.087	78.4703 77	77.7623 15	78.0657 7	77.9023 71	77.9023 71	78.5015	77.8012	77.3265	77.1865	77.1709
5.224	79.3790 35	78.6627 74	78.9697 43	78.8044 52	78.8044 52	79.4105 19	78.7021	78.2219	78.0803	78.0645
5.364	80.2584 47	79.5342 51	79.8446 21	79.6774 98	79.6774 98	80.2902 8	79.5740 42	79.0885 92	78.9453 44	78.9294 276
5.508	81.1318 08	80.3997 31	80.7134 78	80.5445 38	80.5445 38	81.1639 87	80.4399 55	79.9492 22	79.8044 16	79.7883 264
5.656	81.9880 25	81.2482 22	81.5652 8	81.3945 56	81.3945 56	82.0205 43	81.2888 7	80.7929 59	80.6466 24	80.6303 646
5.808	82.7968 42	82.0497 41	82.3699 27	82.1975 19	82.1975 19	82.8296 81	82.0907 9	81.5899 86	81.4422 08	81.4257 882
5.964	83.6207 86	82.8662 5	83.1896 23	83.0154 99	83.0154 99	83.6539 52	82.9077 08	82.4019 21	82.2526 72	82.2360 888
6.124	84.3963 23	83.6347 89	83.9611 61	83.7854 22	83.7854 22	84.4297 97	83.6766 32	83.1661 53	83.0155 2	82.9987 83
6.289	85.1436 21	84.3753 44	84.7046 06	84.5273 11	84.5273 11	85.1773 91	84.4175 57	83.9025 59	83.7505 92	83.7337 068

6.458	85.8929 37	85.1178 99	85.4500 58	85.2712 03	85.2712 03	85.9270 04	85.1604 83	84.6409 52	84.4876 48	84.4706 142
6.631	86.6200 65	85.8384 66	86.1734 37	85.9930 68	85.9930 68	86.6544 21	85.8814 11	85.3574 82	85.2028 8	85.1857 02
6.809	87.3300 49	86.5420 44	86.8797 6	86.6979 13	86.6979 13	87.3646 87	86.5853 41	86.0571 17	85.9012 48	85.8839 292
6.992	88.0208 72	87.2266 33	87.5670 21	87.3837 35	87.3837 35	88.0557 83	87.2702 72	86.7378 7	86.5807 68	86.5633 122
7.18	88.6874 9	87.8872 36	88.2302 02	88.0455 28	88.0455 28	88.7226 66	87.9312 06	87.3947 72	87.2364 8	87.2188 92
7.373	89.3258 71	88.5198 56	88.8652 91	88.6792 88	88.6792 88	89.3613	88.5641 43	88.0238 47	87.8644 16	87.8467 014
7.571	89.9612 26	89.1494 78	89.4973 7	89.3100 44	89.3100 44	89.9969 07	89.1940 8	88.6499 41	88.4893 76	88.4715 354
7.774	90.5643 09	89.7471 19	90.0973 43	89.9087 61	89.9087 61	90.6002 29	89.7920 2	89.2442 34	89.0825 92	89.0646 318
7.983	91.1522 64	90.3297 7	90.6822 67	90.4924 61	90.4924 61	91.1884 18	90.3749 62	89.8236 19	89.6609 28	89.6428 512
8.198	91.6837 44	90.8564 53	91.2110 06	91.0200 93	91.0200 93	91.7201 08	90.9019 09	90.3473 52	90.1837 12	90.1655 298
8.418	92.2081 64	91.3761 41	91.7327 22	91.5407 17	91.5407 17	92.2447 36	91.4218 57	90.8641 28	90.6995 52	90.6812 658
8.644	92.7335 92	91.8968 29	92.2554 42	92.0623 42	92.0623 42	92.7703 73	91.9428 05	91.3818 98	91.2163 84	91.1979 936
8.877	93.2408 68	92.3995 27	92.7601 02	92.5659 46	92.5659 46	93.2778 5	92.4457 55	91.8817 79	91.7153 6	91.6968 69
9.115	93.7178 88	92.8722 43	93.2346 62	93.0395 14	93.0395 14	93.7550 59	92.9187 07	92.3518 46	92.1845 76	92.1659 904
9.36	94.1636 45	93.3139 78	93.6781 21	93.4820 44	93.4820 44	94.2009 93	93.3606 63	92.7911 06	92.6230 4	92.6043 66
9.611	94.5912 49	93.7377 24	94.1035 2	93.9065 53	93.9065 53	94.6287 67	93.7846 21	93.2124 77	93.0436 48	93.0248 892
9.869	95.0027 17	94.1454 79	94.5128 67	94.3150 42	94.3150 42	95.0403 98	94.1925 8	93.6179 48	93.4483 84	93.4295 436
10.13 5	95.4061 17	94.5452 39	94.9141 87	94.7155 22	94.7155 22	95.4439 58	94.5925 4	94.0154 68	93.8451 84	93.8262 636
10.40 5	95.7691 77	94.9050 23	95.2753 75	95.0759 54	95.0759 54	95.8071 62	94.9525 04	94.3732 36	94.2023 04	94.1833 116
10.68 5	96.1372 8	95.2698 04	95.6415 79	95.4413 92	95.4413 92	96.1754 1	95.3174 67	94.7359 73	94.5643 84	94.5453 186
10.97 5	96.4731 1	95.6026 04	95.9756 78	95.7747 92	95.7747 92	96.5113 74	95.6504 34	95.0669 08	94.8947 2	94.8755 88
11.27	96.7877 62	95.9144 17	96.2887 08	96.0871 66	96.0871 66	96.8261 51	95.9624 03	95.3769 74	95.2042 24	95.1850 296
11.57	97.0862 78	96.2102 39	96.5856 84	96.3835 22	96.3835 22	97.1247 85	96.2583 73	95.6711 38	95.4978 56	95.4786 024
11.88	97.3565 56	96.4780 78	96.8545 69	96.6518 43	96.6518 43	97.3951 7	96.5263 46	95.9374 77	95.7637 12	95.7444 048
12.2	97.6137 24	96.7329 25	97.1104 1	96.9071 49	96.9071 49	97.6524 4	96.7813 21	96.1908 96	96.0166 72	95.9973 138
12.52 5	97.8537 47	96.9707 83	97.3491 96	97.1454 35	97.1454 35	97.8925 58	97.0192 97	96.4274 2	96.2527 68	96.2333 622
12.86 5	98.0816 68	97.1966 47	97.5759 42	97.3717 06	97.3717 06	98.1205 7	97.2452 75	96.6520 19	96.4769 6	96.4575 09
13.21 5	98.2995 04	97.4125 17	97.7926 54	97.5879 65	97.5879 65	98.3384 92	97.4612 53	96.8666 8	96.6912 32	96.6717 378
13.57	98.5102 8	97.6213 92	98.0023 44	97.7972 16	97.7972 16	98.5493 52	97.6702 32	97.0743 84	96.8985 6	96.8790 24
13.93	98.7049 21	97.8142 76	98.1959 81	97.9904 48	97.9904 48	98.7440 7	97.8632 13	97.2661 87	97.0900 16	97.0704 414
14.3	98.8864 51	97.9941 68	98.3765 75	98.1706 64	98.1706 64	98.9256 72	98.0431 95	97.4450 71	97.2685 76	97.2489 654
14.68 5	99.0568 87	98.1630 67	98.5461 33	98.3398 66	98.3398 66	99.0961 76	98.2121 78	97.6130 24	97.4362 24	97.4165 796
15.08	99.2031 2	98.3079 8	98.6916 11	98.4850 4	98.4850 4	99.2424 66	98.3571 63	97.7571 25	97.5800 64	97.5603 906
15.48 5	99.3433 01	98.4468 96	98.8310 7	98.6242 07	98.6242 07	99.3827 03	98.4961 49	97.8952 63	97.7179 52	97.6982 508
15.90 5	99.4764 23	98.5788 17	98.9635 05	98.7563 66	98.7563 66	99.5158 78	98.6281 36	98.0264 44	97.8488 96	97.8291 684
16.33	99.5913	98.6927	99.0778	98.8705	98.8705	99.6308	98.7421	98.1397	97.9619	97.9422

5	92	49	82	02	02	93	25	38	84	336
16.77	99.7114 04	98.8116 77	99.1972 74	98.9896 45	98.9896 45	99.7509 52	98.8611 13	98.258	98.0800 32	98.0602 578
17.22	99.8152 79	98.9146 16	99.3006 14	99.0927 69	99.0927 69	99.8548 69	98.9641 03	98.3603 61	98.1822 08	98.1624 132
17.68 5	99.9100 78	99.0085 59	99.3949 24	99.1868 82	99.1868 82	99.9497 05	99.0580 93	98.4537 78	98.2754 56	98.2556 424
18.16	100.000 84	99.0985 05	99.4852 21	99.2769 9	99.2769 9	100.040 51	99.1480 84	98.5432 2	98.3647 36	98.3449 044
18.64 5	100.083 54	99.1804 56	99.5674 92	99.3590 88	99.3590 88	100.123 24	99.2300 76	98.6247 12	98.4460 8	98.4262 32
19.14 5	100.153 13	99.2494 15	99.6367 2	99.4281 71	99.4281 71	100.192 85	99.2990 69	98.6932 84	98.5145 28	98.4946 662
19.66	100.222 71	99.3183 73	99.7059 47	99.4972 54	99.4972 54	100.262 46	99.3680 62	98.7618 56	98.5829 76	98.5631 004
20.19	100.283 22	99.3783 37	99.7661 45	99.5573 26	99.5573 26	100.323 56	99.4280 56	98.8214 84	98.6424 96	98.6226 084
20.73 5	100.337 68	99.4323 05	99.8203 24	99.6113 9	99.6113 9	100.377 48	99.4820 51	98.8751 5	98.6960 64	98.6761 656
21.29	100.398 19	99.4922 69	99.8805 22	99.6714 62	99.6714 62	100.438 01	99.5420 45	98.9347 78	98.7555 84	98.7356 736
21.86	100.443 57	99.5372 42	99.9256 7	99.7165 16	99.7165 16	100.483 41	99.5870 4	98.9794 99	98.8002 24	98.7803 046
22.45	100.485 93	99.5792 17	99.9678 09	99.7585 67	99.7585 67	100.525 79	99.6290 36	99.0212 38	98.8418 88	98.8219 602
23.05 5	100.529 3	99.6221 91	100.010 95	99.8016 18	99.8016 18	100.569 17	99.6720 32	99.0639 72	98.8845 44	98.8646 076
23.67 5	100.562 58	99.6551 71	100.044 06	99.8346 58	99.8346 58	100.602 46	99.7050 29	99.0967 67	98.9172 8	98.8973 37
24.31	100.588 8	99.6811 55	100.070 15	99.8606 89	99.8606 89	100.628 69	99.7310 26	99.1226 06	98.9430 72	98.9231 238
24.96	100.623 09	99.7151 35	100.104 26	99.8947 3	99.8947 3	100.663 23	99.7650 23	99.1563 95	98.9768	98.9568 45
25.63	100.648 3	99.7401 2	100.129 34	99.9197 6	99.9197 6	100.688 22	99.7900 2	99.1812 4	99.0016	98.9816 4
26.32	100.674 52	99.7661 04	100.155 43	99.9457 91	99.9457 91	100.714 45	99.8160 17	99.2070 79	99.0273 92	99.0074 268
27.03	100.695 7	99.7870 92	100.176 5	99.9668 16	99.9668 16	100.735 64	99.8370 15	99.2279 49	99.0482 24	99.0282 546
27.75 5	100.713 85	99.8050 81	100.194 55	99.9848 38	99.9848 38	100.753 8	99.8550 14	99.2458 37	99.0660 8	99.0461 07
28.5	100.734 02	99.8250 69	100.214 62	100.004 86	100.004 86	100.773 98	99.8750 12	99.2657 13	99.0859 2	99.0659 43
29.26 5	100.749 15	99.8400 6	100.229 67	100.019 88	100.019 88	100.789 11	99.8900 1	99.2806	99.1008	99.0808 2
30.05	100.761 25	99.8520 53	100.241 71	100.031 89	100.031 89	100.801 22	99.9020 09	99.2925 46	99.1127 04	99.0927 216
30.86	100.774 36	99.8650 45	100.254 75	100.044 91	100.044 91	100.814 33	99.9150 08	99.3054 65	99.1256	99.1056 15
31.69	100.781 42	99.8720 41	100.261 78	100.051 92	100.051 92	100.821 39	99.9220 07	99.3124 22	99.1325 44	99.1125 576
32.54	100.797 56	99.8880 31	100.277 83	100.067 94	100.067 94	100.837 54	99.9380 05	99.3283 22	99.1484 16	99.1284 264
33.41 5	100.805 63	99.8960 26	100.285 85	100.075 95	100.075 95	100.845 61	99.9460 04	99.3362 73	99.1563 52	99.1363 608
34.31	100.816 72	99.9070 2	100.296 89	100.086 96	100.086 96	100.856 71	99.9570 03	99.3472 05	99.1672 64	99.1472 706
35.23	100.819 75	99.9100 18	100.299 9	100.089 96	100.089 96	100.859 73	99.9600 03	99.3501 86	99.1702 4	99.1502 46
36.18	100.825 8	99.9160 14	100.305 92	100.095 97	100.095 97	100.865 79	99.9660 02	99.3561 49	99.1761 92	99.1561 968
37.15	100.830 84	99.9210 11	100.310 94	100.100 98	100.100 98	100.870 83	99.9710 02	99.3611 18	99.1811 52	99.1611 558
38.14 5	100.832 86	99.9230 1	100.312 94	100.102 98	100.102 98	100.872 85	99.9730 02	99.3631 05	99.1831 36	99.1631 394
39.17	100.836 89	99.9270 08	100.316 96	100.106 98	100.106 98	100.876 88	99.9770 01	99.3670 81	99.1871 04	99.1671 066
40.22 5	100.839 92	99.9300 06	100.319 97	100.109 99	100.109 99	100.879 91	99.9800 01	99.3700 62	99.1900 8	99.1700 82
41.30 5	100.841 93	99.9320 05	100.321 97	100.111 99	100.111 99	100.881 93	99.9820 01	99.3720 5	99.1920 64	99.1720 656

42.41 5	100.843 95	99.9340 04	100.323 98	100.113 99	100.113 99	100.883 95	99.9840 01	99.3740 37	99.1940 48	99.1740 492
43.55 5	100.845 97	99.9360 02	100.325 99	100.116	100.116	100.885 96	99.986	99.3760 25	99.1960 32	99.1760 328
44.72 5	100.847 98	99.9380 01	100.327 99	100.118	100.118	100.887 98	99.988	99.3780 12	99.1980 16	99.1780 164
45.93	100.847 98	99.9380 01	100.327 99	100.118	100.118	100.887 98	99.988	99.3780 12	99.1980 16	99.1780 164
47.16 5	100.847 98	99.9380 01	100.327 99	100.118	100.118	100.887 98	99.988	99.3780 12	99.1980 16	99.1780 164
48.43	100.847 98	99.9380 01	100.327 99	100.118	100.118	100.887 98	99.988	99.3780 12	99.1980 16	99.1780 164
49.73	100.848 99	99.9390 01	100.329	100.119	100.119	100.888 99	99.989	99.3790 06	99.1990 08	99.1790 082
51.06 5	100.848 99	99.9390 01	100.329	100.119	100.119	100.888 99	99.989	99.3790 06	99.1990 08	99.1790 082
52.43 5	100.848 99	99.9390 01	100.329	100.119	100.119	100.888 99	99.989	99.3790 06	99.1990 08	99.1790 082
53.84 5	100.848 99	99.9390 01	100.329	100.119	100.119	100.888 99	99.989	99.3790 06	99.1990 08	99.1790 082
55.29	100.848 99	99.9390 01	100.329	100.119	100.119	100.888 99	99.989	99.3790 06	99.1990 08	99.1790 082
56.77 5	100.85	99.94	100.33	100.12	100.12	100.89	99.99	99.38	99.2	99.18
58.30 5	100.85	99.94	100.33	100.12	100.12	100.89	99.99	99.38	99.2	99.18
59.87	100.85	99.94	100.33	100.12	100.12	100.89	99.99	99.38	99.2	99.18
61.47 5	100.85	99.94	100.33	100.12	100.12	100.89	99.99	99.38	99.2	99.18
63.13	100.85	99.94	100.33	100.12	100.12	100.89	99.99	99.38	99.2	99.18
64.82 5	100.85	99.94	100.33	100.12	100.12	100.89	99.99	99.38	99.2	99.18
66.56 5	100.85	99.94	100.33	100.12	100.12	100.89	99.99	99.38	99.2	99.18
68.35 5	100.85	99.94	100.33	100.12	100.12	100.89	99.99	99.38	99.2	99.18
70.19	100.85	99.94	100.33	100.12	100.12	100.89	99.99	99.38	99.2	99.18
72.07 5	100.85	99.94	100.33	100.12	100.12	100.89	99.99	99.38	99.2	99.18
74.01	100.85	99.94	100.33	100.12	100.12	100.89	99.99	99.38	99.2	99.18
76	100.85	99.94	100.33	100.12	100.12	100.89	99.99	99.38	99.2	99.18
78.04 5	100.85	99.94	100.33	100.12	100.12	100.89	99.99	99.38	99.2	99.18
80.14	100.85	99.94	100.33	100.12	100.12	100.89	99.99	99.38	99.2	99.18
82.29	100.85	99.94	100.33	100.12	100.12	100.89	99.99	99.38	99.2	99.18
84.5	100.85	99.94	100.33	100.12	100.12	100.89	99.99	99.38	99.2	99.18
86.77	100.85	99.94	100.33	100.12	100.12	100.89	99.99	99.38	99.2	99.18
89.10 5	100.85	99.94	100.33	100.12	100.12	100.89	99.99	99.38	99.2	99.18
91.5	100.85	99.94	100.33	100.12	100.12	100.89	99.99	99.38	99.2	99.18
93.95 5	100.85	99.94	100.33	100.12	100.12	100.89	99.99	99.38	99.2	99.18
96.48	100.85	99.94	100.33	100.12	100.12	100.89	99.99	99.38	99.2	99.18
99.08	100.85	99.94	100.33	100.12	100.12	100.89	99.99	99.38	99.2	99.18
101.7 5	100.85	99.94	100.33	100.12	100.12	100.89	99.99	99.38	99.2	99.18
104.5	100.85	99.94	100.33	100.12	100.12	100.89	99.99	99.38	99.2	99.18
107.3	100.85	99.94	100.33	100.12	100.12	100.89	99.99	99.38	99.2	99.18
110.1 5	100.85	99.94	100.33	100.12	100.12	100.89	99.99	99.38	99.2	99.18
113.1	100.85	99.94	100.33	100.12	100.12	100.89	99.99	99.38	99.2	99.18
116.1 5	100.85	99.94	100.33	100.12	100.12	100.89	99.99	99.38	99.2	99.18
119.3	100.85	99.94	100.33	100.12	100.12	100.89	99.99	99.38	99.2	99.18
122.5	100.85	99.94	100.33	100.12	100.12	100.89	99.99	99.38	99.2	99.18
125.7 5	100.85	99.94	100.33	100.12	100.12	100.89	99.99	99.38	99.2	99.18
129.1 5	100.85	99.94	100.33	100.12	100.12	100.89	99.99	99.38	99.2	99.18
132.6	100.85	99.94	100.33	100.12	100.12	100.89	99.99	99.38	99.2	99.18

5										
136.2	100.85	99.94	100.33	100.12	100.12	100.89	99.99	99.38	99.2	99.18
139.8	100.85	99.94	100.33	100.12	100.12	100.89	99.99	99.38	99.2	99.18
5										
143.6	100.85	99.94	100.33	100.12	100.12	100.89	99.99	99.38	99.2	99.18
147.4	100.85	99.94	100.33	100.12	100.12	100.89	99.99	99.38	99.2	99.18
5										
151.4	100.85	99.94	100.33	100.12	100.12	100.89	99.99	99.38	99.2	99.18
155.4	100.85	99.94	100.33	100.12	100.12	100.89	99.99	99.38	99.2	99.18
5										
159.6	100.85	99.94	100.33	100.12	100.12	100.89	99.99	99.38	99.2	99.18
5										
163.9	100.85	99.94	100.33	100.12	100.12	100.89	99.99	99.38	99.2	99.18
5										
168.3	100.85	99.94	100.33	100.12	100.12	100.89	99.99	99.38	99.2	99.18
5										
172.9	100.85	99.94	100.33	100.12	100.12	100.89	99.99	99.38	99.2	99.18
177.5	100.85	99.94	100.33	100.12	100.12	100.89	99.99	99.38	99.2	99.18
5										
182.3	100.85	99.94	100.33	100.12	100.12	100.89	99.99	99.38	99.2	99.18
187.2	100.85	99.94	100.33	100.12	100.12	100.89	99.99	99.38	99.2	99.18
192.2	100.85	99.94	100.33	100.12	100.12	100.89	99.99	99.38	99.2	99.18
5										
197.4	100.85	99.94	100.33	100.12	100.12	100.89	99.99	99.38	99.2	99.18

**Table B.3 Calculated Chi-square value for each cell of Tables B.1 and B.2**

Chi-square value for each cell										
Size (micro n)	Sample 3-1	Sample 3-2	Sample 3-3	Sample 3-4	Sample 3-5	Sample 3-6	Sample 3-7	Sample 3-8	Sample 3-9	Sample 3-10
0.507	0.000175	0.000962	7.35E-05	5.94E-05	0.006367	0.000118	0.001674	0.0019	0.000786	0.004707
0.52	0.008768	0.004046	5.96E-07	0.00581	0.001026	0.006765	0.003316	1.05E-05	0.006292	0.000431
0.534	0.012305	0.003207	0.000848	0.008007	0.00028	0.006315	0.004581	0.000125	0.006563	7.28E-06
0.549	0.010994	0.004471	0.001637	0.011844	6.78E-05	0.007122	0.005414	8.48E-05	0.003568	0.000126
0.564	0.041764	0.00493	0.00783	0.010575	0.000193	0.011909	0.000571	0.002719	0.01245	1.6E-05
0.579	0.034556	0.005111	0.008023	0.011841	0.000139	0.015037	0.000177	0.004117	0.010943	1.13E-06
0.594	0.039061	0.002031	0.007482	0.005278	0.000519	0.012367	2.7E-06	0.001866	0.018261	0.001509
0.61	0.036214	0.003795	0.008686	0.003684	0.000806	0.014246	9.17E-06	0.001964	0.018356	0.001307
0.627	0.035745	0.003679	0.00849	0.003577	0.000573	0.014075	6.61E-05	0.001994	0.019159	0.001235
<=0.627	0.215862	0.027977	0.040901	0.048404	3.8E-05	0.084081	0.003979	0.01192	0.09549	0.001473
0.644	0.034107	0.006108	0.004924	0.001941	0.000796	0.013445	0.000204	0.000407	0.019003	0.001217
0.661	0.035685	0.006232	0.005692	0.00169	0.000922	0.012664	0.000155	0.000206	0.020114	0.000533
0.678	0.031547	0.00787	0.004507	0.006635	0.001605	0.011294	0.000768	0.000392	0.013772	0.000338
0.697	0.029575	0.006979	0.004919	0.007092	0.0016	0.014555	0.000574	0.000412	0.012436	0.000847
0.716	0.035755	0.008458	0.003585	0.008714	0.002816	0.011261	0.000304	0.001459	0.013961	0.001786
0.735	0.038597	0.006682	0.004185	0.009469	0.002146	0.011672	0.000843	0.000841	0.012915	0.002835
0.754	0.041413	0.009811	0.002158	0.010186	0.002239	0.01173	0.000435	0.001803	0.015566	0.002819
0.775	0.048376	0.010145	0.004302	0.009383	0.00127	0.013941	2.55E-05	0.002804	0.018121	0.001276
0.796	0.047967	0.010913	0.00366	0.008929	0.001355	0.013934	4.32E-05	0.002959	0.020712	0.001113
0.817	0.051581	0.01041	0.004528	0.00759	0.001025	0.018692	2.84E-05	0.001772	0.020537	0.001219

0.839	0.05591 4	0.01197 9	0.00461 4	0.00751 9	0.00082 7	0.02213 1	0.0006	0.00297 7	0.02020 2	0.00159 5
0.861	0.05108 5	0.00920 7	0.00628 3	0.00991 3	0.00079 4	0.02003 7	0.00064 9	0.00475 1	0.02099 3	0.00045 9
0.884	0.04654 4	0.00945 7	0.00569 5	0.00964 1	0.00065 7	0.02204 1	0.00048 1	0.00479 8	0.02030 6	0.00065 9
0.908	0.04645 5	0.01038 4	0.00503 8	0.01121 1	0.00028 4	0.02336 8	2.47E- 05	0.00437 5	0.01926 1	0.00095
0.933	0.04312 2	0.00969 3	0.00405 6	0.01000 9	4.73E- 05	0.02141 5	1.4E-06	0.00445 7	0.02065 2	0.00050 3
0.958	0.04332 8	0.00912 9	0.00570 4	0.00951 6	0.00018	0.02442 8	0.00020 3	0.00464 9	0.02485 5	5.47E- 05
0.983	0.04336	0.00818 1	0.00515 3	0.01002 9	2.71E- 07	0.02563 1	7.97E- 05	0.00601 6	0.02380 2	0.00051 7
1.01	0.04416	0.00774 3	0.00529 7	0.01206	3.13E- 05	0.02425 8	1.18E- 05	0.00677 7	0.02680 6	0.00032 3
1.037	0.03868	0.00658 2	0.00360 7	0.01009 7	0.00015 1	0.02706 5	0.00022 8	0.00521 3	0.02978 6	0.00033 6
1.065	0.03962 2	0.00719 1	0.00582 4	0.01035 1	0.00040 3	0.02730 1	0.00012 2	0.00409	0.02455 7	0.00038 5
1.094	0.04113 5	0.00686 3	0.00607 4	0.00951 1	5.01E- 05	0.02888 3	0.00025 7	0.00366 5	0.0233	0.00023 6
1.123	0.04183 7	0.00939 9	0.00565 1	0.00886	0.00012	0.02963 7	0.00041 4	0.00605 7	0.02357 7	0.00074 5
1.153	0.03720 2	0.00909	0.00692	0.00710 1	0.00044 5	0.03327 8	0.00040 6	0.00630 9	0.02372 9	0.00166 4
1.184	0.03928 8	0.01158 7	0.00639 4	0.00790 2	0.00040 2	0.03531 6	5.3E-05	0.00554 4	0.02017 9	0.00323 9
1.215	0.03680 1	0.00993 9	0.00564	0.00698 4	0.00089 2	0.03605	0.00017 8	0.00462 7	0.02159 6	0.00398 2
1.248	0.03777 7	0.01178 7	0.00567 4	0.00658	0.00038 6	0.03855 9	6.68E- 05	0.00620 7	0.02598 9	0.00324 5
1.282	0.03475 6	0.00963 5	0.00608 3	0.00797 4	0.00087 8	0.04086 7	1.2E-05	0.00564 4	0.02516 7	0.00462 7
1.316	0.03581 2	0.01008 7	0.00725 8	0.00645 7	0.00094	0.03799 4	5.14E- 06	0.00588	0.02967 1	0.00333 4
1.351	0.03620 5	0.00713 2	0.00833 4	0.00557 7	0.00144 8	0.03540 2	7.94E- 06	0.00404 5	0.02913	0.00410 3
1.388	0.03256 5	0.00705 1	0.01054	0.00675 9	0.00300 3	0.03663	5.98E- 05	0.00544 8	0.02990 7	0.00281 8
1.425	0.03330 2	0.00722 9	0.01045 8	0.00638 9	0.00175 1	0.03874 5	0.00045 1	0.00505 5	0.02866	0.00134
1.464	0.02897 4	0.00562 4	0.01309 1	0.00573 9	0.00178 2	0.03598 1	0.00031 7	0.00577	0.02683 6	0.00110 6
1.503	0.02929 7	0.00545 6	0.01409 1	0.00703 4	0.002	0.03966	0.00031 2	0.00686 3	0.02733 8	0.00163 4
1.543	0.02865 9	0.00386 6	0.01422 6	0.00716 5	0.00270 8	0.04006 1	0.00060 9	0.0062	0.02702 7	0.00221 5
1.584	0.03076 5	0.00425	0.01408	0.00829 8	0.00238 9	0.04024 3	0.00032 1	0.00637 6	0.02774 3	0.00224 2
1.627	0.03096 8	0.00498 4	0.01003 1	0.01172 8	0.00338 4	0.04373 8	0.00030 4	0.00485 4	0.03024 3	0.00200 2
1.671	0.03193 7	0.00474	0.00815 9	0.01025 6	0.00350 3	0.03852 3	0.00054 4	0.00493 3	0.03392 9	0.00149
1.716	0.03182 5	0.00393 3	0.00860 7	0.00966 1	0.00360 1	0.03957 8	0.00086 6	0.00429	0.03431 1	0.00133 8
1.762	0.03066 5	0.00429 8	0.00828 3	0.00986 1	0.00235 1	0.04135 9	0.00078 3	0.00401 6	0.02841 2	0.00160 5
1.809	0.03018 6	0.00559 4	0.00636	0.01039 7	0.00151 7	0.03997 5	0.00062 6	0.00337 6	0.02327 9	0.00149 9
1.858	0.02508 3	0.00600 5	0.00473 7	0.01127 5	0.00118 7	0.03933 4	0.00072 2	0.00431 2	0.02390 4	0.00061 3
1.908	0.02615 3	0.00564 6	0.00564 2	0.01141 9	0.00090 8	0.03734 5	0.00020 9	0.00313 8	0.02241 2	0.00047 3
1.959	0.02165 2	0.00553	0.00474 1	0.01027 4	0.00125 1	0.04108	0.00025 9	0.00264 3	0.02197 4	0.00087 8
2.012	0.02456 1	0.00648 9	0.00463 8	0.00824 5	0.00103 7	0.04038 5	8.78E- 05	0.00160 1	0.02054	0.00158 3
2.066	0.02438 1	0.00710 4	0.00385 8	0.00813 5	0.00187 6	0.04295 4	0.00034 4	0.00056	0.01770 3	0.00196 4
2.121	0.02018	0.00952	0.00376	0.00842	0.00257	0.04486	0.00037	0.00048	0.01463	0.00141

	6	1	1	5	1	8			7	5
2.178	0.020287	0.0104	0.002864	0.007188	0.003317	0.040442	0.000407	0.000124	0.01466	0.00107
2.237	0.017302	0.01	0.002066	0.006935	0.002239	0.04218	0.00011	9.55E-05	0.014202	0.001415
2.297	0.015758	0.010429	0.001976	0.006886	0.003003	0.040549	8.75E-05	0.000135	0.013374	0.001658
2.358	0.019162	0.009939	0.001628	0.007765	0.002608	0.038588	5.2E-06	5.18E-06	0.013855	0.001772
2.421	0.020266	0.009802	0.001143	0.007711	0.00222	0.036066	1.66E-05	1.72E-05	0.012753	0.0023
2.486	0.020248	0.008811	0.001359	0.008101	0.001898	0.034279	3.08E-05	1.21E-05	0.011056	0.002025
2.553	0.019772	0.008919	0.001828	0.007769	0.002319	0.036028	8.96E-06	1.75E-05	0.010067	0.002276
2.622	0.019492	0.008711	0.001939	0.006484	0.002144	0.038058	1.61E-05	0.000561	0.008842	0.002649
2.693	0.018762	0.010634	0.001108	0.005959	0.002211	0.037838	6.93E-06	0.000781	0.007956	0.002751
2.765	0.01518	0.009015	0.001005	0.004836	0.000946	0.040996	2.84E-06	0.000846	0.00801	0.002026
2.839	0.014082	0.009924	0.000878	0.00482	0.000815	0.043246	0.000111	0.000876	0.008671	0.002152
2.915	0.014044	0.010359	0.000448	0.002613	0.00056	0.037581	0.000158	0.001	0.0094	0.002303
2.994	0.011717	0.009987	0.000196	0.002118	0.000467	0.039903	0.000116	0.001215	0.010409	0.002079
3.074	0.010198	0.011193	8.83E-05	0.000858	0.000443	0.039779	6.21E-05	0.001863	0.010367	0.001757
3.157	0.011621	0.010039	2.47E-05	0.000599	0.000586	0.035682	2.38E-05	0.003065	0.009593	0.002016
3.241	0.011191	0.008234	9.17E-06	0.000741	0.000978	0.034686	1.11E-05	0.003864	0.010078	0.00204
3.328	0.010673	0.007536	5.13E-06	0.00023	0.000915	0.030819	2.59E-08	0.004107	0.010108	0.002207
3.418	0.010268	0.007031	0.000237	8.45E-05	0.000954	0.027396	1.78E-06	0.004822	0.01059	0.002348
3.51	0.010072	0.00659	0.000533	0.000217	0.001225	0.026099	1.95E-05	0.005618	0.010604	0.002771
3.604	0.010727	0.005713	0.000824	0.000218	0.001468	0.026186	3.19E-06	0.006582	0.010515	0.003452
3.701	0.011342	0.005658	0.000995	5.92E-05	0.001512	0.02239	8.16E-05	0.008309	0.010478	0.003761
3.8	0.011978	0.005427	0.000944	3.73E-06	0.001114	0.021015	5.66E-05	0.009254	0.009959	0.0032
3.902	0.010153	0.004463	0.001327	9.16E-06	0.001545	0.021916	2.81E-05	0.011653	0.009362	0.004035
4.007	0.00979	0.003942	0.001837	2.65E-05	0.002004	0.020237	1.24E-07	0.01323	0.008178	0.00466
4.115	0.008441	0.002971	0.001828	4.56E-05	0.001516	0.019153	4.62E-06	0.012736	0.007574	0.004704
4.225	0.008776	0.002105	0.001861	0.000153	0.00098	0.018575	3.12E-05	0.013508	0.008166	0.005188
4.339	0.008008	0.001781	0.001987	0.000316	0.001255	0.018299	8.81E-06	0.014891	0.006915	0.006444
4.455	0.007986	0.001042	0.002384	0.000238	0.001416	0.017245	4.49E-05	0.017745	0.006263	0.007538
4.575	0.007595	0.000233	0.001934	0.000413	0.001172	0.016588	3.57E-05	0.01814	0.006337	0.008657
4.698	0.007245	1.72E-05	0.002584	0.000759	0.000962	0.016284	5.64E-07	0.019796	0.007557	0.008707
4.824	0.006966	6.73E-06	0.003629	0.001073	0.000928	0.013843	2.81E-06	0.022426	0.006587	0.01003
4.954	0.008213	3.02E-05	0.004332	0.001588	0.000571	0.012564	1.22E-06	0.024236	0.006108	0.011515
5.087	0.007946	9.89E-05	0.005997	0.001295	0.000405	0.012447	9.91E-07	0.025951	0.005584	0.01247
5.224	0.007683	0.00012	0.007128	0.001604	0.000116	0.011593	4.26E-05	0.028458	0.005088	0.012167
5.364	0.006308	0.000267	0.008532	0.00156	8.54E-05	0.010082	0.000232	0.027643	0.005113	0.013688

5.508	0.00517 9	0.00066	0.00930 3	0.00280 7	2.57E- 05	0.00840 6	0.00012 4	0.02663 4	0.00553 2	0.01430 4
5.656	0.00456 8	0.00127 4	0.00959 6	0.00301 6	3.78E- 05	0.00779 2	0.00012 6	0.02613	0.00601 7	0.01556 8
5.808	0.00410 7	0.00158 2	0.01119	0.00412 8	3.35E- 05	0.00661 7	1.87E- 05	0.02648 4	0.00694 7	0.01474 7
5.964	0.00443 8	0.00216 7	0.01301 1	0.00425 7	7.23E- 06	0.00468 5	1.26E- 05	0.02558 3	0.00688 7	0.01597 3
6.124	0.00446 2	0.00329 8	0.01412	0.00527 1	3.51E- 07	0.00358 6	2.25E- 05	0.02727 7	0.00669 5	0.01819 2
6.289	0.00376 8	0.00351 6	0.01290 2	0.00635 1	3.55E- 06	0.00345 7	4.62E- 05	0.02762 9	0.00569 4	0.01907 2
6.458	0.00323 4	0.00398 1	0.01314 8	0.00748 3	5.27E- 06	0.00271 5	4.47E- 06	0.02661 7	0.00527 6	0.01941 5
6.631	0.00288 5	0.00464 6	0.01246 9	0.00814 5	4.63E- 05	0.00229 1	2.75E- 05	0.02522 9	0.00531 4	0.01970 8
6.809	0.00242 2	0.00441 3	0.01368 1	0.00959 5	8.91E- 05	0.00152 8	2.48E- 06	0.02300 8	0.00556 2	0.01889 6
6.992	0.00209 2	0.00489 4	0.01465 9	0.00981 8	0.00020 5	0.00142 5	4.46E- 06	0.02350 5	0.00519 7	0.01902 5
7.18	0.00182 7	0.00610 9	0.01604 5	0.00929 1	0.00035	0.00099 6	3.93E- 05	0.02322 8	0.00494	0.02024 7
7.373	0.00165 2	0.00618 9	0.01606 2	0.01040 8	0.00025 1	0.00053 5	2.37E- 05	0.02368 3	0.00388 7	0.02126 3
7.571	0.00127 6	0.00683 4	0.01589 3	0.01119 6	0.00013 6	0.00041 4	3.51E- 05	0.02504 1	0.00392 5	0.02126 2
7.774	0.00132 5	0.00700 4	0.01552 4	0.01137 4	0.00039 6	0.00031 8	5.15E- 05	0.02369 7	0.00355 3	0.02090 9
7.983	0.00090 8	0.00726 8	0.01555 7	0.01235 9	0.00040 9	0.00011 3	2.5E-06	0.02256 3	0.00314 4	0.01922 7
8.198	0.00089 4	0.00783 2	0.01656	0.01165 4	0.00044	3.91E- 05	1.56E- 06	0.02130 4	0.00315 9	0.01919 4
8.418	0.00068 8	0.00779 3	0.01668 8	0.01157 3	0.00028 2	6.92E- 06	1.11E- 05	0.02078 1	0.00275 1	0.01925 1
8.644	0.00041 6	0.00719 6	0.01760 9	0.01169 6	0.00025 2	4.47E- 06	1.17E- 05	0.01970 5	0.00228 3	0.01904 8
8.877	0.00038 4	0.00782 8	0.01711 2	0.01177 6	0.00023	6.5E-05	7.17E- 06	0.01872 8	0.00226 1	0.0192
9.115	0.00039 4	0.00829 6	0.01507	0.01186 1	0.00010 6	0.00011 8	0.00010 5	0.01807 1	0.00195 5	0.01794 3
9.36	0.00033 6	0.00713 6	0.01391 9	0.01243	0.00013 4	0.00018 2	0.00010 9	0.01606 9	0.00158 4	0.01726 3
9.611	0.00023 4	0.00774 9	0.01277 6	0.01137 3	0.00014 5	0.00046 1	5.94E- 05	0.01551 2	0.00112 6	0.01560 6
9.869	8.02E- 05	0.00775 6	0.01227 6	0.01070 8	0.00019 3	0.00046 6	4.16E- 05	0.01432 2	0.00095 3	0.01439 1
10.135	4.28E- 05	0.00754 8	0.01108 7	0.01065 3	0.00025 5	0.00067 6	1.91E- 05	0.01323 5	0.00092 8	0.01234 6
10.405	4.53E- 06	0.00734 6	0.00997	0.01039 3	0.00022 4	0.00086 1	1.11E- 05	0.01197 9	0.00067 6	0.01155 7
10.685	7.7E-08	0.00723 4	0.00881 9	0.00962 8	0.00018 1	0.00103 4	5.85E- 07	0.01047 1	0.00058 1	0.01111 9
10.975	1.78E- 06	0.00698 9	0.00814 8	0.00972 7	0.00016 3	0.00127 9	1.14E- 06	0.00943 2	0.00036	0.01130 4
11.27	1.47E- 05	0.00611 1	0.00806 6	0.00886 3	0.00029 1	0.00154	1.6E-06	0.0077	0.00016 2	0.01019 4
11.57	5.99E- 05	0.006	0.00755 7	0.00815 3	0.00031 2	0.00203 7	3.51E- 06	0.00637 8	6.35E- 05	0.00903 1
11.88	0.00016 5	0.00540 2	0.00703 5	0.00726 8	0.00023 9	0.00241 7	4.17E- 07	0.00536 6	5.87E- 06	0.00798 6
12.2	0.00018 3	0.00502 3	0.00625 8	0.00648 7	0.00028 8	0.00301 3	8.5E-06	0.00467 9	1.96E- 05	0.00713
12.525	0.00034 5	0.00448 1	0.00548 6	0.00601 7	0.00028 2	0.00289 7	1.71E- 05	0.00408 2	0.00011 9	0.00654 1
12.865	0.00054 7	0.00425 8	0.00479 6	0.00500 8	0.00033 9	0.00297 8	2.06E- 05	0.00281 9	0.00018 3	0.00548 7
13.215	0.00073 9	0.00391 4	0.00428 5	0.00435 7	0.00028 9	0.00294 9	2.44E- 05	0.00234 6	0.00026 1	0.00466 8
13.57	0.00110 7	0.00342 9	0.00364 5	0.00371 5	0.00022 2	0.00317 5	3.66E- 05	0.00212 7	0.00046 1	0.00322 6
13.93	0.00127	0.00293	0.00359	0.00331	0.00020	0.00333	3.3E-05	0.00178	0.00075	0.00300

	6	4	3		1	7		1	1	9
14.3	0.001285	0.002611	0.003113	0.002963	0.000174	0.00335	2.88E-06	0.001444	0.000814	0.002166
14.685	0.001671	0.002317	0.00268	0.002544	0.000228	0.003587	6.23E-07	0.001004	0.001213	0.001456
15.08	0.001891	0.002078	0.002037	0.002195	0.000214	0.00378	1.68E-06	0.000575	0.001402	0.001052
15.485	0.002255	0.001905	0.001531	0.001838	0.000156	0.004028	1.95E-06	0.000351	0.001417	0.000488
15.905	0.002681	0.001886	0.001144	0.001569	0.000248	0.004456	1.78E-05	0.000116	0.001563	0.000227
16.335	0.002835	0.001599	0.000921	0.001381	0.0002	0.004653	2.32E-05	3.64E-05	0.001784	0.000153
16.77	0.00339	0.001448	0.000644	0.001102	0.00017	0.004926	2.42E-05	1.04E-05	0.001974	5.03E-05
17.22	0.00367	0.001206	0.000442	0.000833	0.000152	0.005118	6.78E-06	8.17E-05	0.002423	5.93E-08
17.685	0.003974	0.001044	0.000345	0.000698	0.000189	0.005327	4.84E-06	0.000162	0.0028	3.01E-05
18.16	0.004367	0.000857	0.000273	0.000547	0.000189	0.005481	2.72E-05	0.000219	0.002913	0.000135
18.645	0.004668	0.000788	0.000127	0.000406	0.000168	0.005667	2.51E-05	0.000277	0.00323	0.000381
19.145	0.004797	0.000633	6.96E-05	0.000297	0.00014	0.005961	2.61E-05	0.000392	0.003599	0.000562
19.66	0.004927	0.00054	1.95E-05	0.000177	0.000116	0.005647	1.03E-05	0.000574	0.003616	0.000835
20.19	0.005073	0.000494	1.92E-06	0.000106	0.000138	0.005803	1.03E-05	0.000785	0.003866	0.001087
20.735	0.005423	0.000434	1.07E-06	6.2E-05	0.000125	0.005868	7.85E-06	0.001003	0.004072	0.001342
21.29	0.005428	0.000354	1.64E-05	3.44E-05	0.000148	0.006027	7.85E-06	0.001136	0.004606	0.001575
21.86	0.005358	0.0003	5.73E-05	2.87E-05	0.000136	0.006265	1.09E-05	0.001241	0.004677	0.001869
22.45	0.005537	0.000293	9.57E-05	2.65E-05	0.000141	0.006459	1.68E-05	0.001373	0.00479	0.002031
23.055	0.005735	0.000283	0.000171	1.48E-05	0.000103	0.006672	7.85E-06	0.001583	0.005033	0.002286
23.675	0.005935	0.000241	0.000207	6.43E-06	0.000132	0.006724	2.25E-06	0.001808	0.005135	0.002762
24.31	0.005876	0.000222	0.000289	3.73E-06	0.000123	0.006824	8.42E-06	0.001843	0.005195	0.002914
24.96	0.006094	0.000182	0.000339	2.24E-07	0.000156	0.006893	1.23E-05	0.002168	0.005431	0.003205
25.63	0.006174	0.000144	0.000397	8.86E-06	0.000144	0.006978	1.6E-05	0.002311	0.005507	0.003617
26.32	0.00627	0.00013	0.000463	2.1E-05	0.000158	0.006914	1.94E-05	0.002449	0.005569	0.003915
27.03	0.006447	0.000151	0.000558	2.19E-05	0.000187	0.006932	1.85E-05	0.00254	0.005706	0.004159
27.755	0.006416	0.000132	0.000597	3.01E-05	0.000182	0.007067	2.03E-05	0.002664	0.005891	0.004186
28.5	0.006417	0.00011	0.000597	5.6E-05	0.000182	0.007068	1.23E-05	0.002562	0.006047	0.004723
29.265	0.00666	0.0001	0.000673	6.38E-05	0.000169	0.007153	9E-06	0.00293	0.006127	0.004794
30.05	0.006694	9.61E-05	0.000736	6.7E-05	0.000174	0.007358	1.44E-05	0.003018	0.006096	0.005048
30.86	0.006744	9.03E-05	0.000753	9E-05	0.000156	0.00741	6.25E-06	0.003097	0.006207	0.005295
31.69	0.006695	7.75E-05	0.000792	0.000104	0.000149	0.007531	7.84E-06	0.00313	0.006255	0.005487
32.54	0.006631	6.73E-05	0.000885	0.000116	0.000116	0.007637	4.84E-06	0.003176	0.00632	0.005698
33.415	0.006762	5.48E-05	0.000933	0.000112	0.000134	0.007603	5.76E-06	0.003314	0.006352	0.005882
34.31	0.006779	5.33E-05	0.001001	0.000114	0.000137	0.007621	1.69E-06	0.003303	0.006498	0.006179
35.23	0.006829	4.9E-05	0.000958	0.000121	0.000144	0.007673	4E-06	0.003268	0.00645	0.006291

36.18	0.006928	4.1E-05	0.000995	0.000112	0.000134	0.007779	1.96E-06	0.003314	0.006515	0.006516
37.15	0.007012	4.76E-05	0.001027	0.000123	0.000146	0.007867	8.1E-07	0.00349	0.006596	0.006598
38.145	0.006879	4.49E-05	0.00104	0.000128	0.000151	0.007903	2.89E-06	0.003467	0.006564	0.006565
39.17	0.006946	3.97E-05	0.001066	0.000137	0.000161	0.007797	1.69E-06	0.003538	0.006662	0.006663
40.225	0.006996	4.9E-05	0.001021	0.000144	0.000144	0.00785	1E-06	0.003502	0.006613	0.006615
41.305	0.007029	4.63E-05	0.001033	0.000149	0.000149	0.007886	6.4E-07	0.003598	0.006581	0.006746
42.415	0.007063	4.36E-05	0.001046	0.000154	0.000154	0.007921	2.56E-06	0.003695	0.006548	0.006713
43.555	0.007097	4.1E-05	0.001059	0.000159	0.000159	0.00778	1.96E-06	0.003671	0.006516	0.006846
44.725	0.00713	3.85E-05	0.001072	0.000139	0.000164	0.007816	1.44E-06	0.003769	0.006484	0.006813
45.93	0.00713	3.85E-05	0.001072	0.000139	0.000164	0.007816	1.44E-06	0.003769	0.006484	0.006813
47.165	0.00713	3.85E-05	0.001072	0.000139	0.000164	0.007816	1.44E-06	0.003769	0.006484	0.006813
48.43	0.00713	3.85E-05	0.001072	0.000139	0.000164	0.007816	1.44E-06	0.003769	0.006484	0.006813
49.73	0.007147	3.72E-05	0.001079	0.000141	0.000141	0.007833	1.21E-06	0.003756	0.006468	0.006796
51.065	0.007147	3.72E-05	0.001079	0.000141	0.000141	0.007833	1.21E-06	0.003756	0.006468	0.006796
52.435	0.007147	3.72E-05	0.001079	0.000141	0.000141	0.007833	1.21E-06	0.003756	0.006468	0.006796
53.845	0.007147	3.72E-05	0.001079	0.000141	0.000141	0.007833	1.21E-06	0.003756	0.006468	0.006796
55.29	0.007147	3.72E-05	0.001079	0.000141	0.000141	0.007833	1.21E-06	0.003756	0.006468	0.006796
56.775	0.007164	3.6E-05	0.001085	0.000144	0.000144	0.007851	1E-06	0.003868	0.006452	0.00678
58.305	0.007164	3.6E-05	0.001085	0.000144	0.000144	0.007851	1E-06	0.003868	0.006452	0.00678
59.87	0.007164	3.6E-05	0.001085	0.000144	0.000144	0.007851	1E-06	0.003868	0.006452	0.00678
61.475	0.007164	3.6E-05	0.001085	0.000144	0.000144	0.007851	1E-06	0.003868	0.006452	0.00678
63.13	0.007164	3.6E-05	0.001085	0.000144	0.000144	0.007851	1E-06	0.003868	0.006452	0.00678
64.825	0.007164	3.6E-05	0.001085	0.000144	0.000144	0.007851	1E-06	0.003868	0.006452	0.00678
66.565	0.007164	3.6E-05	0.001085	0.000144	0.000144	0.007851	1E-06	0.003868	0.006452	0.00678
68.355	0.007164	3.6E-05	0.001085	0.000144	0.000144	0.007851	1E-06	0.003868	0.006452	0.00678
70.19	0.007164	3.6E-05	0.001085	0.000144	0.000144	0.007851	1E-06	0.003868	0.006452	0.00678
72.075	0.007164	3.6E-05	0.001085	0.000144	0.000144	0.007851	1E-06	0.003868	0.006452	0.00678
74.01	0.007164	3.6E-05	0.001085	0.000144	0.000144	0.007851	1E-06	0.003868	0.006452	0.00678
76	0.007164	3.6E-05	0.001085	0.000144	0.000144	0.007851	1E-06	0.003868	0.006452	0.00678
78.045	0.007164	3.6E-05	0.001085	0.000144	0.000144	0.007851	1E-06	0.003868	0.006452	0.00678
80.14	0.007164	3.6E-05	0.001085	0.000144	0.000144	0.007851	1E-06	0.003868	0.006452	0.00678
82.29	0.007164	3.6E-05	0.001085	0.000144	0.000144	0.007851	1E-06	0.003868	0.006452	0.00678
84.5	0.007164	3.6E-05	0.001085	0.000144	0.000144	0.007851	1E-06	0.003868	0.006452	0.00678
86.77	0.007164	3.6E-05	0.001085	0.000144	0.000144	0.007851	1E-06	0.003868	0.006452	0.00678
89.105	0.007164	3.6E-05	0.001085	0.000144	0.000144	0.007851	1E-06	0.003868	0.006452	0.00678
91.5	0.007164	3.6E-05	0.001085	0.000144	0.000144	0.007851	1E-06	0.003868	0.006452	0.00678

	4		5	4	4	1		8	2	
93.955	0.00716 4	3.6E-05	0.00108 5	0.00014 4	0.00014 4	0.00785 1	1E-06	0.00386 8	0.00645 2	0.00678
96.48	0.00716 4	3.6E-05	0.00108 5	0.00014 4	0.00014 4	0.00785 1	1E-06	0.00386 8	0.00645 2	0.00678
99.08	0.00716 4	3.6E-05	0.00108 5	0.00014 4	0.00014 4	0.00785 1	1E-06	0.00386 8	0.00645 2	0.00678
101.75	0.00716 4	3.6E-05	0.00108 5	0.00014 4	0.00014 4	0.00785 1	1E-06	0.00386 8	0.00645 2	0.00678
104.5	0.00716 4	3.6E-05	0.00108 5	0.00014 4	0.00014 4	0.00785 1	1E-06	0.00386 8	0.00645 2	0.00678
107.3	0.00716 4	3.6E-05	0.00108 5	0.00014 4	0.00014 4	0.00785 1	1E-06	0.00386 8	0.00645 2	0.00678
110.15	0.00716 4	3.6E-05	0.00108 5	0.00014 4	0.00014 4	0.00785 1	1E-06	0.00386 8	0.00645 2	0.00678
113.1	0.00716 4	3.6E-05	0.00108 5	0.00014 4	0.00014 4	0.00785 1	1E-06	0.00386 8	0.00645 2	0.00678
116.15	0.00716 4	3.6E-05	0.00108 5	0.00014 4	0.00014 4	0.00785 1	1E-06	0.00386 8	0.00645 2	0.00678
119.3	0.00716 4	3.6E-05	0.00108 5	0.00014 4	0.00014 4	0.00785 1	1E-06	0.00386 8	0.00645 2	0.00678
122.5	0.00716 4	3.6E-05	0.00108 5	0.00014 4	0.00014 4	0.00785 1	1E-06	0.00386 8	0.00645 2	0.00678
125.75	0.00716 4	3.6E-05	0.00108 5	0.00014 4	0.00014 4	0.00785 1	1E-06	0.00386 8	0.00645 2	0.00678
129.15	0.00716 4	3.6E-05	0.00108 5	0.00014 4	0.00014 4	0.00785 1	1E-06	0.00386 8	0.00645 2	0.00678
132.65	0.00716 4	3.6E-05	0.00108 5	0.00014 4	0.00014 4	0.00785 1	1E-06	0.00386 8	0.00645 2	0.00678
136.2	0.00716 4	3.6E-05	0.00108 5	0.00014 4	0.00014 4	0.00785 1	1E-06	0.00386 8	0.00645 2	0.00678
139.85	0.00716 4	3.6E-05	0.00108 5	0.00014 4	0.00014 4	0.00785 1	1E-06	0.00386 8	0.00645 2	0.00678
143.6	0.00716 4	3.6E-05	0.00108 5	0.00014 4	0.00014 4	0.00785 1	1E-06	0.00386 8	0.00645 2	0.00678
147.45	0.00716 4	3.6E-05	0.00108 5	0.00014 4	0.00014 4	0.00785 1	1E-06	0.00386 8	0.00645 2	0.00678
151.4	0.00716 4	3.6E-05	0.00108 5	0.00014 4	0.00014 4	0.00785 1	1E-06	0.00386 8	0.00645 2	0.00678
155.45	0.00716 4	3.6E-05	0.00108 5	0.00014 4	0.00014 4	0.00785 1	1E-06	0.00386 8	0.00645 2	0.00678
159.65	0.00716 4	3.6E-05	0.00108 5	0.00014 4	0.00014 4	0.00785 1	1E-06	0.00386 8	0.00645 2	0.00678
163.95	0.00716 4	3.6E-05	0.00108 5	0.00014 4	0.00014 4	0.00785 1	1E-06	0.00386 8	0.00645 2	0.00678
168.35	0.00716 4	3.6E-05	0.00108 5	0.00014 4	0.00014 4	0.00785 1	1E-06	0.00386 8	0.00645 2	0.00678
172.9	0.00716 4	3.6E-05	0.00108 5	0.00014 4	0.00014 4	0.00785 1	1E-06	0.00386 8	0.00645 2	0.00678
177.55	0.00716 4	3.6E-05	0.00108 5	0.00014 4	0.00014 4	0.00785 1	1E-06	0.00386 8	0.00645 2	0.00678
182.3	0.00716 4	3.6E-05	0.00108 5	0.00014 4	0.00014 4	0.00785 1	1E-06	0.00386 8	0.00645 2	0.00678
187.2	0.00716 4	3.6E-05	0.00108 5	0.00014 4	0.00014 4	0.00785 1	1E-06	0.00386 8	0.00645 2	0.00678
192.25	0.00716 4	3.6E-05	0.00108 5	0.00014 4	0.00014 4	0.00785 1	1E-06	0.00386 8	0.00645 2	0.00678
197.4	0.00716 4	3.6E-05	0.00108 5	0.00014 4	0.00014 4	0.00785 1	1E-06	0.00386 8	0.00645 2	0.00678

Calculations for results presented in Figure 4.2, c=10 g/L

**Table B.4 Observed values of cumulative particle size distributions presented in Figure 4.2 for 6 different mixtures having the same concentration (c=10 g/L)**

Observed values: cumulative %							
Size	sample1	sample2	sample3	sample4	sample5	sample6	Total

( $\mu\text{m}$ )							
<=0.627	22.41	22.73	23.38	22.95	23.56	23.14	138.170
0.644	5.6	5.54	5.78	5.66	5.9	5.68	34.160
0.661	5.73	5.65	5.9	5.78	6.02	5.78	34.860
0.678	6.61	6.51	6.76	6.68	6.93	6.64	40.130
0.697	6.74	6.64	6.86	6.83	7.04	6.75	40.860
0.716	7.99	7.89	8.14	8.03	8.28	7.93	48.260
0.735	8.28	8.17	8.43	8.37	8.6	8.31	50.160
0.754	8.95	8.87	9.1	9	9.32	8.99	54.230
0.775	10.16	10.14	10.44	10.28	10.64	10.33	61.990
0.796	10.35	10.33	10.63	10.45	10.86	10.51	63.130
0.817	11.38	11.33	11.63	11.48	11.96	11.59	69.370
0.839	12.1	12.1	12.41	12.24	12.75	12.32	73.920
0.861	13.07	13.12	13.36	13.14	13.71	13.23	79.630
0.884	13.3	13.36	13.65	13.33	13.97	13.49	81.100
0.908	14.11	14.19	14.6	14.19	14.84	14.32	86.250
0.933	14.73	14.85	15.29	14.82	15.56	14.96	90.210
0.958	15.78	15.88	16.38	15.86	16.68	15.97	96.550
0.983	16.59	16.78	17.27	16.76	17.59	16.84	101.830
1.01	17.32	17.51	17.98	17.42	18.32	17.53	106.080
1.037	18.17	18.29	18.79	18.2	19.14	18.36	110.950
1.065	19.02	19.07	19.64	19.03	19.98	19.21	115.950
1.094	20.22	20.31	21	20.37	21.23	20.52	123.650
1.123	20.92	21.07	21.61	21.11	21.93	21.19	127.830
1.153	21.73	21.84	22.41	21.83	22.68	21.92	132.410
1.184	22.88	22.97	23.57	22.97	23.85	23.12	139.360
1.215	23.65	23.66	24.29	23.65	24.63	23.87	143.750
1.248	24.72	24.83	25.41	24.69	25.73	24.95	150.330
1.282	25.6	25.64	26.24	25.4	26.59	25.75	155.220
1.316	26.52	26.56	27.2	26.31	27.47	26.73	160.790
1.351	27.59	27.52	28.29	27.32	28.48	27.77	166.970
1.388	28.68	28.57	29.29	28.3	29.59	28.72	173.150
1.425	29.6	29.54	30.27	29.23	30.54	29.7	178.880
1.464	30.59	30.55	31.24	30.09	31.6	30.67	184.740
1.503	31.6	31.58	32.28	31.05	32.53	31.58	190.620
1.543	32.86	32.77	33.5	32.15	33.65	32.72	197.650
1.584	33.77	33.7	34.41	33.04	34.47	33.62	203.010
1.627	35	34.81	35.57	34.1	35.51	34.79	209.780
1.671	36.15	35.95	36.67	35.21	36.64	35.91	216.530
1.716	37.14	36.9	37.64	36.14	37.62	36.92	222.360
1.762	38.21	38.02	38.85	37.21	38.79	38.08	229.160
1.809	39.24	39.07	39.91	38.34	39.89	39.15	235.600
1.858	40.27	40.17	40.9	39.29	40.92	40.09	241.640
1.908	41.46	41.32	42.14	40.51	42.07	41.3	248.800
1.959	42.6	42.39	43.24	41.63	43.21	42.31	255.380
2.012	43.58	43.31	44.23	42.59	44.22	43.31	261.240
2.066	44.73	44.27	45.33	43.59	45.24	44.39	267.550
2.121	45.73	45.2	46.19	44.41	46.16	45.27	272.960
2.178	46.81	46.15	47.2	45.42	47.24	46.3	279.120
2.237	47.82	47.21	48.2	46.5	48.3	47.36	285.390
2.297	48.93	48.27	49.26	47.52	49.33	48.33	291.640
2.358	49.93	49.22	50.33	48.53	50.3	49.27	297.580
2.421	50.94	50.26	51.32	49.48	51.33	50.24	303.570
2.486	51.97	51.3	52.51	50.48	52.41	51.33	310.000
2.553	53.11	52.34	53.68	51.59	53.54	52.47	316.730
2.622	54.11	53.2	54.81	52.48	54.53	53.44	322.570
2.693	55.21	54.25	55.93	53.66	55.52	54.55	329.120
2.765	56.15	55.29	56.96	54.71	56.46	55.57	335.140
2.839	57.27	56.41	57.99	55.88	57.5	56.75	341.800
2.915	58.29	57.44	59.07	56.91	58.49	57.77	347.970
2.994	59.27	58.4	59.96	57.99	59.51	58.69	353.820
3.074	60.2	59.26	60.92	58.91	60.55	59.61	359.450
3.157	61.13	60.06	61.83	59.9	61.46	60.48	364.860
3.241	62.09	60.9	62.72	60.79	62.36	61.43	370.290
3.328	63.05	61.84	63.63	61.7	63.27	62.38	375.870
3.418	63.98	62.71	64.54	62.63	64.23	63.26	381.350
3.51	64.95	63.59	65.45	63.5	65.15	64.19	386.830
3.604	65.92	64.47	66.36	64.47	66.1	65.15	392.470
3.701	66.87	65.32	67.37	65.36	67.02	66.05	397.990

3.8	67.74	66.18	68.27	66.29	67.95	66.96	403.390
3.902	68.72	67	69.24	67.24	68.83	67.87	408.900
4.007	69.74	67.9	70.23	68.18	69.84	68.81	414.700
4.115	70.7	68.91	71.21	69.25	70.89	69.84	420.800
4.225	71.62	69.85	72.25	70.45	71.91	70.91	426.990
4.339	72.64	70.77	73.24	71.47	72.91	71.96	432.990
4.455	73.61	71.61	74.18	72.58	73.86	72.94	438.780
4.575	74.54	72.54	75.12	73.6	74.83	74.06	444.690
4.698	75.45	73.41	76.06	74.59	75.74	75.11	450.360
4.824	76.38	74.25	77.06	75.63	76.64	76.1	456.060
4.954	77.22	75.08	77.95	76.65	77.59	77.02	461.510
5.087	78.08	75.91	78.97	77.68	78.54	77.95	467.130
5.224	78.9	76.73	79.87	78.7	79.45	78.88	472.530
5.364	79.76	77.61	80.83	79.72	80.39	79.82	478.130
5.508	80.59	78.49	81.72	80.53	81.3	80.73	483.360
5.656	81.45	79.34	82.61	81.41	82.16	81.65	488.620
5.808	82.25	80.12	83.45	82.36	83	82.47	493.650
5.964	83.04	80.95	84.32	83.3	83.83	83.3	498.740
6.124	83.78	81.66	85.09	84.09	84.63	84.17	503.420
6.289	84.51	82.38	85.87	84.89	85.34	84.97	507.960
6.458	85.25	83.14	86.58	85.78	86.07	85.78	512.600
6.631	85.93	83.89	87.32	86.58	86.78	86.56	517.060
6.809	86.61	84.65	87.97	87.39	87.51	87.25	521.380
6.992	87.25	85.31	88.68	88.13	88.25	87.93	525.550
7.18	87.87	85.97	89.39	88.84	88.92	88.64	529.630
7.373	88.53	86.58	90.07	89.52	89.58	89.34	533.620
7.571	89.2	87.16	90.66	90.11	90.24	89.96	537.330
7.774	89.72	87.79	91.2	90.68	90.91	90.56	540.860
7.983	90.3	88.4	91.74	91.33	91.47	91.15	544.390
8.198	90.82	88.96	92.29	91.89	91.96	91.74	547.660
8.418	91.38	89.49	92.78	92.49	92.53	92.21	550.880
8.644	91.91	90.04	93.26	92.99	93.05	92.75	554.000
8.877	92.42	90.57	93.77	93.44	93.53	93.25	556.980
9.115	92.94	91.06	94.17	93.97	94.03	93.72	559.890
9.36	93.37	91.57	94.61	94.44	94.45	94.24	562.680
9.611	93.79	92.01	95.04	94.84	94.88	94.65	565.210
9.869	94.18	92.46	95.43	95.22	95.23	95.04	567.560
10.135	94.56	92.9	95.83	95.58	95.6	95.42	569.890
10.405	94.93	93.31	96.13	95.92	95.92	95.83	572.040
10.685	95.31	93.74	96.51	96.22	96.26	96.14	574.180
10.975	95.65	94.12	96.77	96.53	96.57	96.48	576.120
11.27	95.92	94.52	97.03	96.8	96.83	96.79	577.890
11.57	96.21	94.89	97.34	97.03	97.1	97.09	579.660
11.88	96.5	95.22	97.53	97.31	97.36	97.32	581.240
12.2	96.74	95.52	97.75	97.52	97.63	97.58	582.740
12.525	96.98	95.8	97.95	97.74	97.84	97.82	584.130
12.865	97.19	96.13	98.16	97.97	98.04	98.02	585.510
13.215	97.42	96.39	98.35	98.15	98.19	98.2	586.700
13.57	97.65	96.62	98.52	98.3	98.35	98.4	587.840
13.93	97.85	96.85	98.65	98.43	98.51	98.56	588.850
14.3	98.04	97.07	98.79	98.59	98.67	98.71	589.870
14.685	98.19	97.3	98.94	98.71	98.8	98.8	590.740
15.08	98.34	97.52	99.03	98.86	98.92	98.93	591.600
15.485	98.5	97.71	99.16	98.98	99.03	98.99	592.370
15.905	98.6	97.92	99.23	99.08	99.13	99.09	593.050
16.335	98.73	98.08	99.32	99.19	99.23	99.18	593.730
16.77	98.86	98.29	99.4	99.26	99.32	99.24	594.370
17.22	98.97	98.45	99.47	99.32	99.39	99.31	594.910
17.685	99.05	98.58	99.51	99.38	99.46	99.41	595.390
18.16	99.14	98.69	99.56	99.43	99.52	99.47	595.810
18.645	99.23	98.79	99.61	99.49	99.56	99.51	596.190
19.145	99.31	98.89	99.67	99.55	99.59	99.57	596.580
19.66	99.39	99	99.7	99.58	99.65	99.62	596.940
20.19	99.44	99.1	99.75	99.64	99.69	99.66	597.280
20.735	99.5	99.19	99.77	99.65	99.73	99.7	597.540
21.29	99.55	99.27	99.8	99.69	99.77	99.73	597.810
21.86	99.6	99.33	99.83	99.73	99.78	99.77	598.040
22.45	99.64	99.39	99.84	99.76	99.81	99.8	598.240
23.055	99.7	99.46	99.85	99.8	99.84	99.82	598.470

23.675	99.72	99.52	99.87	99.82	99.86	99.83	598.620
24.31	99.75	99.55	99.9	99.83	99.88	99.85	598.760
24.96	99.77	99.62	99.91	99.85	99.89	99.86	598.900
25.63	99.8	99.66	99.92	99.87	99.91	99.88	599.040
26.32	99.82	99.7	99.93	99.89	99.92	99.89	599.150
27.03	99.83	99.73	99.95	99.91	99.93	99.9	599.250
27.755	99.85	99.76	99.96	99.92	99.95	99.92	599.360
28.5	99.87	99.77	99.96	99.94	99.95	99.93	599.420
29.265	99.89	99.82	99.97	99.94	99.96	99.94	599.520
30.05	99.9	99.84	99.97	99.94	99.97	99.94	599.560
30.86	99.92	99.86	99.97	99.95	99.97	99.94	599.610
31.69	99.93	99.87	99.98	99.95	99.97	99.95	599.650
32.54	99.96	99.89	99.98	99.96	99.97	99.97	599.730
33.415	99.96	99.91	99.98	99.96	99.98	99.98	599.770
34.31	99.97	99.92	99.98	99.97	99.99	99.98	599.810
35.23	99.97	99.92	99.99	99.99	99.99	99.99	599.850
36.18	99.98	99.93	99.99	99.99	99.99	100	599.880
37.15	99.98	99.95	99.99	99.99	99.99	100	599.900
38.145	99.98	99.95	99.99	99.99	99.99	100	599.900
39.17	99.98	99.96	100	99.99	100	100	599.930
40.225	99.99	99.96	100	100	100	100	599.950
41.305	99.99	99.97	100	100	100	100	599.960
42.415	99.99	99.98	100	100	100	100	599.970
43.555	99.99	99.98	100	100	100	100	599.970
44.725	99.99	99.99	100	100	100	100	599.980
45.93	99.99	99.99	100	100	100	100	599.980
47.165	99.99	99.99	100	100	100	100	599.980
48.43	99.99	99.99	100	100	100	100	599.980
49.73	100	99.99	100	100	100	100	599.990
51.065	100	99.99	100	100	100	100	599.990
52.435	100	99.99	100	100	100	100	599.990
53.845	100	99.99	100	100	100	100	599.990
55.29	100	99.99	100	100	100	100	599.990
56.775	100	100	100	100	100	100	600.000
58.305	100	100	100	100	100	100	600.000
59.87	100	100	100	100	100	100	600.000
61.475	100	100	100	100	100	100	600.000
63.13	100	100	100	100	100	100	600.000
64.825	100	100	100	100	100	100	600.000
66.565	100	100	100	100	100	100	600.000
68.355	100	100	100	100	100	100	600.000
70.19	100	100	100	100	100	100	600.000
72.075	100	100	100	100	100	100	600.000
74.01	100	100	100	100	100	100	600.000
76	100	100	100	100	100	100	600.000
78.045	100	100	100	100	100	100	600.000
80.14	100	100	100	100	100	100	600.000
82.29	100	100	100	100	100	100	600.000
84.5	100	100	100	100	100	100	600.000
86.77	100	100	100	100	100	100	600.000
89.105	100	100	100	100	100	100	600.000
91.5	100	100	100	100	100	100	600.000
93.955	100	100	100	100	100	100	600.000
96.48	100	100	100	100	100	100	600.000
99.08	100	100	100	100	100	100	600.000
101.75	100	100	100	100	100	100	600.000
104.5	100	100	100	100	100	100	600.000
107.3	100	100	100	100	100	100	600.000
110.15	100	100	100	100	100	100	600.000
113.1	100	100	100	100	100	100	600.000
116.15	100	100	100	100	100	100	600.000
119.3	100	100	100	100	100	100	600.000
122.5	100	100	100	100	100	100	600.000
125.75	100	100	100	100	100	100	600.000
129.15	100	100	100	100	100	100	600.000
132.65	100	100	100	100	100	100	600.000
136.2	100	100	100	100	100	100	600.000
139.85	100	100	100	100	100	100	600.000
143.6	100	100	100	100	100	100	600.000

147.45	100	100	100	100	100	100	600.000
151.4	100	100	100	100	100	100	600.000
155.45	100	100	100	100	100	100	600.000
159.65	100	100	100	100	100	100	600.000
163.95	100	100	100	100	100	100	600.000
168.35	100	100	100	100	100	100	600.000
172.9	100	100	100	100	100	100	600.000
177.55	100	100	100	100	100	100	600.000
182.3	100	100	100	100	100	100	600.000
187.2	100	100	100	100	100	100	600.000
192.25	100	100	100	100	100	100	600.000
197.4	100	100	100	100	100	100	600.000
Total	16618.47	16495.8	16719.96	16598.48	16706.22	16634.99	99773.920

**Table B.5 Expected values for data presented in Table B.4**

Expected values						
Size (µm)	sample1	sample2	sample3	sample4	sample5	sample6
<=0.627	23.01498	22.84365	23.15453	22.98596	23.13518	23.03708
0.644	5.690031	5.647673	5.724533	5.682858	5.71975	5.695497
0.661	5.80663	5.763404	5.841839	5.79931	5.836958	5.812208
0.678	6.684454	6.634693	6.724985	6.676027	6.719367	6.690875
0.697	6.80605	6.755384	6.847319	6.79747	6.841598	6.812588
0.716	8.038668	7.978826	8.087411	8.028534	8.080654	8.04639
0.735	8.355151	8.292953	8.405813	8.344618	8.39879	8.363177
0.754	9.033091	8.965846	9.087863	9.021703	9.080271	9.041768
0.775	10.32567	10.24881	10.38828	10.31266	10.37961	10.33559
0.796	10.51556	10.43728	10.57933	10.50231	10.57049	10.52566
0.817	11.55496	11.46894	11.62502	11.54039	11.61531	11.56606
0.839	12.31285	12.22119	12.38751	12.29733	12.37716	12.32468
0.861	13.26397	13.16523	13.3444	13.24725	13.33325	13.27671
0.884	13.50883	13.40826	13.59074	13.4918	13.57938	13.5218
0.908	14.36666	14.25971	14.45378	14.34855	14.4417	14.38046
0.933	15.02628	14.91442	15.11739	15.00734	15.10476	15.04071
0.958	16.08233	15.96261	16.17985	16.06206	16.16633	16.09778
0.983	16.96182	16.83555	17.06467	16.94044	17.05042	16.97812
1.01	17.66975	17.53821	17.77689	17.64747	17.76204	17.68672
1.037	18.48094	18.34336	18.593	18.45764	18.57747	18.49869
1.065	19.31379	19.17001	19.4309	19.28944	19.41467	19.33234
1.094	20.59638	20.44305	20.72127	20.57041	20.70396	20.61616
1.123	21.29264	21.13413	21.42175	21.2658	21.40386	21.3131
1.153	22.05553	21.89135	22.18927	22.02773	22.17073	22.07672
1.184	23.2132	23.04039	23.35395	23.18393	23.33444	23.23549
1.215	23.94444	23.76619	24.08963	23.91425	24.0695	23.96744
1.248	25.04047	24.85406	25.1923	25.0089	25.17126	25.06452
1.282	25.855	25.66252	26.01177	25.8224	25.99004	25.87983
1.316	26.78279	26.58341	26.94519	26.74902	26.92268	26.80852
1.351	27.81219	27.60515	27.98083	27.77713	27.95746	27.83891
1.388	28.8416	28.62689	29.01648	28.80523	28.99224	28.8693
1.425	29.79604	29.57423	29.97671	29.75848	29.95167	29.82466
1.464	30.77214	30.54306	30.95873	30.73335	30.93287	30.8017
1.503	31.75157	31.5152	31.9441	31.71154	31.91741	31.78207
1.543	32.92256	32.67747	33.12219	32.88105	33.09452	32.95418
1.584	33.81538	33.56364	34.02042	33.77274	33.99199	33.84786
1.627	34.94305	34.68293	35.15493	34.899	35.12556	34.97662
1.671	36.0674	35.7989	36.2861	36.02193	36.25578	36.10205
1.716	37.03851	36.76278	37.26309	36.99181	37.23196	37.07408
1.762	38.17118	37.88702	38.40263	38.12306	38.37055	38.20785
1.809	39.24389	38.95175	39.48185	39.19442	39.44886	39.28159
1.858	40.24997	39.95034	40.49403	40.19923	40.4602	40.28864
1.908	41.44262	41.1341	41.6939	41.39037	41.65907	41.48242
1.959	42.53865	42.22198	42.79658	42.48502	42.76083	42.57951
2.012	43.51475	43.19081	43.7786	43.45989	43.74203	43.55655
2.066	44.5658	44.23404	44.83603	44.50962	44.79857	44.60861
2.121	45.46695	45.12848	45.74264	45.40963	45.70442	45.51062
2.178	46.49302	46.14691	46.77493	46.4344	46.73585	46.53768
2.237	47.53741	47.18353	47.82566	47.47748	47.7857	47.58307

2.297	48.57847	48.21684	48.87303	48.51723	48.8322	48.62514
2.358	49.5679	49.1989	49.86846	49.50541	49.8268	49.61551
2.421	50.56565	50.18923	50.87226	50.50191	50.82976	50.61423
2.486	51.6367	51.2523	51.9498	51.5716	51.9064	51.6863
2.553	52.75772	52.36497	53.07761	52.6912	53.03327	52.80839
2.622	53.73048	53.3305	54.05628	53.66275	54.01112	53.7821
2.693	54.82152	54.41341	55.15393	54.7524	55.10785	54.87418
2.765	55.82427	55.4087	56.16276	55.75389	56.11584	55.87789
2.839	56.93363	56.50979	57.27884	56.86185	57.23099	56.98831
2.915	57.96136	57.52988	58.31281	57.88829	58.2641	58.01704
2.994	58.9358	58.49706	59.29316	58.8615	59.24362	58.99241
3.074	59.87359	59.42787	60.23663	59.7981	60.18631	59.9311
3.157	60.77473	60.3223	61.14324	60.69811	61.09216	60.83311
3.241	61.67921	61.22005	62.0532	61.60144	62.00136	61.73845
3.328	62.60867	62.14259	62.98829	62.52973	62.93567	62.66881
3.418	63.52147	63.0486	63.90663	63.44139	63.85324	63.58249
3.51	64.43427	63.9546	64.82497	64.35304	64.77082	64.49617
3.604	65.37373	64.88707	65.77012	65.29131	65.71518	65.43652
3.701	66.29319	65.79969	66.69516	66.20962	66.63945	66.35687
3.8	67.19267	66.69247	67.6001	67.10796	67.54362	67.25721
3.902	68.11047	67.60344	68.52346	68.0246	68.46622	68.1759
4.007	69.07658	68.56235	69.49543	68.98949	69.43737	69.14293
4.115	70.09266	69.57086	70.51766	70.00429	70.45875	70.15998
4.225	71.12372	70.59426	71.55498	71.03406	71.49521	71.19204
4.339	72.12314	71.58624	72.56046	72.03222	72.49985	72.19242
4.455	73.08758	72.5435	73.53075	72.99544	73.46932	73.15779
4.575	74.07201	73.5206	74.52115	73.97863	74.45889	74.14316
4.698	75.01647	74.45802	75.47133	74.92189	75.40828	75.08852
4.824	75.96591	75.4004	76.42653	75.87014	76.36269	76.03888
4.954	76.87372	76.30145	77.33985	76.7768	77.27523	76.94756
5.087	77.80984	77.2306	78.28165	77.71175	78.21625	77.88458
5.224	78.70932	78.12338	79.18658	78.61009	79.12042	78.78493
5.364	79.64211	79.04923	80.12503	79.54171	80.05809	79.71861
5.508	80.51328	79.91391	81.00147	80.41177	80.9338	80.59061
5.656	81.38943	80.78354	81.88294	81.28682	81.81453	81.46761
5.808	82.22728	81.61515	82.72587	82.12361	82.65676	82.30626
5.964	83.07512	82.45668	83.57885	82.97039	83.50903	83.15492
6.124	83.85467	83.23043	84.36312	83.74895	84.29264	83.93522
6.289	84.6109	83.98103	85.12394	84.50423	85.05282	84.69217
6.458	85.38378	84.74816	85.90151	85.27614	85.82974	85.4658
6.631	86.12668	85.48553	86.64891	86.0181	86.57653	86.20941
6.809	86.84627	86.19976	87.37286	86.73678	87.29987	86.92969
6.992	87.54086	86.88918	88.07167	87.4305	87.99809	87.62495
7.18	88.22047	87.56373	88.7554	88.10925	88.68125	88.30521
7.373	88.88508	88.22339	89.42404	88.77302	89.34933	88.97046
7.571	89.50306	88.83677	90.04576	89.39022	89.97054	89.58903
7.774	90.09105	89.42038	90.63732	89.97747	90.5616	90.17759
7.983	90.67904	90.004	91.22888	90.56472	91.15266	90.76614
8.198	91.22373	90.54463	91.77686	91.10872	91.70019	91.31135
8.418	91.76008	91.07699	92.31647	91.6444	92.23935	91.84822
8.644	92.27978	91.59282	92.83932	92.16344	92.76176	92.36842
8.877	92.77616	92.0855	93.33871	92.65919	93.26073	92.86528
9.115	93.26088	92.56661	93.82637	93.1433	93.74798	93.35046
9.36	93.72561	93.02788	94.29391	93.60744	94.21514	93.81564
9.611	94.14703	93.44617	94.71789	94.02834	94.63876	94.23746
9.869	94.53847	93.83469	95.1117	94.41928	95.03225	94.62928
10.135	94.92658	94.21991	95.50217	94.8069	95.42238	95.01776
10.405	95.2847	94.57537	95.86246	95.16457	95.78238	95.37623
10.685	95.64116	94.92918	96.22108	95.52058	96.1407	95.73303
10.975	95.96431	95.24992	96.54619	95.84332	96.46553	96.05649
11.27	96.25914	95.54255	96.84281	96.13778	96.7619	96.3516
11.57	96.55397	95.83519	97.13942	96.43224	97.05827	96.64671
11.88	96.81715	96.09641	97.4042	96.69509	97.32283	96.91015
12.2	97.067	96.3444	97.65557	96.94463	97.57399	97.16024
12.525	97.29853	96.57421	97.88851	97.17587	97.80673	97.39199
12.865	97.5284	96.80237	98.11977	97.40544	98.03779	97.62208
13.215	97.72662	96.99911	98.31919	97.60341	98.23705	97.82049
13.57	97.91651	97.18759	98.51023	97.79306	98.42793	98.01056
13.93	98.08474	97.35457	98.67948	97.96109	98.59704	98.17896

14.3	98.25465	97.52321	98.85041	98.13077	98.76783	98.34903
14.685	98.39956	97.66704	98.99621	98.27551	98.91351	98.49408
15.08	98.54281	97.80923	99.14033	98.41858	99.0575	98.63747
15.485	98.67107	97.93653	99.26936	98.54667	99.18643	98.76585
15.905	98.78434	98.04896	99.38332	98.6598	99.30029	98.87923
16.335	98.89761	98.16138	99.49727	98.77292	99.41415	98.9926
16.77	99.00421	98.26719	99.60452	98.87939	99.52131	99.09931
17.22	99.09416	98.35647	99.69502	98.96923	99.61173	99.18934
17.685	99.17411	98.43583	99.77546	99.04908	99.6921	99.26937
18.16	99.24407	98.50527	99.84584	99.11895	99.76243	99.3394
18.645	99.30737	98.56809	99.90952	99.18217	99.82605	99.40276
19.145	99.37233	98.63257	99.97488	99.24705	99.89136	99.46778
19.66	99.4323	98.69209	100.0352	99.30694	99.95163	99.52781
20.19	99.48893	98.7483	100.0922	99.3635	100.0086	99.58449
20.735	99.53224	98.79129	100.1358	99.40675	100.0521	99.62784
21.29	99.57721	98.83593	100.181	99.45167	100.0973	99.67286
21.86	99.61552	98.87395	100.2195	99.48993	100.1358	99.71121
22.45	99.64884	98.90702	100.2531	99.52321	100.1693	99.74456
23.055	99.68715	98.94505	100.2916	99.56147	100.2078	99.7829
23.675	99.71213	98.96984	100.3167	99.58642	100.2329	99.80791
24.31	99.73545	98.99299	100.3402	99.60971	100.2564	99.83125
24.96	99.75877	99.01614	100.3637	99.633	100.2798	99.8546
25.63	99.78209	99.03928	100.3871	99.65629	100.3033	99.87794
26.32	99.80042	99.05747	100.4056	99.67459	100.3217	99.89628
27.03	99.81707	99.074	100.4223	99.69123	100.3384	99.91295
27.755	99.8354	99.09219	100.4407	99.70953	100.3568	99.93129
28.5	99.84539	99.10211	100.4508	99.71951	100.3669	99.9413
29.265	99.86205	99.11864	100.4676	99.73615	100.3836	99.95797
30.05	99.86871	99.12525	100.4743	99.7428	100.3903	99.96464
30.86	99.87704	99.13352	100.4826	99.75112	100.3987	99.97298
31.69	99.8837	99.14013	100.4893	99.75777	100.4054	99.97964
32.54	99.89703	99.15336	100.5028	99.77108	100.4188	99.99298
33.415	99.90369	99.15997	100.5095	99.77774	100.4255	99.99965
34.31	99.91035	99.16659	100.5162	99.78439	100.4322	100.0063
35.23	99.91701	99.1732	100.5229	99.79105	100.4389	100.013
36.18	99.92201	99.17816	100.5279	99.79604	100.4439	100.018
37.15	99.92534	99.18147	100.5312	99.79936	100.4473	100.0213
38.145	99.92534	99.18147	100.5312	99.79936	100.4473	100.0213
39.17	99.93034	99.18643	100.5363	99.80435	100.4523	100.0263
40.225	99.93367	99.18973	100.5396	99.80768	100.4556	100.0297
41.305	99.93534	99.19139	100.5413	99.80935	100.4573	100.0313
42.415	99.937	99.19304	100.543	99.81101	100.459	100.033
43.555	99.937	99.19304	100.543	99.81101	100.459	100.033
44.725	99.93867	99.19469	100.5446	99.81267	100.4607	100.0347
45.93	99.93867	99.19469	100.5446	99.81267	100.4607	100.0347
47.165	99.93867	99.19469	100.5446	99.81267	100.4607	100.0347
48.43	99.93867	99.19469	100.5446	99.81267	100.4607	100.0347
49.73	99.94033	99.19635	100.5463	99.81434	100.4623	100.0363
51.065	99.94033	99.19635	100.5463	99.81434	100.4623	100.0363
52.435	99.94033	99.19635	100.5463	99.81434	100.4623	100.0363
53.845	99.94033	99.19635	100.5463	99.81434	100.4623	100.0363
55.29	99.94033	99.19635	100.5463	99.81434	100.4623	100.0363
56.775	99.942	99.198	100.548	99.816	100.464	100.038
58.305	99.942	99.198	100.548	99.816	100.464	100.038
59.87	99.942	99.198	100.548	99.816	100.464	100.038
61.475	99.942	99.198	100.548	99.816	100.464	100.038
63.13	99.942	99.198	100.548	99.816	100.464	100.038
64.825	99.942	99.198	100.548	99.816	100.464	100.038
66.565	99.942	99.198	100.548	99.816	100.464	100.038
68.355	99.942	99.198	100.548	99.816	100.464	100.038
70.19	99.942	99.198	100.548	99.816	100.464	100.038
72.075	99.942	99.198	100.548	99.816	100.464	100.038
74.01	99.942	99.198	100.548	99.816	100.464	100.038
76	99.942	99.198	100.548	99.816	100.464	100.038
78.045	99.942	99.198	100.548	99.816	100.464	100.038
80.14	99.942	99.198	100.548	99.816	100.464	100.038
82.29	99.942	99.198	100.548	99.816	100.464	100.038
84.5	99.942	99.198	100.548	99.816	100.464	100.038
86.77	99.942	99.198	100.548	99.816	100.464	100.038

89.105	99.942	99.198	100.548	99.816	100.464	100.038
91.5	99.942	99.198	100.548	99.816	100.464	100.038
93.955	99.942	99.198	100.548	99.816	100.464	100.038
96.48	99.942	99.198	100.548	99.816	100.464	100.038
99.08	99.942	99.198	100.548	99.816	100.464	100.038
101.75	99.942	99.198	100.548	99.816	100.464	100.038
104.5	99.942	99.198	100.548	99.816	100.464	100.038
107.3	99.942	99.198	100.548	99.816	100.464	100.038
110.15	99.942	99.198	100.548	99.816	100.464	100.038
113.1	99.942	99.198	100.548	99.816	100.464	100.038
116.15	99.942	99.198	100.548	99.816	100.464	100.038
119.3	99.942	99.198	100.548	99.816	100.464	100.038
122.5	99.942	99.198	100.548	99.816	100.464	100.038
125.75	99.942	99.198	100.548	99.816	100.464	100.038
129.15	99.942	99.198	100.548	99.816	100.464	100.038
132.65	99.942	99.198	100.548	99.816	100.464	100.038
136.2	99.942	99.198	100.548	99.816	100.464	100.038
139.85	99.942	99.198	100.548	99.816	100.464	100.038
143.6	99.942	99.198	100.548	99.816	100.464	100.038
147.45	99.942	99.198	100.548	99.816	100.464	100.038
151.4	99.942	99.198	100.548	99.816	100.464	100.038
155.45	99.942	99.198	100.548	99.816	100.464	100.038
159.65	99.942	99.198	100.548	99.816	100.464	100.038
163.95	99.942	99.198	100.548	99.816	100.464	100.038
168.35	99.942	99.198	100.548	99.816	100.464	100.038
172.9	99.942	99.198	100.548	99.816	100.464	100.038
177.55	99.942	99.198	100.548	99.816	100.464	100.038
182.3	99.942	99.198	100.548	99.816	100.464	100.038
187.2	99.942	99.198	100.548	99.816	100.464	100.038
192.25	99.942	99.198	100.548	99.816	100.464	100.038
197.4	99.942	99.198	100.548	99.816	100.464	100.038

**Table B.6 Calculated Chi-square value for each cell of Tables B.4 and B.5**

Chi-square value for each cell						
Size (µm)	sample1	sample2	sample3	sample4	sample5	sample6
<=0.627	0.015903	0.000565	0.002196	5.63E-05	0.007801	0.00046
0.644	0.001425	0.002053	0.000537	9.19E-05	0.00568	4.22E-05
0.661	0.001011	0.002231	0.000579	6.43E-05	0.00574	0.000178
0.678	0.000829	0.002343	0.000182	2.36E-06	0.006603	0.000387
0.697	0.000641	0.001971	2.35E-05	0.000156	0.005754	0.000575
0.716	0.000295	0.000989	0.000342	2.68E-07	0.004918	0.001684
0.735	0.000676	0.001823	6.96E-05	7.72E-05	0.00482	0.000338
0.754	0.000764	0.001025	1.62E-05	5.22E-05	0.006329	0.000296
0.775	0.002658	0.001155	0.000257	0.000103	0.006533	3.03E-06
0.796	0.002607	0.001103	0.000243	0.000261	0.007929	2.33E-05
0.817	0.002649	0.001683	2.13E-06	0.000316	0.010229	4.96E-05
0.839	0.00368	0.001202	4.08E-05	0.000267	0.011231	1.78E-06
0.861	0.002837	0.000155	1.82E-05	0.000868	0.010646	0.000164
0.884	0.003228	0.000174	0.000258	0.00194	0.011236	7.48E-05
0.908	0.004585	0.000341	0.001479	0.001752	0.010985	0.000254
0.933	0.005842	0.000278	0.001971	0.002338	0.01372	0.000433
0.958	0.005684	0.000428	0.002476	0.002542	0.016321	0.001014
0.983	0.008151	0.000183	0.002471	0.001922	0.017076	0.001124
1.01	0.006923	4.54E-05	0.002321	0.002932	0.017528	0.001389
1.037	0.005232	0.000155	0.002087	0.003596	0.017034	0.00104
1.065	0.004469	0.000522	0.00225	0.003489	0.016462	0.000774
1.094	0.006878	0.000866	0.003749	0.001953	0.013366	0.000449
1.123	0.006522	0.000195	0.001654	0.001141	0.012934	0.000711
1.153	0.004805	0.00012	0.002196	0.001775	0.011698	0.001113
1.184	0.004783	0.000215	0.001999	0.001974	0.011391	0.000574
1.215	0.003621	0.000474	0.001667	0.00292	0.013052	0.000396
1.248	0.004101	2.33E-05	0.001881	0.004066	0.012403	0.000523
1.282	0.002515	1.98E-05	0.002003	0.00691	0.01385	0.000651
1.316	0.002578	2.06E-05	0.00241	0.007206	0.011127	0.00023
1.351	0.001775	0.000263	0.003416	0.007523	0.009767	0.000171

1.388	0.000905	0.000113	0.002578	0.008862	0.012325	0.000772
1.425	0.00129	3.96E-05	0.00287	0.009385	0.011556	0.000521
1.464	0.001078	1.57E-06	0.002555	0.013467	0.014388	0.000563
1.503	0.000724	0.000133	0.003532	0.013801	0.011757	0.001285
1.543	0.000119	0.000262	0.00431	0.016254	0.009324	0.001664
1.584	6.09E-05	0.000554	0.004461	0.015898	0.006722	0.001534
1.627	9.28E-05	0.000466	0.004901	0.018293	0.004208	0.000996
1.671	0.000189	0.000638	0.004062	0.018301	0.004072	0.001022
1.716	0.000278	0.000512	0.003812	0.019615	0.004044	0.00064
1.762	3.95E-05	0.000467	0.005212	0.021868	0.004585	0.000428
1.809	3.86E-07	0.000359	0.004643	0.018626	0.004933	0.000441
1.858	9.96E-06	0.001208	0.00407	0.020565	0.005225	0.000979
1.908	7.29E-06	0.00084	0.004773	0.018725	0.004053	0.000802
1.959	8.85E-05	0.000669	0.004594	0.017207	0.004718	0.001706
2.012	9.79E-05	0.000329	0.004654	0.017412	0.005223	0.001396
2.066	0.000605	2.92E-05	0.005442	0.019	0.00435	0.001071
2.121	0.001522	0.000113	0.004375	0.022005	0.004541	0.001272
2.178	0.002161	2.07E-07	0.003863	0.022161	0.005438	0.001214
2.237	0.00168	1.49E-05	0.00293	0.020125	0.005535	0.001046
2.297	0.002544	5.86E-05	0.003064	0.020497	0.005075	0.001791
2.358	0.002645	9.05E-06	0.004272	0.019219	0.004494	0.002406
2.421	0.002771	9.98E-05	0.003941	0.020678	0.004923	0.002767
2.486	0.002151	4.44E-05	0.006041	0.023106	0.004886	0.002456
2.553	0.002352	1.19E-05	0.006837	0.023014	0.004842	0.002168
2.622	0.002681	0.000319	0.010509	0.026068	0.004985	0.002176
2.693	0.002753	0.000491	0.01092	0.021795	0.003082	0.001915
2.765	0.001901	0.000254	0.011317	0.019545	0.002111	0.001697
2.839	0.001987	0.000176	0.008829	0.016954	0.001264	0.000997
2.915	0.001863	0.00014	0.009832	0.016533	0.000876	0.001052
2.994	0.001895	0.000161	0.0075	0.012903	0.001198	0.00155
3.074	0.00178	0.000474	0.007753	0.01319	0.002198	0.00172
3.157	0.002077	0.001141	0.007714	0.010494	0.002215	0.00205
3.241	0.002736	0.001673	0.007165	0.010689	0.002075	0.001541
3.328	0.003111	0.001473	0.006537	0.01101	0.001776	0.001331
3.418	0.00331	0.001818	0.006277	0.010377	0.002223	0.001636
3.51	0.004128	0.002079	0.006026	0.011308	0.00222	0.001453
3.604	0.004565	0.002681	0.00529	0.010331	0.002253	0.001255
3.701	0.005019	0.003497	0.006828	0.010902	0.002173	0.001419
3.8	0.004458	0.003938	0.006639	0.00997	0.002445	0.001313
3.902	0.005455	0.005386	0.007493	0.00905	0.001933	0.001373
4.007	0.006372	0.006399	0.007765	0.009498	0.002335	0.001603
4.115	0.005263	0.006278	0.006797	0.008127	0.002639	0.001459
4.225	0.003463	0.007847	0.006751	0.004802	0.002407	0.001117
4.339	0.003704	0.009307	0.006364	0.004388	0.00232	0.000748
4.455	0.003734	0.012012	0.005733	0.002364	0.002077	0.000648
4.575	0.002957	0.013079	0.004812	0.001938	0.00185	9.33E-05
4.698	0.002505	0.014751	0.004592	0.00147	0.001459	6.14E-06
4.824	0.002257	0.017552	0.005251	0.00076	0.001007	4.91E-05
4.954	0.00156	0.019553	0.004814	0.000209	0.001282	6.82E-05
5.087	0.000938	0.022582	0.006053	1.3E-05	0.00134	5.49E-05
5.224	0.000462	0.024852	0.005898	0.000103	0.001373	0.000115
5.364	0.000174	0.026204	0.006203	0.0004	0.001376	0.000129
5.508	7.31E-05	0.025371	0.006374	0.000174	0.001657	0.000241
5.656	4.51E-05	0.025795	0.006456	0.000187	0.001459	0.000408
5.808	6.28E-06	0.027391	0.006339	0.00068	0.001425	0.000326
5.964	1.48E-05	0.027531	0.006572	0.001309	0.001234	0.000253
6.124	6.65E-05	0.029632	0.006263	0.001389	0.00135	0.000657
6.289	0.00012	0.030522	0.006539	0.001761	0.00097	0.000911
6.458	0.00021	0.030516	0.005359	0.002977	0.000673	0.001155
6.631	0.000449	0.029779	0.005197	0.003671	0.000478	0.001426
6.809	0.000643	0.027863	0.004081	0.004919	0.000506	0.00118
6.992	0.000966	0.028701	0.004202	0.005596	0.000721	0.001062
7.18	0.001392	0.029007	0.004537	0.006061	0.000643	0.001269
7.373	0.001419	0.030613	0.004666	0.006285	0.000595	0.001535
7.571	0.001026	0.031649	0.00419	0.005796	0.000807	0.001536
7.774	0.001528	0.029726	0.003493	0.005485	0.00134	0.001622
7.983	0.001584	0.028586	0.002864	0.006467	0.001105	0.001623
8.198	0.001787	0.027733	0.002869	0.0067	0.000736	0.002012
8.418	0.001574	0.027653	0.002327	0.007802	0.000916	0.001425

8.644	0.001482	0.026326	0.001906	0.007413	0.000896	0.001576
8.877	0.001367	0.024941	0.001993	0.00658	0.000777	0.001594
9.115	0.001104	0.024522	0.001259	0.007337	0.000848	0.001463
9.36	0.001349	0.022847	0.00106	0.007405	0.000585	0.00192
9.611	0.001354	0.022072	0.001095	0.007006	0.000615	0.001806
9.869	0.001359	0.02014	0.001065	0.00679	0.000412	0.001783
10.135	0.001416	0.01849	0.001125	0.006304	0.000331	0.001703
10.405	0.00132	0.01693	0.000747	0.005997	0.000198	0.002159
10.685	0.001147	0.014897	0.000868	0.005121	0.000148	0.00173
10.975	0.001029	0.013404	0.000519	0.00492	0.000113	0.001867
11.27	0.001195	0.010944	0.000362	0.004562	4.79E-05	0.001995
11.57	0.001225	0.009322	0.000414	0.003705	1.79E-05	0.002033
11.88	0.001039	0.007993	0.000162	0.00391	1.42E-05	0.001733
12.2	0.001102	0.007054	9.13E-05	0.003415	3.22E-05	0.001813
12.525	0.001043	0.006207	3.86E-05	0.003275	1.13E-05	0.001881
12.865	0.001174	0.00467	1.65E-05	0.003272	4.96E-08	0.001622
13.215	0.000962	0.003825	9.66E-06	0.003061	2.25E-05	0.001472
13.57	0.000725	0.003315	9.7E-07	0.002628	6.17E-05	0.001547
13.93	0.000562	0.002615	8.81E-06	0.002245	7.68E-05	0.001479
14.3	0.000469	0.002106	3.69E-05	0.002149	9.69E-05	0.001325
14.685	0.000446	0.001379	3.19E-05	0.001921	0.00013	0.00095
15.08	0.000417	0.000855	0.000123	0.00198	0.000191	0.000868
15.485	0.000297	0.000524	0.00012	0.001905	0.000247	0.000509
15.905	0.000344	0.00017	0.000237	0.00179	0.000292	0.000449
16.335	0.000284	6.75E-05	0.000316	0.001761	0.000341	0.000355
16.77	0.00021	5.29E-06	0.00042	0.001465	0.000407	0.0002
17.22	0.000156	8.89E-05	0.000508	0.001243	0.000494	0.000147
17.685	0.000155	0.000211	0.000706	0.001106	0.00054	0.000199
18.16	0.000109	0.000346	0.000818	0.000976	0.000589	0.000172
18.645	6.03E-05	0.0005	0.000898	0.000955	0.000709	0.000116
19.145	3.91E-05	0.000672	0.00093	0.000925	0.000909	0.000105
19.66	1.8E-05	0.000961	0.001123	0.000751	0.00091	8.54E-05
20.19	2.41E-05	0.001253	0.00117	0.000769	0.001015	5.72E-05
20.735	1.04E-05	0.001609	0.001336	0.000595	0.001037	5.23E-05
21.29	7.44E-06	0.001906	0.001449	0.000571	0.00107	3.28E-05
21.86	2.42E-06	0.002103	0.001514	0.000579	0.001264	3.47E-05
22.45	7.84E-07	0.002358	0.001702	0.000563	0.001289	3.08E-05
23.055	1.66E-06	0.00268	0.001944	0.000571	0.00135	1.38E-05
23.675	6.21E-07	0.003058	0.001989	0.000548	0.001388	4.89E-06
24.31	2.12E-06	0.003134	0.001931	0.000487	0.001413	3.52E-06
24.96	1.26E-06	0.003683	0.002051	0.000473	0.001515	2.92E-07
25.63	3.21E-06	0.00389	0.002174	0.000458	0.001542	4.25E-08
26.32	3.84E-06	0.004168	0.002252	0.000466	0.001608	3.95E-07
27.03	1.67E-06	0.004344	0.002221	0.00048	0.001662	1.68E-06
27.755	2.14E-06	0.004501	0.002301	0.000444	0.001649	1.28E-06
28.5	6.07E-06	0.004501	0.002398	0.000488	0.001732	1.28E-06
29.265	7.82E-06	0.004963	0.002464	0.000417	0.001788	3.23E-06
30.05	9.8E-06	0.005154	0.002531	0.00039	0.00176	6.07E-06
30.86	1.85E-05	0.005324	0.002615	0.000397	0.001831	1.09E-05
31.69	2.15E-05	0.005373	0.002582	0.00037	0.001888	8.79E-06
32.54	3.97E-05	0.005473	0.002719	0.000358	0.002006	5.28E-06
33.415	3.17E-05	0.005673	0.002789	0.000333	0.001976	3.86E-06
34.31	3.56E-05	0.005724	0.00286	0.000345	0.001947	6.93E-06
35.23	2.81E-05	0.005624	0.002825	0.000397	0.002006	5.28E-06
36.18	3.37E-05	0.005699	0.002878	0.000377	0.002051	3.24E-06
37.15	2.99E-05	0.005955	0.002914	0.000364	0.002082	4.55E-06
38.145	2.99E-05	0.005955	0.002914	0.000364	0.002082	4.55E-06
39.17	2.47E-05	0.006033	0.002861	0.000345	0.002036	6.93E-06
40.225	3.18E-05	0.005982	0.002896	0.000371	0.002067	8.8E-06
41.305	2.99E-05	0.006112	0.002914	0.000364	0.002082	9.81E-06
42.415	2.81E-05	0.006243	0.002932	0.000358	0.002097	1.09E-05
43.555	2.81E-05	0.006243	0.002932	0.000358	0.002097	1.09E-05
44.725	2.64E-05	0.006376	0.00295	0.000352	0.002112	1.2E-05
45.93	2.64E-05	0.006376	0.00295	0.000352	0.002112	1.2E-05
47.165	2.64E-05	0.006376	0.00295	0.000352	0.002112	1.2E-05
48.43	2.64E-05	0.006376	0.00295	0.000352	0.002112	1.2E-05
49.73	3.56E-05	0.00635	0.002968	0.000345	0.002128	1.32E-05
51.065	3.56E-05	0.00635	0.002968	0.000345	0.002128	1.32E-05
52.435	3.56E-05	0.00635	0.002968	0.000345	0.002128	1.32E-05

53.845	3.56E-05	0.00635	0.002968	0.000345	0.002128	1.32E-05
55.29	3.56E-05	0.00635	0.002968	0.000345	0.002128	1.32E-05
56.775	3.37E-05	0.006484	0.002987	0.000339	0.002143	1.44E-05
58.305	3.37E-05	0.006484	0.002987	0.000339	0.002143	1.44E-05
59.87	3.37E-05	0.006484	0.002987	0.000339	0.002143	1.44E-05
61.475	3.37E-05	0.006484	0.002987	0.000339	0.002143	1.44E-05
63.13	3.37E-05	0.006484	0.002987	0.000339	0.002143	1.44E-05
64.825	3.37E-05	0.006484	0.002987	0.000339	0.002143	1.44E-05
66.565	3.37E-05	0.006484	0.002987	0.000339	0.002143	1.44E-05
68.355	3.37E-05	0.006484	0.002987	0.000339	0.002143	1.44E-05
70.19	3.37E-05	0.006484	0.002987	0.000339	0.002143	1.44E-05
72.075	3.37E-05	0.006484	0.002987	0.000339	0.002143	1.44E-05
74.01	3.37E-05	0.006484	0.002987	0.000339	0.002143	1.44E-05
76	3.37E-05	0.006484	0.002987	0.000339	0.002143	1.44E-05
78.045	3.37E-05	0.006484	0.002987	0.000339	0.002143	1.44E-05
80.14	3.37E-05	0.006484	0.002987	0.000339	0.002143	1.44E-05
82.29	3.37E-05	0.006484	0.002987	0.000339	0.002143	1.44E-05
84.5	3.37E-05	0.006484	0.002987	0.000339	0.002143	1.44E-05
86.77	3.37E-05	0.006484	0.002987	0.000339	0.002143	1.44E-05
89.105	3.37E-05	0.006484	0.002987	0.000339	0.002143	1.44E-05
91.5	3.37E-05	0.006484	0.002987	0.000339	0.002143	1.44E-05
93.955	3.37E-05	0.006484	0.002987	0.000339	0.002143	1.44E-05
96.48	3.37E-05	0.006484	0.002987	0.000339	0.002143	1.44E-05
99.08	3.37E-05	0.006484	0.002987	0.000339	0.002143	1.44E-05
101.75	3.37E-05	0.006484	0.002987	0.000339	0.002143	1.44E-05
104.5	3.37E-05	0.006484	0.002987	0.000339	0.002143	1.44E-05
107.3	3.37E-05	0.006484	0.002987	0.000339	0.002143	1.44E-05
110.15	3.37E-05	0.006484	0.002987	0.000339	0.002143	1.44E-05
113.1	3.37E-05	0.006484	0.002987	0.000339	0.002143	1.44E-05
116.15	3.37E-05	0.006484	0.002987	0.000339	0.002143	1.44E-05
119.3	3.37E-05	0.006484	0.002987	0.000339	0.002143	1.44E-05
122.5	3.37E-05	0.006484	0.002987	0.000339	0.002143	1.44E-05
125.75	3.37E-05	0.006484	0.002987	0.000339	0.002143	1.44E-05
129.15	3.37E-05	0.006484	0.002987	0.000339	0.002143	1.44E-05
132.65	3.37E-05	0.006484	0.002987	0.000339	0.002143	1.44E-05
136.2	3.37E-05	0.006484	0.002987	0.000339	0.002143	1.44E-05
139.85	3.37E-05	0.006484	0.002987	0.000339	0.002143	1.44E-05
143.6	3.37E-05	0.006484	0.002987	0.000339	0.002143	1.44E-05
147.45	3.37E-05	0.006484	0.002987	0.000339	0.002143	1.44E-05
151.4	3.37E-05	0.006484	0.002987	0.000339	0.002143	1.44E-05
155.45	3.37E-05	0.006484	0.002987	0.000339	0.002143	1.44E-05
159.65	3.37E-05	0.006484	0.002987	0.000339	0.002143	1.44E-05
163.95	3.37E-05	0.006484	0.002987	0.000339	0.002143	1.44E-05
168.35	3.37E-05	0.006484	0.002987	0.000339	0.002143	1.44E-05
172.9	3.37E-05	0.006484	0.002987	0.000339	0.002143	1.44E-05
177.55	3.37E-05	0.006484	0.002987	0.000339	0.002143	1.44E-05
182.3	3.37E-05	0.006484	0.002987	0.000339	0.002143	1.44E-05
187.2	3.37E-05	0.006484	0.002987	0.000339	0.002143	1.44E-05
192.25	3.37E-05	0.006484	0.002987	0.000339	0.002143	1.44E-05
197.4	3.37E-05	0.006484	0.002987	0.000339	0.002143	1.44E-05

## Appendix C: Effect of FPIA mixer speed on kaolinite PSD

Concentration: 20 g/L

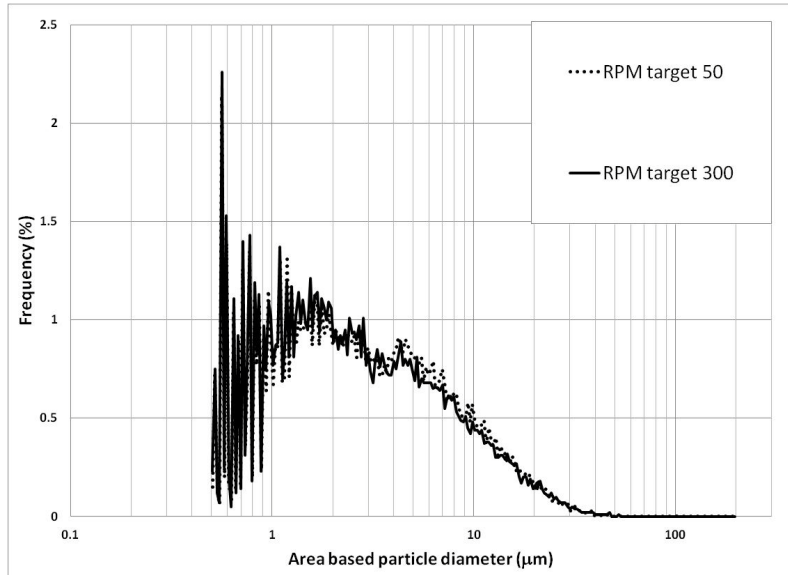


Figure C.1 Effect of FPIA mixer speed on the measured PSD (c=20 g/L, RPM=50, 300)

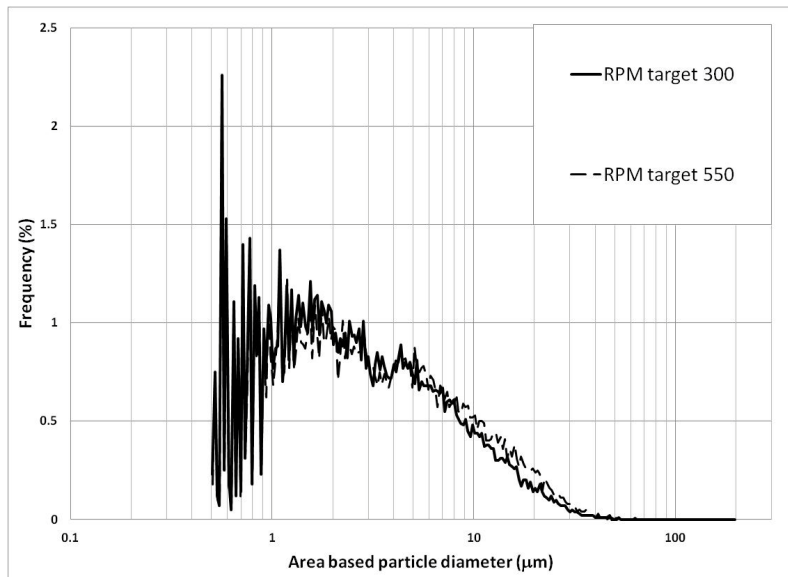


Figure C.2 Effect of FPIA mixer speed on the measured PSD (c=20 g/L, RPM=300, 550)

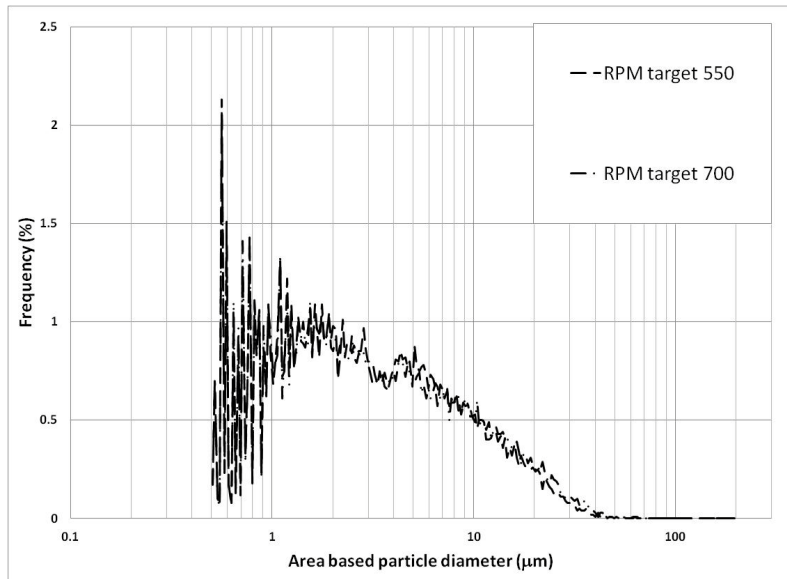


Figure C.3 Effect of FPIA mixer speed on the measured PSD (c=20 g/L RPM=550, 700)

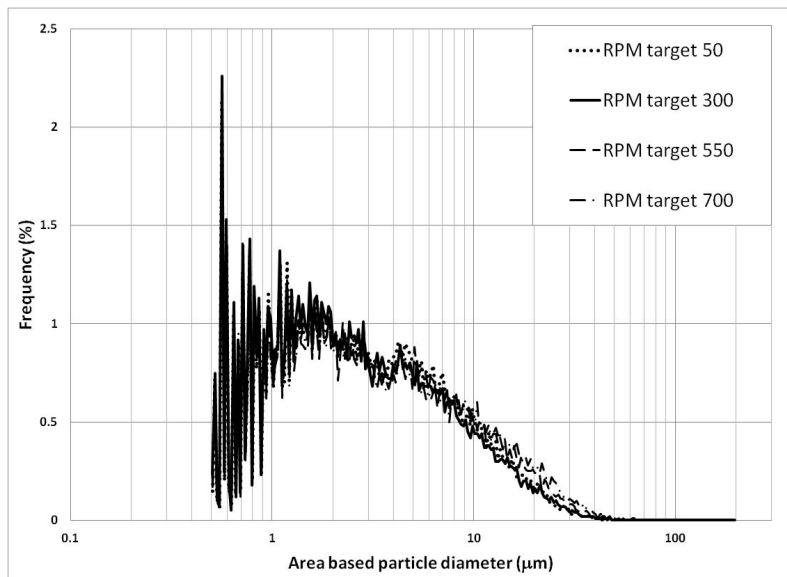


Figure C.4 Effect of FPIA mixer speed on the measured PSD (c=20 g/L RPM=50, 300, 550, 700)

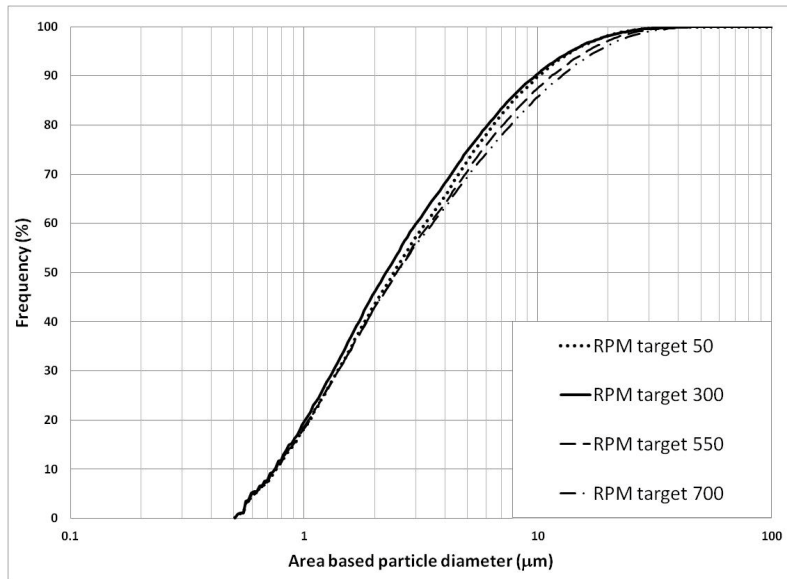


Figure C.5 Effect of RPM target on the cumulative particle size distribution (c=20 g/L)

Concentration: 40 g/L

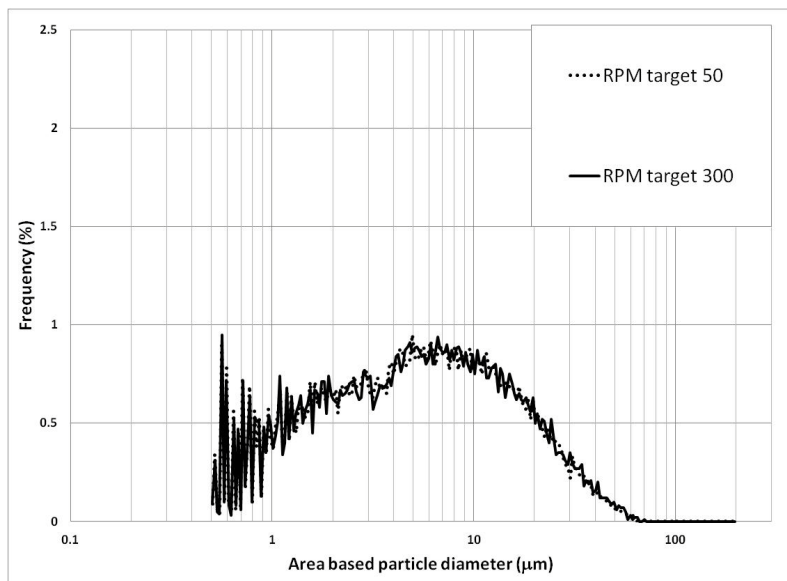


Figure C.6 Effect of FPIA mixer speed on the measured PSD (c=40 g/L, RPM=50, 300)

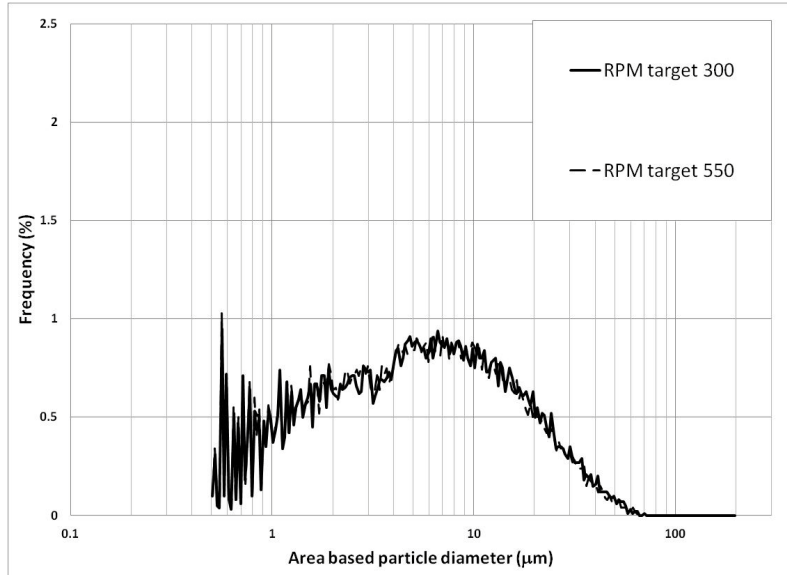


Figure C.7 Effect of FPIA mixer speed on the measured PSD (c=40 g/L, RPM=300, 550)

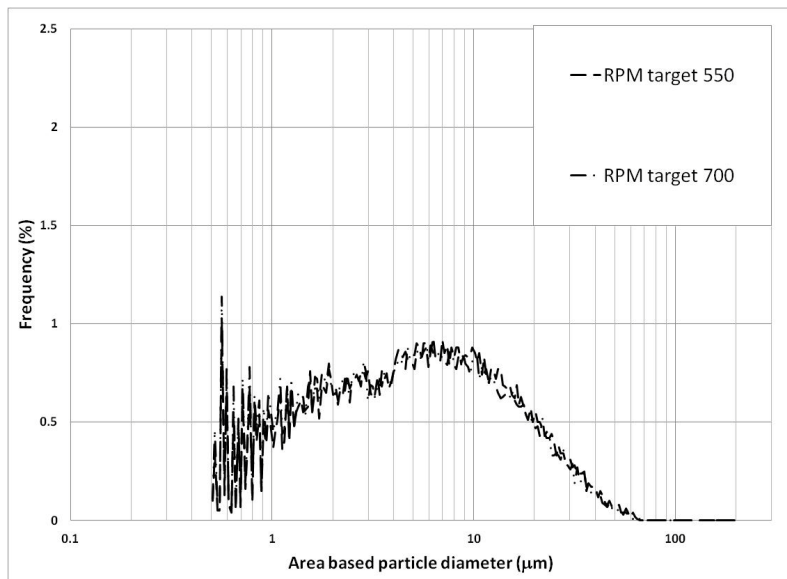


Figure C.8 Effect of FPIA mixer speed on the measured PSD (c=40 g/L RPM=550, 700)

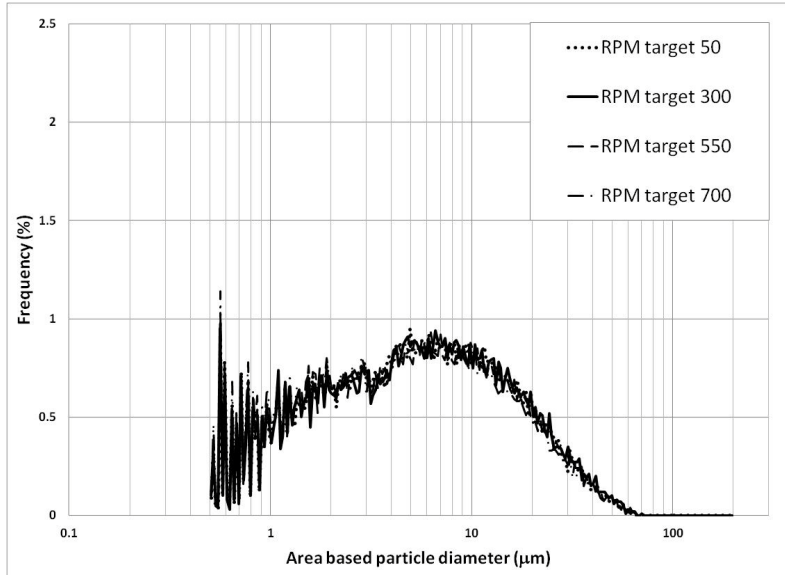


Figure C.9 Effect of FPIA mixer speed on the measured PSD (c=40 g/L RPM=50, 300, 550, 700)

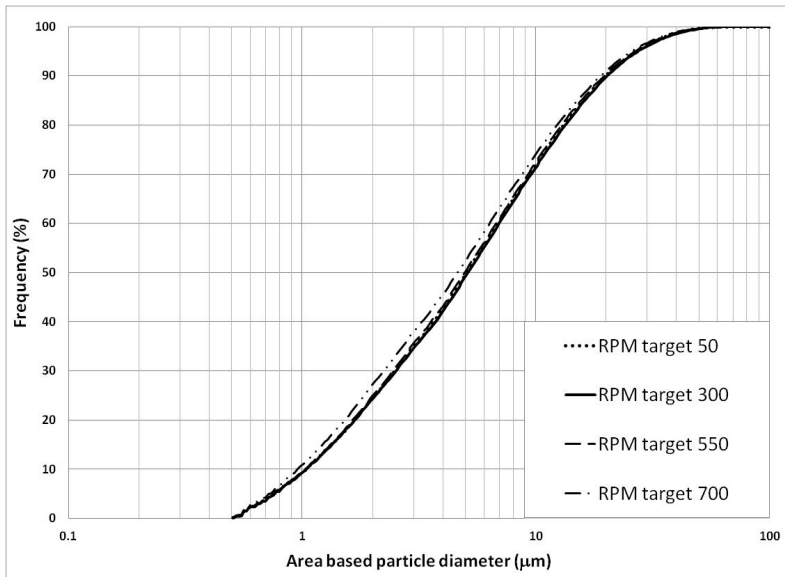


Figure C.10 Effect of RPM target on the cumulative particle size distribution (c=40 g/L)

## Appendix D: Effect of sonication time- Comparison of particle size distributions

Concentration: 40 g/L

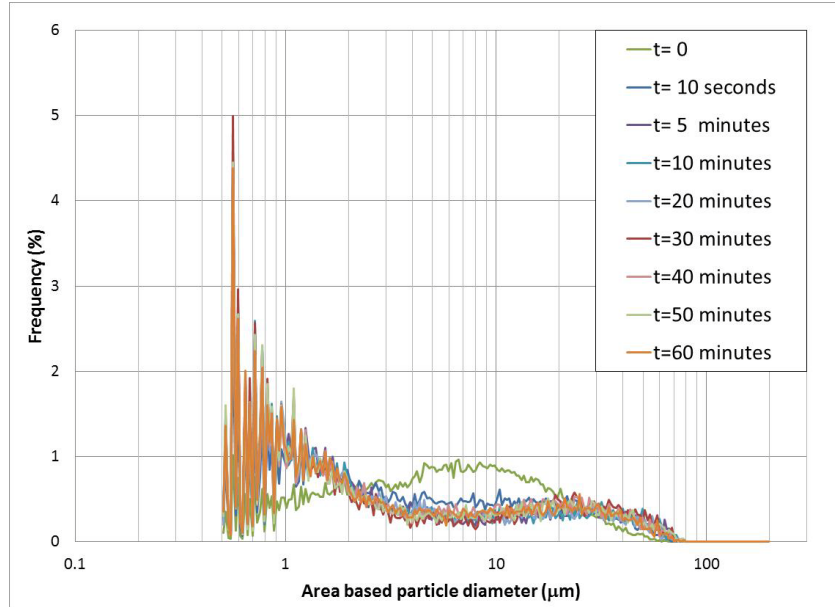


Figure D.1 Effect of sonication time on the kaolinite PSD: c=40 g/L; pH~4.6;  
Sonication amplitude: 75%

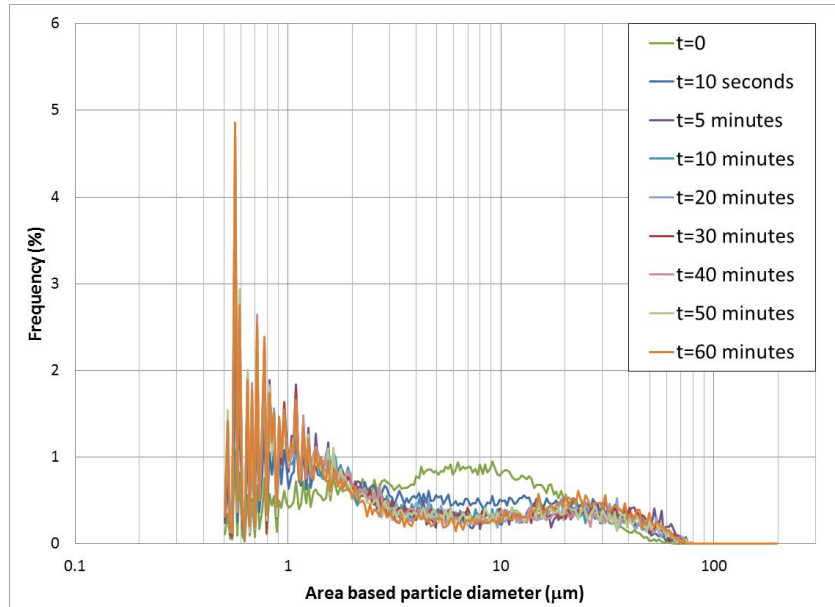
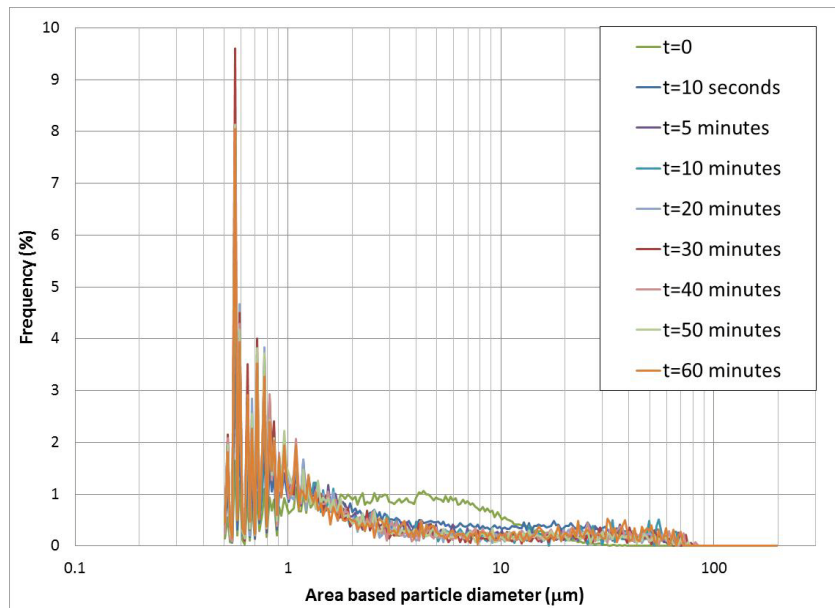
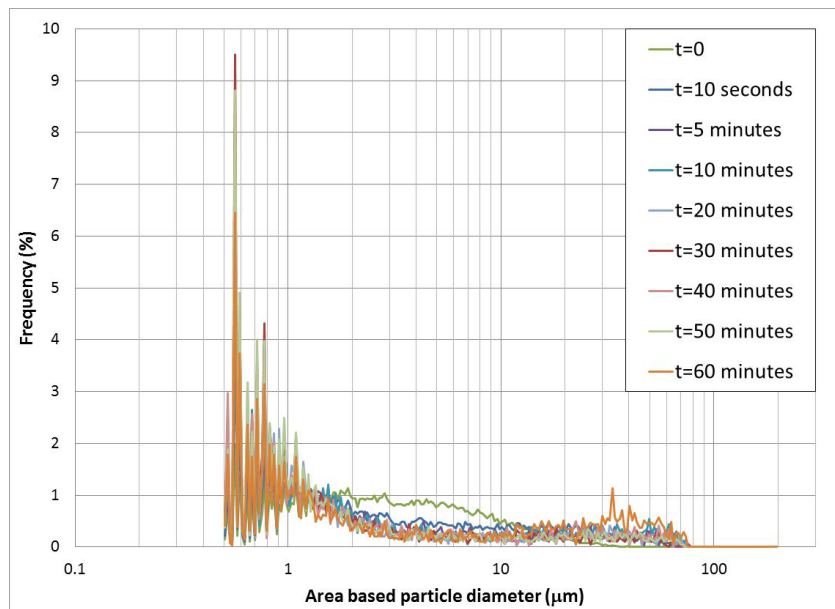


Figure D.2 Effect of sonication time on the kaolinite PSD: c=40 g/L; pH~4.6;  
Sonication amplitude: 50%

Concentration: 20 g/L



**Figure D.3** Effect of sonication time on the kaolinite PSD: c=20 g/L; pH~4.6;  
Sonication amplitude: 75%



**Figure D.4** Effect of sonication time on the kaolinite PSD: c=20 g/L; pH~4.6;  
Sonication amplitude: 50%

Concentration: 10 g/L

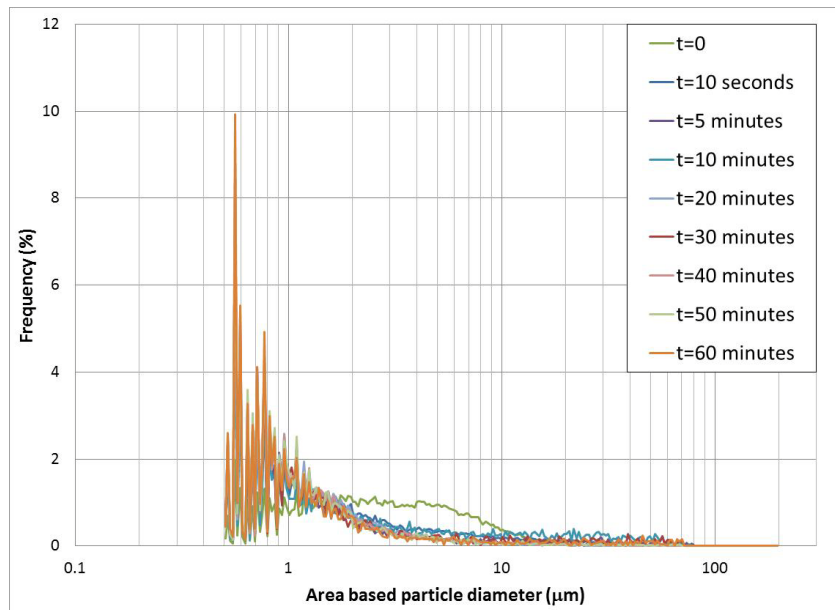


**Figure D.5 Effect of sonication time on the kaolinite PSD: c=10 g/L; pH~4.6; Sonication amplitude: 75%**

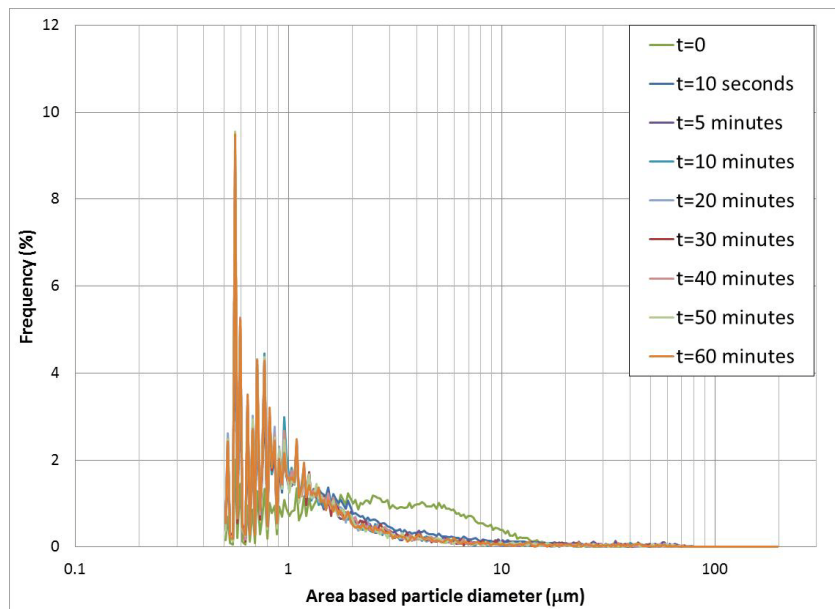


**Figure D.6 Effect of sonication time on the kaolinite PSD: c=10 g/L; pH~4.6; Sonication amplitude: 50%**

## Appendix E: Effect of sonication time- Comparison of populations of primary particles, flocs, and aggregates

Amplitude: 75%

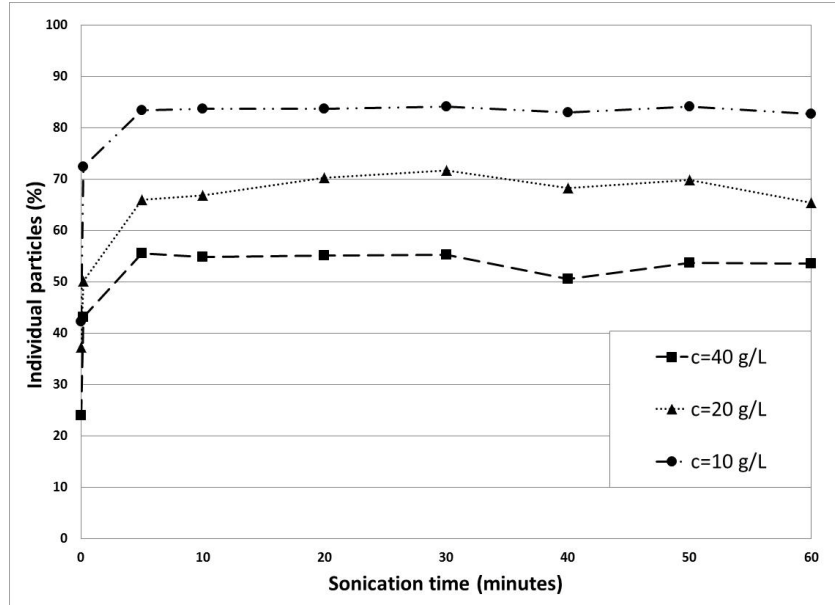


Figure E.1 Proportion of the dispersed phase population of primary particles, expressed in %, as a function of sonication time, for sample concentrations of 10, 20, and 40 g/L.

Sonication amplitude: 75%

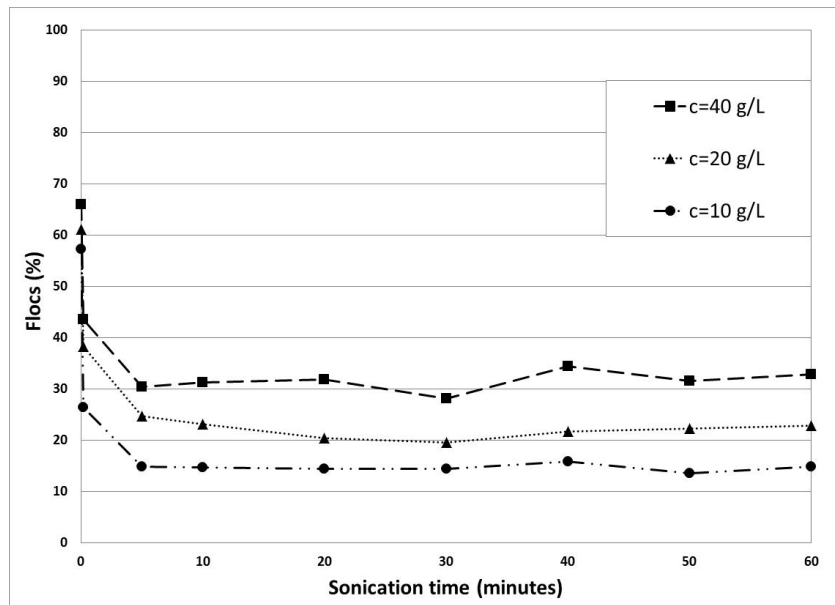


Figure E.2 Proportion of the dispersed phase population of flocs, expressed in %, as a function of sonication time, for sample concentrations of 10, 20, and 40 g/L. Sonication amplitude: 75%

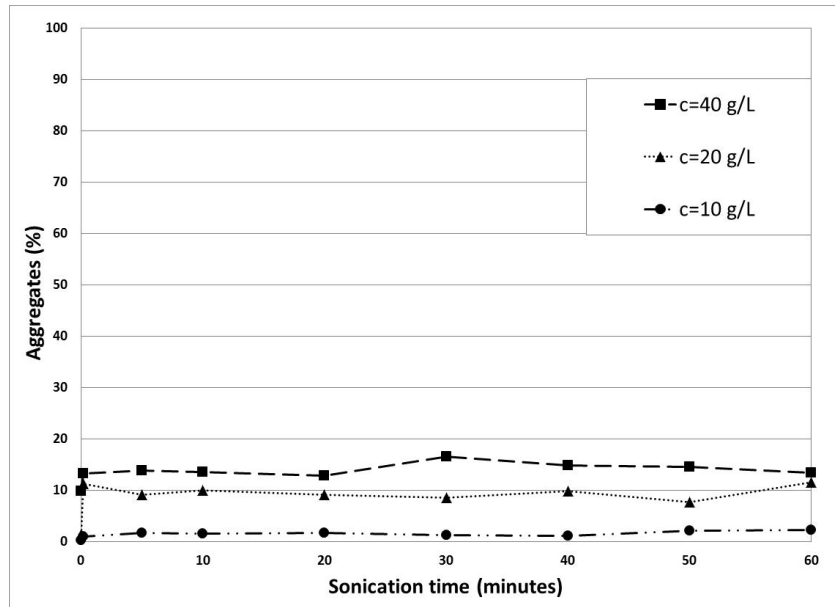


Figure E.3 Proportion of the dispersed phase population of aggregates, expressed in %, as a function of sonication time, for sample concentrations of 10, 20, and 40 g/L. Sonication amplitude: 75%

Amplitude: 50%

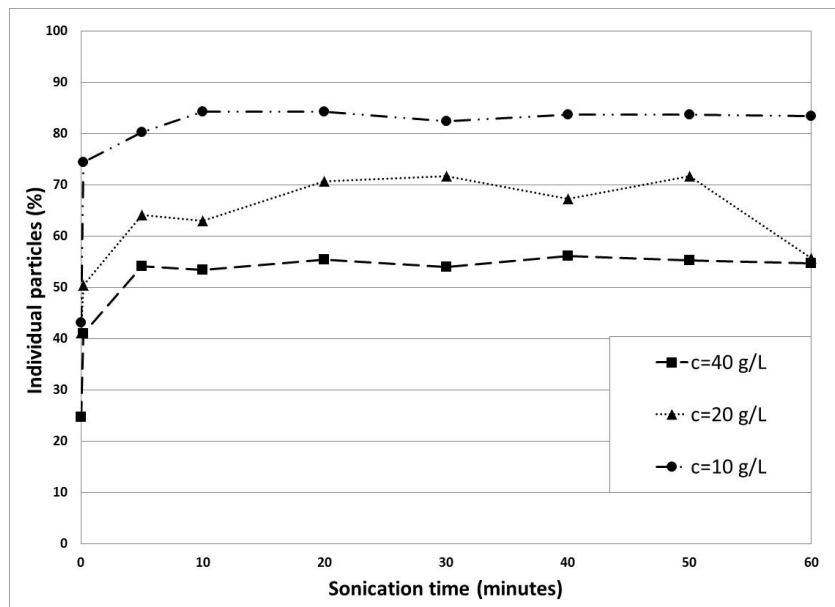
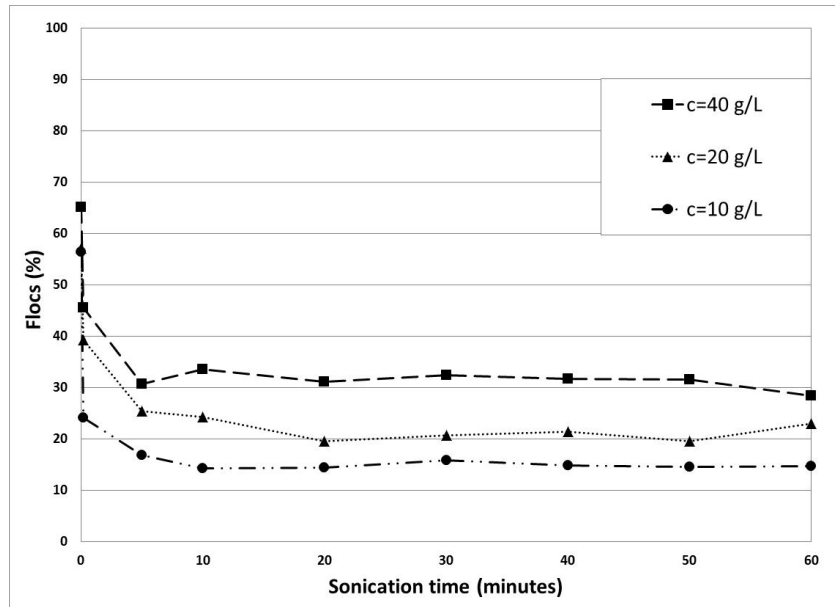
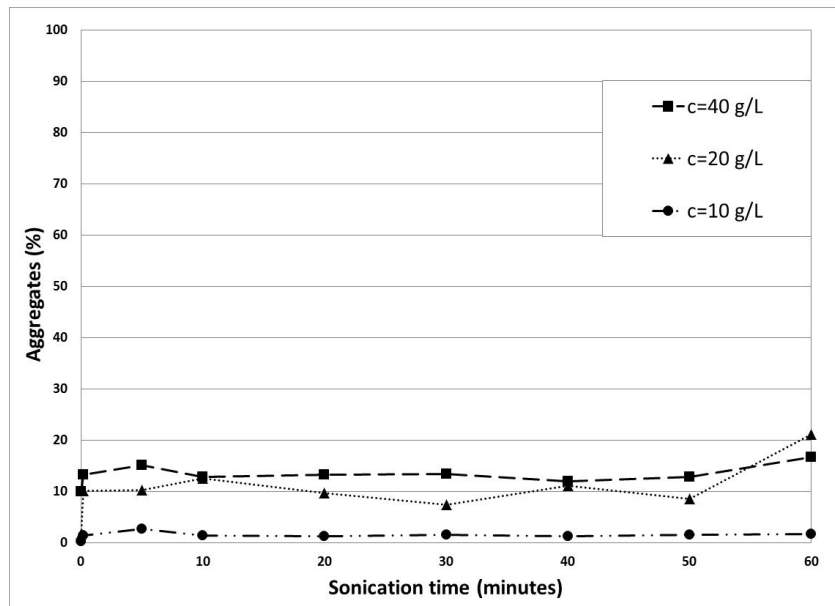


Figure E.4 Proportion of the dispersed phase population of primary particles, expressed in %, as a function of sonication time, for sample concentrations of 10, 20, and 40 g/L. Sonication amplitude: 50%



**Figure E.5** Proportion of the dispersed phase population of flocs, expressed in %, as a function of sonication time, for sample concentrations of 10, 20, and 40 g/L. Sonication amplitude: 50%



**Figure E.6** Proportion of the dispersed phase population of aggregates, expressed in %, as a function of sonication time, for sample concentrations of 10, 20, and 40 g/L. Sonication amplitude: 50%

## Appendix F: Effect of sonication time- Evaluation of the Floc Reduction Ratio (FRR)

Amplitude: 75%

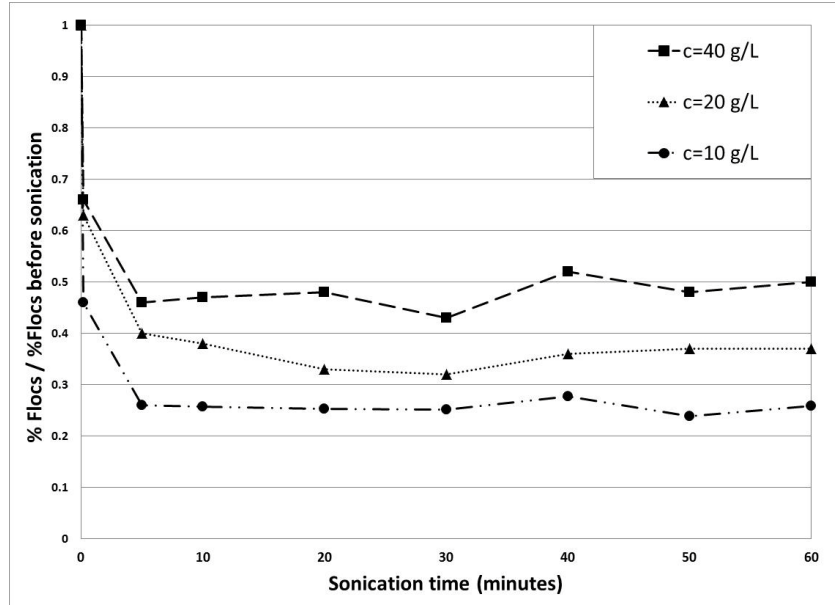


Figure F.1 Floc reduction ratio (FRR) at each sonication time: c=10, 20, and 40 g/L; Sonication amplitude: 75%

Amplitude: 50%

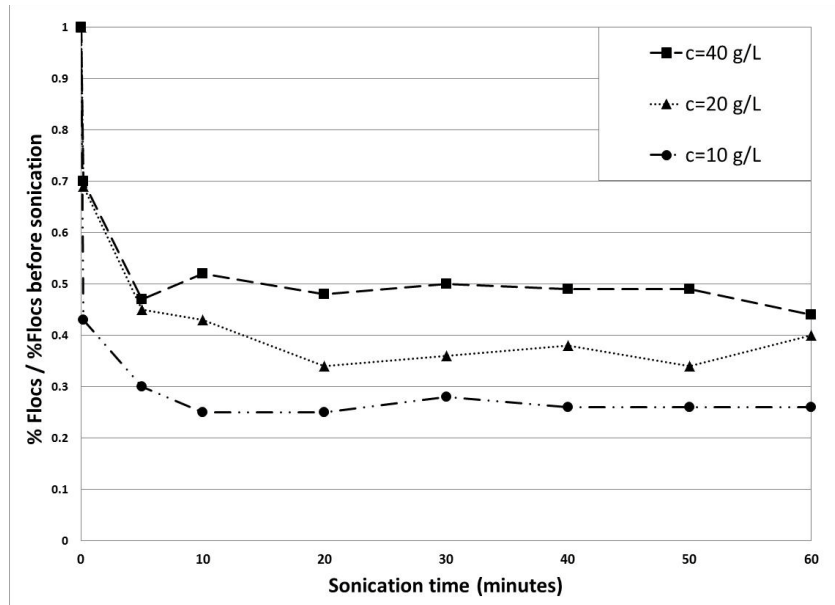


Figure F.2 Floc reduction ratio (FRR) at each sonication time: c=10, 20, and 40 g/L; Sonication amplitude: 50%

## Appendix G: Laser diffraction method

Concentration: 40 g/L

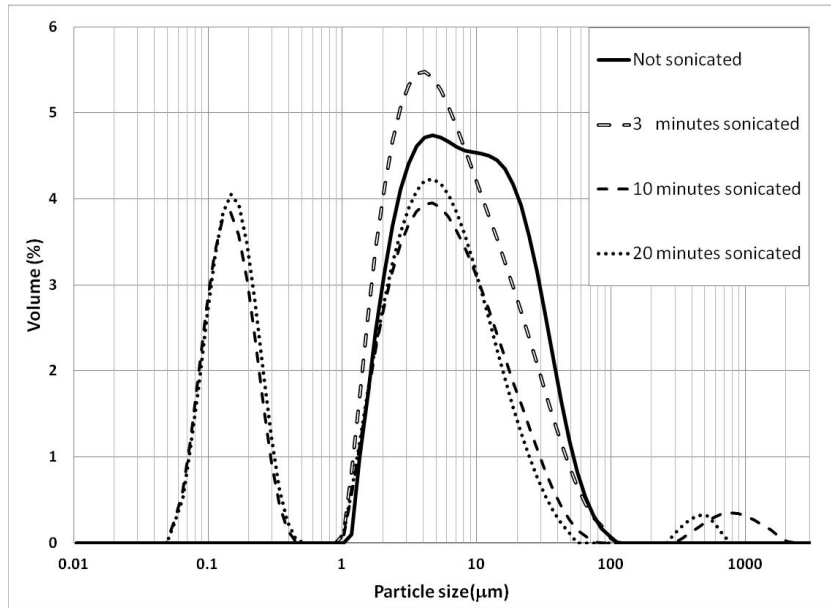


Figure G.1 Kaolinite PSD after different sonication times measured by Malvern Mastersizer  
c=40 g/L, Sonication times: 0, 3, 10, and 20 minutes, Sonication amplitude: 100%

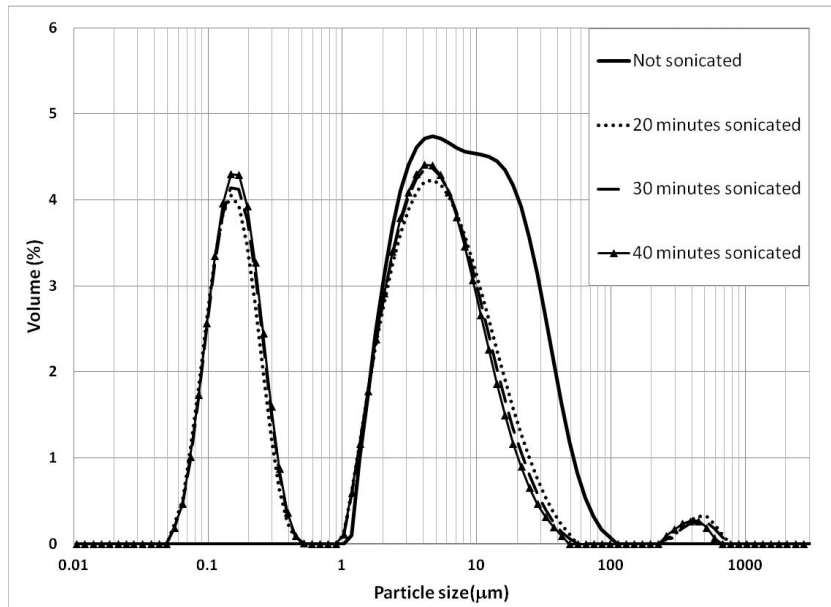
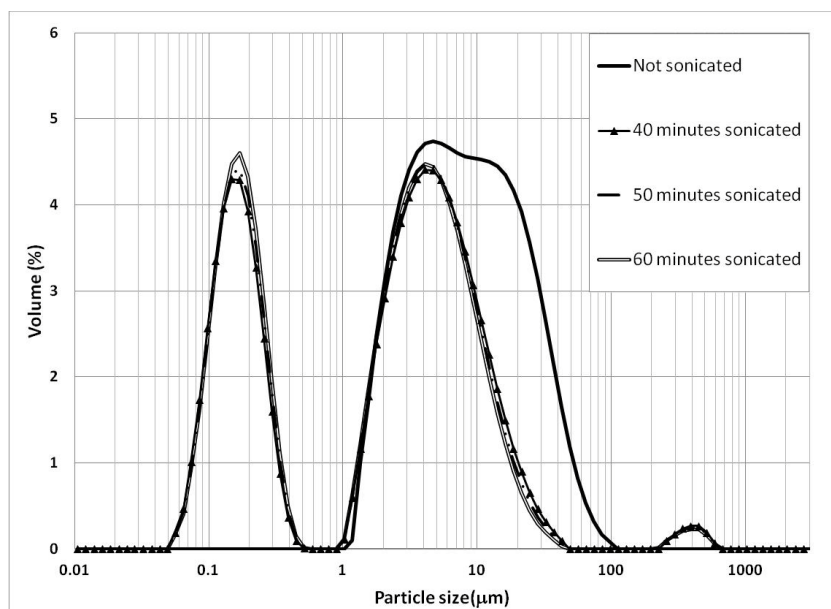
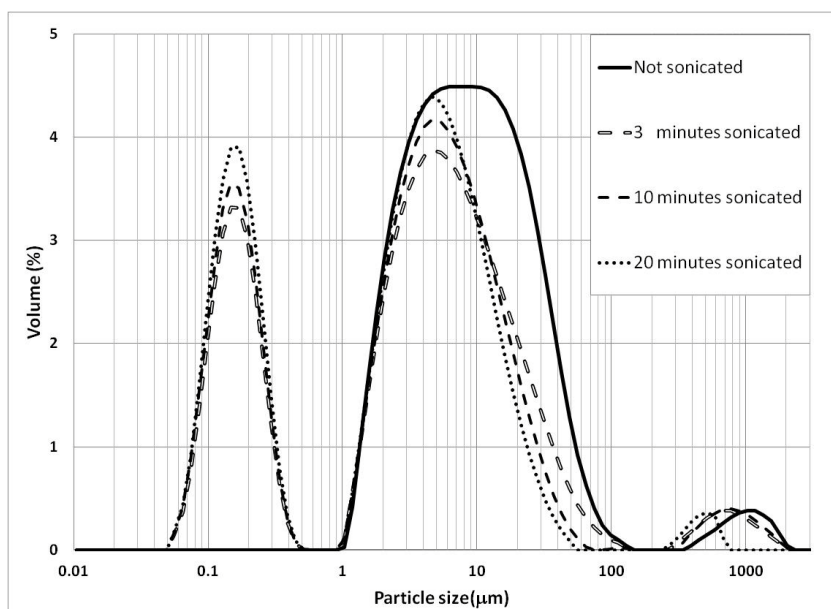


Figure G.2 Kaolinite PSD after different sonication times measured by Malvern Mastersizer  
c=40 g/L, Sonication times: 0, 20, 30, and 40 minutes, Sonication amplitude: 100%



**Figure G.3 Kaolinite PSD after different sonication times measured by Malvern Mastersizer**  
**c=40 g/L, Sonication times: 0, 40, 50, and 60 minutes, Sonication amplitude: 100%**

Concentration: 10 g/L



**Figure G.4 Kaolinite PSD after different sonication times measured by Malvern Mastersizer**  
**c=10 g/L, Sonication times: 0, 3, 10, and 20 minutes, Sonication amplitude: 100%**

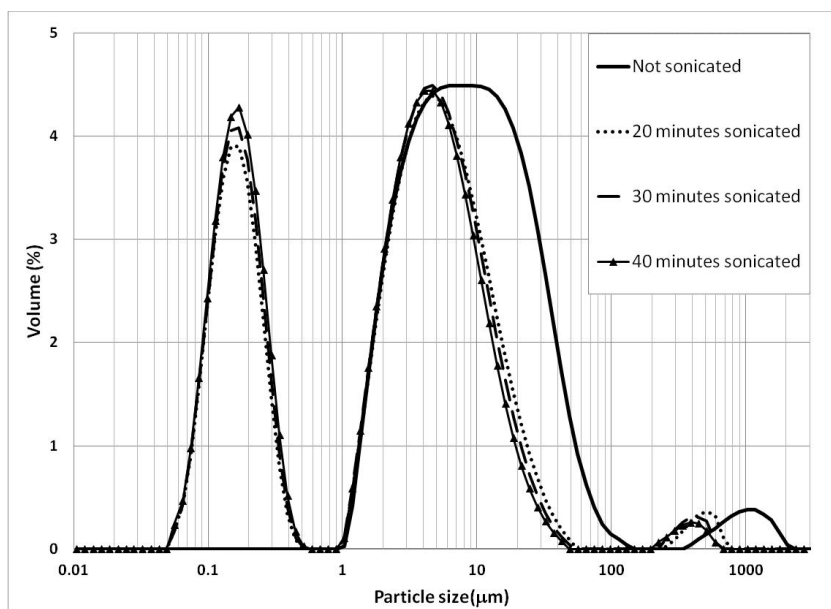


**Figure G.5 Kaolinite PSD after different sonication times measured by Malvern Mastersizer**  
**c=10 g/L, Sonication times: 0, 20, 30, and 40 minutes, Sonication amplitude: 100%**

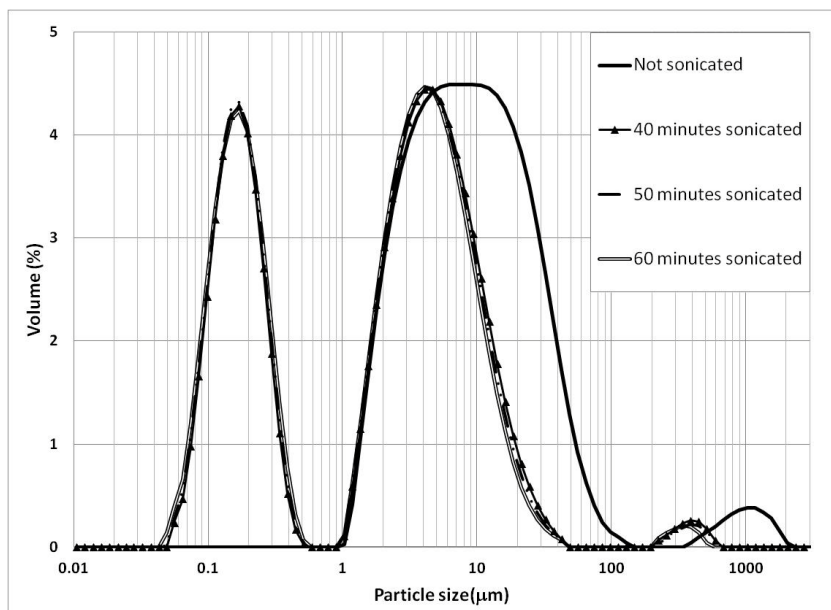


**Figure G.6 Kaolinite PSD after different sonication times measured by Malvern Mastersizer**  
**c=10 g/L, Sonication times: 0, 40, 50, and 60 minutes, Sonication amplitude: 100%**

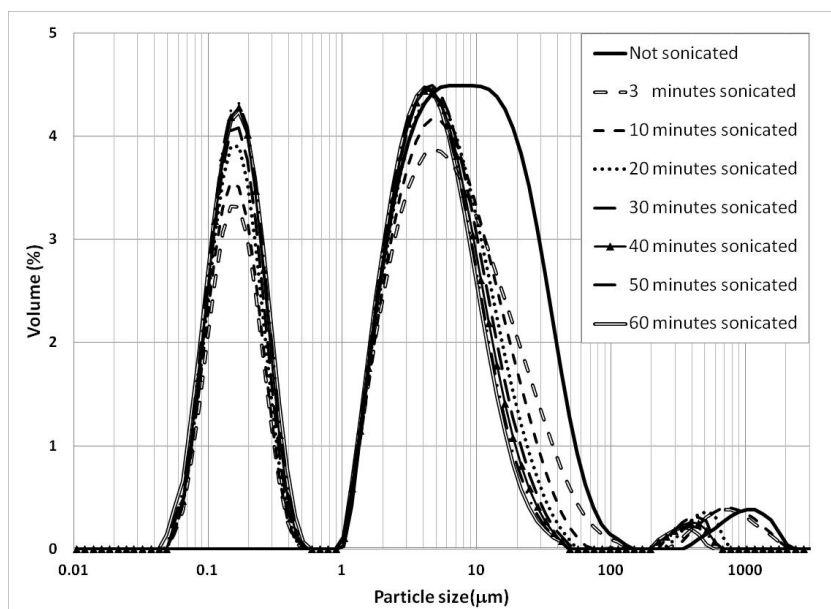


Figure G.7 Kaolinite PSD after different sonication times measured by Malvern Mastersizer;  $c=10$  g/L; Sonication times: 0, 3, 10, 20, 30, 40, 50, and 60 minutes; Amplitude: 100%

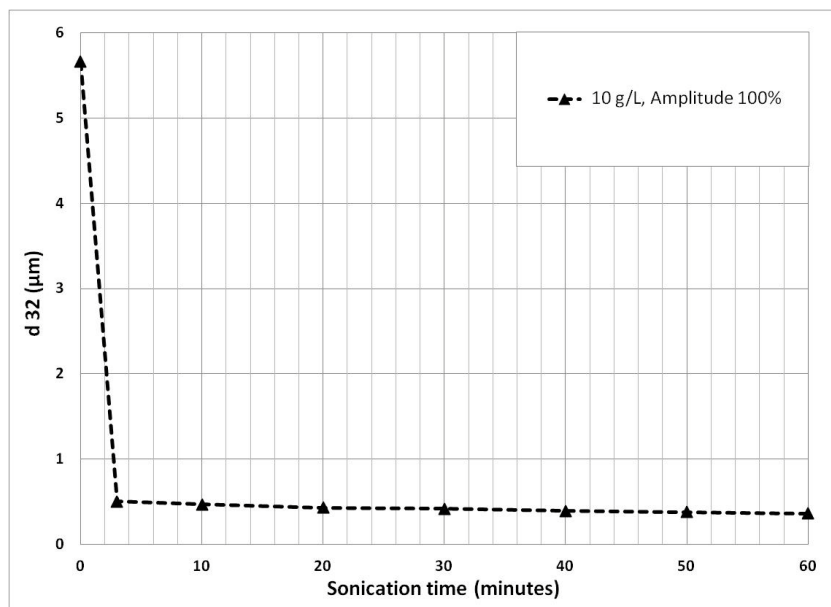


Figure G.8 Sauter mean diameter ( $d_{32}$ ) of kaolinite sample at different sonication times measured by Malvern Mastersizer software;  $c=10$  g/L; Amplitude: 100%

## Appendix H: Cryogenic SEM studies

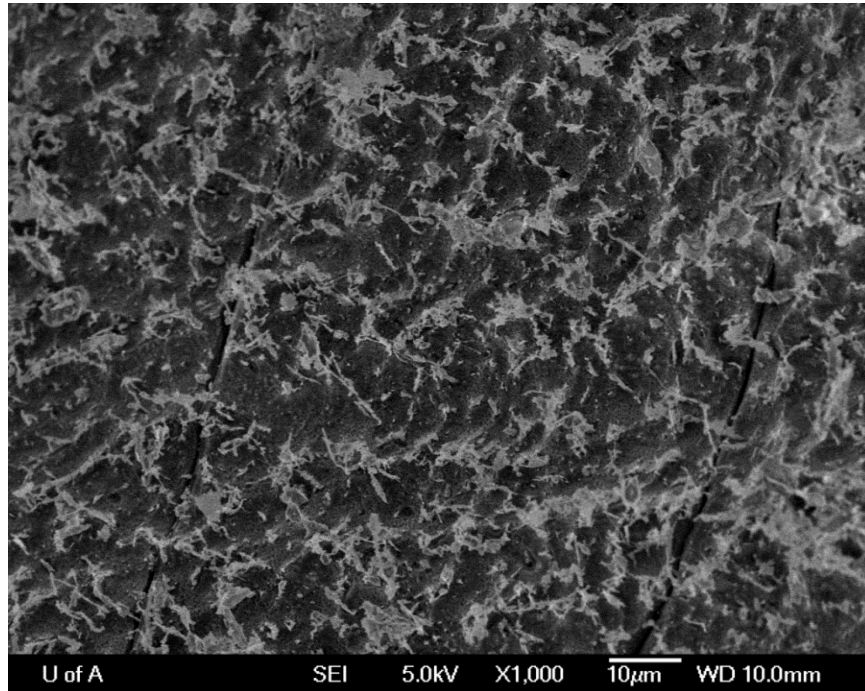


Figure H.1 Cryo-SEM image of non-sonicated kaolinite sample; sample (2-1);  $c=10$  g/L, 1000X

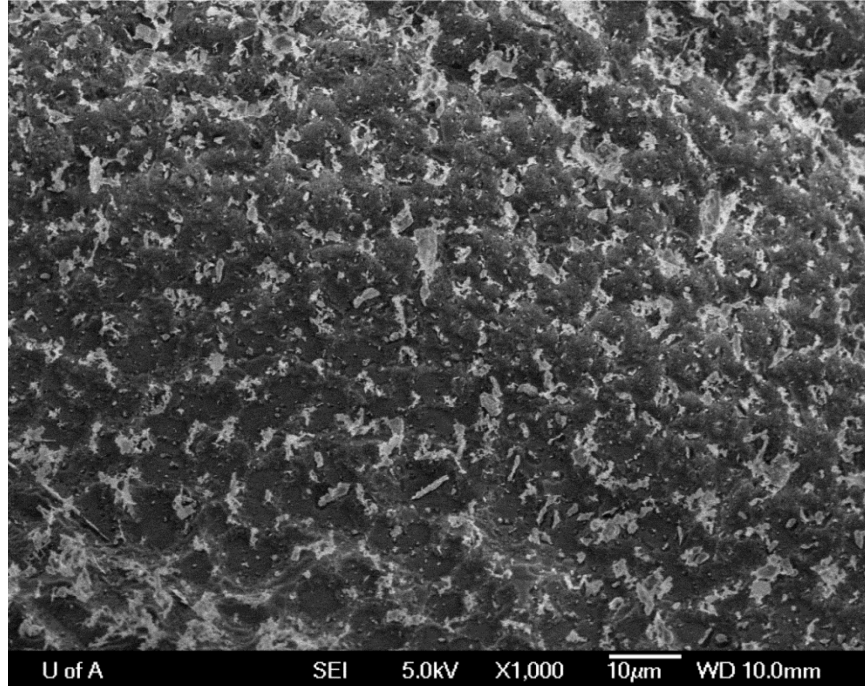
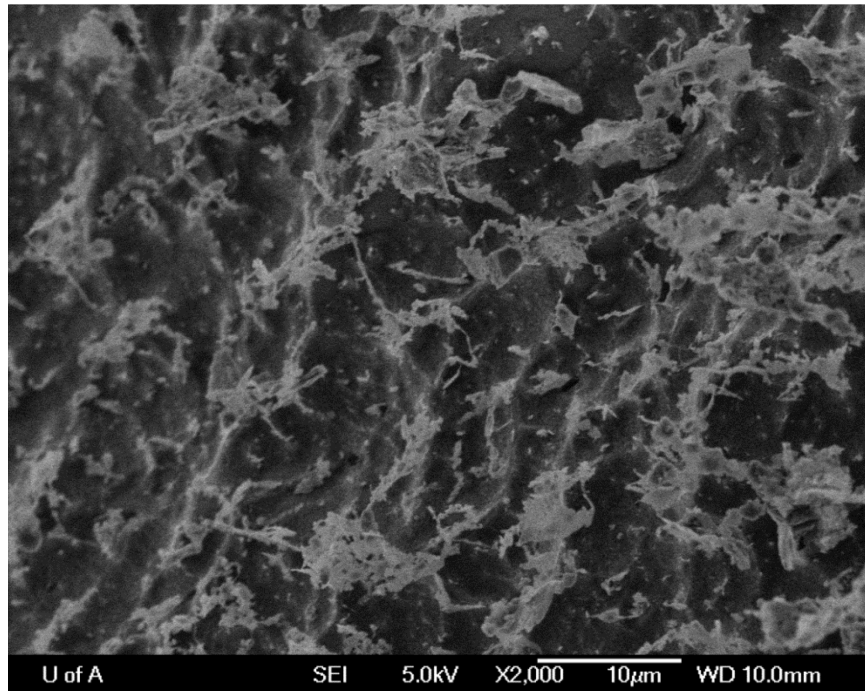
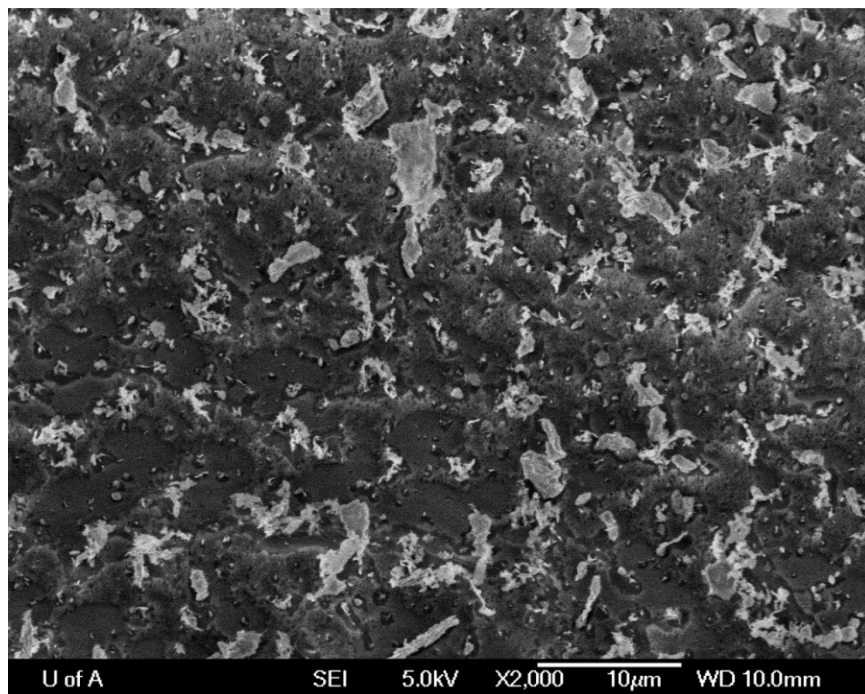


Figure H.2 Cryo-SEM image of sonicated kaolinite sample; sample (2-2);  $c=10$  g/L; 1000X; sonication time: 30 minutes; amplitude: 100%



**Figure H.3** Cryo-SEM image of non-sonicated kaolinite sample; sample (2-1); c=10 g/L, 2000X



**Figure H.4** Cryo-SEM image of sonicated kaolinite sample; sample (2-2); c=10 g/L; 2000X; sonication time: 30 minutes; amplitude: 100%

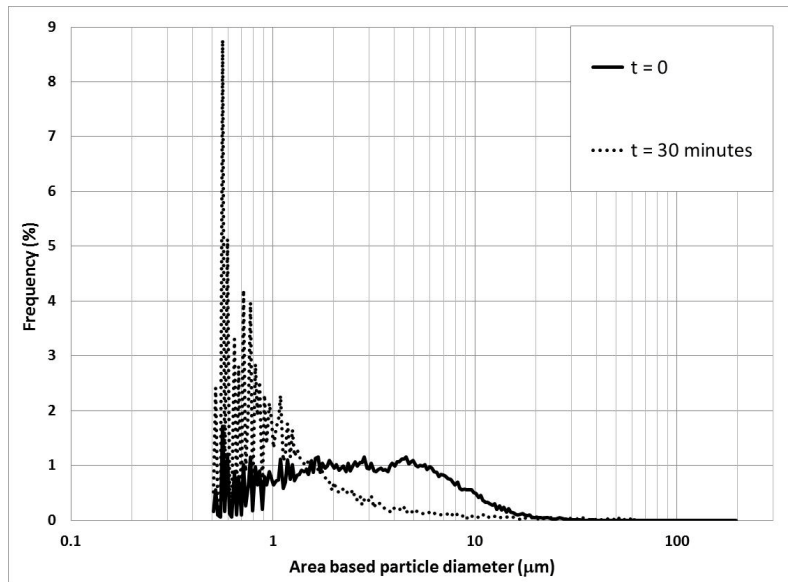


**Figure H.5 Sample PSD measured by FPIA; Sample (2-1) and (2-2); c=10 g/L; Sonication time: 30 minutes; amplitude: 100%**

## Appendix I: Effect of sonication amplitude on the kaolinite PSD

Concentration: 40 g/L

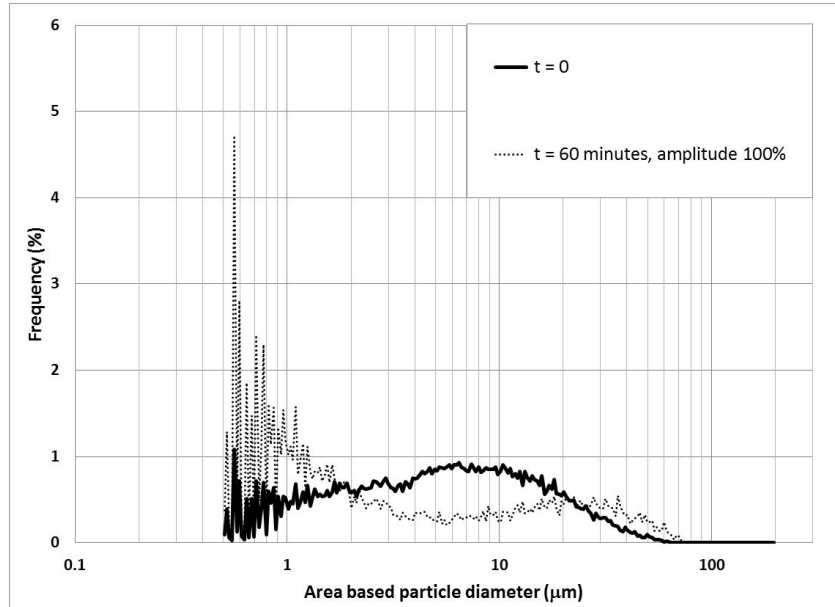


Figure I.1 Effect of sonication amplitude on the kaolinite PSD: c=40 g/L, Amplitude: 100%

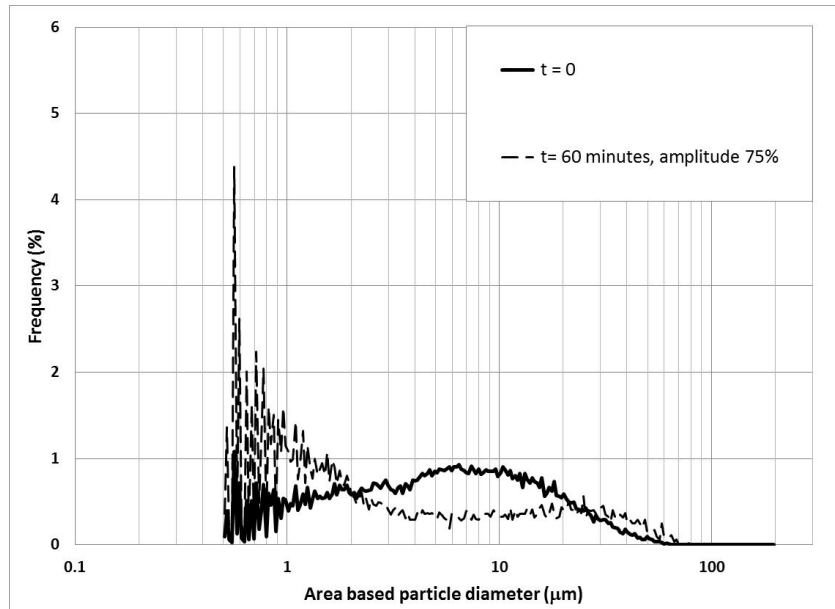


Figure I.2 Effect of sonication amplitude on the kaolinite PSD: c=40 g/L, Amplitude: 75%

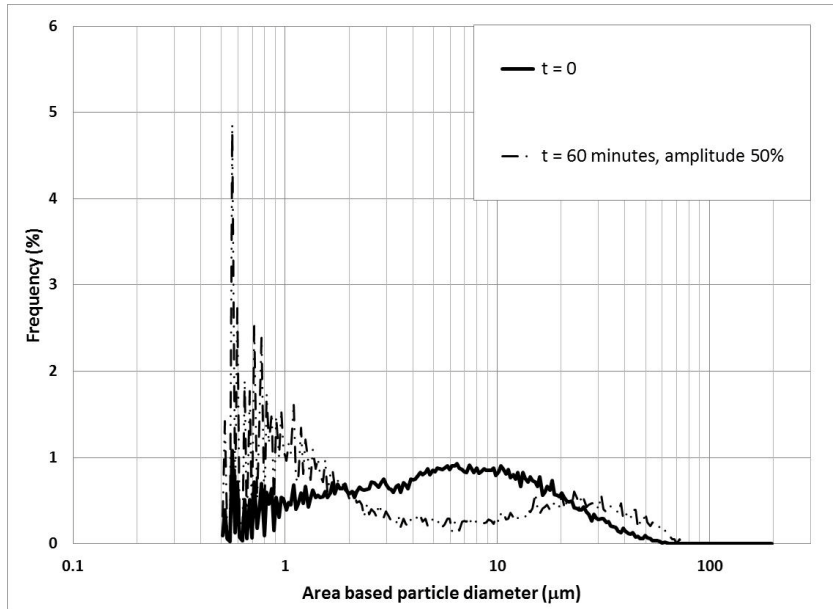


Figure I.3 Effect of sonication amplitude on the kaolinite PSD:  $c=40$  g/L, Amplitude: 50%

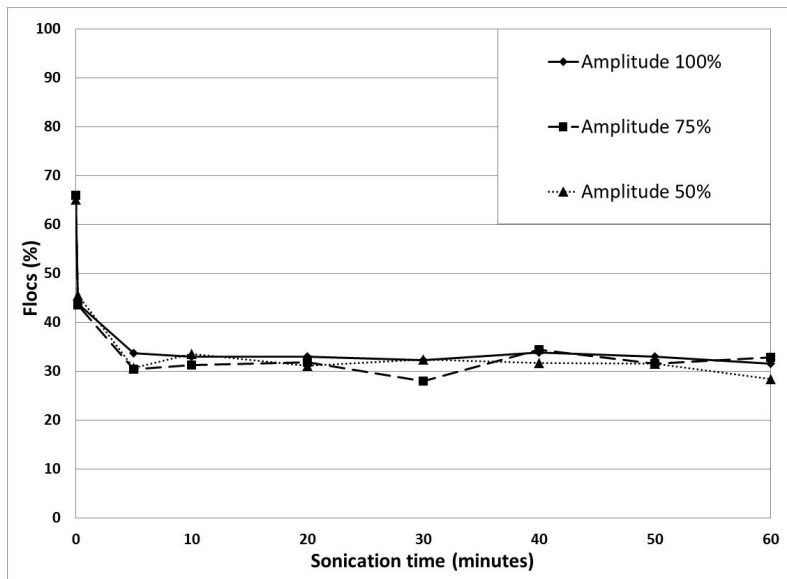


Figure I.4 Effect of sonication amplitude on the percentage of the proportion of the dispersed phase population of flocs, expressed in %, as a function of sonication time,  $c=40$  g/L sonication amplitudes: 50%, 75%, 100%

Concentration: 20 g/L

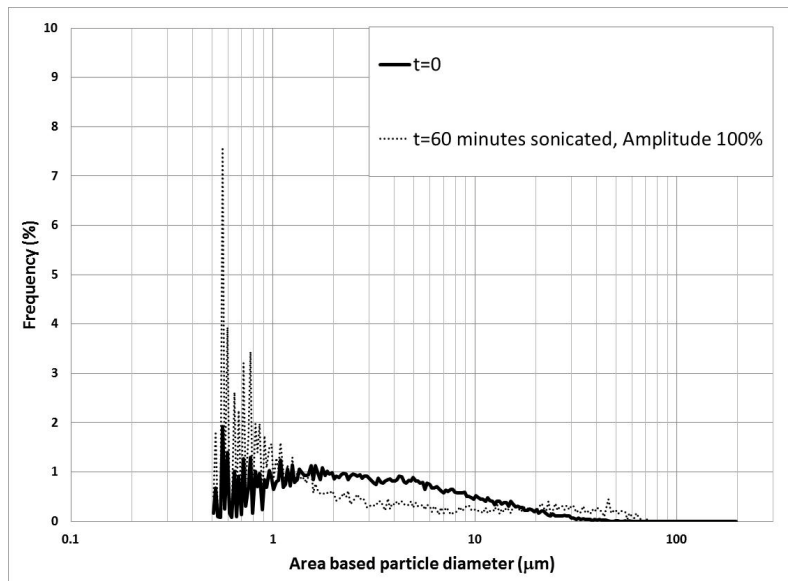


Figure I.5 Effect of sonication amplitude on the kaolinite PSD: c=20 g/L, Amplitude: 100%

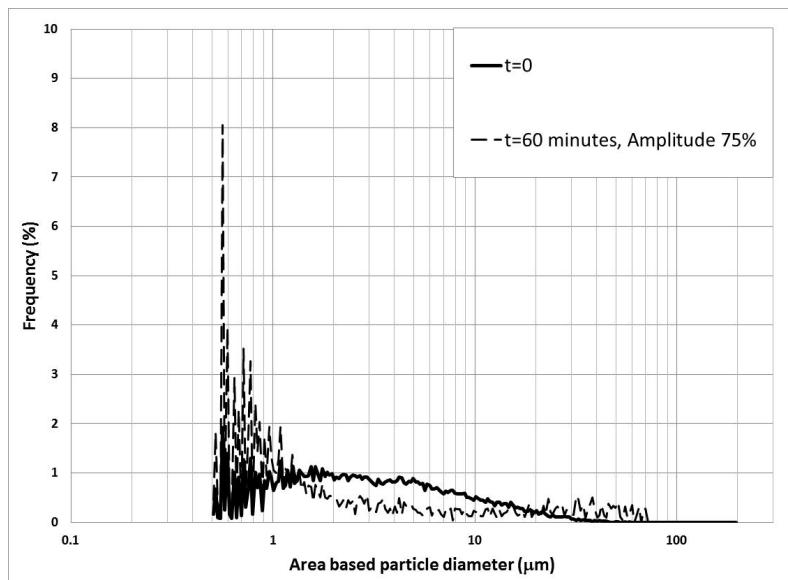


Figure I.6 Effect of sonication amplitude on the kaolinite PSD: c=20 g/L, Amplitude: 75%

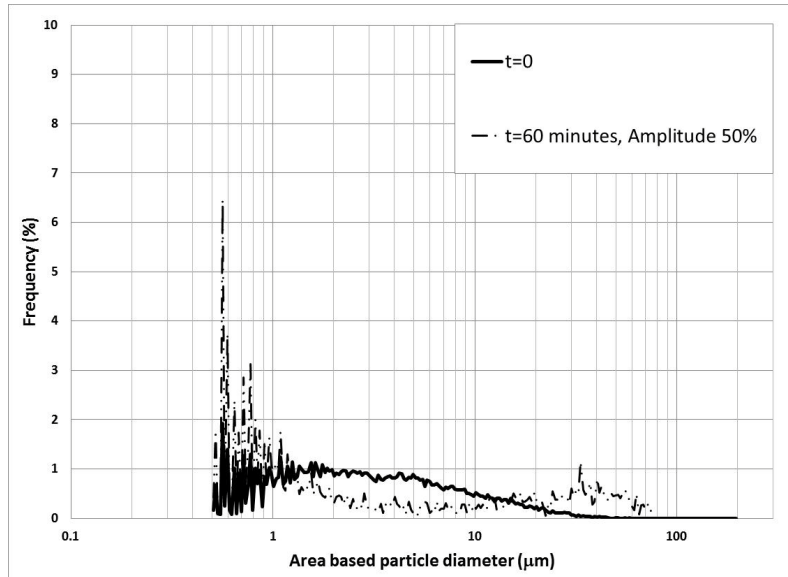


Figure I.7 Effect of sonication amplitude on the kaolinite PSD:  $c=20$  g/L, Amplitude: 50%

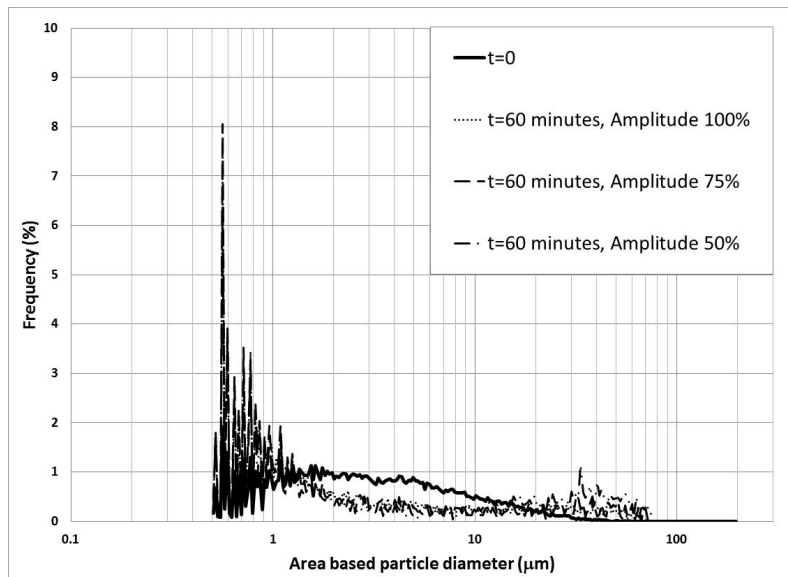


Figure I.8 Effect of sonication amplitude on the kaolinite PSD:  $c=20$  g/L, Amplitude: 50%, 75%, and 100%

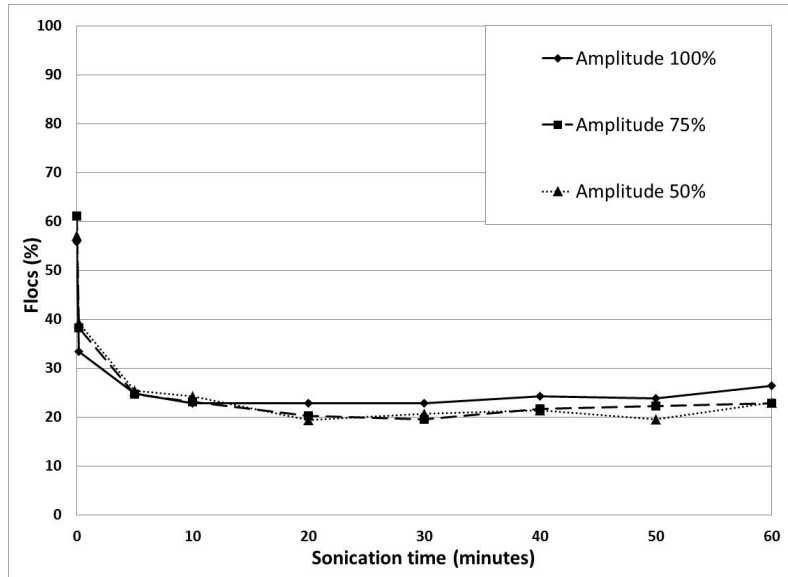


Figure I.9 Effect of sonication amplitude on the percentage of the proportion of the dispersed phase population of flocs, expressed in %, as a function of sonication time,  $c=20$  g/L sonication amplitudes: 50%, 75%, 100%

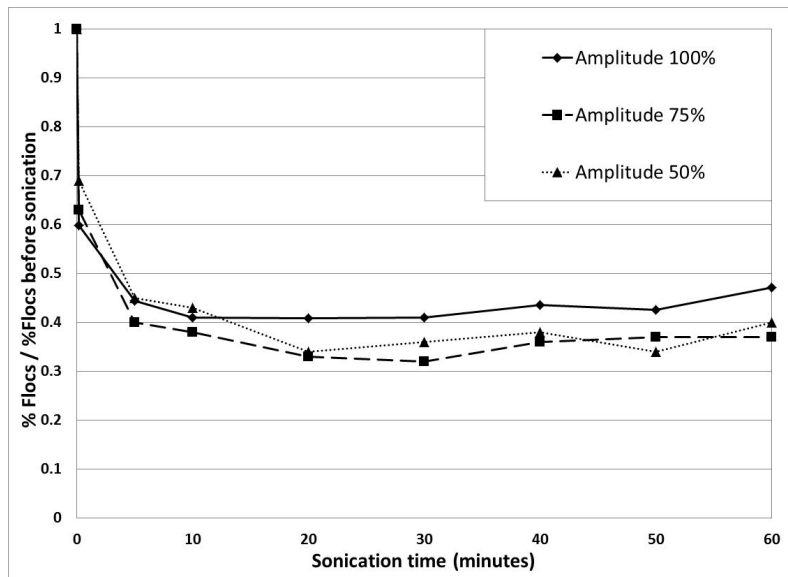


Figure I.10 Effect of sonication amplitude on the floc reduction ratio (FRR):  $c=20$  g/L

Concentration: 10 g/L

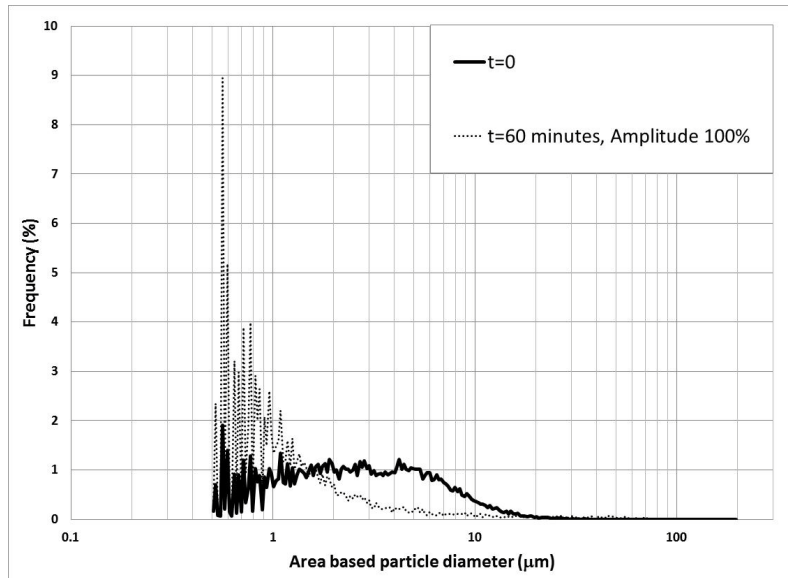


Figure I.11 Effect of sonication amplitude on the kaolinite PSD: c=10 g/L, Amplitude: 100%

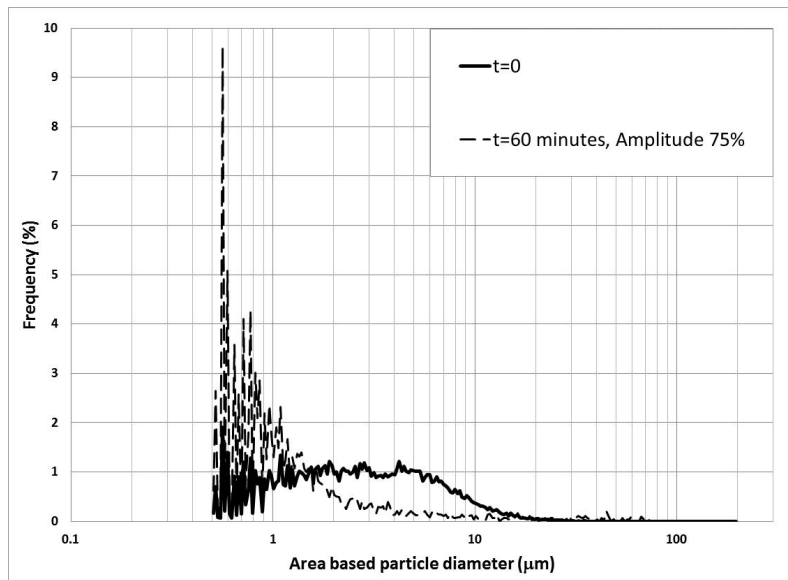
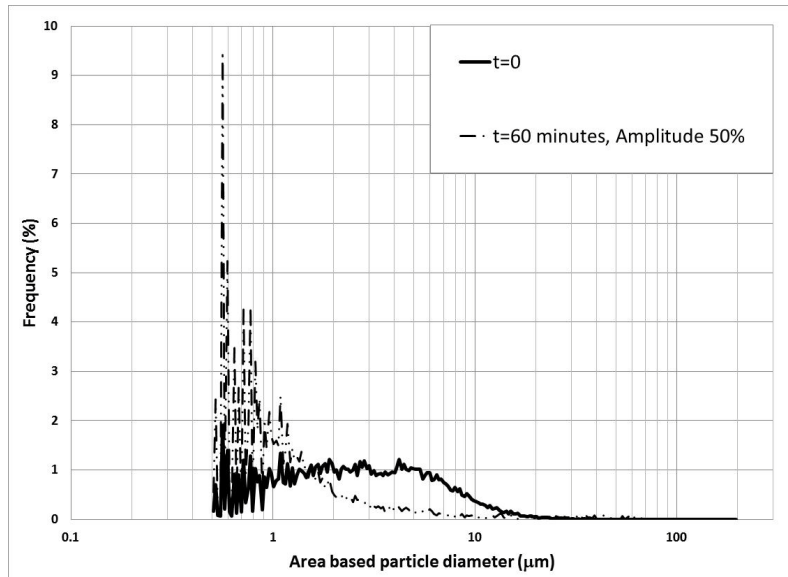
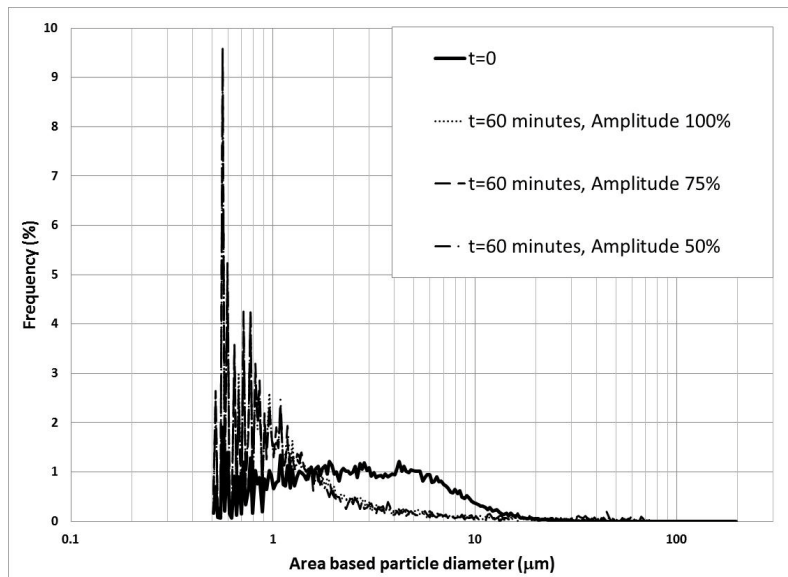


Figure I.12 Effect of sonication amplitude on the kaolinite PSD: c=10 g/L, Amplitude: 75%



**Figure I.13 Effect of sonication amplitude on the kaolinite PSD: c=10 g/L, Amplitude: 50%**



**Figure I.14 Effect of sonication amplitude on the kaolinite PSD: c=10 g/L, Amplitude: 50%, 75%, and 100%**

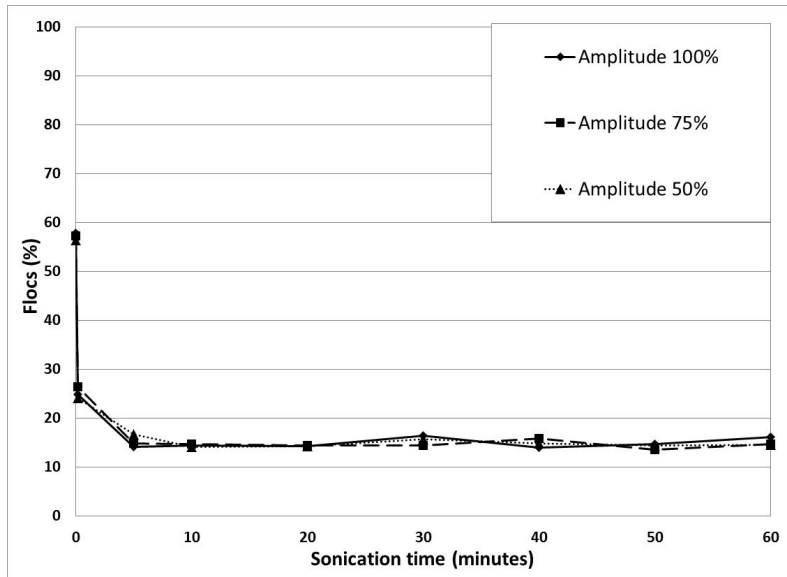


Figure I.15 Effect of sonication amplitude on the percentage of the proportion of the dispersed phase population of flocs, expressed in %, as a function of sonication time,  $c=10$  g/L sonication amplitudes: 50%, 75%, 100%

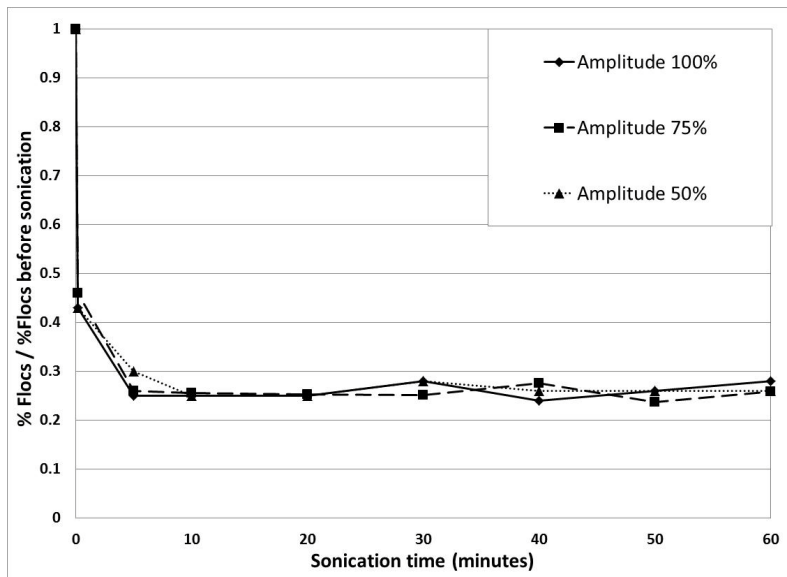
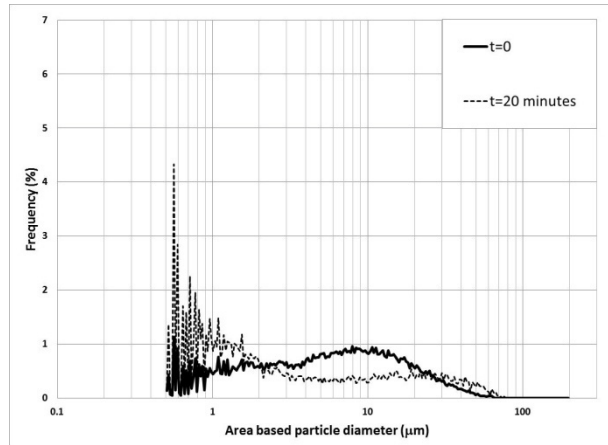
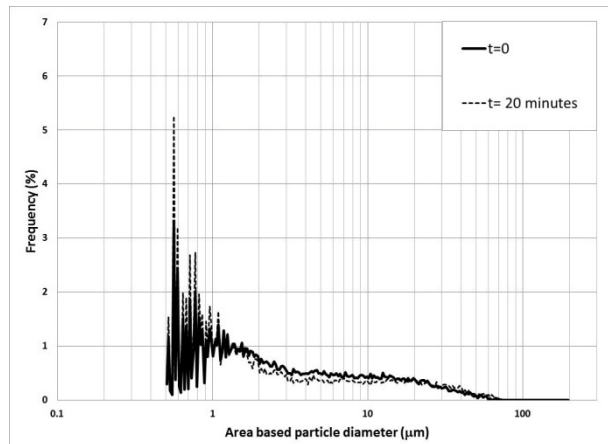


Figure I.16 Effect of sonication amplitude on the floc reduction ratio (FRR):  $c=10$  g/L

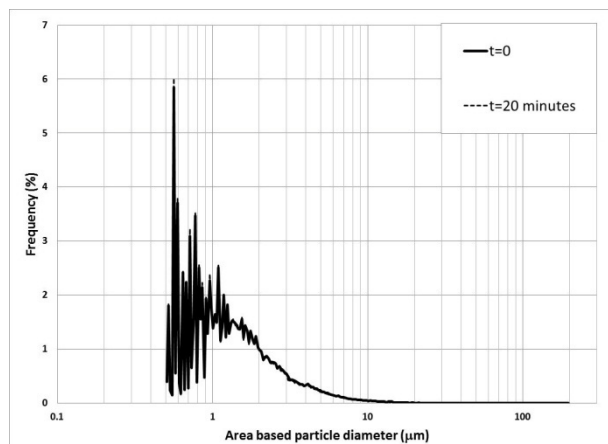
## Appendix J: Case study I: effect of sample pH



(a)

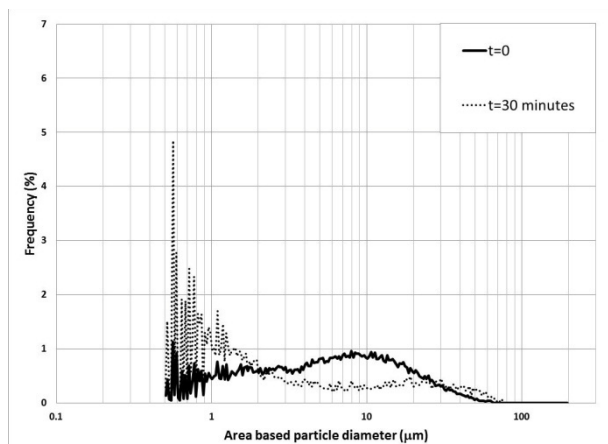


(b)

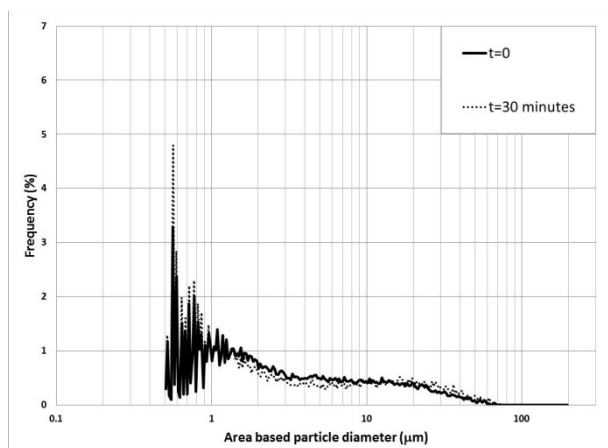


(c)

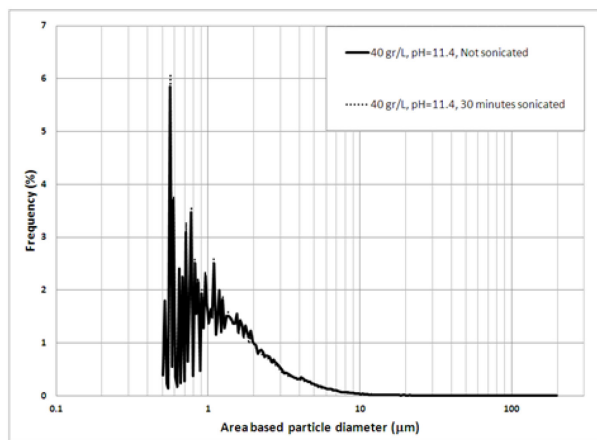
Figure J.1 (a)-(c) Influence of pH on the sonication effect ( $t=20$  minutes,  $c=40$  g/L);  
(a) pH=4.6; (b): pH=8.2; (c):pH=11.4; Sonication amplitude: 100%



(a)



(b)



(c)

**Figure J.2 (a)-(c) Influence of pH on the sonication effect (t=30 minutes, c= 40 g/L);  
 (a) pH=4.6; (b): pH=8.2; (c):pH=11.4; Sonication amplitude: 100%**

## Appendix K: Case study II: effect of flocculant addition

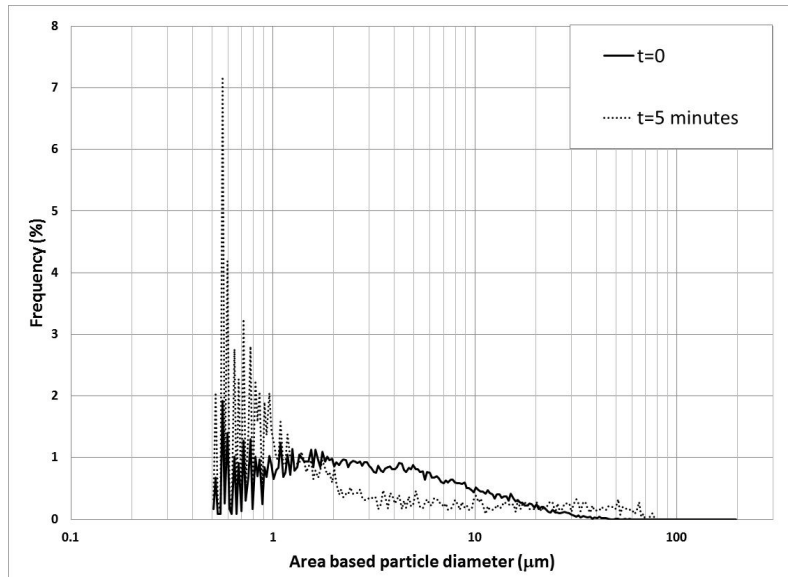


Figure K.1 Effect of sonication on the non-flocculated kaolinite sample:  $c=20$  g/L; sonication time: 5 minutes; amplitude: 100%

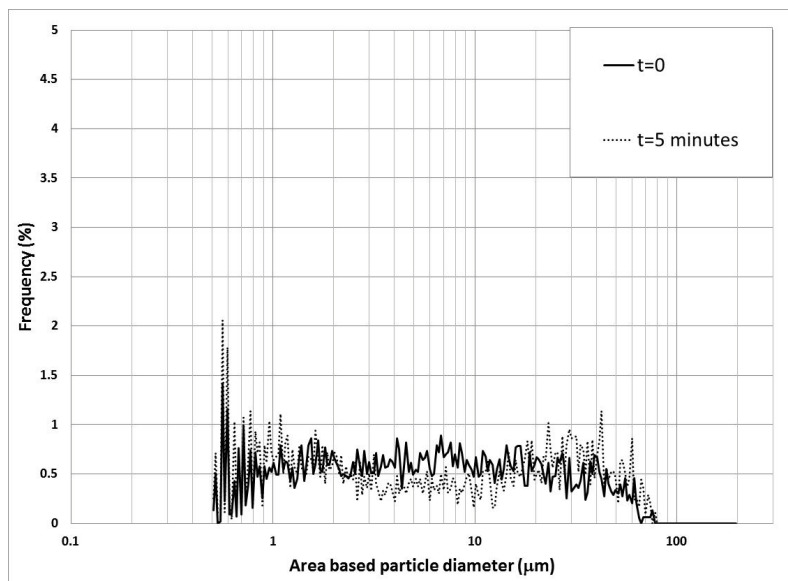
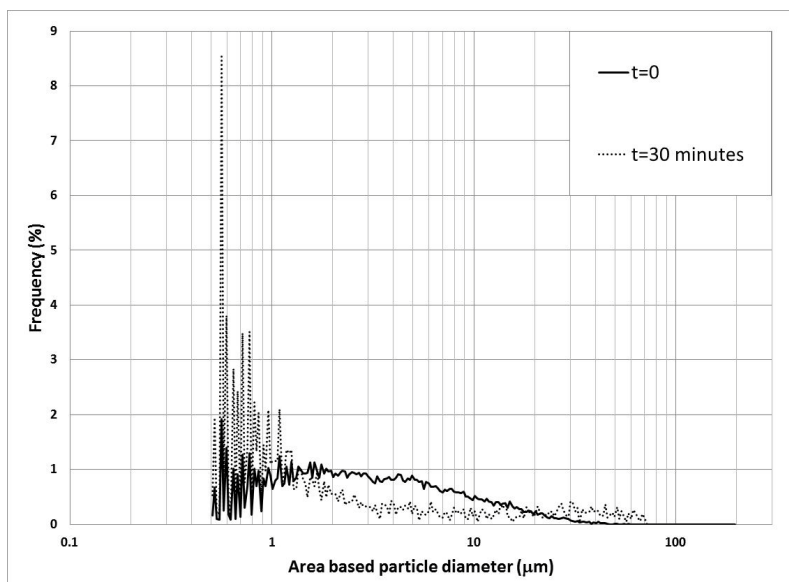
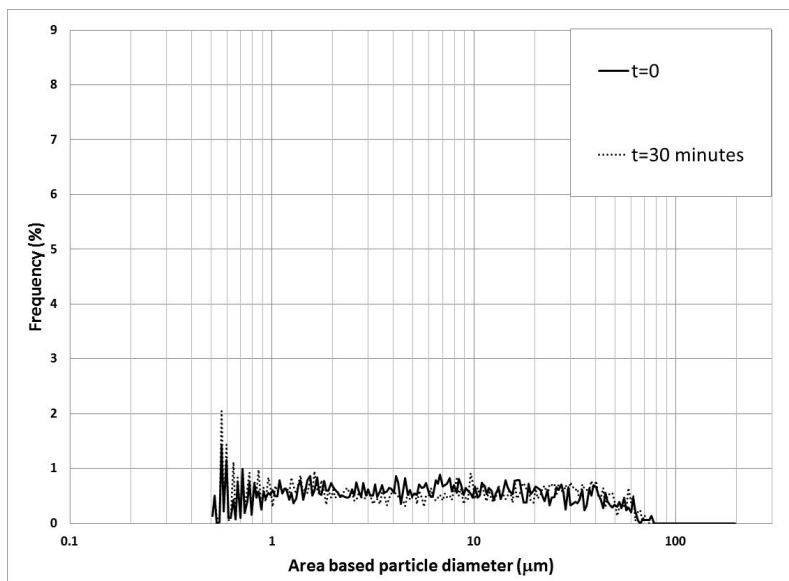


Figure K.2 Effect of sonication on the flocculated kaolinite sample:  $c=20$  g/L;  $\text{CaCl}_2$  to kaolinite mass ratio = 0.1; sonication time: 5 minutes; sonication amplitude: 100%



**Figure K.3 Effect of sonication on the non-flocculated kaolinite sample:  $c=20$  g/L; sonication time: 30 minutes; amplitude: 100%**



**Figure K.4 Effect of sonication on the flocculated kaolinite sample:  $c=20$  g/L;  $\text{CaCl}_2$  to kaolinite mass ratio = 0.1; sonication time: 30 minutes; sonication amplitude: 100%**

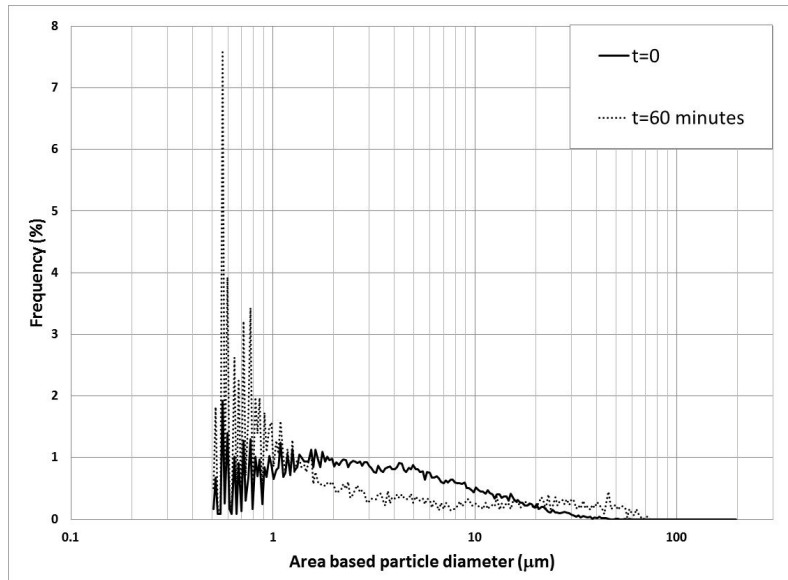


**Figure K.5 Effect of sonication on the non-flocculated kaolinite sample:  $c=20$  g/L; sonication time: 60 minutes; amplitude: 100%**

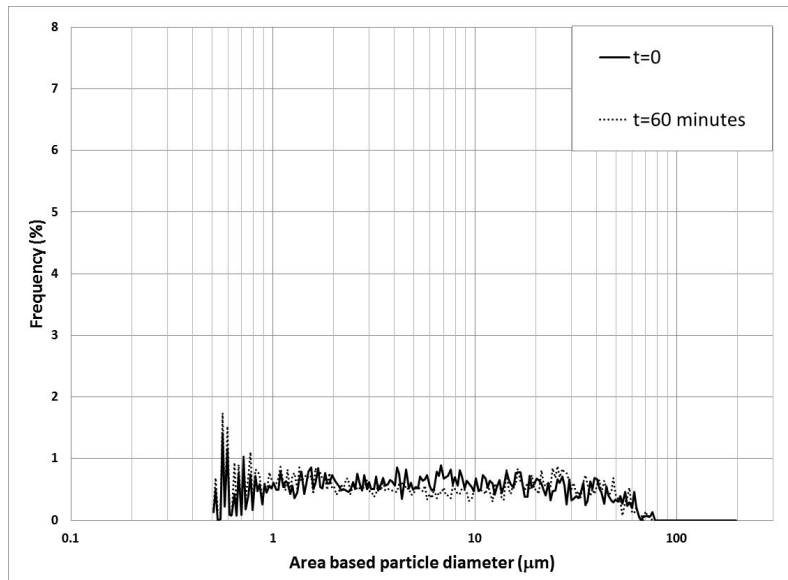


**Figure K.6 Effect of sonication on the flocculated kaolinite sample:  $c=20$  g/L;  $\text{CaCl}_2$  to kaolinite mass ratio = 0.1; sonication time: 60 minutes; sonication amplitude: 100%**